UNIVERSITY OF CALIFORNIA

Santa Barbara

Modeling the Hydrologic Impacts of Vegetation and Channel Network Change for a Semi-arid, Mountainous, Meso-scale Catchment: the Baviaanskloof, South Africa

A dissertation submitted in partial satisfaction of the

requirements for the degree Doctor of Philosophy

in Environmental Science & Management

by

Julia Ann Glenday

Committee in charge:

Professor Arturo Keller, Chair

Professor Thomas Dunne

Professor John Melack

Professor Naomi Tague

December 2015

The dissertation of Julia Ann Glenday is approved.

_____

Thomas Dunne

_____

John Melack

_____

Naomi Tague

_____

Arturo Keller, Committee Chair

November 2015

Modeling the Hydrologic Impacts of Vegetation and Channel Network Change for a Semi-arid, Mountainous, Meso-scale Catchment: the Baviaanskloof, South Africa

ACKNOWLEDGEMENTS

I want to give an enormous thanks to all the family, friends, and faculty who have helped me on my journey. I am extremely grateful to my parents for their love and support and for bringing me up to know that anyone can achieve anything when they set their minds and energy to it. I'd like to thank my supervisor, Professor Arturo Keller, and committee members, Professors Thomas Dunne, Naomi Tague, and John Melack, for their assistance and advice, for believing in me, and for investing in my growth. To all of the LivingLands memebers past and present, thank you for your support, friendship, fun, and constant inspiration: Dieter van den Broeck, Marijn Zwinkels, Odirilwe Selomane, Jennifer Foley, Maura Talbot, Ebie van de Merwe, Bart van Enk, Noel Isaacs, Silvia Weel, Stephie Mendelson, Justin Gird, Elwin Malgas, Miranda Sofika, Matt Zylstra, Alejandra Vargas. To Rebecca Joubert Powell, thank you for being the best field work mate anyone could ask for! Thanks to Rebecca and Mike Powell for help of all kinds and warm hospitality. Thank you to everyone at Rhodes University who has assisted me with academic advice and use of labs, equipment, and computing facilities, particularly Professor Kate Rowntree, Professor Fred Ellery, and Abe Ngoepe. I'm very grateful to the Tchnuganoo community farm for friendship and assistance on many a field trip, particularly Lois Stahl, Melloson Allen, and Anthony, and to the whole Baviaanskloof community for your warmth, hospitality, many cups of tea, and ability to fix cars. Special thanks to Piet Kruger and Chris Lamprecht for allowing me free access to your properties for my fieldwork. Thank you to the many organizations that have given me information, advice, and logistical support: Working for Wetlands, particularly Japie Buckle; Working for Water and Gamtoos Irrigation Board, particularly Vuyani Dlomo,Yolande Vermaak and Pierre Joubert; South African Environmental Observation Network (SAEON), particularly Nicky Allsopp and Abri de Buys; Center for Science and Industrial Research (CSIR), Patrick O'Farrel, Rene Wright, Lindie Adao-Smith, and the sweatshop crew; and, for weather data, Agricultural Research Council and South African Weather Services. Thanks also to Eastern Cape Parks and Tourism Agency (ECPTA), Sizwe Mukhulise and all the rangers, for allowing me to do research in the Baviaanskloof Nature Reserve and providing buffalo protection! I am so grateful for all the people who helped me in the field, in heat and dust and rain and mud, particularly Lucaan and Burtlan Kleinboi, and all the PRESENCE students, particularly Jordy (Baron) Stockhoff, Mark Bruggeling, Stefan Smit, Romel Torcat-Gil, Ana Ndeketya, Joep van Doornik, Opaline Lysaik and the WfJ crew: Jan van de Werken, Erik Stevens, and Lieke Jager. To friends, housemates, and officemates in Santa Barbara, thank you for your friendship and support: Ariana and Chris Arcenas-Utley, Theresa Morgan, Meredith Brockreide, Emily de Moor, Cameron Brick, Erin Bray, Yemi (aqueous media manager) Adeleye, and Xiaoli Chen. Thanks of course the merry salseros and salseras of SB for keeping me sane. I also want to express gratitude to many furry and the feathered friends that have been excellent company, taken me for walks, made me run, and kept me in the present: Zorro, Scratchy, Mila, Ponkle & Lex, Po & Kivet, Abby & Champ, and all the baboons in the Baviaanskloof! I am grateful to the mountains and rivers that always fed my soul.

I owe so much to so many and I strive to 'pay-it-forward'.

VITA OF JULIA ANN GLENDAY
November 2015

EDUCATION

Bachelor of Science in Environmental Science, Brown University, May 2004 (summa cum laude)
Doctor of Philosophy in Environmental Science, University of California, Santa Barbara, December 2015 (expected)

PROFESSIONAL EMPLOYMENT

2001-2002: Tutor, Department of Chemistry, Brown University
2002-2003: Teaching Assistant, Department of Environmental Studies, Brown University
2004-2005: Contracted Research, Critical Ecosystems Partnership Fund/Conservation International, Kenya
2006-2008: Research and Communications, EThekwini Municipality Environmental Management Department, South Africa
2009-2010: Teaching Assistant, School of Environmental Science & Management, University of California, Santa Barbara
2011-2014: Research Associate & Research Coordinator, LivingLands, South Africa

PUBLICATIONS

Keller, A. A., Chen, X., Fox, J., Fulda, M., Dorsey, R., Seapy, B., Glenday, J., Bray, E. (2014). Attenuation Coefficients for Water Quality Trading. *Environmental Science & Technology*, *48*(12), 6788–6794.

Petz, K., Glenday, J., & Alkemade, R. (2014). Land management implications for ecosystem services in a South African rangeland. *Ecological Indicators, 45*, 692–703.

Van Luijk, G., Cowling, R.M., Riksen, M., & Glenday, J. (2013) Hydrologic implications of degradation of South African semi-arid subtropical thicket. *Journal of Arid Environments*. 91: 14-21

Glenday, J (2008) Carbon storage and emissions offset potential in an African Dry Forest, the Arabuko-Sokoke Forest, Kenya. *Environmental Monitoring and Assessment.* 142 (1-3): 85-95

Glenday, J (2008) Carbon storage and emissions offset potential in an African Riverine Forest, the Lower Tana River Forests, Kenya. *Journal of East African Natural History*. 97 (2): 207-223

Glenday, J (2006) Carbon storage and emissions offset potential in an East African tropical rainforest. *Forest Ecology and Management.* 235: 72-83

AWARDS

Royce Fellowship, Brown University, 2003

Faculty Scholar Award, Brown University, 2004

Chancellors Fellowship, University of California, Santa Barbara, 2008

ABSTRACT

Modeling the Hydrologic Impacts of Vegetation and Channel Network Change for a Semi-arid, Mountainous, Meso-scale Catchment: the Baviaanskloof, South Africa

by

Julia Ann Glenday

This dissertation employs hydrologic modeling to assess probable impacts of changes in vegetation cover and in the channel network on streamflow and floodplain groundwater levels in the Baviaanskloof catchment, South Africa. The Baviaanskloof serves as a case study of a semi-arid, mountainous, meso-scale catchment that has been subject to agricultural land use and is regionally important for water supply. In this catchment livestock grazing has resulted in a loss of subtropical thicket cover on hillslopes and the channel network in the central valley has become increasingly connected and incised.

In order to build an appropriate model of the Baviaanskloof, streamflow, groundwater, surface runoff, and soil moisture data were analyzed for diagnostic patterns that revealed information about hydrologic connectivity at different spatial and temporal scales. Critical results of these analyses were that: a) the central valley alluvial aquifer is recharged by subsurface flows from surrounding mountain areas following two major pathways, a likely interflow contribution following large rainfall events and a more temporally consistent

contribution from the bedrock aquifer, and b) the dominant direction of exchange of water between the alluvial aquifer and the main floodplain channel regularly fluctuates between losing and gaining. To capture the observed patterns, the numeric model structure consisted of a coarse-scale sub-model of the mountain tributary subcatchments surrounding the central valley alluvial fill, and a higher resolution, coupled hydraulic-hydrologic sub-model of the central valley alluvial fans and floodplain. This model was calibrated in a multi-criteria calibration process using various observational datasets. It was found that including multiple streamflow-based criteria and including criteria based on additional data types improved model performance and better constrained the model parameter space.

Alternative scenarios of further degradation and of restoration of the hillslope vegetation, alluvial fan surfaces, and floodplain channel were modeled individually and in combination. Models were run using 38 years of local climate data and differences between model predictions for the current catchment state and each alternative scenario were assessed. Outputs suggested that, of the individual restoration intervention scenarios considered, hillslope thicket restoration would have the most significant impact on streamflow, driven by large reductions in storm event runoff and floodplain channel restoration would have the largest impact on the floodplain water table, driven by decreased drainage into the channel and increased recharge due to overbank flooding. Results indicated that restoring hillslopes could reduce flood peaks by 56-60% and annual average yield by 22-27%. Greater modeled water retention and evapotranspiration on vegetated hillslopes reduced runoff to the floodplain, resulting in a deepened water table and decreased baseflow in the model. Restoring alluvial fans was predicted to reduce flood

peaks by 11-17% compared to the current scenario, but modeled impacts on average yield, baseflow, and floodplain aquifer levels were not statistically detectable. Comparing the alluvial fan restoration scenario to a more extreme channelized case did show small, but detectable, increases in baseflow and floodplain groundwater levels. Reducing floodplain channel incision was predicted to reduce peak flows by 14-20%. Modeled impacts on average yield and baseflow were not statistically detectable. Groundwater levels were predicted to rise with channel restoration, with average depth decreasing 17-21%. Simultaneous restoration at all three positions was predicted to reduce flood peaks more substantially than any individual intervention (69-71%) while also decreasing the average depth of the floodplain water table (8-11%). Average annual yield was predicted to decrease by 32-37% as was baseflow, with a 20-40% decrease in average annual minimum monthly flow.

These results highlight various potential tradeoffs that would need to be considered in restoration planning and catchment management. Predictions made here would need further integration into reservoir and water supply system models, as well as sediment transport models to consider reservoir sedimentation, in order to better understand implications for local and downstream water supply availability. Nevertheless a net decrease in annual average available supply appears likely.

The catchment and climatic contexts of these changes were shown to be important in determining the magnitude and direction of the predicted impacts, with dispersive flow paths through central valley alluvium dampening impacts of hillslope vegetation changes

and with the frequency and magnitude of storm events determining how often different thresholds of flow path connectivity were reached. This highlighted the importance of including best available understanding of a landscape's hydrologic connectivity in modeling, even when focusing on a local scale change, and of modeling impacts over a long time period to include long-term weather patterns.

TABLE OF CONTENTS

LIST OF TABLES

LIST OF FIGURES

Chapter 2 Multi-criteria calibration of a hydrologic model for a semi-arid, mountainous, meso-scale catchment

Chapter 3 Impacts of subtropical thicket degradation and restoration on streamflow and groundwater in a semi-arid meso-scale catchment

Chapter 4 Streamflow and groundwater impacts of channelization on alluvial fans in a meso-scale, semi-arid, mountainous catchment

Chapter 5 Streamflow and groundwater impacts of floodplain channel incision in a meso-scale, semi-arid catchment

Chapter 6 Modeling cumulative hydrologic impacts of both vegetation and channel restoration in a semi-arid, meso-scale catchment

Chapter 1 : Development of a conceptual hydrologic model for a semi-arid, meso-scale catchment for water supply management using field data

1.1 Introduction

The development of hydrologic models to assist in catchment management entails balancing the purpose of the modeling exercise and the available data and level of knowledge about hydrologic processes in the catchment (Young et al., 1996; Wagener et al., 2001; Vaché and McDonnell, 2006). Both concerns will affect the decisions and assumptions made in selecting a model structure. In the last decade, catchment model structure development research has focused on methods for making 'best use' of all available information (Gupta et al., 2008; McMillan et al., 2011; Clark et al., 2011; Gupta et al., 2012). Such methods include systematic assessments of data-based diagnostics: patterns in observed data that are indicative of the occurrence, dominance, and thresholds of occurrence of different processes or flow paths. These provide formal frameworks for the various decisions made in moving from conceptual to numeric models (as described by Gupta et al., 2012). Despite the development of such procedures, (Fenicia et al., 2014) note that in the majority of cases, the grounds for applying particular conceptual and numeric models are still not well documented, hindering model assessment and further development. In addition, much exploratory model structure research has focused on small, headwater catchments in relatively wet environments without express consideration of an applied use of model outputs for management. This study employed multiple data sources, streamflow,

groundwater, and other hydrometric data, to develop a conceptual and numeric catchment model of a semi-arid, meso-scale catchment: the Baviaanskloof catchment, South Africa. The desired use of model in this case was to assess local and regional water supply impacts of proposed vegetation cover and river channel restoration activities. This application was explicitly considered in the development of the model structure.

Meso-scale catchments (10-10,000 km^2) are of a size typically relevant for catchment and water supply management and modeling at this scale can entail a large set of model structure decisions (Tetzlaff et al., 2010; Uhlenbrook et al., 2004). Drier environments tend to have greater temporal and spatial variability in flow path connectivity and can need higher resolution models to achieve similar accuracies to coarser models of wetter regions (Clark et al., 2008; Maneta et al., 2008). Data-based diagnostics can be used to guide the level of model complexity warranted by existing information (Gupta et al., 2008). The desired application of the model for management may require smaller-scale processes to be explicitly conceptualized, regardless of data available to resolve them, as outputs of internal catchment states and processes may be needed for decision making. Modeling possible future scenarios that differ from conditions for which historic data exists may also require more physics-based mechanistic process representations than the existing data supports.

The process of balancing available information on catchment processes and model structure requirements for a particular management application was explored through the development of a model for the 1,234 km^2 semi-arid watershed of the Baviaanskloof River in the Eastern Cape of South Africa. This catchment feeds a major regional water supply

reservoir. The loss of hillslope canopy cover due to livestock grazing (Mills et al., 2005; Sigwela et al., 2009) and channel modification and enhanced incision on alluvial fans and the main floodplain are thought to negatively influence water supply availability for users downstream of the reservoir and local users drawing from the alluvial aquifer (Jansen, 2008). The potential for vegetation and channel restoration interventions to impact local groundwater levels and downstream water yields are key management questions for the area and the motivation for modeling the catchment. This goal places constraints on the necessary model structure in terms of spatial and process discretization in order to differentiate scenario parameterizations and produce the desired outputs of both catchment water yield and floodplain groundwater levels. Within these constraints, field data were used to answer questions of flow path connectivity within and between landscape units.

The goals of this study are to use information on catchment physical properties and diagnostics from available streamflow, groundwater, soil moisture and runoff data to guide the development of conceptual and numeric models, adding to the knowledge base for semi-arid systems, and to ensure the model structure meets the needs of its application in terms of scales of process representation and outputs. A second stage of this process, described in a separate chapter, is multi-criteria calibration of the resulting model, assessing it against performance thresholds that are relevant to its application.

1.1.1 Development of model structure

Recent research in catchment model development emphasizes the need for targeted use of available data and information to inform model structure decisions as well as parameter value selection, as opposed to assuming applicability of a commonly used model structure and focusing on the use of observational data to parameterize this structure (Fenicia et al., 2008a; Gupta et al., 2008, 2012; Seibert and McDonnell, 2002). 'Top-down' modeling approaches use data-based diagnostics to identify dominant processes at different scales and the level of complexity required or warranted in their model representation (Gupta et al., 2008; Sivakumar, 2004; Sivapalan et al., 2003; Young, 2003). Streamflow, groundwater levels, soil moisture, and isotopic data have all been used to determine dominant processes and connectivity from the hillslope to the catchment scale based on diagnostic patterns (Clark et al., 2009, 2011; Karen, 2009; McMillan et al., 2011; Seibert and McDonnell, 2002; Tromp-van Meerveld and McDonnell, 2006; Vaché and McDonnell, 2006; Wittenberg, 2003). For example, McMillan et al. (2011) used the timing of streamflow peaks after rainfall peaks compared to flow path length to infer relative dominance of sub-surface pathways in the quickflow response and used the speed at which soil moisture decreases after a wetting event to infer the importance of drainage versus retention and evapotranspiration (ET) on hillslopes. Baseflow recession analyses have been used to indicate the degree to which water storage dictates outflow and whether or not a single linear reservoir is an appropriate representation of the process (Clark et al., 2009, 2011; McMillan et al., 2011). Seasonal variation in recession characteristics can indicate whether evapotranspiration (ET) has a dominant effect on the storages feeding baseflow (Wittenberg, 2003). Karen (2009) and Jencso et al. (2010) used relative elevations of groundwater and

river water surfaces to assess connectivity between river reaches and alluvial aquifers or riparian zones.

Top-down model development can be done in a hierarchic, step-wise manner: identifying first-order controls on outputs, and the simplest applicable algorithmic representations of them (e.g., a linear reservoir), and then sequentially testing the additions of more refined representations of internal processes (e.g., outflow thresholds, non-linear outflow, multiple reservoirs) until there is no further significant improvement in model accuracy against the available data (Fenicia et al., 2008b; Sivakumar, 2004; Vaché and McDonnell, 2006). Ensemble model structure testing procedures have been developed in which many alternative model structures, with ranges of complexity and different options of process representations, are tested against one another (Clark et al., 2008, 2011; Fenicia et al., 2014). This approach aims to prevent initial selection of a basic model structure from first-order data patterns that could later become inappropriate when finer scale processes are sequentially added. Most comparative model structure assessments, particularly ensemble assessments, have been limited to lumped models or small catchments due to computational intensity.

These methods contrast with 'bottom-up' model development in which catchment-scale models are built by combining physics-based, mechanistic, algorithmic descriptions of as many internal component processes as can be described given existing physical understanding. Arguments against the applicability of this approach in many situations are that processes described at fine scales may not be relevant at the scale of analysis (Clark et

al., 2009; Savenije, 2010; Sivapalan et al., 2003). For example, modeling subsurface flow using the Darcy-Richards equations parameterized by soil sampling in cases where hillslope-scale flows may be dominated by macro-pore flow or bedrock topography fill-and-spill effects, processes that are not detectable at the point scale and not well represented by Darcy-Richards equation based algorithms and parameters (Clark et al., 2009; Gupta et al., 2012; Tromp-van Meerveld and McDonnell, 2006). Bottom-up approaches can lead to development and use of highly parameterized, complex, and computationally intensive, models for areas where there is insufficient data to resolve the uncertainties in the many parameter values, leading to high levels of equifinality (Beven and Freer, 2001; Savenije, 2010). The resulting application of the model may then be stochastic, perhaps without reaching levels of output accuracy that could be achieved with simpler structures.

There are cases where physics-based, bottom-up modeling approaches are needed and useful regardless of uncertainties and complexities they introduce. A downward model development approach cannot be directly applied to ungauged or data-poor catchments. Model structures and parameters developed through a downward approach in gauged catchments could, in principle, be regionalized to ungauged catchments if guiding catchment physical properties are reliably defined, but this has only been developed in a few select areas (Gupta et al 2012). Modeling scenarios of change that affect processes which are not modeled with physics-based algorithms can also be difficult.

1.1.2 Dominant processes, connectivity observations, and modeling experience in meso-scale, semi-arid, mountainous catchments and floodplain systems

Semi-arid meso-scale catchments provide significant challenges to modeling with similar accuracy to humid, headwater catchments, due to both the relative scarcity of hydrometric data and the dominance of complex surface-subsurface flow pathways in contributing to streamflow (Clark et al., 2008; Maneta et al., 2008; Tetzlaff et al., 2008). Existing process and model research on meso-scale catchments and in semi-arid and mountainous locations have identified characteristic patterns in processes that can be brought to bear in model development decisions, such as the level of spatial and process discretization and landscape and process connectivity and its model representation.

Meso-scale catchments can encompass both steep headwater areas and sizeable floodplains, including a range of geologic and topographic landscape features with different hydrologic response characteristics. As such different flow pathways may be dominant at different scales and times. It has been generally observed that for micro-scale ($<1km^2$) headwater catchments, surface and shallow subsurface runoff generating processes are first-order determinants of streamflow patterns, while for meso-scale catchments the spatial distribution of rainfall and channel routing of runoff become important (Uhlenbrook et al., 2004). In addition, as catchment scales increase, there can be an increasing proportional contribution of bedrock groundwater to total catchment outflows (McGrane et al., 2014; Ophori and Tóth, 1990).

The importance of spatial variability at the meso-scale and in semi-arid environments makes lumped catchment models less appropriate and so decisions must be made about spatial scales for process representation. Including spatially variable precipitation and spatial discretization of threshold-controlled surface and shallow sub-surface processes has been found to improve model performance in arid and semi-arid catchments (Fenicia et al., 2008b; Maneta et al., 2008). However, a fully gridded approach does not necessarily provide improvement in runoff modeling over a semi-lumped model at the meso-scale (Das et al., 2008; Winsemius et al., 2006). A common approach has been to identify landscape units thought to have distinctly different first-order dominant processes and to model surface and near surface processes of each of these units separately (Gao et al., 2014; McGlynn et al., 2004; Savenije, 2010; Van den Bos et al., 2006). As an example of potential differences in processes between topographic units, Savenije 2010 observed that in many systems plateaus are dominated by water storage and/or vertical drainage to deep groundwater, hillslopes are dominated by storage excess subsurface flow, and lowland riparian areas more often have saturation excess surface flow as well as subsurface drainage. Data-diagnostics and top-down modelling approaches have supported the physical process reasoning that lithology and topography differentiate areas of distinct runoff responses that are emergent in meso-scale catchment runoff patterns (Clark et al., 2009; Fenicia et al., 2014; Gao et al., 2014; Uhlenbrook et al., 2004; Van den Bos et al., 2006). Sub-catchment hydrograph analyses (Van den Bos et al., 2006) and ensemble model testing (Fenicia et al., 2014) have also supported separating process representation by areas of different dominant lithology. Similarly, isotope water balance unmixing (Tromp-van Meerveld et al., 2007), flow recession analyses (Clark et al., 2009), hierarchical model development (Fenicia et al.,

2008a) and ensemble model testing (Gao et al., 2014) studies have supported discretization at the level of topographic units, such as hillslopes and valley bottoms, in meso-scale catchments.

Conceptualization of the surface and subsurface connectivity between separately modeled land units can significantly influence model performance at the meso-scale as dominant flow paths feeding streamflow are likely to include multiple units. Model structure studies have used data-based diagnostics and physical process reasoning to determine whether to model hydrologic response units (HRUs) in parallel, each individual unit directly connected to a channel network, or as a cascading series of units, in which only the most downslope unit is directly connected to the channel. Van den Bos et al. (2006) used channelized sub-catchments as HRUs and so they could be reasonably modeled in parallel, using channel routing to account for each unit's distance from the catchment outlet. While theoretically, when using smaller-scale, less channelized HRUs, surface and shallow surface runoff from upslope areas would flow across and through a catena of topographic landscape units, in some cases data analyses have supported a simpler, parallel model structure. For example, in the Panola Experimental Watershed, Clark et al. (2009) supported modeling hillslopes and riparian zones as parallel reservoirs. In this case, field measurements found that precipitation thresholds to initiate hillslope surface and shallow-subsurface runoff were only met during infrequent extreme events, while the riparian areas consistently contributed to streamflow, being often saturated and slow draining (Clark et al., 2009; Tromp-van Meerveld and McDonnell, 2006). Hillslopes therefore rarely if ever contributed runoff to riparian zone storage, only producing runoff during large events in which the riparian zone

would already have been saturated through direct precipitation. As such, the threshold-triggered outflow from the hillslope unit could reasonably be routed directly to the river channel, assuming quick passage across a saturated riparian area, without considering infiltration on the riparian zone and its antecedent storage.

Based on physical reasoning, Savenije (2010) and Winsemius et al. (2009) suggest linking topographic units in series in a flow path catena in meso-scale systems that have areas of deep and permeable soils, capable of infiltrating the majority of the surface flows they receive, and in systems in which subsurface flows dominate and hillslope flows are a significant source feeding riparian zone storage. Data-based approaches have also supported linking units in series in cases where subsurface lateral flow is dominant (Fenicia et al., 2008a). In a multi-scale study, using isotope, groundwater level, and streamflow monitoring at different landscape positions in a mountainous catchment, McGlynn et al. (2004) found that in small headwater catchments, riparian areas were consistent sources of streamflow, while in larger catchments, the valley bottom areas only contributed to streamflow after high rainfall events or those occurring with wet-antecedent conditions. This supports linking upslope hillslope units in series to valley bottom areas of large catchments, because floodplains would more often have storage space for flows originating upslope, particularly in arid areas. Field observations of relative groundwater and stream elevations, and correlations between groundwater levels and streamflow, have been used to describe the nature and thresholds of connectivity between floodplain areas and the channel network (Banks et al., 2011; Hammersmark et al., 2008; Jencso and McGlynn, 2011; Karen, 2009; Phillips et al., 2011).

The potentially dynamic connectivity between floodplain alluvial aquifers and channel flows is not typically explicitly modeled at the catchment scale, however observations have suggested that this can be an important factor in determining runoff peaks and recessions (Essaid and Hill, 2014; Hammersmark et al., 2008; Maneta et al., 2008; Smith et al., 2013). Particularly in more arid environments, channel flows originating higher up in the catchment can be a source of recharge to a low-land alluvial aquifer in dry periods, through infiltration of channel flow and of overbank flood water in extreme events. The direction of flow can reverse in wetter periods, when high aquifer groundwater levels contribute flows into the stream. Observational and modeling studies have indicated that the dimensions of the floodplain channel, hence its capacity to contain flood flows and the level of incision relative to the groundwater table, influence streamflow magnitude and timing (Essaid and Hill, 2014; Hammersmark et al., 2008; Loheide and Booth, 2011; Loheide and Gorelick, 2007; Ohara et al., 2014; Tague et al., 2008). Coupled hydraulic and hydrologic models (Hammersmark et al., 2008) and coupled coarse-scale catchment and fine-scale floodplain channel-groundwater models (Hipsey et al., 2011) have been used to better represent this interaction at the catchment scale.

In large, mountainous catchments, in which the bedrock is porous or highly fractured and the soils are thin and/or fast draining, percolation into bedrock aquifers and contributions from bedrock aquifers to recharging alluvial aquifers and catchment outlet flows can be substantial, with estimated values of 10-70% of recharge or outflow coming via bedrock in various cases (Katsuyama et al., 2010; Magruder et al., 2009; Tromp-van

Meerveld et al., 2007; Van den Bos et al., 2006; Welch and Allen, 2012). Conceptualization of mountain block recharge (MBR) of alluvial aquifers has received increased attention in models of mountainous catchments as it has been recognized as a significant contributor to alluvial groundwater levels and hence to streamflow (Kao et al., 2012; Magruder et al., 2009). Savenije et al (2010) suggest that, while representation of surface and shallow subsurface processes benefits from discretizing topographic units, the slower bedrock groundwater flows, about which there is generally less information and diagnostic data, are more reasonably modeled using single reservoirs receiving recharge from all the overlying land units.

Flow recession analyses can be used to guide how groundwater storage and outflow should be represented in a model (Clark et al., 2009). The relationship between the rate of flow decline to the flow volume, and hence to catchment storage, indicates whether or not a simple linear reservoir model can be an appropriate representation of outflow from the storages feeding catchment baseflow. Semi-arid and topographically complex catchments are unlikely to have simple storage-outflow relationships (Clark et al., 2009; Maneta et al., 2008; Tetzlaff et al., 2008), however the effects of local complexities and spatial heterogeneities can be smoothed in the flow responses at large catchment scales (Sivapalan et al., 2003). Non-linear recession patterns can be recreated with multiple linear reservoirs feeding catchment outflows in parallel or linked in series, and the degree of non-linearity indicates the number of reservoirs that may be needed, representing different storages and flow pathways through the catchment (Clark et al., 2009). Non-linear recessions with smooth curves can be recreated by combining high numbers of linear reservoirs. Recession

patterns that instead have different distinct slopes at different stages of the recession can be recreated by a smaller number of linear reservoirs with large differences in their drainage constants. Seasonal differences in recession patterns indicate the influence of factors other than catchment water stores, such as ET, on the flow paths supplying recession flows (Wittenberg, 2003).

1.1.3 Model development

A completely data-driven top-down approach to model development was not considered appropriate here given process representation requirements of the model's intended application: to assess the impacts of changes in hillslope vegetation cover and in alluvial fan and floodplain channels on water supply. Therefore, the level spatial discretization and process representation needed to use the model to consider the effects of vegetation and channel change scenarios was identified, following a bottom-up approach. Diagnostic patterns in the available hydrologic data were then used to further determine where additional complexity was warranted, to infer connectivity between processes and flow paths, and to parameterize processes. Due to the scale of the catchment, discretization at the scale of broad topographic units was assumed to be a reasonable starting level of complexity and data-diagnostics from catchment streamflow, floodplain groundwater, and hillslope runoff and soil moisture observations were used to infer dominant processes and connectivity between these units. Where data was insufficient to specify the needed process representation, literature on similar cases was used to inform the model structure. A priori

parameter ranges were defined using inferences from the available data and relevant literature.

1.2 Study site and model use

1.2.1 Catchment description

The study site is the 1,234 km^2 catchment of the Baviaanskloof River, a semi-arid, mountainous watershed in the Eastern Cape Province of South Africa (Figure 1-1). Situated in the Cape Fold Mountain Belt, the catchment was shaped by geologic faulting and successive uplift events and has a half graben structure (Holmes, 2012). The result is a trellis drainage pattern in which a central valley floodplain, running between parallel mountain ranges (Baviaans Mountains, the footwall side to the north, and Kouga Mountains, the hanging wall to the south), is fed by steep, deeply incised, tributary valleys oriented perpendicular to the main valley line (Figure 1-2). Many of these tributary valleys terminate in alluvial fans at the floodplain margin. The central valley floodplain and fans make up 5% of the catchment area with a 0.6% average longitudinal slope (Powell, 2015), compared to the 38% average terrain slope over the entire catchment (calculated using a 30m resolution digital elevation model, DEM, from NASA satellite radar topography mission, SRTM, datasets).

The lithology is primarily quartzitic sandstones of the Table Mountain Group (TMG) with interbedded shale layers. An overlying Enon Conglomerate layer formed in the central

valley has largely eroded away; however, outcrops remain on some lower slopes and likely underlie parts of the current floodplain. TMG quartzitic sandstones are fractured, while the less permeable shales and conglomerates create aquicludes. Surface springs appear at interfaces between quartzitic sandstones and shales as well as at major fault zones. Studies of TMG fractured sandstone aquifers in other parts of the Cape Fold Belt indicate that there is generally a more highly fractured surface layer, and that fractures and faults become progressively cemented by mineral deposits at depth (Xu et al., 2003, 2009). Soils on the cliffs, hillslopes, and plateaus are thin (0-100 cm) and are generally loamy sands with high rock content (30-40% by volume). Research on the connection between surface and groundwater in areas with TMG lithologies has indicated that interflow in the highly fractured bedrock surface and/or at the soil-rock interface can make up significant portions of river and wetland annual hydrographs, over 50% in some cases, particularly in headwater streams and water bodies near TMG mountain footslopes (Midgley and Scott, 1994; Roets et al., 2008; Xu et al., 2002, 2003). These outflows can then feed lowland alluvial aquifers

Differential uplift of fault blocks, and the differing hardnesses of the TMG layers exposed as a result, has meant that the main valley floodplain varies in width: wide sediment basins (1 km wide between hillslopes), carved from erodible lithologies, alternate with narrow valley reaches (100-300 m wide) crossing outcrops of harder layers. Resistivity measurements in the wide floodplain basins indicate that the alluvial deposit is 20-35 m thick (Soltau et al., 2011) and floodplain soil profiles have sand and cobble deposits overlain by 50-200 cm of sandy loam/loamy sand.

Based on daily gage data obtained from the South African Weather Services (SAWS) and the Agricultural Research Council (ARC), the average annual rainfall for the period 1970-2013 was 270 mm and with annual average maximum and minimum temperatures of 32 and 5^{o}C. Average annual potential evapotranspiration (PET), estimated using the method of (Hargreaves and Samani, 1982), for the same period was 1335 mm. Interannual variation in precipitation is high (recorded annual values range from 100 to 500mm) and there is no consistent seasonal pattern of large rainfall events. Winter rainfall tends to be dominated by frontal systems while summer receives convective rainfall with short, intense events. The outlet of the catchment is the confluence with the Kouga River, below which lies the Kouga water supply reservoir. The Baviaanskloof River flows perennially at its outlet and in upstream narrow valley reaches, but surface flow in the wide floodplain basins is ephemeral, flowing for months to years in wet periods. Surface flows in tributary valley channels are ephemeral typically lasting hours to days following large storms. Surface groundwater springs from the bedrock aquifer are evident at faults and interfaces between sandstone and significant shale layers.

The distribution of indigenous vegetation generally follows the topography with fynbos (characterized by woody shrubs, grasses, and herbs) on the plateaus and upper slopes, subtropical thicket (characterized by large succulents and woody shrubs) on the cliffs and lower slopes, riparian forest in the narrow tributary gorges and narrow reaches of the main valley, and savannah woodland on the wide floodplains (Euston-Brown 2006). Small areas of reed dominated permanent wetland exist on the floodplain close to bedrock groundwater seeps. Livestock farming with goats has been practiced for over a century in much of the

catchment, significantly reducing the thicket vegetation cover on the hillslopes, which would otherwise have had a closed canopy (Euston-Brown, 2006; Sigwela et al., 2009). In 2012 roughly 11% of the floodplain area was used for irrigated agriculture, down from 25% 1970. Direct channel modification, in the forms of ditching, straightening, and berm construction, occurred on many alluvial fans and reaches of the main channel to protect fields and infrastructure from floods.

Figure 1-1 Location of the Baviaanskloof catchment area within South Africa

Figure 1-2 Map of rainfall, streamflow, and groundwater monitoring sites in the Baviaanskloof catchment (above) and higher resolution map of Gannaland (GN) tributary and Joachimskraal (JK) floodplain sites (below)

Monitoring site name codes are written above each instrumented site. Two additional rainfall gauges used are off the map, shown in Figure 1-3. Delineated tributary valleys feeding the central valley floodplain based on the DEM shown, sourced from NASA's 30m SRTM data. Working for Wetlands proposed location for a permeable weir to trap sediment shown for Joachimskraal site.

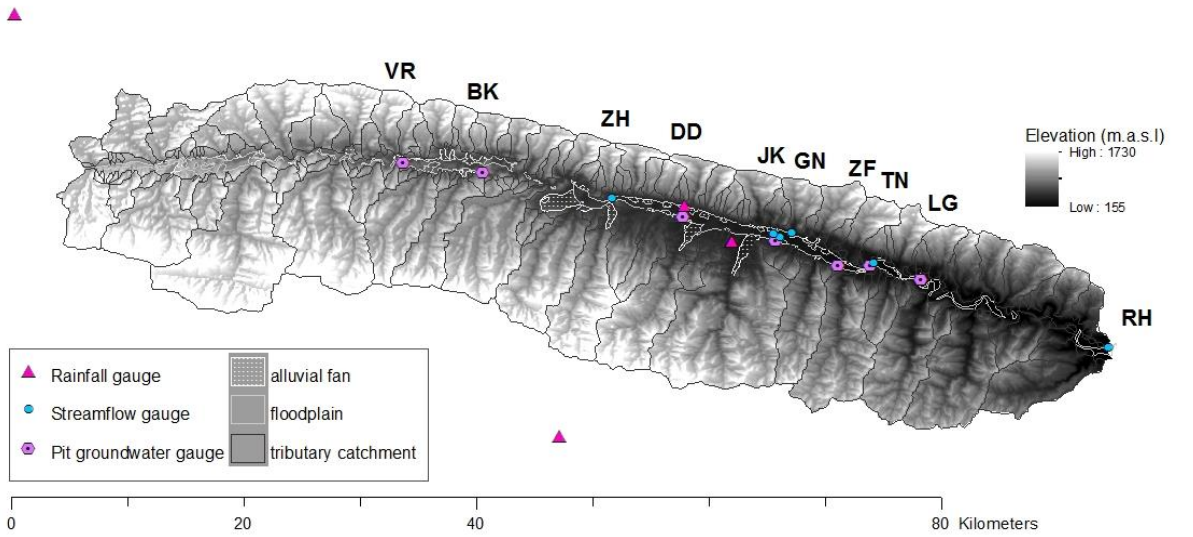

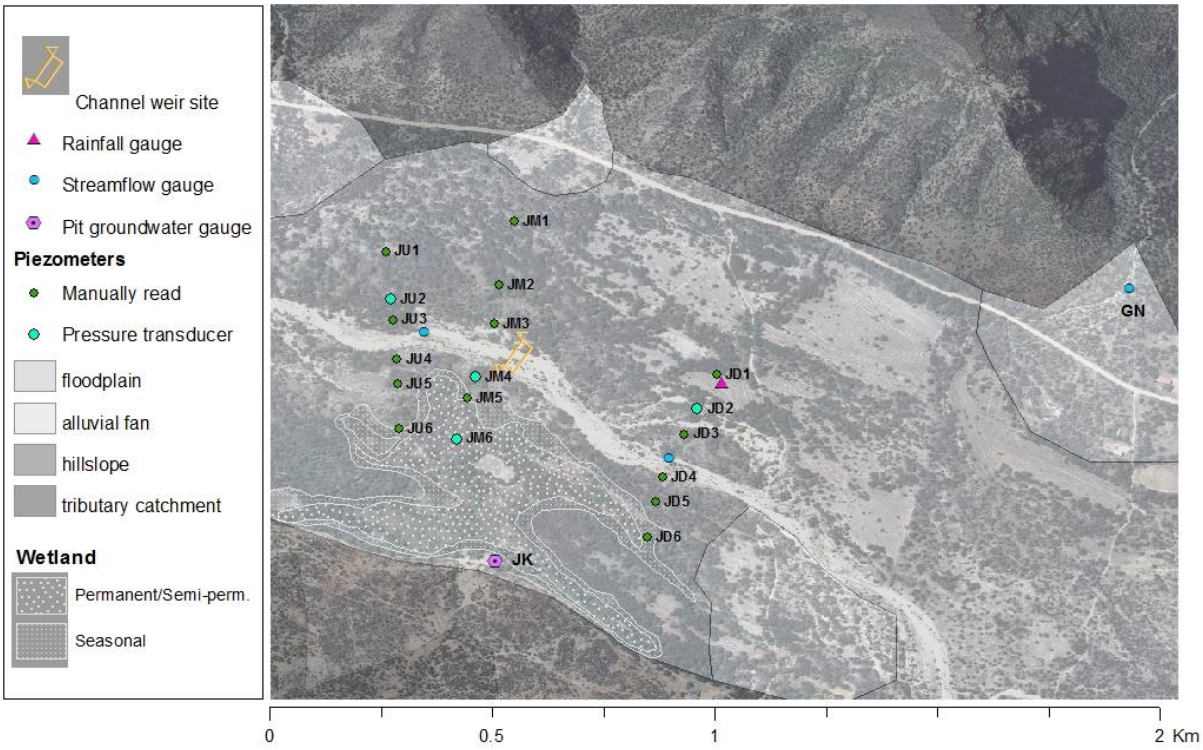

1.2.2 Model use and implications for structure and scale

The purpose of developing a model of the Baviaanskloof catchment is to quantify potential impacts of various landscape and river channel restoration interventions on the river flow regime and water supply. The proposed restoration interventions are reduced grazing and replanting indigenous thicket vegetation on degraded hillslopes, restoring more dispersive surface flow paths across alluvial fans, and channel restoration measures on the trunk river to counteract incision and channel-floodplain disconnection. These activities have been advocated on the grounds of increasing biodiversity by restoring subtropical thicket and floodplain wetland habitats, improving carbon stocks, regaining lost agricultural potential, and for potential water supply benefits (Jansen, 2008; Mander et al., 2010; Mills and Cowling, 2006). Baviaanskloof catchment residents obtain water from the floodplain aquifer, while the downstream reservoir supplies coastal urban areas and commercial agriculture outside the catchment. The flashy hydrology, reservoir storage capacity, and downstream water demand have meant that uncontrolled overtop spillage losses in wet periods and low reservoir levels in dry periods requiring water use restrictions have become regular occurrences (Jansen, 2008). The degree to which proposed restoration interventions could play a role in improving the reliability of water supply, by increasing the proportion of flow through the catchment coming via slower subsurface pathways compared to fast surface run-off, such that the reservoir is fed more evenly over time, is of interest for catchment management. As such, outputs that the catchment model needs to produce are groundwater levels in the floodplain aquifer, affecting local supply, and streamflow to the catchment outlet, feeding the Kouga reservoir.

Table 1-1 documents proximal processes that would be affected by the various restoration interventions and the implications this has for the model structure. The model will need to be discretized at the level of different landscape units in its conceptualization of surface processes. Modeling sub-surface flows will need to differentiate processes in alluvial aquifer from the surrounding mountain areas. Separate consideration of the alluvial aquifer is needed to assess impacts on groundwater levels relevant to irrigation. If the exchange of water between the trunk channel and the floodplain aquifer changes direction and magnitude frequently, then assessment of the impacts of floodplain channel change will require that relative channel and groundwater elevations be calculated to estimate flows between these pools. Whereas saturated zone outflows could be represented by simple reservoirs for the other landscape units, a gridded groundwater model may be warranted for the alluvial aquifer such that the water level gradients in multiple directions can be considered. A monthly scale of assessment would be sufficient to look at water supply outcomes, however some relevant processes that impact supplies and are predicted to change, such as overbank flooding, occur at daily or sub-daily time-steps.

There is no available streamflow and groundwater data from the time before hillslope vegetation cover was heavily impacted by livestock. Without this, a top-down model development approach cannot be used to infer parameterizations for restoration scenarios. As such the effected surface and shallow subsurface hillslope processes need to be considered in a bottom-up, mechanistic fashion with parameters related to measurable differences in canopy cover and soil properties that can be used to distinguish scenarios.

Table 1-1 Model structure implications of the intended model use in impact assessment for various restoration interventions

Change due to restoration intervention	Proximal hydrologic processes affected	Model structure implications
Hillslope vegetation cover and associated soil properties	• Canopy interception • Evapotranspiration • Soil infiltration vs. surface runoff production • Soil water retention vs. lateral subsurface flow & percolation	• Discretization separates hillslope surface processes from other topographic units • Canopy interception storage capacity and AET calculations based on vegetation cover properties • Soil water content thresholds for runoff and percolation linked to measurable soil properties
Alluvial fan surface flow channelization	• Partitioning of channelized vs. dispersed fan surface flow • Infiltration on the fan	• Discretization separates alluvial fans • Separate surface and subsurface flows reaching the fan from tributary catchments • Partitioning of incoming surface flows between channel and fan surface based on channel characteristics • Overland flow on fan surface available for infiltration
Floodplain channel dimensions	• Overbank flooding and floodplain aquifer recharge • Water exchange between floodplain aquifer and channel	• Discretization separates floodplain • Channel routing explicit • Channel flow exceeding channel capacity routed to floodplain surface • (*If overbank flooding occurs when the floodplain is not saturated*) Overbank flood water available for infiltration • (*If the channel is regularly fed by the alluvial aquifer*) Flow between channel and alluvial aquifer based on relative water surface elevations ○ Riparian area groundwater surface elevation and channel water surface elevation dynamically calculated

1.3 Methods

1.3.1 Topographic analysis

The application of the model requires discretization at the level of vegetation type and topographic land forms, at a minimum, in order to parameterize vegetation cover and channel connectivity scenarios. The catchment was classified into six topographic land units: high plateaus, hillslopes, cliffs, canyon floors, alluvial fans, and floodplains. These land units were assumed to have different dominant processes, warranting separate model conceptualization and parameterization based on previous literature (Clark et al., 2009; Fenicia et al., 2008b; Gao et al., 2014; Savenije, 2010; Van den Bos et al., 2006). Local physical characteristics and observation data were used characterize the processes of, and connectivity between, delineated topographic units in the Baviaanskloof catchment, as described further below.

Land unit mapping was done using a 30 m DEM based on slope and a topographic position index (TPI) as described by Jenness (2006), automated into Topography Tools 9.3 (Dilts, 2010) for ArcGIS. While other studies have used slope and elevation to delineate topographic land units (Gao et al., 2014), the west to east elevation decline along the Baviaanskloof's 82 km longitudinal profile meant that elevation alone was not sufficient to differentiate flat areas into floodplains and plateaus over the entire catchment area. The TPI is the degree to which the elevation of cell is higher or lower than the average of the cells surrounding it within a user defined radius, or neighborhood window. TPI thresholds, based on the standard deviation of TPI values for the landscape considered, are then combined

with slope value thresholds to define slope-position classes. For example, a TPI value close to zero could occur either on a flat plain, in which case the slope would be close to zero, or at the middle of an even gradient hillslope, in which case the slope would be higher. A second level of classification into landforms was then done by combining two sets of slope-position classes calculated using different neighborhood window sizes (Jenness, 2006). For example, an area classified as a flat plain using the smaller window and as a valley using the large window would be a floodplain, whereas a small window flat plain, large window mountain ridge would be a high plateau. Cliffs were defined as any area in which the slope was greater than 60%. Alluvial fans were mapped separately by Bobbins (2011) using stereography.

1.3.2 Data collection & available data

Precipitation and temperature were measured hourly using tipping bucket rainfall gages and temperature sensors at two locations in the catchment from 2011-2013. Daily rainfall and temperature from 1970 onward are also available for two gages within the catchment and five within 20 km from the South African Weather Services (SAWS) and the Agricultural Research Council (ARC). Stream discharge was calculated over two years (2012-2013) at 6 locations in the catchment, using pressure transducers (Solinst Levelogger Junior Edge 5M, ± 5 mm accuracy) logging water depth hourly and channel surveys and manual flow measurements to derive rating curves. These locations were the catchment outlet (RH), two sites upstream on perennially flowing narrow valley reaches (ZH,TN), two on an ephemeral wide valley reach (JK), and one on an ephemeral tributary valley channel

(GN) upstream of the alluvial fan (Figure 1-2). To obtain a longer-term record of albeit lower-resolution data, monthly flows at the catchment outlet were estimated for the period from 1972-2013 using the measured inflow to the Kouga reservoir and gage data on the Kouga River sourced from the South African Department of Water Services.

To create rating curves for gauged sites on the main river, 14-16 manual flow measurements were taken at each site. To calculate flow at a gauged cross-section, water velocity readings were taken using a Marsh-McBirney Flo-Mate at 20%, 40%, and 80% of the water depth at 8-10 equally spaced points across the wetted channel width. Measurements were taken in flow conditions ranging from bankfull to low flows with depths close to 15 cm and water velocities close to instrument detection limits (0.015 m/s). It was not feasible to take measurements during flood events when flow exceeded bankfull depths. Flow, slope, and wetted cross section measurements were used to determine Manning's n roughness values for the channels, while an n value of 0.1 was assumed for the floodplain (Hammersmark et al., 2008) to extend rating curves to peak flow values. At each gauged site, 100-200m wide floodplain and channel topography cross sections were surveyed using a differential GPS system (Thales ProMark 3 and base station), with widths extending beyond the active floodplain as discerned by vegetation and debris deposits.

Groundwater levels in the floodplain alluvium were collected at two spatial and temporal scales. Levels were manually read from staff gages in groundwater pits used for farm water supply at near monthly intervals at seven locations from 2011 to 2013 (Table 1-4). Some of these pits are located in the centers of wide floodplain basins while others are up against

mountain fronts. Test readings taken before and after irrigation pumping indicated that pit water levels recover within 6-10 hours and levels were recorded prior to pumping. In addition, eighteen 2 m piezometers were installed in three transects along a 1 km floodplain reach that is no longer actively farmed at a site called Joachimskraal (JK) (Figure 1-2). These were placed to examine the local groundwater impacts of a pilot floodplain channel restoration intervention: berm removal and construction of an in-channel sediment-trapping gabian weir. Four piezometers were instrumented with hourly recording pressure transducers starting in July 2012, while the remaining fourteen were measured manually on a monthly basis. The site includes a small area of permanent wetland, and one of the instrumented piezometers was placed in the wetland. Both at the water supply pits and the piezometer transects, river stage at an adjacent cross section was measured at the same interval as the groundwater level. Topographic surveys done with a differential GPS system (Thales ProMark 3 and base station), allowed relative assessment of groundwater and surface water elevations at these sites. Soil texture, bulk density, rock content, and conductivity were sampled from distinct soil layers during piezometer installation. Conductivity was measured in field using a double-ring infiltrometer. Rock content was measured using 10 L wet samples sieved and weighed in the field and wet-dry weight ratios of rock and soil calculated using 500g sub-samples dried in the lab.

Soil moisture data from six 600 mm long capacitance probes (DFM), with sensors at 100 mm intervals, installed on a hillslope are available for 2011-2013 from van Luijk et al. (2013) and continued data collection at this site. The soils on this hillslope were shallow, such that the bottoms of the probes were in regolith. Probes were installed along either side

of a fence-line separating an area of ongoing grazing (5% shrub canopy cover) and an area that has had 30 years of vegetation recovery without grazing (45% cover). This study also included data collection on relative quantities of surface runoff and sediment transport in the different vegetation cover densities, assessed with Gerlach troughs, and estimation of canopy interception using tipping bucket gages in the open and under the canopy (van Luijk et al., 2013).

1.3.3 Data diagnostics

Available climate, streamflow, groundwater, soil moisture, and surface runoff time-series were analyzed for diagnostic patterns indicative of different processes, flow paths, and landscape connectivity at the scales of the data (Table 1-2). Because surface flows in the tributaries are short lived and infrequent (e.g., only one flow event in the instrumented tributary in two years of observation), the majority of the available streamflow data represent large catchment areas (635-1,234 km^2). This signal integrates what is likely to be a variety of different dominant processes at different scales as well as spatial variation of rainfall patterns. Data were not available at the appropriate scales to discern dominant processes for all the landscape units considered. Process studies and literature on catchments with similar characteristics were also assessed to suggest dominant processes at these scales, means of numerical representation, and parameter ranges.

Table 1-2 Hydrometric data diagnostics applied to guide model development

Scale	Data types	Analysis	Process interpretation	Model structure decisions affected
Catchment	Streamflow, precipitation	Average annual runoff ratio	Low ratios indicate large ET withdrawals from dominant flow paths and/or significant storage in relatively inactive groundwater.	ET influence on dominant model reservoirs and/or significant percolation to slow outflow groundwater
Catchment	Streamflow	Quick vs. slow response flow proportions and output variability	Relative dominance of surface and subsurface runoff pathways. Variability in slow-flow output indicates variability in aquifer storage and/or sensitive storage-outflow relationship.	Balance of parameters driving partitioning between quick and slow flow paths and releases. Importance of modelling baseflow contributions dynamically.
Catchment	Streamflow, precipitation	Storm event precipitation threshold for quick-flow runoff response	Reflects cumulative surface and shallow subsurface processes of contributing landscape units. (Thresholds at smaller scales contribute.)	Maximum combined storage of land unit surface and shallow sub-surface reservoirs. Seasonal trend indicates ET influences antecedent storage in relevant reservoirs.
Catchment	Streamflow, precipitation	Peak-forming storm event runoff ratio	High ratios indicate dominance of quickflow paths vs. slower flow paths, storage, and/or ET. Seasonal trends indicate ET effects on quickflow flow production.	Balance of parameters driving production of quickflow vs. slow flow or storage, when above thresholds
Catchment	Streamflow, precipitation	Shape of flow recession curve	The degree of non-linearity and linear portions of curves can reflect the number of significantly different subsurface flow paths contributing to baseflow.	Minimum number of linear or non-linear reservoirs needed to represent catchment storage-outflow relationship (non-linear will require more than one linear reservoir in the model). ET influence on baseflow reservoirs.
Hillslope	Surface runoff presence / absence, precipitation	Storm event precipitation threshold for surface runoff response	Clear threshold indicates saturation excess surface runoff.	Saturation excess surface runoff included.
Hillslope	Soil moisture, precipitation	Time to decline post storm peak	Fast declines (1-3 days) indicate dominant vertical drainage	Parameterization of drainage from soil reservoir
Hillslope	Soil moisture, precipitation	Peak timing & magnitude at different locations	Delayed and higher peaks downslope compared to upslope indicate lateral subsurface flow.	Inclusion of lateral flow or an interflow reservoir or pathway

Scale	Data types	Analysis	Process interpretation	Model structure decisions affected
Tributary catchment	Tributary streamflow, precipitation	Precipitation threshold for streamflow initiation	Reflects cumulative surface and shallow subsurface processes of land units in tributary catchments.	Maximum combined storage of plateau, hillslope, and canyon floor surface and shallow sub-surface reservoirs.
		…vs. for hillslope surface runoff	Less rain needed than for hillslope surface runoff indicates significant subsurface runoff. More indicates hillslope surface runoff detected below the tributary threshold must infiltrate.	Connectivity and routing of hillslope surface and subsurface to tributary channel flow
		…vs. for catchment streamflow peak	Less rain needed than for catchment flow peaks indicates tributary surface outflows infiltrate on their flow path when below catchment response thresholds. More indicates subsurface flow from tributaries and/or that catchment peaks can come from the floodplain response alone	Connectivity of tributary catchment catena surface and subsurface flows via alluvial fan and floodplain to the catchment outlet
Alluvial aquifer	Groundwater level, precipitation	Groundwater level change following precipitation at different locations	Responsiveness indicates notable recharge through direct infiltration/percolation and/or contributions from tributary catchments. No change indicates net recharge is not significant and/or another water source dominates. Seasonality indicates recharge is notably affected by ET.	Connectivity between alluvial aquifer and tributary catchments and/or mountain block aquifer
Alluvial aquifer	Groundwater level, precipitation	Groundwater rise post-storm compared to maximum direct floodplain infiltration	A rise greatly in excess of that predicted from only potential direct infiltration on the floodplain indicates influx from tributary catchments.	Connectivity between alluvial aquifer and tributary catchments

Scale	Data types	Analysis	Process interpretation	Model structure decisions affected
Alluvial aquifer	Groundwater level, precipitation	Peak timing post-storm at different locations	Delayed peaks at downstream sites indicate subsurface flow connectivity. Similar peak timing indicates direct floodplain surface recharge and/or local tributary catchment sources dominate	Connectivity between alluvial aquifer and tributary catchments
Alluvial aquifer	Groundwater level, precipitation, PET	Groundwater level decline correlation with PET	Responsiveness of the alluvial aquifer water table to PET demand indicates plant roots are able to reach water table	ET withdrawals from the alluvial aquifer
River channel	Streamflow	Time periods when river reaches are gaining or losing flow	A losing stream indicates streamflow infiltration into the alluvial aquifer. A gaining stream could be supplied by the alluvial aquifer, direct mountain bedrock outflow in narrow reaches, and tributary surface flows.	Connectivity between alluvial aquifer and river channel.
Alluvial aquifer - river channel	Groundwater level, river stage	Relative elevation of groundwater and river water surface during baseflow	Groundwater levels above the river surface indicate possible groundwater flow into the channel. The reverse indicates possible channel infiltration.	Lateral connectivity between alluvial aquifer and river channel. Need to explicitly calculate ground and river water elevations.
Alluvial aquifer - river channel	Groundwater level, streamflow	Streamflow correlation with groundwater level during baseflow	Strong correlation indicates likely flow contribution from alluvial aquifer. Correlation only above a threshold indicates aquifer storage level not available to the channel.	Lateral connectivity between alluvial aquifer and river channel. Dead storage in the alluvial aquifer reservoir and threshold of connectivity
Alluvial aquifer	Groundwater level	Longitudinal vs. lateral water table slope	Longitudinal slopes much greater than lateral ones indicates down-valley flows, with longer flow paths dominate.	Travel time through alluvial aquifer to river channel. Need to dynamically calculate groundwater elevations.

Figure 1-3 Mean annual precipitation (MAP) surface from Lynch (2003) and the rainfall gauges used as daily timeseries for interpolation.

Interpolation was done using mean monthly precipitation surfaces. The MAP surface is shown for demonstration. Rainfall gauges from SAWS and ARC.

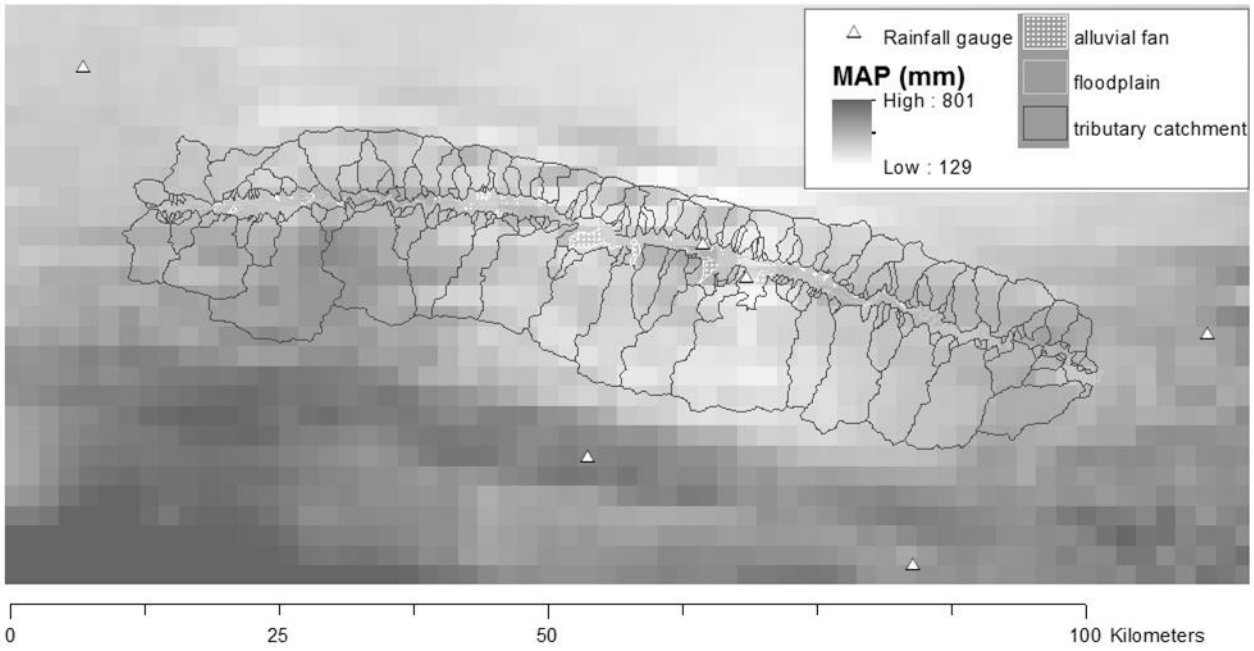

1.3.3.1 Runoff production at catchment and sub-catchment scale

Annual average runoff ratios, storm event quickflow runoff ratios, and thresholds of precipitation to initiate a streamflow peak were calculated from precipitation and streamflow data for the 1,234 km^2 catchment (RH gauge, Figure 1-2) , the 635 km^2 sub-catchment (ZH gauge), and the 9km^2 tributary sub-catchment (GN gauge). Runoff ratios indicate the proportion of precipitation that is not either lost to ET or to groundwater storage not connected to the streamflow at this scale (Clark et al., 2011; McMillan et al., 2011). Storm event quickflow-runoff ratios and a separation of fast and slow changing portions of the hydrograph indicate the relative importance of quick versus slow flow pathways in feeding water to the catchment outlet. The catchment area is dominated by steep hillslopes and cliffs which would promote high runoff ratios during storms, despite the high PET, however vegetation cover, permeable soils and bedrock, and the buffering effects of the fans and floodplains would be expected to reduce these. Large seasonal differences in storm runoff ratios indicate a notable effect of antecedent water storage, affected by ET, on quickflow production. Differences in thresholds and ratios between the catchment sizes could occur due to differences in land type distribution, vegetation cover, and/or scale dependent differences in connectivity thresholds. If less rainfall is needed to create runoff at a smaller scale than a larger one, this indicates infiltration and/or ET losses along flow paths that may need to be modeled if these smaller units are discretized.

To estimate catchment and sub-catchment-wide precipitation, daily gage data from 6 stations were interpolated to their closest topographic region using monthly rainfall distribution surfaces derived by Lynch, 2003 (Figure 1-3). Streamflow data were aggregated

to a daily time-step to correspond to rainfall. Based on visual hydrograph analysis, a flow peak response was defined as starting when streamflow increased by 30% in a 24-hour period and ending when the daily decline in flow during the recession was less than 20%. The rain event quick-response runoff was defined as the sum of runoff during the event above the extrapolated pre and post event baseflows. Rainfall events were defined as starting when the catchment averaged daily rainfall was 1mm or more and ending when the average daily rainfall over the following three days declined below 1mm.

1.3.3.2 Slow flow and flow recession analyses

To estimate the proportion of the streamflow arriving via slower flow paths versus quicker surface and near-surface flow responses to storms, a simple signal processing recursive filter algorithm, described and applied by Hughes et al. (2004), Nathan and McMahon (1990), Smakhtin (2001), and Xu et al. (2009), was applied to the 2012-2013 daily and 1973-2013 monthly flow time-series. This signal filtering technique has no inherent assumptions about hydrologic processes and the user must determine if the outcomes are meaningful. To address this, iterative separation outputs were compared to observed patterns of floodplain groundwater levels to select a separation in which the slow flow portion corresponds to flows passing through the alluvial aquifer. At the Joachimskraal (JK) site, in the middle of a wide floodplain reach, the river water surface elevation and the groundwater table elevations in alluvial aquifer piezometers were both measured continuously at multiple sites using pressure transducers. It was assumed that the greater the elevation of the groundwater table above the river water surface, the more flow in the river

channel would be coming from lateral flows from the alluvial aquifer. Therefore the slow flow portions of different separation attempts for the 2012-2013 streamflow record were also compared to the time-series of height differentials between the groundwater and river water surface.

Flow recession analyses, relating the rate of flow decline to the flow volume and hence to catchment storage, were used to determine if a simple linear reservoir model could be an appropriate representation of outflow from the storages feeding catchment baseflow. Flow recession periods were defined when there were five or more consecutive days without rainfall. For these periods, dQ/dt vs. Q curves (Q being streamflow and t being time) were created using variable length time-steps following the accumulated volume method described by Rupp and Selker (2006). This method smoothes data in low flow periods to account for flow variability approaching measurement accuracy when values are small. A critical accumulated flow volume per time-step of 43,000 m^3 was selected such that a daily average flow of 0.5 m^3/s would give a one day time-step. This value was chosen based on the day to day flow variability in dry periods. Recession curves were plotted as log dQ/dt vs. log Q for recession periods that had with four or more time steps of consistently declining flows. Linear regression of the log-log plots was used to determine the form and explanatory power of the best-fit exponential equation ($dQ/dt = aQ^b$) to describe the recession. If the exponent, b, was found to be 1, the recession could be described by a linear reservoir for which the constant, a, was the recession constant.

1.3.3.3 Runoff production and soil moisture patterns at the hillslope scale

Data from the instrumented hillslope were analyzed to determine the presence of precipitation thresholds to initiate surface runoff. The geology and vegetation type of the site are representative of the catchment's hillslope area: quartzitic sandstone with moderately degraded thicket (Euston-Brown 2006). The site's slope is 28%, somewhat lower than catchment average of 41% (range: 11-90%). Because the surface runoff volumes caught in the Gerlach troughs came from an undefined surface area, volumes were only used for presence-absence of surface flow and relative comparison between storm events. Rainfall data for this assessment came from a weather station at the hillslope site itself. Because of the spatial variability in rainfall across the catchment, responses to specific events on the hillslope were not compared to the catchment event response. However, if a precipitation threshold to initiate surface runoff on the hillslope is much lower than the catchment average precipitation needed to see a peak flow response at the catchment scale, this indicates that hillslope surface runoff is likely to infiltrate along its flow path. This would suggest that either a model structure that routes runoff across land units where it can infiltrate or one that directly estimates net runoff production at a larger scale would be appropriate.

Data from soil moisture probes on the hillslope were examined for patterns that would indicate drainage speed and direction. Probes were positioned on three transects, upslope, midslope, and downslope, spaced roughly 200 m apart (van Luijk et al., 2013). Peaks in soil moisture at different depths and hillslope positions, and the time taken for soil moisture to recede to a relatively constant level after rainfall events, were assessed to look at drainage versus soil moisture retention. Sharp declines in soil moisture over one to two days after

rain events show fast drainage as a dominant process (McMillan et al., 2011). Consistently delayed and larger soil moisture peaks at lower hillslope positions following high rainfall events could indicate lateral subsurface flows moving downslope. Infiltration of surface runoff along its flow path could lead to higher soil moisture peaks at the downslope sites if they are sites of surface flow convergence, but if this was the cause of the higher downslope peak, then the delay in peak timing would be expected to be less than a day.

1.3.3.4 Alluvial aquifer groundwater processes and connectivity

The groundwater level in the floodplain alluvial aquifer and its relationship to rainfall and to water levels in the main river channel were assessed to understand the role of the alluvial aquifer in catchment processes. The intention was to identify dominant pathways of recharge for the alluvial aquifer, when and to what extent the alluvial aquifer contributes to streamflow, and if ET withdrawal from the alluvial aquifer is significant and effects outflow into the river channel. The floodplain aquifer could receive recharge from direct infiltration and percolation of rainfall falling on the floodplain surface, from the surrounding mountain bedrock aquifer, from infiltration of incoming surface flows through river channel beds and overbank flooding, and/or from subsurface flows through alluvium in tributary catchments.

The time-series of groundwater levels at the irrigation pits and piezometers at different locations were compared to rainfall events and PET. If the water table shows no response to a rainfall event, this indicates that direct infiltration and any surface or subsurface flow from tributary catchments were not a major net recharge source in that event. If the water table

does respond and the water table increase represents more water than fell on the floodplain surface, then there must be surface and/or subsurface contributions from the surrounding catchment. The irrigation pits are spread out over 48 km of the valley's longitudinal profile, and so are fed by different sized catchment areas, with some located in the center of the floodplain and some up against the mountain front. Those at the mountain front are closer to both potential hillslope runoff and mountain bedrock subsurface flow sources. The delay in the groundwater level peak after a rainfall event was assessed to indicate the travel time and hence distance of subsurface flows of recharge water reaching the measured site. The change in groundwater level over periods without rainfall was compared to the estimated PET demand for that period. Correlation between PET and the groundwater level decline would indicate ET withdrawals from the alluvial aquifer are notable at the water table depths observed. Much of the floodplain vegetation is dominated by *Acacia karroo* trees, a species known to have root depths of up to 40 m (Selaolo, 1998), so some correlation is expected.

Streamflow and water elevation data indicators were used to look at the relationship between the alluvial aquifer and flow in the main river channel. Streamflow measurements from different points along the river indicated whether a reach was gaining or losing water. Frequent switching between gaining and losing suggests the need to model the aquifer-channel connection dynamically rather than assuming a reach is constantly gaining or constantly losing. A losing reach could be feeding the alluvial aquifer and/or be losing water to evaporation. A gaining reach could be receiving water from the alluvial aquifer and/or channel flows from tributary catchments, however tributary channel flows are infrequent and typically only last days. The floodplain aquifer could feed channel flow if the water

table sits above the channel elevation. The water table slope, the distance over which the gradient exists, and the conductivity of the floodplain material influence the magnitude and timing of this contribution. In this case the material is dominated by sand and cobble deposits with high conductivities and so significant connectivity is expected when there is a gradient toward the channel. The difference between the groundwater and river channel water elevations was determined for different monitored points over time. Both the lateral slope across the floodplain to the adjacent river reach and down-valley longitudinal slopes were assessed. Periods in which the lateral water table slope exceeds the longitudinal slope would be expected to have faster passage of water out of the catchment because the subsurface flow path across the floodplain would be shorter: across, rather than down the floodplain. Groundwater levels were compared to streamflow to determine if any thresholds of connectivity to the alluvial aquifer were reached during the observation period.

1.4 Results

1.4.1 Topographic unit discretization

The topographic discretization showed that the landscape of the 1234 km^2 catchment area is dominated by the hillslopes (40%) and plateaus (29%) while the central valley alluvial fill covers only 5% of the area (Table 1-3). Alluvial fans make up 21% of the alluvial fill area. Not all of the area described as floodplain may still be active floodplain, this area may include abandoned terraces that no longer receiving floods.

Table 1-3 Cover of mapped topographic units in the Baviaanskloof catchment

Landform	Area (km^2)	*Percent of catchment*
Tributary catchments	1,179	*95%*
Plateau	357	*29%*
Hillslope	494	*40%*
Cliff	209	*17%*
Canyon floor	118	*10%*
Central valley alluvial fill	56	*5%*
Floodplain	44	*4%*
Alluvial fan	12	*1%*
Catchment total	1,234	*100%*

1.4.2 Data diagnostics

1.4.2.1 Quick vs. slow flow separation using signal filtering conditioned on groundwater patterns

The pattern of peaks and troughs in the slower portion of the streamflow calculated using the signal filtering algorithm was compared to the pattern of groundwater table fluctuation in the floodplain and to the height difference between the floodplain water table and the river water surface. It was found that a single iteration of the filter algorithm separated a portion of the flow that roughly approximated flows entering the river through the alluvial aquifer. The single iteration appeared to produce a better approximation of the groundwater patterns than the flow separation produced by two or more iterations. It would be expected that peaks in this portion of the streamflow would be close in timing, or slightly delayed, compared to peaks in groundwater levels in the alluvial aquifer. This is seen to be the case both at the Joachimskraal piezometer transects, as shown in Figure 1-4 and Figure 1-5, as well as further upstream where monthly groundwater data from Bookloof and Damsedrif irrigation pits was compared to flow separation at Zaaimanshoek, a site located between these two pits, seen in Figure 1-6. In both cases the portion of flow separated by a single iteration of the filter algorithm better matched the patterns of groundwater levels and slopes toward the river than the portion separated by more iterations.

Additional iterations of the filter algorithm produce a more constant, low flow portion without pronounced peaks which may represent the portion of flow being fed from the mountain bedrock aquifer via the alluvium to the river, rather than quicker flows from

mountain storm runoff infiltrating in the tributary catchments and alluvial fans. This is consistent with the unchanging groundwater levels seen at irrigation pits located right at the mountain front.

Applying this flow separation technique to the 2012-2013 daily data for the outlet of the Baviaanskloof monitored at Rooihoek indicated that as much as 55% of the outflow for this period likely passed through subsurface paths. Because flow peaks are smoothed in monthly data, application of the filter to monthly data produced a separation with only 25% of the flow in the slow flow portion for the same time period. This portion is similar to applying multiple iterations of the filter to the daily data to achieve a relatively constant low flow (22% of total 2012-2013 outflow), the pattern of which may approximate the flow portion that has passed through the mountain block aquifer. Performing the separation on the long-term monthly time-series for the Kouga Dam and that estimated for the Baviaanskloof catchment alone suggests that 20% and 10% of the total flow from these catchments is from this slower flow portion, which likely excludes some of quicker subsurface flows through the alluvium in the weeks following a large storm. In the Baviaanskloof the annual contribution from this slower flow portion ranged from 4 to 44% of the total outflow for a given year.

Figure 1-4 Groundwater and river surface water elevation fluctuation measured at the lower Joachimskraal (JK) transect compared to slow flow portions of streamflow at the site calculated with iterations of a signal filtering algorithm.

Elevations recorded with pressure transducers (solid lines, groundwater at JD-2 and river surface at JD-R) and manually monitored piezometers (points, JD 1, JD4-5)

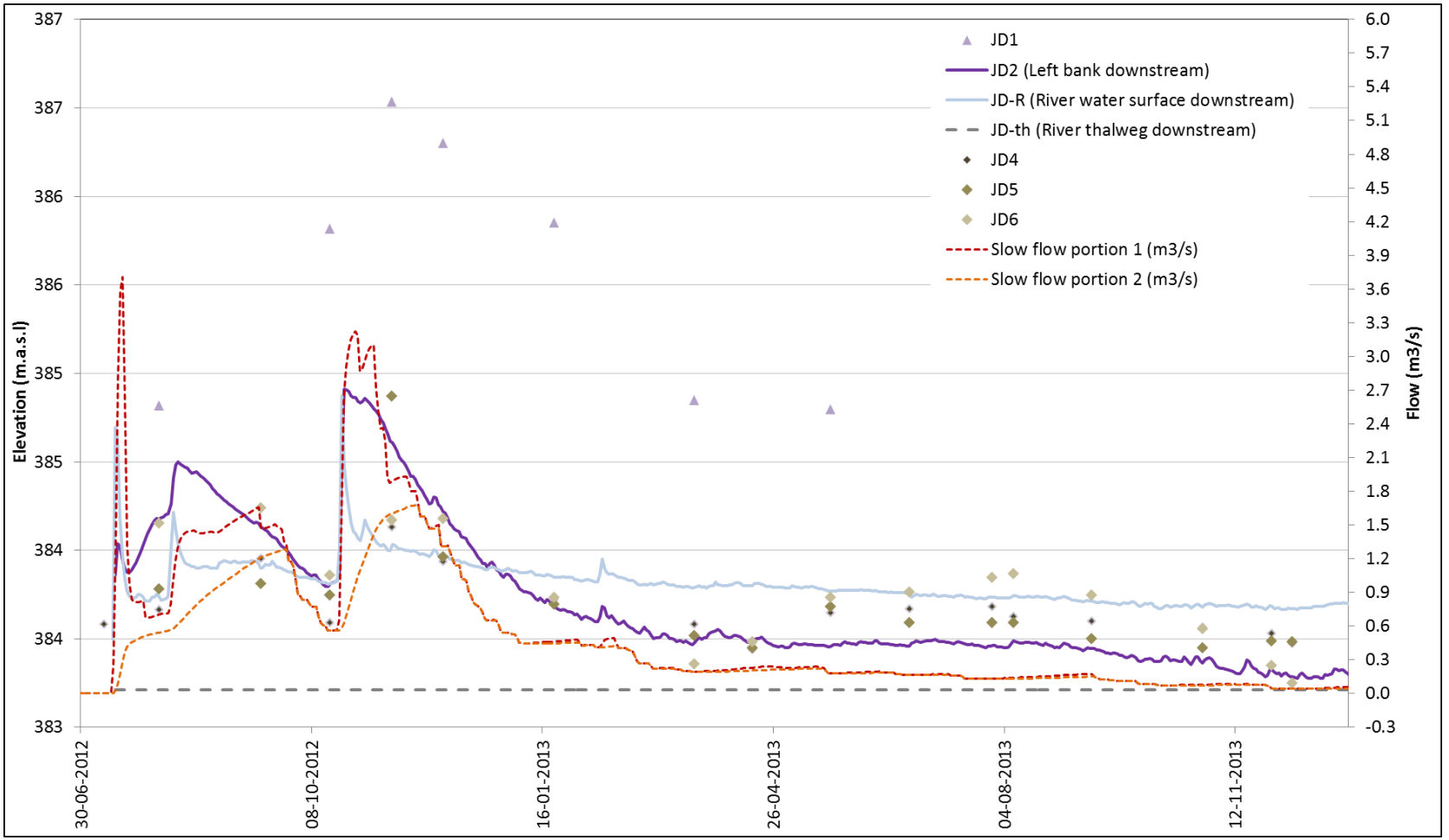

Figure 1-5 Height of groundwater table at piezometer JD2 above the adjacent river water surface compared to slow flow portions of JK streamflow calculated with iterations of a signal filtering algorithm

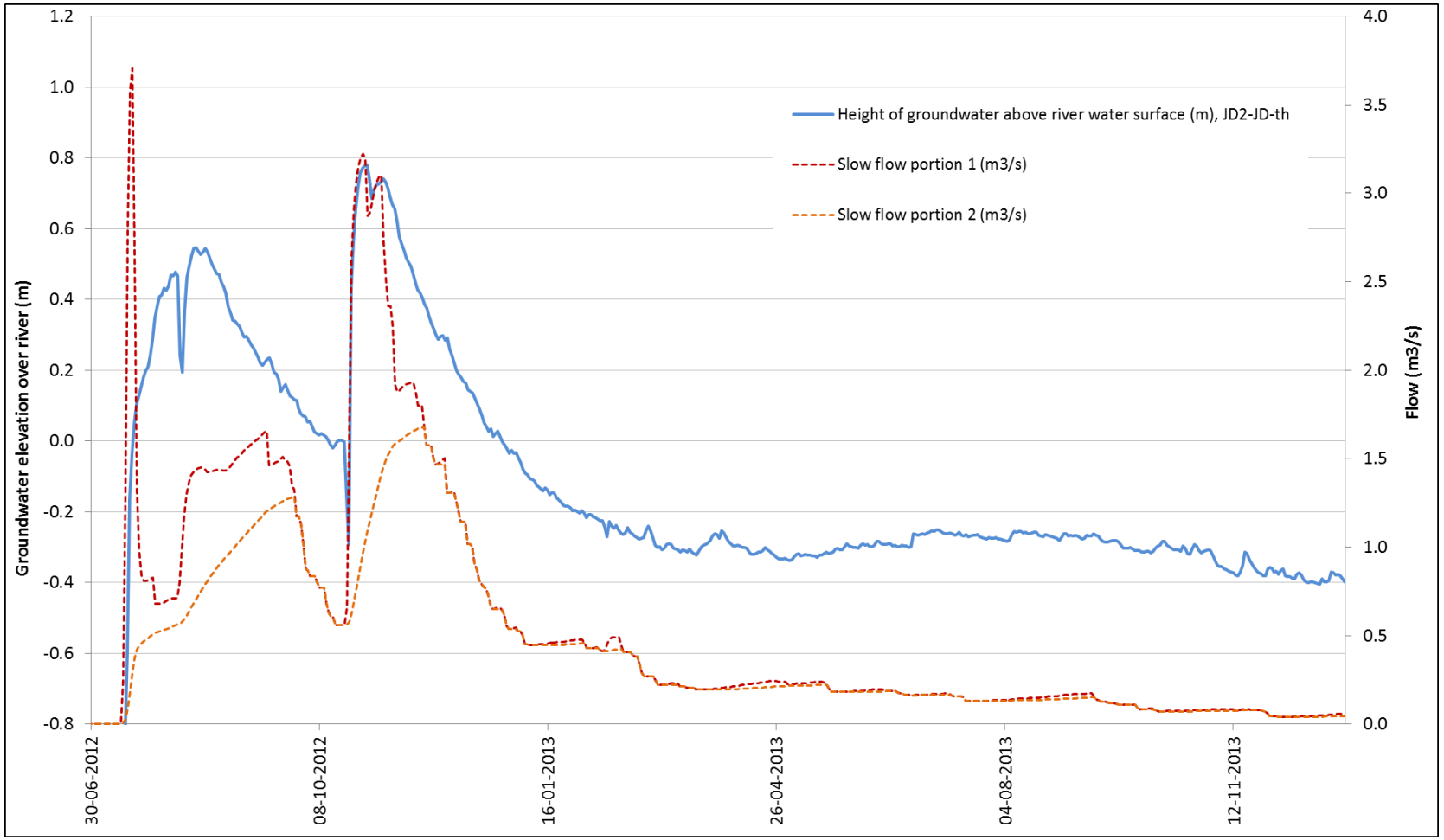

Figure 1-6 Fluctuation in groundwater levels at highly responsive pit sites (BK and DD) and slow flow portions of monthly streamflow data at ZH, separated using iterations of a signal filtering algorithm

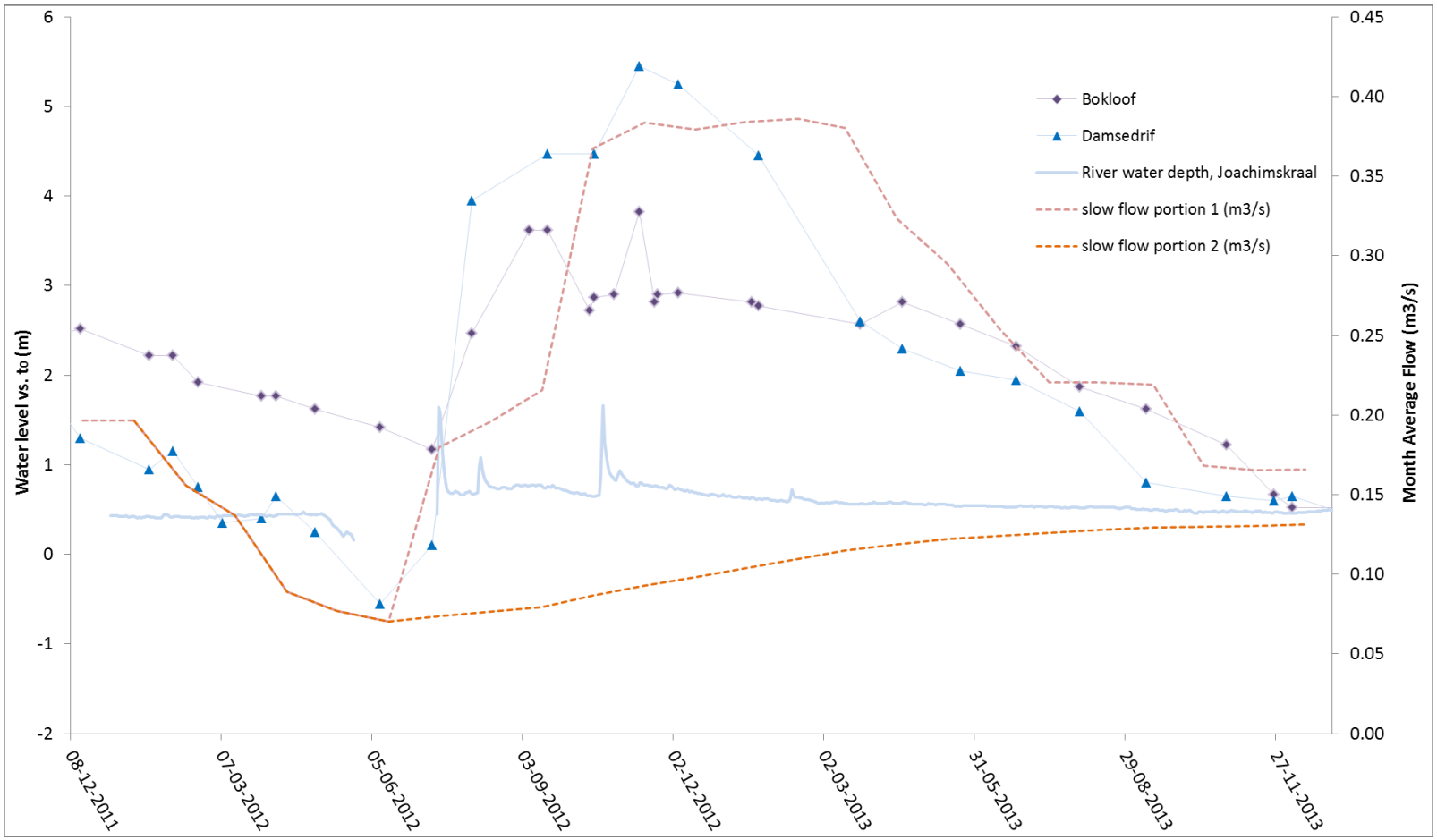

1.4.2.2 Catchment runoff ratios and event quickflow runoff ratios

The annual average precipitation in the Baviaanskloof was 270 mm for the period from 1972 to 2013 and 350 mm for 2012-2013. The estimated average annual runoff ratio for the 1,234 km^2 catchment was 7% for 1972-2013 and 11% for 2012-2013. This indicates over 90% of precipitation, on average, leaves as ET and/or enters groundwater stores not connected to the stream. There was a large inter-annual variation in annual runoff ratios: values ranged from 1-33%. High ratios occurred in years with wet winter and spring months in particular, suggesting that seasonal ET variation plays a significant role in determining overall runoff production. This pattern was consistent in the 2012-2013 dataset: winter and spring flow responses to rainfall were greater than in summer and fall for events of similar precipitation, as described below.

Application of the signal processing filter indicated that, of streamflow leaving the catchment in 2012-2013, 57% of the water came via slow flow pathways that had similar flow fluctuations to the patterns of fluctuation observed in the alluvial aquifer groundwater levels. Applying an 11% runoff ratio, roughly 6% of the precipitation received left the catchment via slow-flow runoff paths and 5% as faster flows. Daily average streamflow was highly variable, from 0.13 to 106 m^3/s, with a mean of 1.8 m^3/s. Of this, the daily flow from the slow pathways ranged from 0.13 to 8.9 m^3/s with a mean of 0.88 m^3/s. When applying the separation filter to monthly data, peaks in subsurface flows occurring at scales of weeks to months are lumped into the faster flow portion. The filter results from the 1972-2013 monthly data therefore reflect even slower flow pathways, such as those sourced from mountain bedrock and/or more distant parts of the catchment. These flows represented 10%

of catchment outflows on average over the long term, with annual proportions ranging from 4 to 44%. Annual average flow ranged from 0.06 to 3.3 m^3/s over these 42 years, while annual average flow from the filtered slow flow pathways ranged from 0.01 to 0.42 m^3/s. For 2012-2013 this even slower slow-flow portion was 25% of the total outflow with flows ranging from 0.13 to 0.76 m^3/s. These results show that baseflow contributions can be high and can vary significantly compared to the total annual average flow over relevant time-scales.

In 2012-2013, 41 rainfall events were recorded, 19 of which coincided with discernable flow peaks (Figure 1-7). Over 23% of the rainfall in these years fell in two major events in the winter and spring of 2012. These events had 71 mm and 81 mm total rainfall, 52 mm and 40 mm occurring in a 24-hour period, and resulted in peaks in the daily average flow of 79 m^3/s and 106 m^3/s, estimated to be 6 and 8-year return flood magnitudes. For 1-2 days during these events, river water surface elevations were 0.5-0.8 m above the surveyed banks at gauged sites, indicating overbank flooding can occur with at least a 6 year frequency. Event quickflow runoff ratios over 1% were only seen for six events: the two large flood events and smaller (8-24 mm) events occurring in weeks following them (Figure 1-7). During the large flood events, 16% and 21% of the precipitation appeared as quickflow runoff, meaning the remainder must have come as baseflow, been stored as groundwater, and/or been lost to ET. These events were followed by several months of elevated baseflow: in winter 2012, prior to the large storms, there was a relatively steady baseflow of 0.18-0.20 m^3/s, whereas in the winter of 2013, a year after the large floods, baseflows were 0.32-0.35 m^3/s.

Thresholds of precipitation needed to produce a flow peak at the catchment outlet varied and effects of antecedent conditions, storm intensity, and season were evident. The smallest event associated with a runoff peak had 5 mm catchment averaged rainfall, whereas the largest event to not produce any peak was 23 mm. In the dry conditions preceding the 2012 floods and in late 2013, a year after the floods, summer rainfall events of up to 20 mm in 24 hours and winter events of up to 10 mm did not produce peaks. This indicates that in dry conditions interception, detention storage, and soil storage can hold up to 20 mm. Given wetter antecedent conditions, likely prolonged due to low winter ET, rainfall events of 5-20 mm occurring within weeks of the major flood events did result in notable flow peaks with runoff ratios of 1-12%. After this period, events with similar rainfall had much lower quick-flow ratios. For roughly 6 months after the floods, discernible flow peaks were observed at the catchment outlet following rain events of under 10 mm per day, event sizes that did not produce peaks in the pre-flood period or later in the recession. This indicates that storages that impact production of quickflow runoff can take weeks to months to drain.

Increased streamflow responsiveness to small rainfall events in the post-flood period could have several explanations. Retained soil moisture could mean storage thresholds for runoff production are met with less rainfall. High PET makes this unlikely to persist into warmer seasons. Significant recharge of groundwater stores during the floods could result in greater outflow responsiveness to any additional recharge, depending on storage-outflow relationships. If alluvial aquifer groundwater elevations are close to river channel elevations, additional recharge bringing the water table above channel would be expected to

increase outflows. It is also possible that some of the minor catchment outflow peaks in the post-flood period reflect decreases in ET being withdrawn from more continuous subsurface flow along its path to the catchment outlet. If the groundwater feeding the prolonged elevated baseflows in the post flood period is more accessible for ET than groundwater was prior to the 2012 floods, then the decline in PET demand around rainfall events could increase net outflows and cause flow peaks that would not occur for similar PET dips in lower baseflow periods. Peaks were seen at the catchment outlet within 2 days of the rain event, so if this was the case, the ET affected pathway either has significant flows close to the outlet and/or has a high enough flow rate for this response timing. There was also more continuous surface flow along the length of the main river channel in the post-flood elevated baseflow period, whereas prior to the floods more channel reaches were dry and alluvial aquifer levels low. In the post-flood period more of the rain falling directly on the channel would remain as channel surface flow rather than infiltrating through the channel bed in dry reaches and/or reaches where the alluvial aquifer water table lies below the river channel.

Figure 1-7 Rainfall, PET, runoff, and event quickflow runoff ratio for the Baviaanskloof catchment 2012-2013

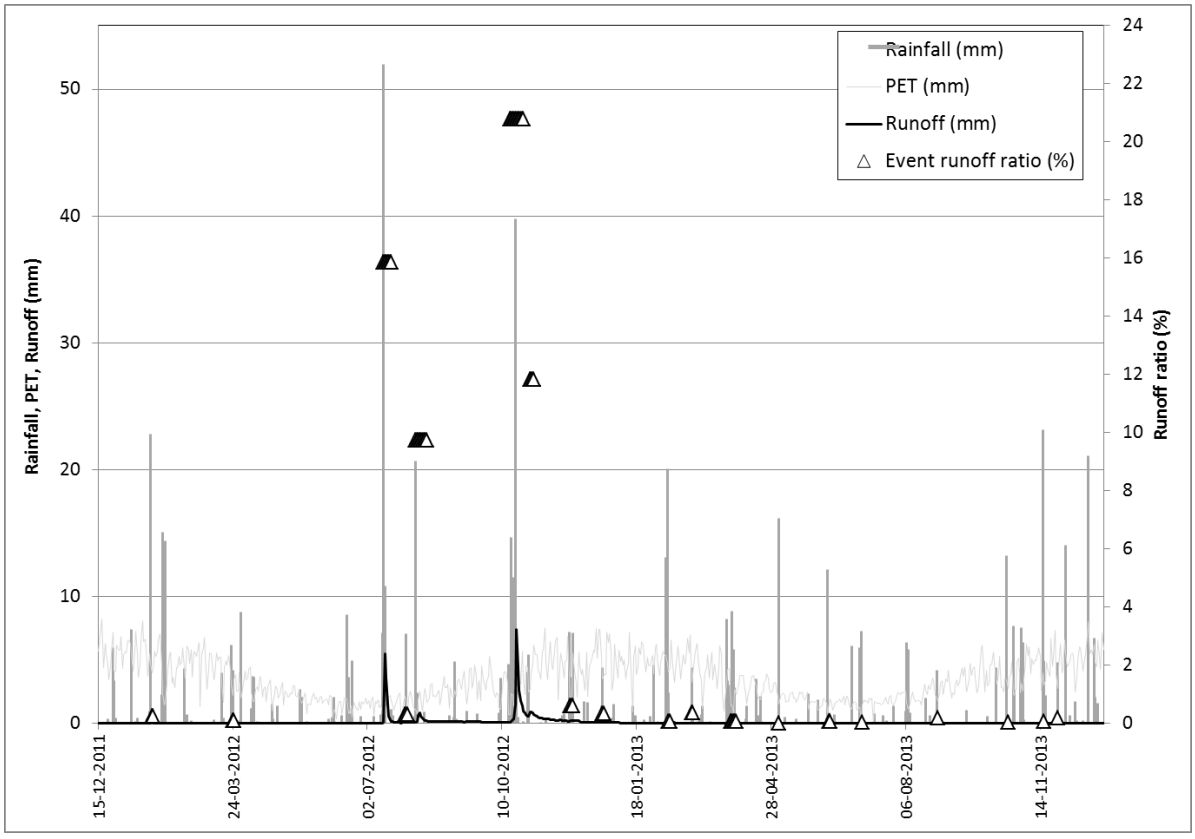

1.4.2.3 Sub-catchment scale runoff ratios and event quickflow runoff ratios

Runoff ratios differed somewhat between the 1234 km^2 catchment and the 635 km^2 sub-catchment. The overall 2012-2013 runoff ratio of the sub-catchment was 12%, close to the 11% in the larger catchment. The total runoff for both was roughly 80 mm, but total estimated precipitation was lower in the sub-catchment (664 mm vs. 710 mm). All rainfall events detected at the catchment scale met the event criteria in the sub-catchment; however, fewer events had associated streamflow peaks at this scale, eight as opposed to nineteen, due to lower responsiveness to small rainfall events in drier periods. For only five of the eleven events with flow peaks at the larger catchment but no peaks at the sub-catchment was the estimated event rainfall less in the sub-catchment; however, the low gauge density reduced the spatial rainfall estimate accuracy. The lowest rainfall event associated with a peak in sub-catchment flow was 8 mm whereas the largest event to produce no flow was 20 mm.

Patterns of quickflow runoff production during the two major floods differed with catchment scale. During the first heavy rainfall event, 15/07/2012, more runoff and a higher quickflow runoff ratio was seen at the outlet of the 635 km^2 sub-catchment compared to the 1,234 km^2 catchment: 16 mm of runoff, with a quickflow runoff ratio of 21%, in the sub-catchment compared to 11 mm and 16% in the larger catchment. This pattern was reversed in the second large event, 20/10/2012, in which the larger catchment had more runoff and a higher ratio: 17mm and 21% quickflow runoff for the large catchment versus 11 mm and 13% in the sub-catchment. In the smaller rainfall events in weeks following the major floods, the sub-catchment had lower runoff ratio than the larger catchment.

Possible explanations for differences in runoff could be differences in rainfall between the two catchments, in the distribution of land units, and/or scale-related runoff connectivity thresholds. The proportion of different land units is similar between the two catchments as was estimated event rainfall, although distribution data is limited. There was a significant difference in the antecedent groundwater level in the alluvial aquifer and surface flow connectivity between the two major storms. Prior to the first event, the main river channel through the wide floodplain reaches was dry and the alluvial aquifer groundwater level was low. When the second storm occurred, groundwater levels were higher and there was continuous surface flow along the main river channel. In the first event, some runoff leaving the sub-catchment would have infiltrated downstream, feeding the alluvial aquifer in the larger catchment. In the second event, a greater proportion of runoff produced in the sub-catchment would have been conveyed as surface flow to the larger catchment outlet. Between the storms, the upper sub-catchment would be expected to become drier earlier as surface and subsurface flows move down the catchment. This is consistent with earlier declines in water tables higher up in the catchment described below. Drier antecedent conditions in the alluvial aquifer could contribute to lower runoff ratios in the sub-catchment in the later storms.

1.4.2.4 Streamflow recession analysis

Recession analyses did not show a single linear relationship between flow and catchment storage at the 635 or the 1,234 km^2 catchment scale (Figure 1-8). Sixteen recession events meeting the criteria described were assessed. Flow-storage relationships differed with season

and with the change in antecedent catchment wetness seen before and after the 2012 flood events. Relationships between dQ/dt and Q for events were generally non-linear: best-fit values for the exponent, b, were all greater than one. Recessions after winter high flow events were closer to being linear with b values of 1.1-1.5 (R^2=0.9), while those in spring had a b value of 2 (R^2=0.8). Low flow events in drier periods were non-linear, with exponents of 3 or above, and weak relationships between recession and flow (R^2<0.5). The weak relationship during low flows indicates that factors other than storage, such as ET or thresholds of drainage in contributing reservoirs, play larger roles in determining recession rates in these conditions. If a linear fit was applied to the more linear sections of high flow recession periods, the values for the constant, a, indicated drainage constants in the range of 3-4 days after the winter flood flows and 13-15 days for the tail end of the recession and those occurring in spring and summer. This could indicate dominance of drainage from different storages, such as surface and near-surface and subsurface flows.

The non-linear recession patterns indicate that a single linear reservoir would not be sufficient to reproduce baseflows. The seasonal variation in the storage-discharge relationships and their shapes, approaching linear at some flows with increasingly non-linear tails, also indicate a single non-linear reservoir would not be appropriate. Clark et al. (2009, 2011) and McMillan et al. (2011) succeeded in reproducing similar recession patterns using multiple linear and threshold-controlled reservoirs with different outflow rate constants.

Figure 1-8 Log-log plot of change in flow (dQ/dt) versus average time-step flow (Q) at the catchment outlet 2012-2013.

Different symbols represent separate recessions following different high flow events.

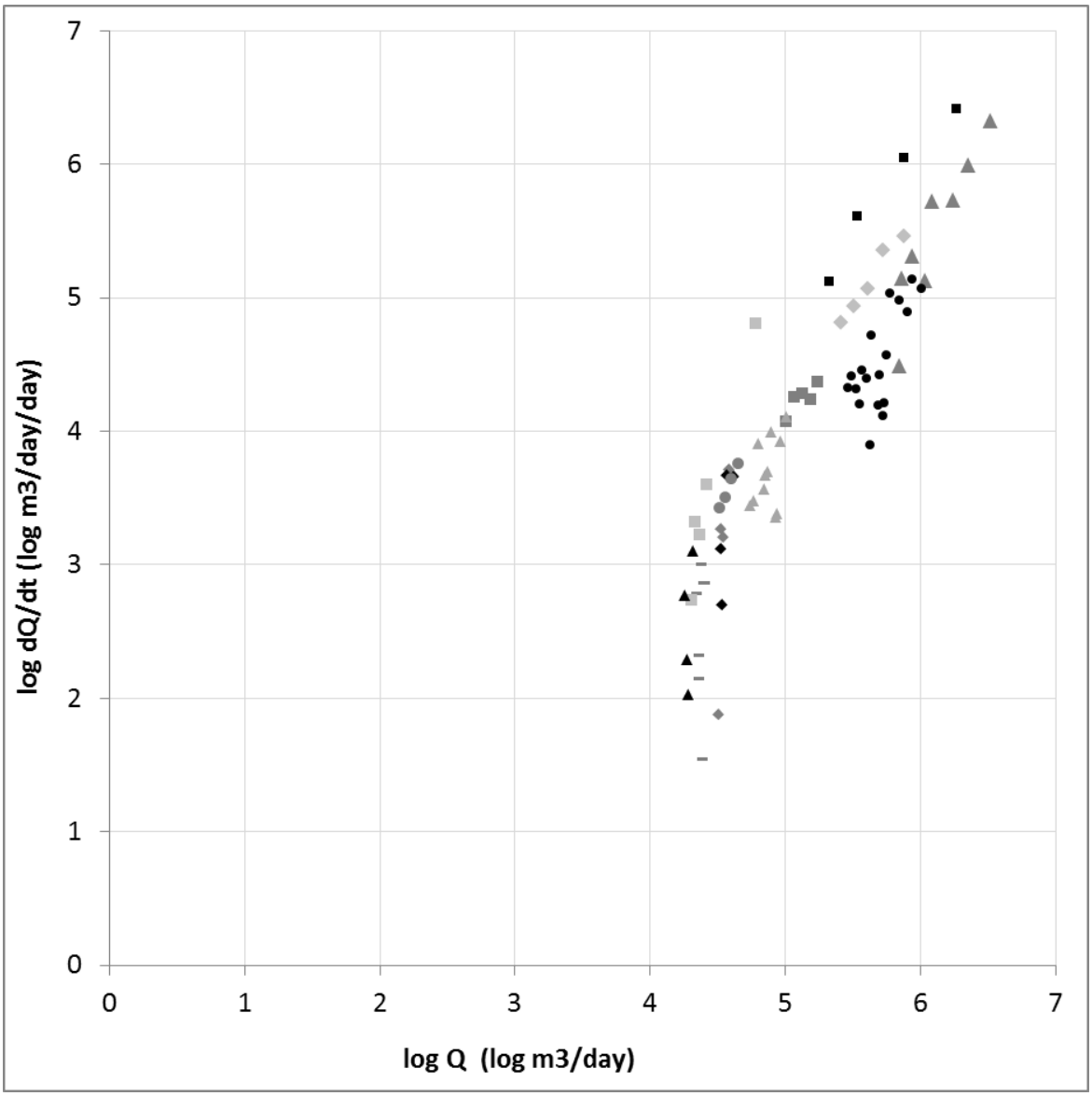

1.4.2.5 Hillslope surface runoff

The relationship between rainfall and the quantity of surface runoff caught in the troughs on the sampled hillslope of van Luijk et al. (2013) varied with event intensity and antecedent conditions. Surface runoff was only found following rainfall events with over 5 mm in 24 hours. In hot, dry periods such as the summers of 2010 and 2011, events over 5 mm did not show evidence of surface runoff. Surface runoff was always detected for events with over 15 mm of rainfall (Figure 1-9). If this hillslope is representative, the observed trends indicate that the model should include a maximum storage for hillslope interception and soils close to 15 mm, and/or the maximum infiltration rate should be in this range, and antecedent soil moisture needs to be considered in determining infiltration. Soil depths on the hillslopes ranged from 100-600 mm, with a capacity between wilting point and saturation of 20-30%, and estimated conductivities of 30-60 mm/hr, which would indicate that more than 15 mm of rainfall would be needed to initiate surface runoff in a dry period. These values take into account the volumetric rock content of the soils; however, the rock cover on the surface of the soil was 30% on average, meaning that the surface infiltration capacity at the scale of the hillslope may be far less than estimated from point soil pit sample properties.

In dry summers, even rainfall events of 20 mm did not produce runoff peaks at the catchment scale, although this magnitude of event always produced surface runoff at the hillslope scale. Surface runoff produced on the hillslopes can re-infiltrate on the toeslope, the alluvial fan, the floodplain, such that thresholds of catchment quickflow runoff need not be the same as the hillslope. This suggests that modeled hillslope runoff should be routed

over other land units in series in the model rather than having land unit runoff connected to the channel in series and/or bed infiltration from channels should be considered in the model.

Figure 1-9 Event rainfall and runoff collected in Gerlach troughs on sample hillslope

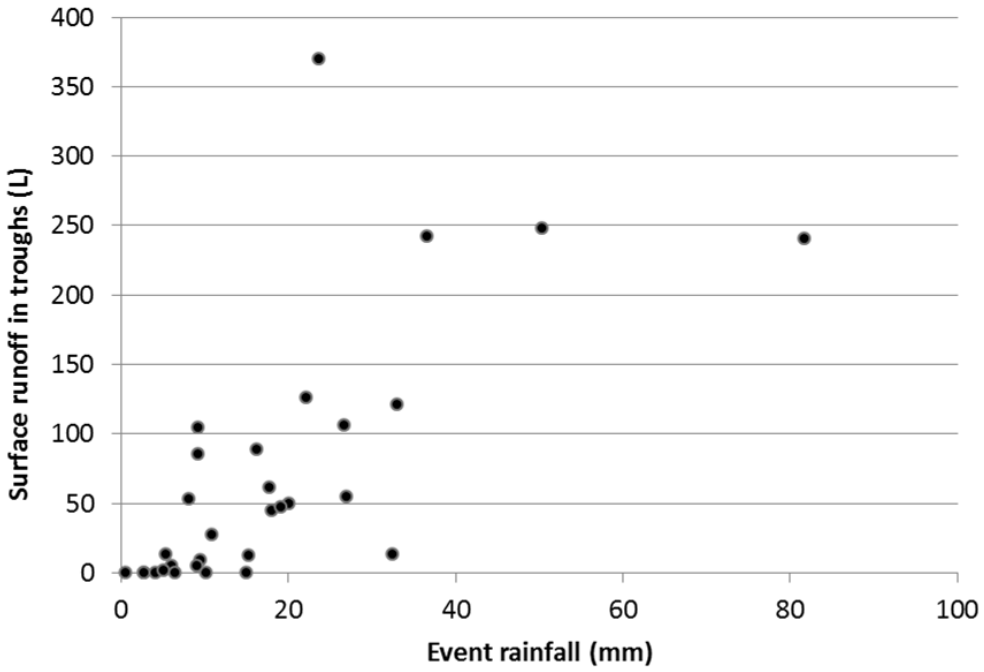

1.4.2.6 Hillslope soil moisture

Similar to the surface runoff, peaks in soil moisture were always present in the top soil layer (0-300 mm) following rain events of over 15 mm, while peaks were sometimes present for smaller events depending on the season and antecedent conditions. Increases in soil moisture by over 5% were only seen following rain events over 7 mm. Soil moisture peaks in the top 300 mm did not start reaching saturation until total event rainfall reached approximately 60 mm. This is consistent with soil properties indicating differences between field capacity and saturation and between wilting point and saturation of 15-20% and 20-25%.

Soil moisture peaked within a day of the maximum event rainfall in the top layers, but soil moisture showed less variability and slower change in the lower layer (300-600 mm) which could peak multiple days after the event. In the top layer, the decline of moisture after wetting up generally occurred relatively fast: moisture decreasing by 5-8%, constituting 10-30% of the peak, per day over the first two to three days after rain. This indicates a significant portion of the infiltrated water drains quickly. However, it could take up to two weeks to reach a relatively stable level at which moisture changed by 2% or less per day. Soil moisture was higher in the lower layer than in the upper except during post-storm peaks. That lower layer moisture declined much less than the upper during warm dry periods indicates that the lower layer is less accessible to ET.

The multi-day delay in the moisture peak in the lower layer could indicate the time needed for vertical percolation, but could also indicate time to concentration of water

draining laterally downslope, potentially at the soil-rock interface. Estimated soil conductivity, 30-60 mm/hr based on texture and infiltrometer measurements, suggests that vertical drainage of water over field capacity though the thin soil profile could occur in less than a day. The hypothesis of lateral flow, which would accumulate vertical recharge moving downslope, feeding soil moisture peaks in the lower soil layer is supported by the observation that the lower layer of the downslope site showed bigger and more delayed peaks than the upslope sites (Figure 1-10). The downslope site was at the toe of steeper slope, having a lower grade than the upper sites, and so could be expected to collect water. A bulge in soil moisture maintained in the lower layer of the downslope site over two weeks after the major storm on 20/10/2012 was not seen upslope. Soil moisture and peaks at the upslope site were lower than at the downslope. For the upper layer, this potentially indicates less infiltration and/or more drainage upslope and/or infiltration of surface runoff at the downslope site. For the lower regolith layer, this further supports hypothesized lateral interflow.

Figure 1-10 Soil moisture at different positions and soil depths and daily rainfall on the sample hillslope

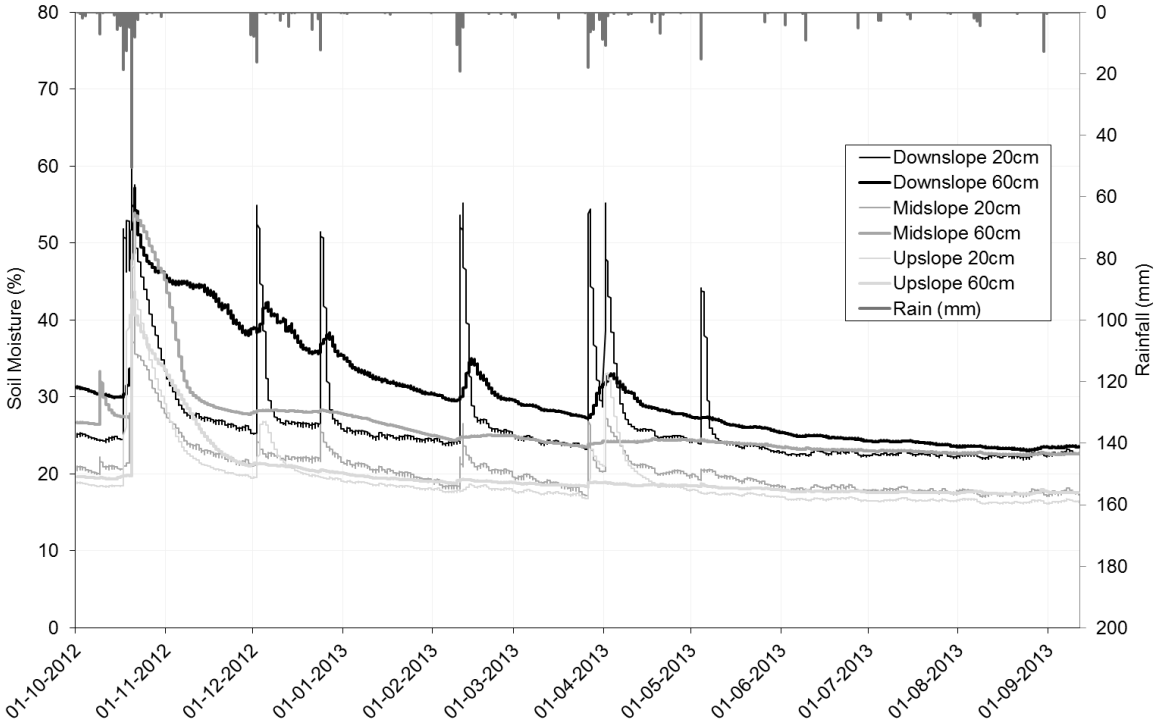

1.4.2.7 Tributary sub-catchment scale runoff

At the instrumented 9 km^2 tributary sub-catchment, channel flow only reached the canyon mouth during the second flood event of 2012. Flows started the same day as the maximum rainfall intensity (40 mm in 24hrs) and continued for 6 days. There is no rain gauge in the mountains of this sub-catchment and the interpolated quantity of rainfall received by this small area during a particular event is more uncertain than averages at the larger scales. However, the quickflow runoff ratio for the event was estimated to be 80-90%, making the overall surface runoff ratio for the 2012-2013 period 12-14%. The instrumented tributary is located in the Baviaanskloof Mountains north of the floodplain. Other tributaries coming from the Kouga Mountains to the south did have channel flows during the first flood event of 2012, presumably due to the spatial distribution of rainfall and potentially the size and landform properties of sub-catchments on the different sides. Tributary sub-catchments did not produce channel outflow in any of the smaller rain events in the observation period, with event totals of 4 to 43 mm with 4 to 23 mm in 24hrs, and catchment residents farming adjacent to these tributaries estimated local rainfall events in the range of 30-50 mm in 24 hours are needed to initiate flows (Powell, 2015). These observations indicate that more precipitation is needed to produce surface flows at the tributary catchment outlet than was observed to produce hillslope surface runoff and a runoff peak response at the catchment outlet.

The vast majority of the 1,234 km^2 catchment area is comprised of tributary sub-catchments. The fact that the larger catchment showed a runoff response to smaller events which produced no surface flow responses in the tributaries can indicate that the large

catchment flow responses to smaller events are a result of processes occurring on the floodplain alone and/or that subsurface flows leaving the tributary catchment areas feed surface runoff at the catchment outlet. Runoff from the hillslopes in the tributary catchments can infiltrate into the alluvium of the canyon floors and alluvial fans at the valley mouth. Some of this water may reach the floodplain aquifer and feed streamflow in the main river without production of surface flows from the tributaries. Evidence of this is seen in alluvial aquifer groundwater level rising in excess of maximum likely direct floodplain infiltration following smaller rainfall events, as described below.

1.4.2.8 Alluvial aquifer water table fluctuation

The alluvial aquifer response to rainfall varied with season, antecedent conditions, and location. Based on their water table fluctuation patterns, monitored sites were classed into three groups: highly responsive, slow responsive, and unresponsive (Figure 1-11). The two sites with groundwater pits in wide floodplain reaches (VR and DD), were 'highly responsive': water tables fluctuated by 4-6 m during 2011-2013, rising sharply following large rainfall events and falling significantly in dry periods (Table 1-4, Figure 1-11). Continuous data from instrumented piezometers in the wide JK floodplain showed a similarly responsive pattern with a smaller, 2 m, amplitude. Piezometers also showed small rises (5-10 cm) following smaller rainfall events (19-36 mm: 29/11/12, 10/2/2013, 17/11/2013) that could not be detected at the resolution of the pit data. The BK site, located at the end of a wide valley at the mouth of a narrow reach, had a dampened responsive pattern, falling in between the highly and the slow responsive sites. The ZH and TN sites,

located at mountain fronts further downstream in the catchment, were considered 'slow responsive'. Water levels rose by 3-4 m during 2011 and by 1 m in 2012 at these locations, but the response was dampened, having a much slower decline in dry periods compared to the highly responsive sites. The 'unresponsive' sites, JK and LG, were also located at mountain fronts, but water levels fluctuated by less than a meter over the observation period. The instrumented piezometer in the JK wetland similarly showed minimal response to rainfall. Water at these two sites was tinted red by oxidized iron, not observed at the other sites, likely indicating they receive mountain bedrock groundwater from iron-rich lithologic layers common to TMG formations (Xu et al., 2009).

Table 1-4 Monitored groundwater pit site descriptions

Site name	Location type	Water color	Catchment area (km^2)	Floodplain surface elevation (m.a.s.l)	Pit depth (m)	Pit depth below river thalweg (m)	Distance to river channel (m)
Veloren Rivier (VR)	Floodplain, wide valley	clear	362	670	7.6	4.8	135
Bokloof (BK)	Mountain front, narrow valley	clear	450	620	10.8	4.3	42
Damsedrif (DD)	Floodplain, wide valley	clear	692	475	9.4	7.6	529
Joachimskraal (JK)	Mountain front, wide valley	red	866	411	3.7	0.03	425
Zandflakte (ZF)	Mountain front, wide valley	clear	931	379	6.1	3.9	150
Tuin (TN)	Mountain front, narrow valley	clear	988	362	3.2	1.6	82
Landsegat (LG)	Mountain front, narrow valley	red	1,023	336	4.2	2.7	177

Figure 1-11 Water level measurements in groundwater pits, continuous water level data from piezometer pressure traducers, rainfall, and PET, 2011-2013

Highly responsive sites shown in blues, slow responsive sites in greens, and unresponsive sites in red and purple

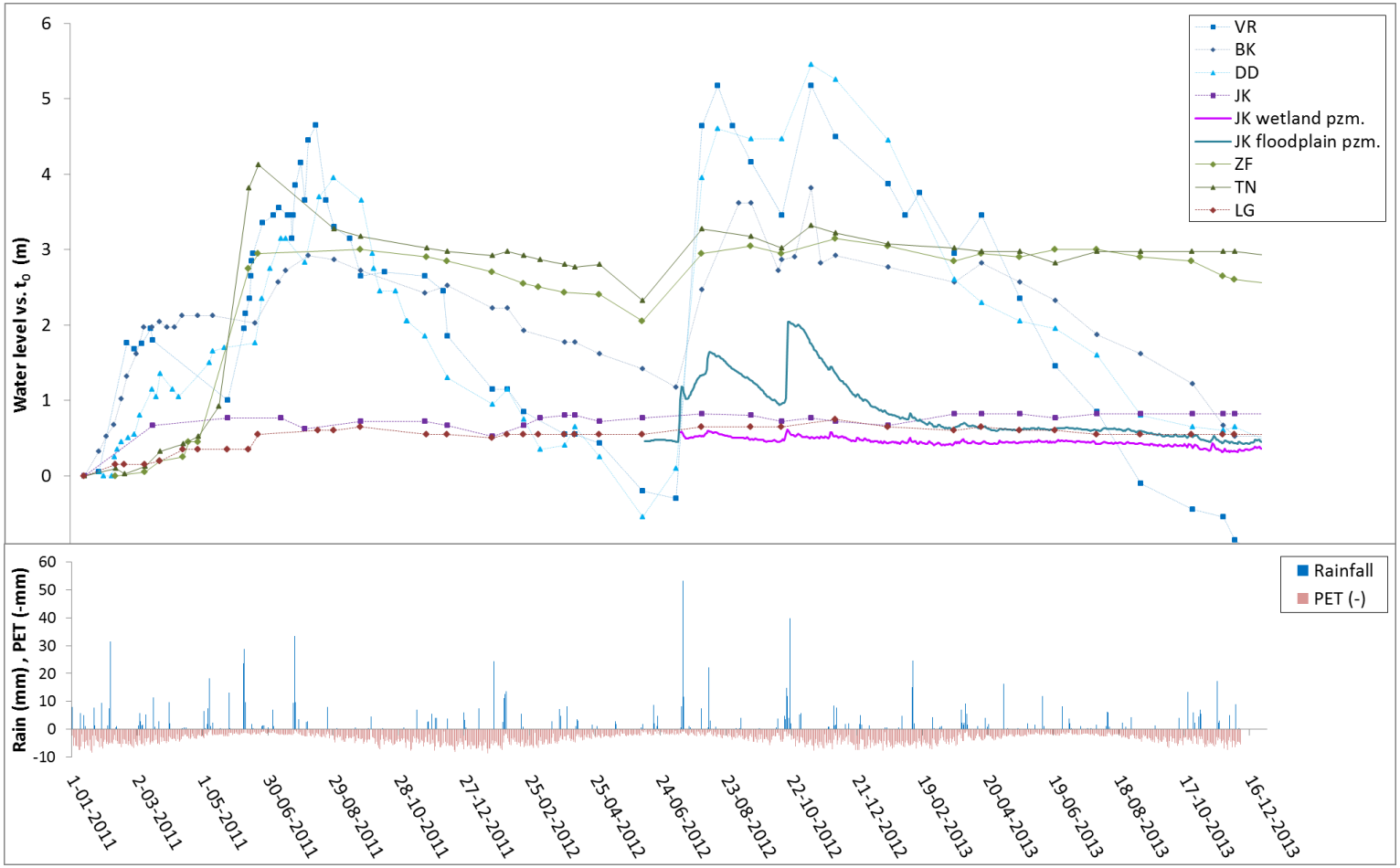

The observation period was preceded by a prolonged dry period (2007-2010) during which high rainfall events fell primarily in warmer months resulting in little runoff and low groundwater levels. A series of closely timed rain events in the summer of 2011 (78 mm over 30 days, including a 40 mm event), was followed by a slow rise in the water table by 1-2 m at the highly responsive sites, peaking 2-4 weeks after the rainy period (Figure 1-11). Two large multi-day storms (62 mm and 53 mm) in the winter of 2011 each resulted in additional rises of 1-2 m. These were followed by a steep recession in spring and summer. In contrast to the response to storms in wet and winter conditions, a 24 mm and a 40 mm storm over two weeks in mid-summer 2012 was followed by a minimal 0.2 m rise. Within nine months of the 2011 winter peak, the water tables at the highly responsive sites had receded back to the level seen at the beginning of the observation period. The larger storms in the winter of 2012 resulted in a 4-6 m rise at the responsive sites which again receded back to pre-storm levels within 10-12 months. Water tables at the slow responding sites rose after the winter storms of 2011 and 2012, but declined more slowly afterwards and did not recede back to pre-storm levels during the observation period.

The magnitudes of the water table responses indicate that the alluvial aquifer is recharged by flows originating elsewhere in the catchment in addition to any direct recharge from the floodplain surface. If the alluvial aquifer was only recharged by rainfall on its surface, to see a rise in the water table of 5 m following a 74 mm rainfall, seen at the VR site following the 14/7/2012 event, the specific yield of the alluvial material would have to be under 0.015. This maximum value was estimated assuming 100% of the precipitation goes into recharge, which would not be the case. For the1.3 m rise observed at the JK piezometer,

the value would have to be under 0.06. These values are well below what would be expected from a sand and cobble aquifer. If it is assumed that the specific yield of the alluvial material is 0.1-0.2, then 10-40% of the 74 mm of rain falling on the catchment area of the site would need to recharge the alluvial aquifer to a result in a water table rise of 5 m over the floodplain area down to VR and a 1.3 m rise for the floodplain area down to JK. This is also likely true for the smaller rainfall events observed to cause water tables to rise at the JK floodplain: more than 19-36 mm of rain would be needed for a 50-100 mm rise in the water table from direct infiltration on the floodplain surface alone, once interception and soil storage are taken into account, although proportionately less additional subsurface flow from the tributary catchments would be needed to make up the difference.

Water tables peaked days to weeks after major rainfall events. Due to the low temporal resolution of the pit gauge data, the date of a peak cannot be determined, nor can short lived responses to smaller events. If the peak is assumed to have occurred within the time interval surrounding the highest water level recorded, peaks generally occurred at the highly responsive pit sites at least two weeks after a major storm, potentially being delayed as much as four weeks. The continuous data at the JK piezometers in 2012 indicated a faster initial rise in groundwater levels, peaking within two days of the first winter storm (14/7/2012) and immediately starting recede (Figure 1-11). This could be due to direct infiltration and infiltration of surface flow from the tributary catchments. However, without further rainfall, this initial peak was followed by a second, slower rise reaching a higher level and appearing to peak and plateau 17 days after this storm, more consistent with trends in the pit data. This is indicative of subsurface flows from the tributary catchments which

would be expected to have longer travel times. Water table peaks were then reached at this site within two to four days of the 7/8/2012 and 20/10/2012 storms, which occurred with higher antecedent groundwater and river level conditions facilitating more surface flow. If there was a greater time to peak at downvalley sites, it was not detectable at the resolution of the pit data except during winter 2011 in which site DD may have peaked 3 days to 3 weeks after site VR. The slower and less

When water tables were receding, the decline in the water table at the JK piezometers over periods without rainfall showed medium correlation with the estimated PET for the time interval (slope=2 mm/mm, R^2=0.5, Figure 1-12). This trend was also seen at the responsive groundwater pits with higher correlations and steeper declines with PET (slopes 5-27 mm/mm, , R^2 0.6-0.9), although there were too few time intervals with receding water tables and no rainfall for the trends to be significant. This indicates that the alluvial aquifer is affected by ET. The range in declines per unit PET would reflect differences in local sediment properties and specific yield, vegetation cover root depth and density (AET vs. PET), and other water flows in and out of the site from downvalley alluvial aquifer flow and tributary catchment and mountain bedrock in puts.

Figure 1-12 Decline in water table compared to estimated PET at responsive pit and piezometer sites for time periods with receding water tables and no rainfall

Linear regression best fit functions shown as dotted lines

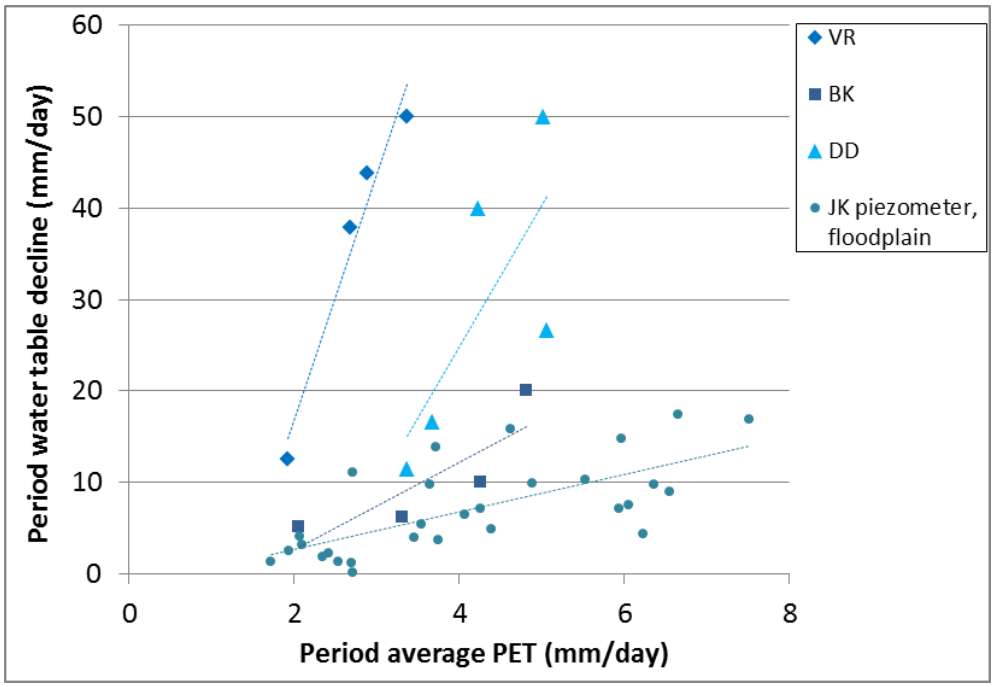

1.4.2.9 Alluvial aquifer – floodplain channel connectivity

Daily average flow at the 1,234 km^2 catchment outlet (RH) ranged from 0.13 to 106 m^3/s with a mean of 1.5 m^3/s. At the most upstream gaged site (ZH), located in a perennially flowing narrow reach fed by a 635 km^2 catchment, it ranged from 0.06 to 51 m^3/s with a mean of 0.79 m^3/s. At the JK site, an ephemeral site in the middle of a wide floodplain reach fed by an 865 km^2 catchment area, it ranged from 0-58 m^3/s having a mean of 0.77 m^3/s. There was no flow at JK for a period in early winter 2012 (12/5/2012-14/7/2012) preceding the flood events described above. Other river channel sites were checked for presence of flow and river stage when groundwater observations were made at adjacent pit sites. Upstream floodplain sites (VR, BK, DD) dried out earlier in 2012 than JK and stopped flowing in the dry fall and winter of 2013. Comparing streamflow at the most upstream and downstream gauged sites, ZH to RH, the 55 km reach was a gaining stream for the majority of 2012-2013, including periods when the intervening floodplain was dry and when streamflow was being fed by the slowest groundwater pathways (Figure 1-13). There were two periods in the summer and fall of 2013 (21 days in February and 18 days in March) during which flow at ZH exceeded the catchment outlet (RH) flow by 7-20%. These occurred during baseflow periods with no significant rainfall, but when groundwater and baseflows were elevated from the 2012 floods. The elevated water table could be more accessible to ET, causing the intervening net loss not seen in when groundwater tables were lower. Both times the reach reverted to a gaining stream after a rainfall event of over 30 mm and it remained so through the following winter and spring.

In contrast, the upstream ZH to JK sub-reach, 15 km completely located in wide floodplain, was most often a losing stream in 2012-2013, only gaining water along its length for days to weeks following heavy rainfall. The sub-reach became a gaining reach immediately following the large rainfall events of 2012. In the first two storms (14/7/2012 and 7/8/2012) flows at JK receded more quickly than at ZH such that the reach became a losing stream again within four to six days. This is consistent with the time period of post-storm surface flow in the instrumented tributary channel. A several week delayed secondary rise in flow occurred after these storms which was bigger at JK than upstream at ZH, making it a gaining reach again for two months in the winter and spring of 2012. This is consistent with the delay in the rise of the alluvial groundwater table. Following the spring 20/10/2012 storm peak, there was again a fast recession, but the reach stayed a gaining reach for four weeks.

Measured relative elevations of the alluvial aquifer water table and the river water surface showed groundwater gradients toward the stream at different time periods for different sites. Water tables over 1 m above the river water surface were observed, even at the upper catchment sites, following the winter storms of 2012. At the pit sites further down in the catchment (JK, ZF, TN, LG), the groundwater surface was higher than the local river water surface at all observation times (Table 1-5). This is consistent with the generally gaining downstream river reach. All observations were made during baseflow periods and it is possible river levels exceeded groundwater levels during storm peaks. Water tables at sites further up in the catchment (VR, BK) fell below the river channel both in the early winter of 2012 and by the middle of 2013, which coincided with the river drying out at these

sites (example, Figure 1-14). At DD, the pit furthest from the river, the water table was only over the adjacent thalweg for four months during late 2012. The piezometer transects at the JK site revealed that the relationship between the aquifer and river can vary at spatial scales of hundreds of meters. Piezometers located in and close to the permanent wetlands on the south side of the floodplain, which had relatively little water level variability, showed water tables consistently higher than in the channel except during storm peaks. Groundwater levels along the most downstream transect and on the northern side of the floodplain were mostly slightly above the channel following the 2012 floods, but had receded below the channel by July 2013.

Figure 1-13 Gains and losses in daily average streamflow for different monitored river reaches, 2012-2013

Calculated as: flow in downstream site – flow at upstream site

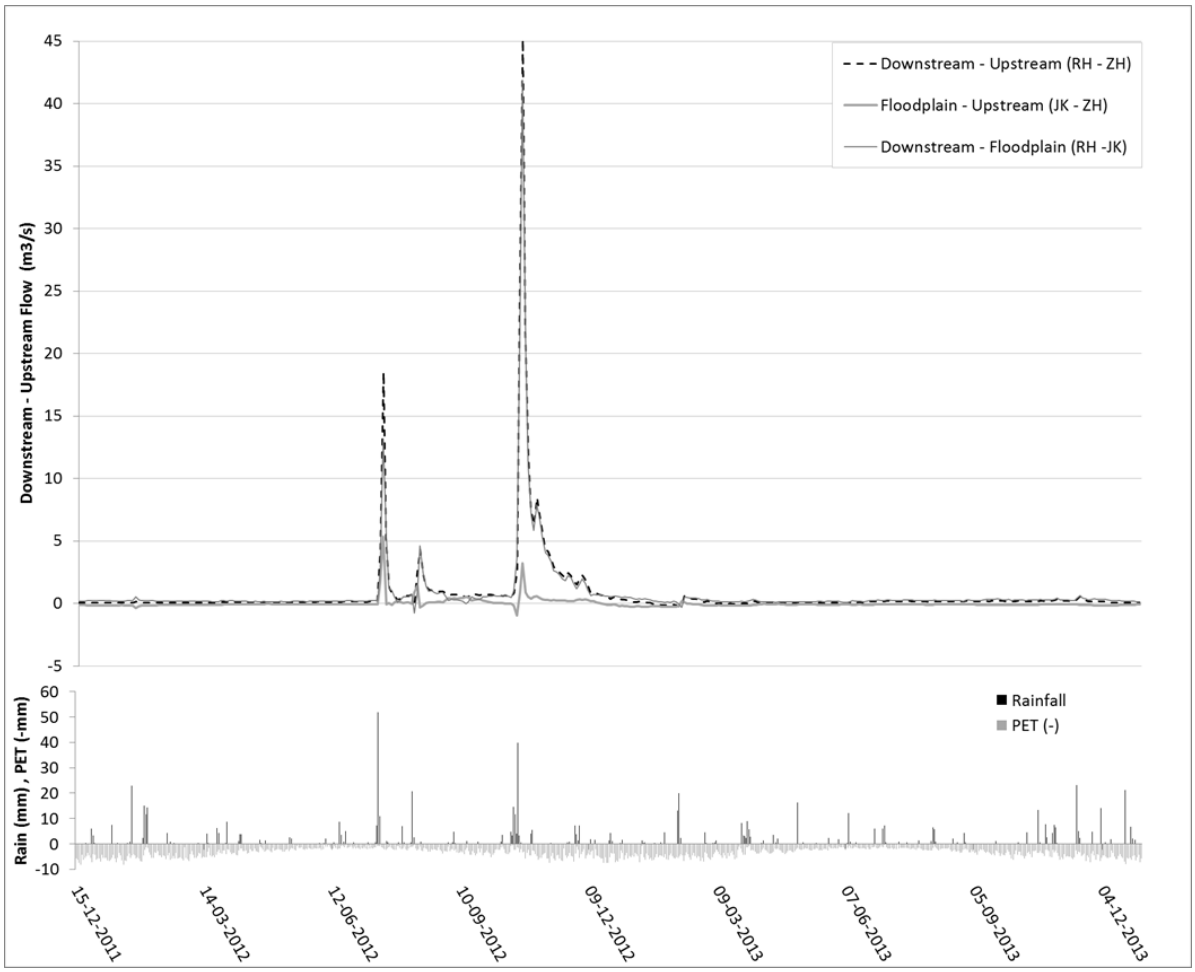

On average over the monitored period, local lateral groundwater gradients were similar to, or lower than, the longitudinal gradient; however at multiple pit sites the lateral gradients exceeded longitudinal for several months following the large rainfall events in 2012 (Table 1-5). The average longitudinal slope of the water table over the 48 km^2 length of floodplain spanned by the monitored groundwater pit sites was 0.7%, the same as the topographic slope over this reach. Despite the notable fluctuations in local groundwater levels at different sites, the large distances and elevation changes between sites meant that observed longitudinal groundwater gradients at this scale did not vary by more than 0.02% over time. Trends at the smaller scale at the JK site showed a 1% local longitudinal gradient and an almost flat lateral water table prior in the dry period prior to the 2012 floods, with the exception of the permanent wetland site which created a local gradient of 0.5% toward the channel. The flood recharge created gradients toward the stream at most locations, however these remained lower than the down-valley slope and a gradient toward the north floodplain developed at the middle transect (Figure 1-15) perhaps due to preferential flow paths such as old channel deposits in the alluvium, patterns of localized subsurface water sources feeding the alluvium, and/or draw-down from dense tree stands.

Table 1-5 Average longitudinal and lateral groundwater gradients observed at pit sites from 2011-2013 and response to the winter 2012 flood events

Pit site	Average groundwater gradient		Maximum slope toward river	Days groundwater above river level post 14/7/2012 flood	Days lateral > longitudinal gradient post 14/7/2012 flood
	Longitudinal (to next site down-valley)	Lateral (to river water surface)			
Veloren Rivier (VR)	0.7%	0.48%	1.2%	240 - 270	150 - 180
Bokloof (BK)	0.8%	0.96%	2.8%	365 - 395	180 - 210
Damsedrif (DD)	0.7%	-0.50%	0.04%	78 - 126	10 - 78
Joachimskraal (JK)	0.6%	0.27%	0.32%	always above	*always below*
Zandflakte (ZF)	0.4%	0.37%	0.49%	always above	345 - 375
Tuin (TN)	0.7%	0.81%	0.88%	always above	always above
Landsegat (LG)	-	0.25%	0.33%	always above	-

Figure 1-14 Groundwater and river water surface elevations at site BK compared to rainfall

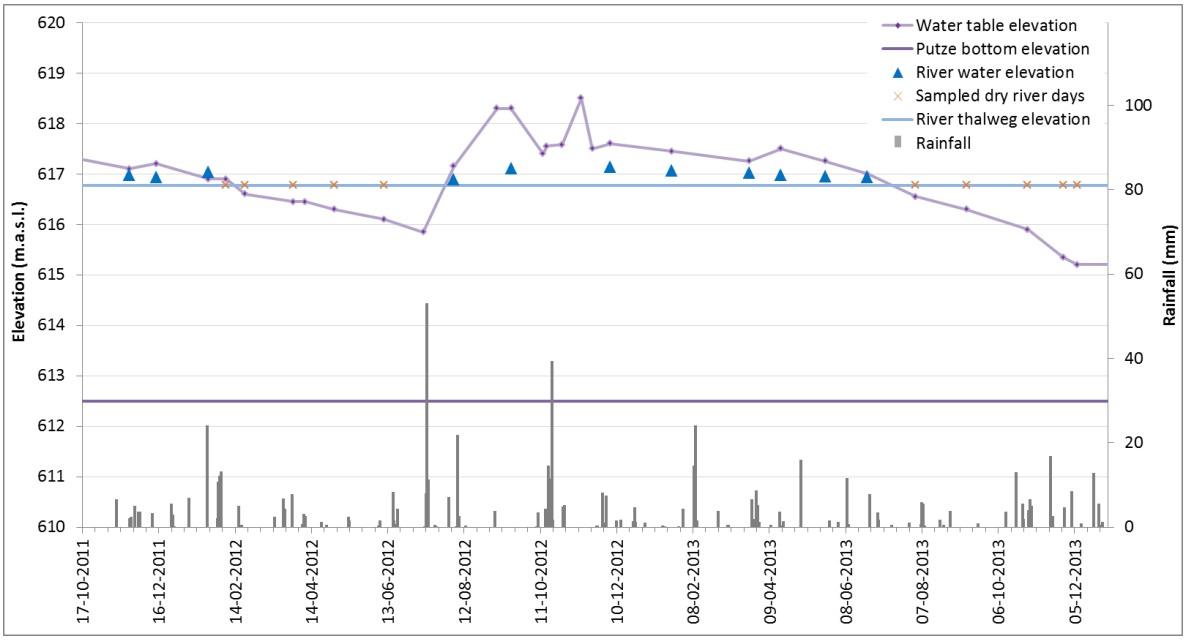

Figure 1-15 Water surface elevation gradients between all piezometers at selected dates

Dotted lines between points and labels indicate measured water table slope between piezometers with no lines indicating dry piezometers. White lines are summed slope vectors of proportional length, slope vector lines were cut short and made thicker when intercepting a flowing channel.

Dry period – no streamflow, winter (10/07/2012)

Post flood, groundwater peak (12/11/2012)

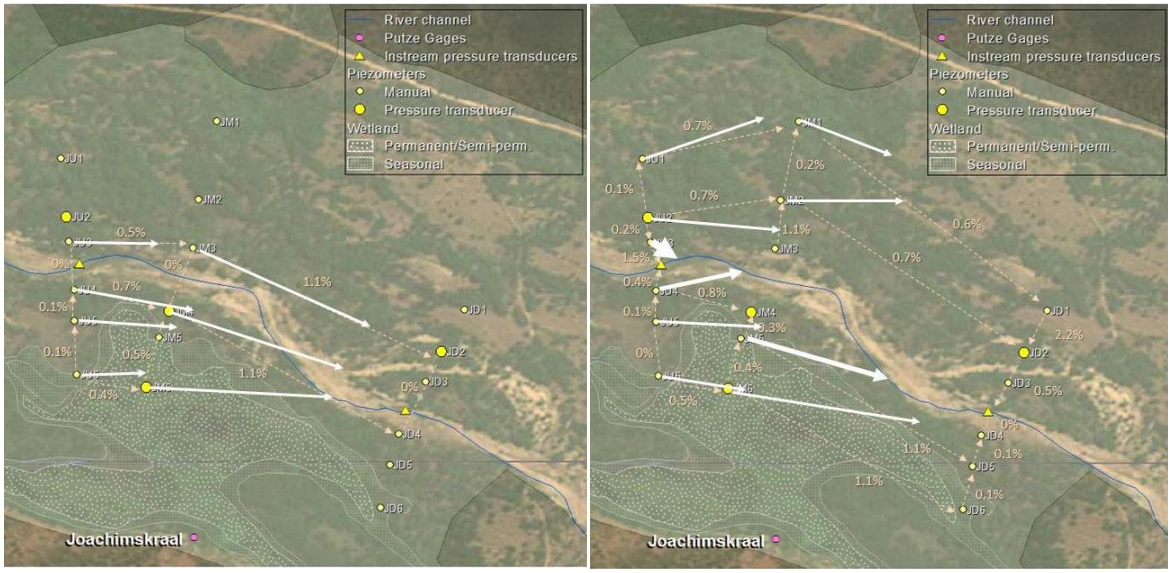

Post flood, winter (03/08/2012)

Dry period, summer (07/12/2013)

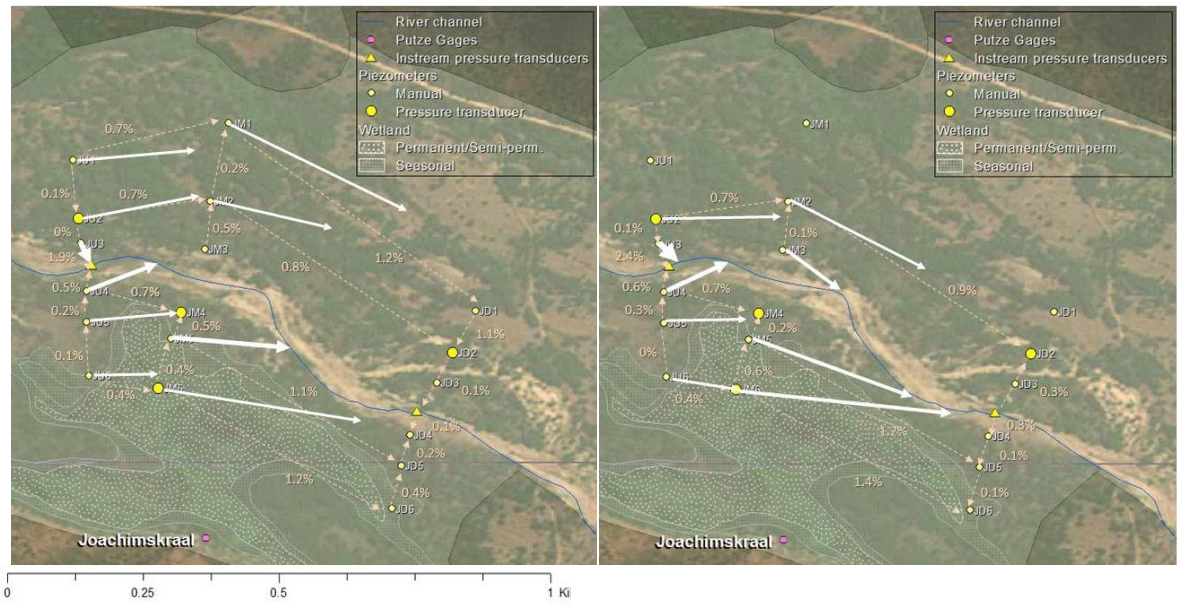

Streamflow showed medium to high positive correlations (R^2 values 0.5-0.8) with groundwater levels during baseflow periods at sites where water-tables were highly responsive to rainfall events. The increase in streamflow associated with a given rise in the water table was not constant over the range of water table depths observed: most sites showed a point of inflection above which much greater increases in flow were observed per unit water table rise (Figure 1-16). This point of inflection occurred close to where the water table reached the level of the adjacent river channel thalweg at the more highly responsive sites, VR, BK, and DD. At the deepest water tables recorded these sites, streamflow correlation appeared weaker, perhaps indicating a threshold of interaction, however there were too few data points at these levels to be conclusive. At JK, ZF, TN, and LG the water table was always above the channel, but some sites still showed evidence of inflection points. Correlations were weakest at the non-responsive sites, JK at the mountain front and piezometers in and around the wetland and at LG, but there appeared to be some relationship between water table and streamflow when only periods of very low flow are considered.

The changing relationships at different flows and water tables may indicate different pathways contributing to baseflow at different water levels. One possible explanation for this would be a change in conductivity of the aquifer material with depth, reaching a less conductive layer as the water table declines. Another explanation is a transition from a state with a steeper groundwater table from the mountain front laterally across the floodplain to the channel into a state in which longitudinal gradient down the valley is dominant. This

could occur as inputs to the floodplain aquifer along the mountain fronts recede after a wet event. In the initial period more groundwater would flow along a shorter path length from a point in the floodplain to the adjacent channel, and streamflow would be highly responsive to a change in this gradient. In the later stage, water would flow longitudinally down the length of the floodplain, traveling much further before intersecting the channel further down-valley. This would take much longer and provide more opportunity for ET losses, such that streamflow is less sensitive to small changes in groundwater levels in this phase. It would also be expected that, as groundwater flows down valley, the water tables at more down-valley sites become stronger determinants of catchment outlet streamflow later in a flow recession period than they had been earlier on. Immediately after a large event the entire catchment would have been contributing flows via faster pathways whereas later on, only the more down valley sites are. This was seen at ZF and LG sites where correlations at high flows were very much weaker and showed large changes in flow with almost no change in groundwater level, but showed much clearer correlations at lower flows.

Figure 1-16 Streamflow and groundwater levels at pits and instrumented piezometers.

Logging piezometers captured data over a larger range of flow conditions than manually read pit sites. For JM6 and JD2 piezometers two scales are shown for visual comparison with pit sites and to show the pattern over the full range of values observed

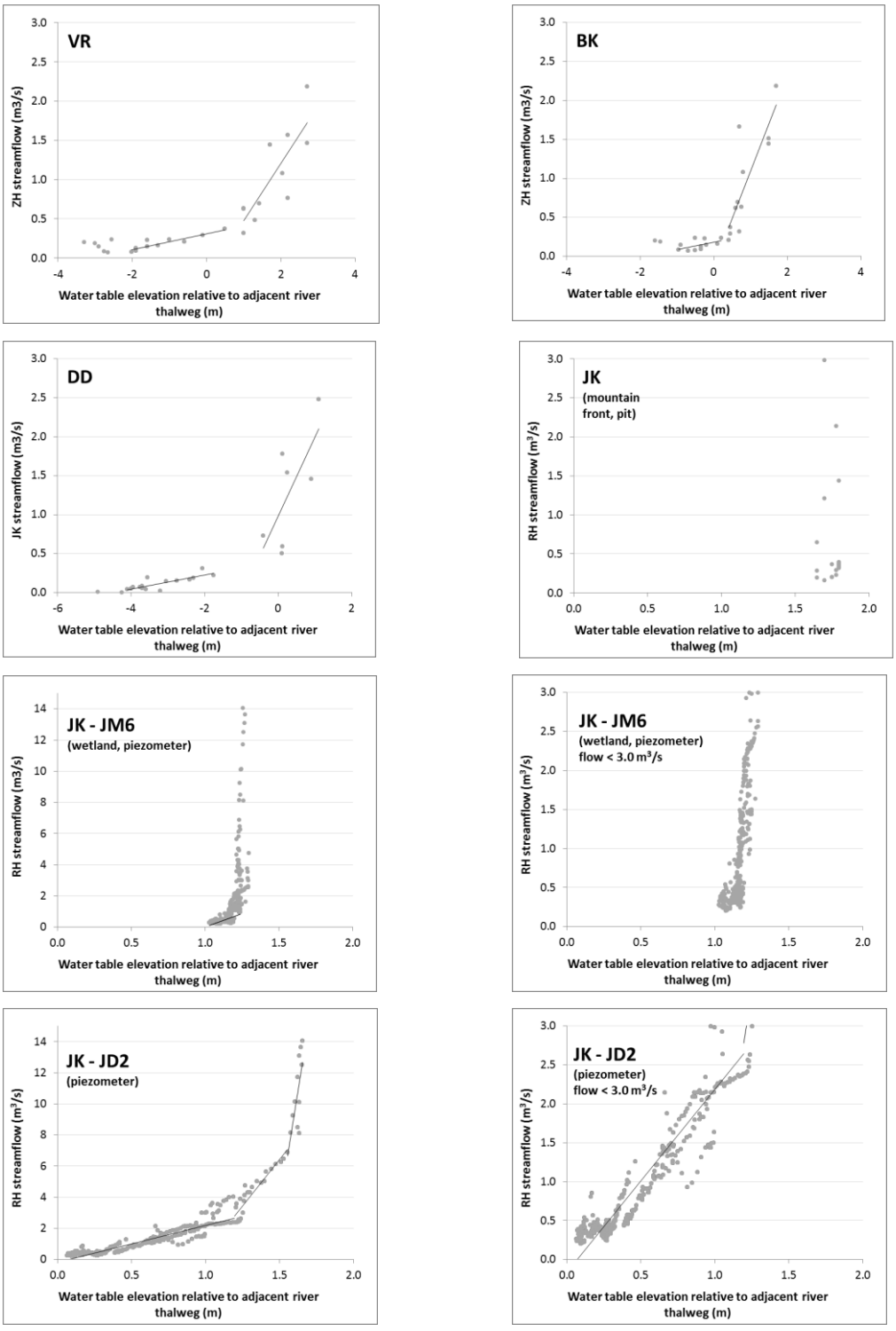

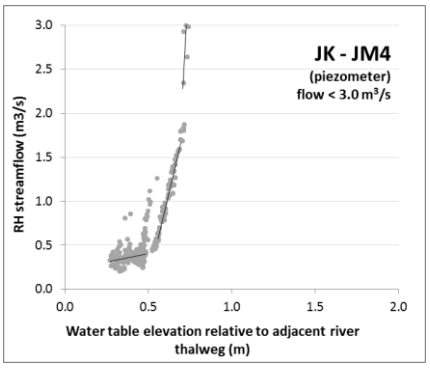
JK - JM4
(piezometer)
flow < 3.0 m³/s
RH streamflow (m3/s)
Water table elevation relative to adjacent river thalweg (m)

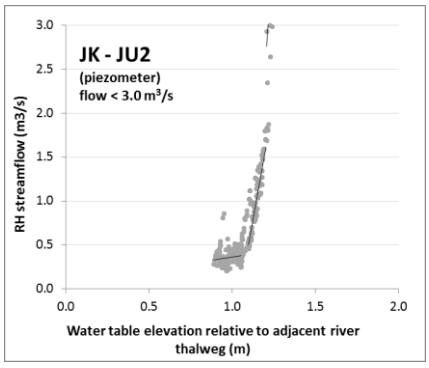
JK - JU2
(piezometer)
flow < 3.0 m³/s
RH streamflow (m3/s)
Water table elevation relative to adjacent river thalweg (m)

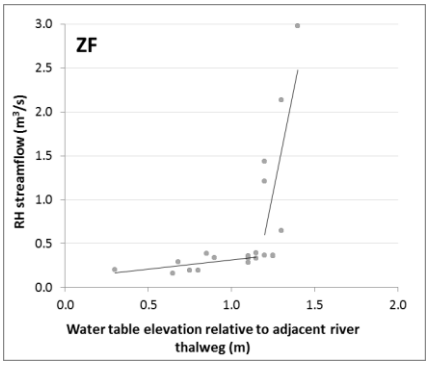
ZF
RH streamflow (m³/s)
Water table elevation relative to adjacent river thalweg (m)

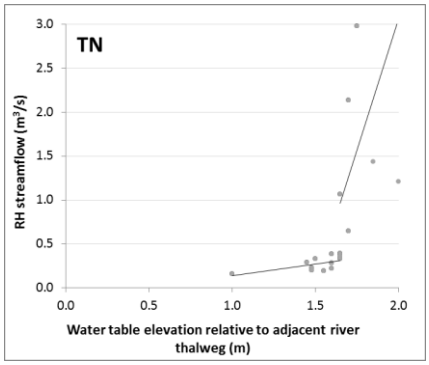
TN
RH streamflow (m³/s)
Water table elevation relative to adjacent river thalweg (m)

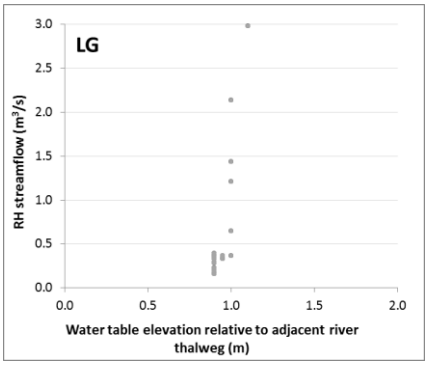
LG
RH streamflow (m³/s)
Water table elevation relative to adjacent river thalweg (m)

Table 1-6 Diagnostic patterns observed in the hydrometric data and resulting model structure

Scale	Data types	Analysis	Patterns observed	Model structure
Catchment	Streamflow, precipitation	Average annual runoff ratio	Low average runoff ratio (7%). High variability with rainfall seasonality and intensity.	High interception and infiltration rate relative to average storm size. ET withdrawals from significant reservoirs on flow path.
Catchment	Streamflow	Quick vs. slow response flow proportions	Slower, subsurface flow pathways can contribute significantly to overall flow (55%) and show high variability.	Baseflow contributions dynamically modelled (as opposed to a temporally static quantity)
Catchment	Streamflow, precipitation	Storm event precipitation threshold for quick-flow runoff response	Dry period threshold of roughly 20mm to see a flow peak. Wet antecedent conditions allow for peaks after much smaller storms.	Combined storage space of various land units in canopy interception, detention storage, and soils is roughly 20mm.
Catchment	Streamflow, precipitation	Peak-forming storm event runoff ratio	Low event quick-flow run-off ratios even for intense storm events (max 21%). Ratios are influenced by antecedent conditions which last weeks to months.	High interception and infiltration rates relative to storm events. Storages that effect quickflow runoff production drain over weeks to months.
Catchment	Streamflow, precipitation	Shape of flow recession curve	Non-linear recession patterns that vary with season and flow. Recessions at high winter flows are most linear. Low-flow and summer periods being highly non-linear with weak relationships to storage.	Baseflows modeled with multiple reservoirs with different drainage rates. ET withdrawls from baseflow reservoirs.
Hillslope	Surface runoff presence / absence, precipitation	Storm event precipitation threshold for surface runoff response	Dry period threshold of roughly 15mm to see surface runoff. Wet antecedent conditions allow for runoff from smaller storms.	Hillslope maximum interception and soil storage close to 15mm (per storm)
Hillslope	Soil moisture, precipitation	Time to decline post storm peak	Fast decline (1-2 days) of soil moisture post-storm.	Fast vertical soil drainage on hillslopes.
Hillslope	Soil moisture, precipitation	Peak timing and magnitude at different locations	Delayed peaks in lower layer (regolith) and greater peaks downslope.	Lateral interflow on hillslopes

Scale	Data types	Analysis	Patterns observed	Model structure
Tributary catchment	Tributary streamflow, precipitation	Precipitation threshold for streamflow initiation	Rainfall over 30mm needed for channel flow	
		…vs. for hillslope surface runoff	More rainfall needed to initiate tributary channel flow than needed for hillslope surface runoff.	Hillslope runoff connected in series to canyon floor and alluvial fan such that infiltration can occur on the flow path
		…vs. for catchment streamflow peak	More rainfall needed to initiate tributary channel flow than needed for a streamflow peak at the catchment outlet (or for rise in alluvial aquifer groundwater in excess of direct infiltration).	Subsurface flow connectivity between tributary catchment land units, the floodplain alluvial aquifer, and the catchment outlet.
Alluvial aquifer	Groundwater level, precipitation	Groundwater level change following precipitation at different locations	Large water table response to large rainfall events, and to those in wet and winter conditions at, sites higher up in the catchment and closer to the floodplain center. Smaller response and recession further down in the catchment. Very little fluctuation in at some mountain front locations.	High conductivity floodplain sediment to allow significant percolation and downvalley flow. Mountain bedrock subsurface flow into alluvial aquifer that fluctuates little or very slowly in response to rainfall.
Alluvial aquifer	Groundwater level, precipitation	Groundwater rise post-storm compared to maximum direct floodplain infiltration	For large storms, water table rise was in great excess of that expected due to recharge from direct infiltration on the floodplain alone. Smaller storms showed a smaller proportional excess.	Subsurface flow connectivity between tributary catchment land units and the floodplain alluvial aquifer
Alluvial aquifer	Groundwater level, precipitation	Peak timing post-storm	Post storm-event water table peaks were delayed days to weeks, with a greater delay with drier antecedent conditions.	Subsurface flow from the tributary catchment to alluvial aquifer has a drainage time in the order of weeks
Alluvial aquifer	Groundwater level, precipitation, PET	Groundwater level decline correlation with PET	Water table declines were correlated with PET at all responsive sites	ET withdrawal from the alluvial aquifer

Scale	Data types	Analysis	Patterns observed	Model structure
River channel	Streamflow	Time periods when river reaches are gaining or losing flow	At larger scales (55km) the stream was predominantly gaining, indicating consistent flow sources. Short periods of net flow loss during summer baseflow with elevated water tables indicate ET effects. Within the wide floodplain, the stream was generally losing, except during flood surface-flow periods and post-flood periods with high alluvial aquifer water tables.	River channel and alluvial aquifer dynamically coupled. Secondary slower draining groundwater reservoir (maintains gaining flows in dry periods).
Alluvial aquifer -river channel	Groundwater level, river stage	Relative elevation of groundwater and river water surface during baseflow	Up-valley and mid-floodplain site groundwater fluctuated above and below the river. Down-valley and mountain front sites were consistently above.	River channel and alluvial aquifer dynamically coupled.
Alluvial aquifer -river channel	Groundwater level, streamflow	Streamflow correlation with groundwater level during baseflow	Medium to high correlations with water tables at responsive sites. Relationships change over the recession indicating different pathways of drainage dominate at different periods. No obvious threshold of interaction at levels observed (up to 5m depth)	Alluvial aquifer represented by multiple baseflow reservoirs with different drainage rates or flow through the alluvial aquifer to the channel calculated dynamically in two dimensions. Dead storage in the alluvial aquifer must be more than 5m deep.
Alluvial aquifer	Groundwater level	Longitudinal vs. lateral water table slope	Water table gradients across the floodplain to the river were smaller than the longitudinal slope on average, but exceeded it for weeks to months after major floods at multiple sites. During this period time travel through the aquifer material to the channel would be shorter and faster.	Flow through the alluvial aquifer dynamically calculated in 2 dimensions.

1.4.3 Proposed conceptual model

The implications of the diagnostic patterns in the hydrometric data for catchment modeling are summarized in Table 1-6 Diagnostic patterns observed in the hydrometric data and resulting model structure. Land units within the tributary catchments, such as hillslopes, are to be modeled separately to enable modeling of different scenarios of hillslope vegetation cover. Data indicate that surface flows from the different land units should be connected in series along a flow path, rather than each unit connecting to the channel network in parallel. Hillslope surface flow was initiated by rainfall events below tributary catchment thresholds for channel flow (15 mm vs. 30 mm), indicating infiltration of hillslope runoff along the flow path. Patterns in streamflow data indicated that capturing variability in subsurface flow pathways is important for estimating streamflow quantity and timing. Even following storm events large enough to result in surface flow connectivity from the tributaries to the catchment outlet, subsurface flows made up substantial portions (roughly 50%) of the resulting runoff reaching the outlet. Baseflow quantities and their contribution to overall catchment water yield also had high inter-annual variation.

Subsurface flows from the tributary catchments appeared to be significant in recharging the alluvial aquifer on a time scale of days to weeks after large rainfall events. Water infiltrated on hillslopes appeared to have relatively fast vertical drainage, however there was some evidence of interflow at the soil-rock interface. In addition, evidence of interflow in shallow, highly fractured surface layers, feeding springs and wetlands has been seen in other studies in TMG geology (Midgley and Scott, 1994; Roets et al., 2008; Xu et al., 2002, 2003), and so interflow is a likely pathway for some of the subsurface recharge of the

alluvium. The effect of ET on the alluvial aquifer is consistent with the deep rooting nature of one of the dominant species, *Acacia karroo*. The mountain bedrock aquifer contributes to the alluvial aquifer, as shown by consistent water levels at some mountain fronts, water color indicative of iron-rich TMG-sourced groundwater, observed groundwater seeps and springs, and that the gain in flow with catchment scale was maintained at perennially flowing reaches even in dry periods.

A dynamic relationship between streamflow and alluvial aquifer was observed that suggests the need for explicit consideration of fluctuating aquifer-channel exchange to predict baseflow responses. The alluvial aquifer feeds river baseflow in relation to its water table elevation. However, patterns of baseflow recession and the relationship between baseflow and the alluvial aquifer water table were variable, indicating contributions of flow pathways with different rates and which are affected by ET. This is consistent with the changes in the magnitude and dominant direction of water table gradients within the floodplain over the course of the recession and changes in surface flow connectivity across wide floodplain reaches. These observations support dynamic modeling of river water elevations and of floodplain groundwater elevation across a two dimensional grid to determine their interactions as dictated by relative elevation and dominant water table gradients. In addition, the coarse nature of the floodplain alluvium would facilitate aquifer recharge given significant floodplain inundation. Overbank flows were seen in the observation period during relatively high frequency (6-8 year) flood magnitudes. This suggests overbank flooding and infiltration be modeled when looking at multidecadal timescales, likely to include floods of greater magnitudes.

As a result of these observations, and literature for land units for which specific data were not available, as well as the model structure requirements laid out in Table 1-1, a conceptual model for each land unit and its connectivity to one another and to channel flow is proposed (Figure 1-17 to Figure 1-20). In this conceptualization, tributary catchments can contribute channelized surface flow to the head of an alluvial fan and subsurface flows to the margin of the alluvial aquifer (Figure 1-18). Depending on the channel properties of the alluvial fan, surface flows arriving at its head will be apportioned to either join the channel network or flow over the fan surface where it can infiltrate into the alluvium (Figure 1-20). The alluvial aquifer contributes water to the river channel in quantities and rates dependent on the level of the water table relative to the channel.

Tributary catchments are comprised of plateau, hillslope, cliff, and canyon floor units (Figure 1-18). Plateau areas have fairly continuous fynbos vegetation cover, low slopes, and shallow soils overlying the fractured bedrock. Dominant processes are therefore expected to be interception, infiltration, and percolation into the fractured bedrock. Hillslopes by contrast produce more surface runoff because of their slope and more open canopy cover in their current state, but infiltration and percolation to the interflow interface are also significant. Cliffs produce even more surface runoff, being steeper with more bare-rock cover. Canyon floors are characterized by coarse alluvial fill and high infiltration. Surface runoff produced by these units flows in a catena from plateau to hillslope and cliff to canyon floor over which there is opportunity to infiltrate. Flow path infiltration would depend on relative runoff velocity across the slope length, determined by gradient and roughness,

compared to the infiltration rate of the unit, determined by its soil and antecedent wetness. In these units, infiltrated water in excess of some effective soil storage limit percolates into an interflow reservoir: the regolith at the soil-rock interface and the fractured rock surface layer. Water in this layer drains into the fan and floodplain alluvial aquifer over multi-week timescales while some would also percolate vertically into the sparser fracture network of the mountain bedrock aquifer. The mountain bedrock aquifer also releases water to the fan and floodplain alluvial aquifer margin at a much slower rate.

Channel flows crossing the combined fan and floodplain alluvial aquifer lose water through bed infiltration into the aquifer when and where the water table sits below the river channel elevation (Figure 1-20 C). The channel receives water from the alluvial aquifer when and where the water table sits above the channel. Within the alluvial aquifer water will flow according to the dominant water table gradient direction and magnitude, which fluctuates with interflow inputs at the floodplain margin and infiltration of surface flows on alluvial fans following rainfall events. For a few weeks following a large rainfall event, these inflows create a dominant water table slope between the mountain fronts and the central floodplain resulting in a shorter subsurface flow path to the river network. As these contributions recede, leaving only slow mountain bedrock inputs from springs at the margins, the dominant gradient becomes more longitudinal such that the path length from a mountain front water source to a lower lying channel reach down-valley is much longer (Figure 1-20 C). Direct infiltration of precipitation on the floodplain surface also contributes to recharging the alluvial aquifer. Water can be withdrawn from the alluvial aquifer to meet PET demand over the full range of water table depths. Due to the high conductivity of the

floodplain material, high vegetation cover, and high PET, surface runoff due to saturation or infiltration excess is minimal on the floodplain surface. Overbank flooding occurs in extreme events, a portion of which will recharge the alluvial aquifer if it is not fully saturated.

Figure 1-17 Overview of flow paths and travel times in conceptual model of the Baviaanskloof catchment based on field data diagnostics

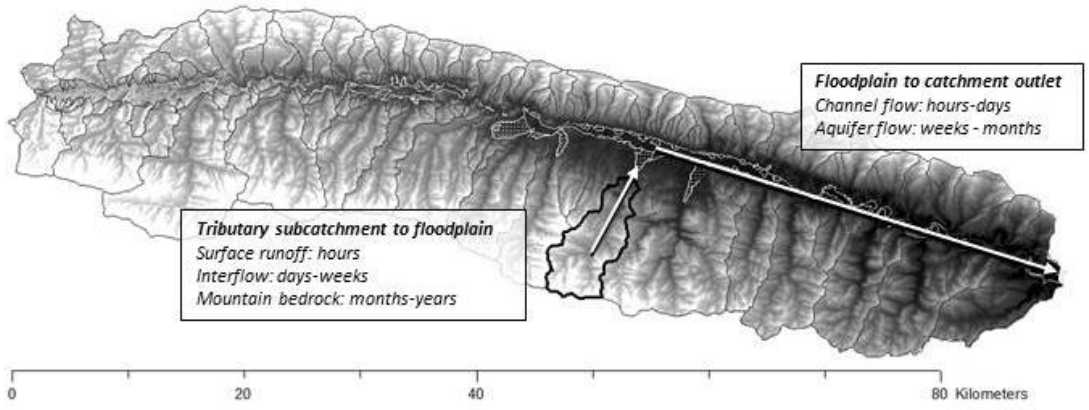

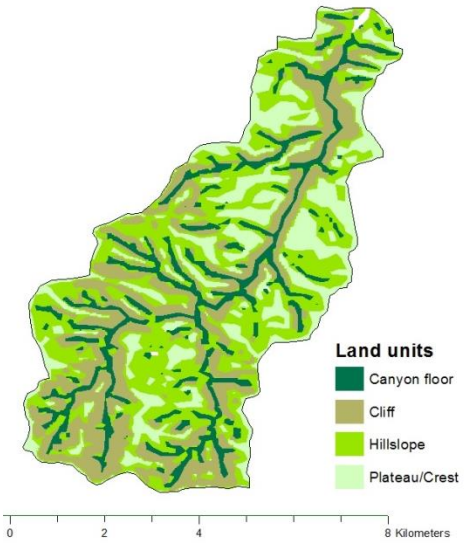

Figure 1-18 Conceptual model of surface and subsurface flows through a tributary subcatchment to the alluvial fan and floodplain.

Topographic land unit discretization of an example subcatchment shown at left.

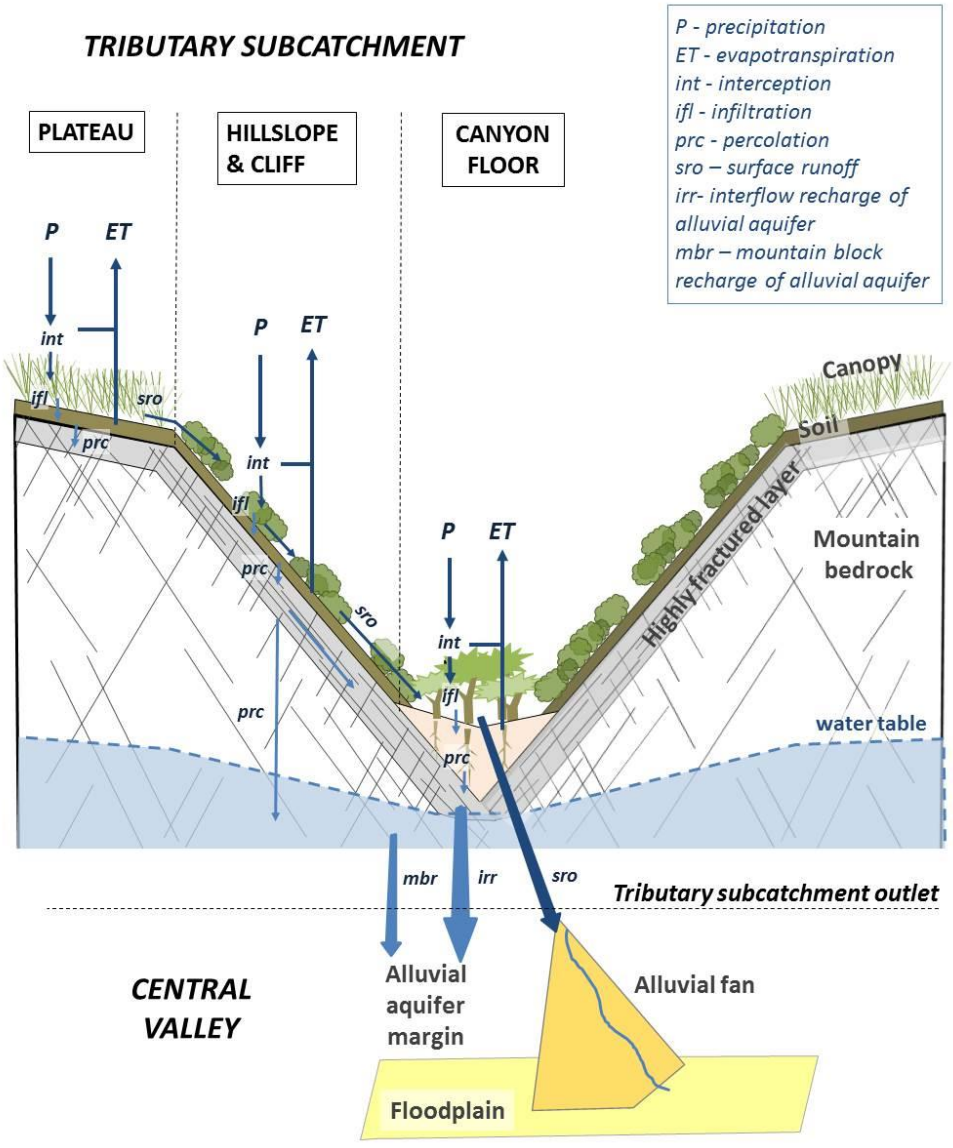

Figure 1-19 Model structure diagram for the numeric representation of a tributary catchment showing outputs to the alluvial fan and alluvial aquifer

P - precipitation
ET - evapotranspiration
int - interception
ifl – infiltration
sat – saturation soil moisture
fc – field capacity soil moisture
wp – wilting point soil moisture
prc - percolation
sro – surface runoff
irr- interflow recharge of alluvial aquifer
mbr – mountain block recharge of alluvial aquifer

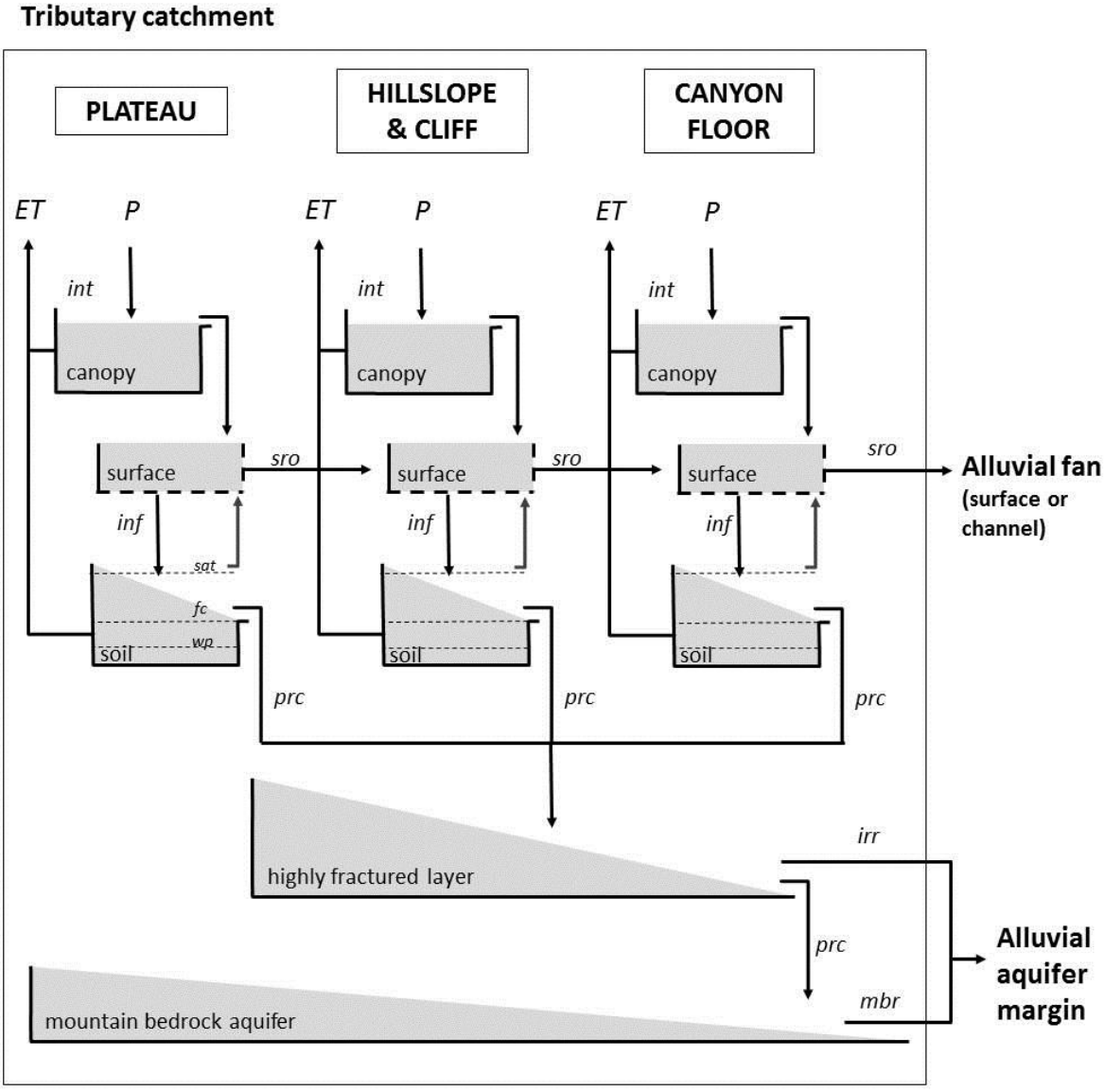

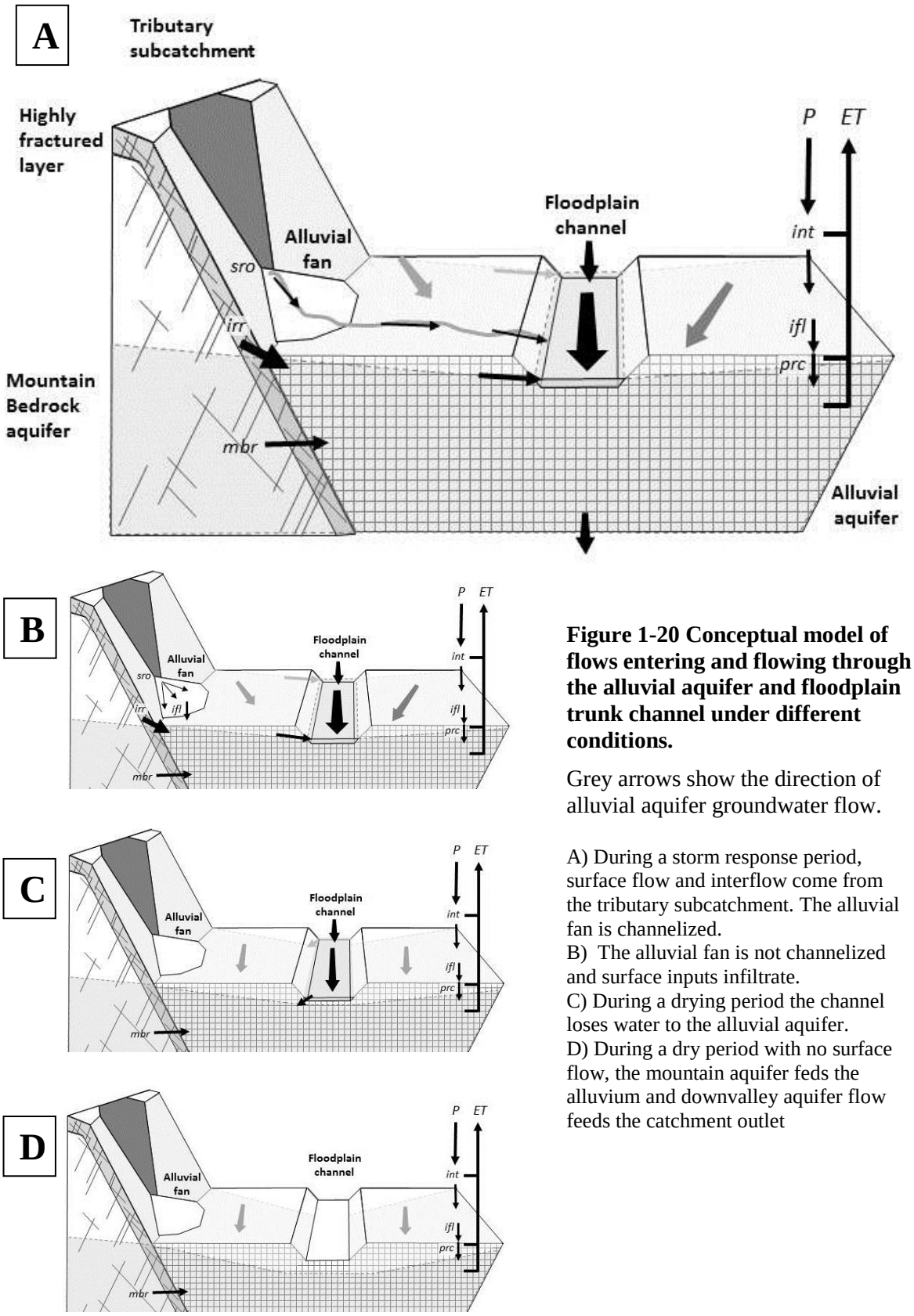

Figure 1-20 Conceptual model of flows entering and flowing through the alluvial aquifer and floodplain trunk channel under different conditions.

Grey arrows show the direction of alluvial aquifer groundwater flow.

A) During a storm response period, surface flow and interflow come from the tributary subcatchment. The alluvial fan is channelized.
B) The alluvial fan is not channelized and surface inputs infiltrate.
C) During a drying period the channel loses water to the alluvial aquifer.
D) During a dry period with no surface flow, the mountain aquifer feds the alluvium and downvalley aquifer flow feeds the catchment outlet

1.4.4 Proposed numeric model structure

The numeric representation proposed for this conceptual model was structured to meet the needs of the model application: the ability to parameterize both vegetation and channel change scenarios and output alluvial groundwater levels in addition to catchment outlet streamflow. To account for the different levels of information and output needs at different spatial scales, particularly regarding subsurface flows, the numeric model was built as two sub-models having different levels of spatial discretization and process representation: a coarser sub-model of the mountain areas coupled to a higher resolution model of the central valley alluvial fans, floodplain, and channel network. To calculate flows between the alluvial aquifer and the floodplain channel based on relative water surface elevations, and to allow for overbank flows, the central valley model required a hydraulic model of the channel linked to a gridded surface and subsurface hydrologic model.

Based on a review of existing catchment models and modeling software systems, the MIKE-SHE/MIKE-11 modeling system by DHI (Graham and Butts, 2005; Refsgaard and Storm, 1995) was selected to build the numeric model of the catchment. This platform allows for different levels of spatial and process representation to be applied to surface and subsurface processes and can integrate a 2-D hydraulic model (MIKE-11) with the hydrologic model's surface and groundwater routines. When processes are conceptualized at the level of hydrologic response units (HRUs), MIKE-SHE allows run-off to be routed across a catena of HRUs such that infiltration of surface flows along a flow path can be considered. Many medium complexity models or modeling systems, such as SWAT (Arnold et al., 1998), WARMF (Herr and Chen, 2012), or ACRU (Schulze, 1995), route

HRU runoff directly to the channel network in parallel. Models such as RHESSyS (Tague and Band, 2004) and HSPF (Bicknell et al., 1993) do consider landscape routing across HRUs, but do not include channel routing and overbank flooding. Other potentially appropriate catchment models that allow for the surface-subsurface exchange of water required to capture floodplain processes include SWATMOD (SWAT linked to MODFLOW, (Sophocleous et al., 1999)), FHM (HSPF linked to MODFLOW, (Ross et al., 1997)), HMS (Yu, 1997), and PAWS ((Shen and Phanikumar, 2010). It would have been possible to build the mountain and central valley submodels in two different modeling platforms, however for simplicity of processing it was decided to build both using MIKE-SHE.

In the mountain area sub-model, for each land unit in a tributary sub-catchment, the interception, infiltration, soil water storage, AET, and vertical percolation were calculated daily and the resulting surface runoff was then routed across the unit to the next unit in the catena (Figure 1-19). Canopy interception was calculated using a maximum interception storage quantity. If daily rainfall plus water remaining on the canopy from the previous day exceeds the maximum storage, the excess is allocated to the soil surface. Infiltration, soil water storage, and vertical percolation were calculated as functions of soil field capacity, wilting point, and conductivity. If the soil layer is not saturated, water on the soil surface is added to the soil layer with the quantity of infiltration in a day being limited by the infiltration rate, the quantity of water required to saturate the soil, and the quantity of water on the soil surface. Water on the soil surface not infiltrating in a day was subject to surface flow. Soil moisture in excess of the field capacity was allocated to the interflow reservoir

with the quantity of daily percolation limited by soil conductivity and the quantity of free water. Lateral subsurface flow was assumed to be dominant only in the interflow zone and was not calculated for overlying soil layers.

In the mountain area model, water on the soil surface of an HRU that did not infiltrate was routed to the next unit in the series based on Manning's equation, considering the HRU as a sloped plane. The depth of available surface water, surface roughness, slope, and slope length were to calculate flow across the edge of the unit in the time step. The resulting rate of flow could mean there was remaining surface water available for ET and for infiltration or overland flow in the subsequent timestep. This was operationalized in the simplified overland flow routing routine for MIKE-SHE (DHI, 2014a) and is the same method as applied in HSPF (Bicknell et al., 1993), WATBAL (Knudsen, 1985), and others descending from the Stanford watershed model. Slope and slope length were assigned to subcatchment HRUs based on average slope and flow path length across delineated land cover units calculated from the DEM while roughness was a calibrated parameter.

AET was calculated based on PET, available interception and surface stores, available soil water, and vegetation type ET rates. This allowed for parameterization of different vegetation cover scenarios in the model based on measured vegetation and soil properties in areas with different levels of canopy cover. Within the mountain area sub-model, plant roots were assumed to fully penetrate the soil layer above bedrock and, being thin, soils were considered as a single layer. A vegetation type ET coefficient, or 'crop coefficient', was used to modify the atmospheric PET demand for the day. The resulting daily ET demand

was first addressed by removing water from the canopy storage, then removing water from the soil surface, and finally by removing water from the soil if there was further outstanding demand. When addressing ET demand from the soil, approximating transpiration removals and evaporation from the soil, the rate of removal was decreased linearly once the soil moisture reached field capacity to equal zero when soil moisture reaches wilting point.

Percolation into and flow out of an assumed interflow reservoir represented the likely preferential subsurface flow pathway at the soil-rock interface and in the highly fractured top layer of bedrock (Figure 1-19). Little is known about the physical properties and spatial variability of this layer and it was not necessary to change its parameterization between scenarios. As such, it was modeled as a simple linear reservoir in which outflow (Q) is a linear function of storage (S) determined by a drainage constant (k) such that $Q = (1/k)*S$. The alluvial aquifer groundwater patterns gave an indication of the drainage rate of faster subsurface flows from tributary catchments after a storm event, suggesting this reservoir has a drainage constant for flow reaching the alluvial aquifer in the order of days to weeks. The interflow reservoir was assumed to be fed by all the land units in the tributary sub-catchment and to drain both laterally, into the alluvial aquifer, as well as vertically, into the mountain bedrock aquifer. Flows in these two directions leaving a subcatchment interflow reservoir in a day were calculated in MIKE-SHE using different drainage rate constants for vertical and horizontal outflow. The linear reservoir equation for a reservoir with two outlets was combined with the continuity equation and the resulting differential equation was solved by assuming the rate of inflow to the reservoir is constant over the timestep (DHI, 2014a).

The mountain bedrock aquifer was modeled in MIKE-SHE as a linear reservoir for each tributary subcatchment, receiving vertical inflow from the interflow reservoir and having a single outlet feeding water to the central valley alluvial aquifer. Based on the relatively constant water levels observed at mountain front sites away from alluvial fans it was assumed that the drainage constant was on the order of years. The interflow and mountain bedrock water stores were assumed not to be accessible for ET; however the alluvial aquifer is subject to ET withdrawals (Figure 1-20), accounting for the observed ET impact on baseflow recessions at the catchment outlet.

The central valley sub-model received surface and subsurface flow from the mountain area sub-model. Daily time-series of surface flows leaving tributary subcatchments were input as surface flow point sources at the heads of corresponding alluvial fans. Subsurface outflows from the interflow and mountain bedrock reservoirs were input as flow boundary conditions at the margin of the alluvial aquifer groundwater model. This linkage was operationalized using codes written in MATLAB 2012 (MathWorks, Inc) and the DHI MATLAB Toolbox.

The major differences in the central valley and the mountain area sub-models were the spatial resolution of process calculations, the calculation of groundwater flow, and the integration of the channel hydraulic model. The central valley sub-model calculated surface and subsurface processes per grid cell over a regular 50 m resolution grid with explicit surface and aquifer bottom topography. This included calculation of canopy interception, infiltration, overland flow, percolation to the saturated zone, and AET. Surface flow in the

channel network was handled by a coupled MIKE-11 hydraulic model. This also included flow on the floodplain surface during events in which the streamflow exceeded the channel capacity as the hydraulic model cross-sections spanned the floodplain. Overland flow on alluvial fan and floodplain surfaces which was not sourced from the main floodplain channel was calculated between grid cells using the finite difference routine to solve the diffusive wave approximation of the St.Venant equations as specified in MIKE-SHE (DHI, 2014a). The spatial extent and depth of surface water on the floodplain surface in the MIKE-11 hydraulic model during a time-step was calculated and this water was available for infiltration and ET in the hydrologic model. The quantity of flow in the hydraulic model would then be updated for the next timestep.

Groundwater flow in the saturated zone of the central valley alluvium was modeled using Darcy's Law to calculate flow between grid cells. This was operationalized using the finite element grid routine in MIKE-SHE (DHI, 2014a) which uses the same iterative solution method as MODFLOW (McDonald and Harbaugh, 1988). A single layer of sand and cobble alluvium was defined in the groundwater module so flow only needed to be calculated in two directions. The thickness of the unsaturated soil zone was determined by the height of the groundwater table. ET withdrawals from the soils were first made from the unsaturated zone, however the root depth of the floodplain vegetation was specified to reach typical water table depths and if ET demand could not be met by the unsaturated zone, water would be withdrawn from the saturated zone of the cell and the water table elevation adjusted.

Channel flow on the alluvial fans and floodplain were modeled in MIKE-11 using diffusive wave simplification of the dynamic wave approach to solving the St. Venant equations of continuity and momentum (DHI, 2014b). The diffusive wave equations were solved using an implicit finite grid scheme over a grid of alternating flow and stage calculation points as described for MIKE-11 (DHI, 2014b). River stages were calculated at nodes that coincided with groundwater grid cells. The direction and magnitude of flow between the channel and the groundwater was calculated using Darcy's Law based on the water surface elevation gradient between the river channel and the neighboring groundwater grid cells and the bed material conductivity (DHI, 2014b).

1.4.4.1 Parameter values guided by data-diagnostics

Parameters needed for this model and a range of *a-priori* values in given in Table 1-7 and Table 1-8. These value ranges were informed by the flow and groundwater data diagnostics, local sampling and remote sensing of vegetation and soil properties (van Luijk et al., 2013; Mills and Cowling, 2006, 2010; Mills and Fey, 2004; Mills et al., 2005; Smit, 2013), and review of parameter values estimated for similar vegetation types and geomorphological settings (Consoli et al., 2013; Ganguly et al., 2013; Hammersmark et al., 2008; McMichael et al., 2006; Schulze, 1995; Steinwand et al., 2001; Tague et al., 2004). Parameters such as land unit slope and slope length and river channel and floodplain dimensions are obtained from available topographic data and are assumed to not require calibration. On plateaus, hillslopes, cliffs, and canyons, roots are assumed to penetrate the full depth of the relatively thin soils. This is based on cliff face, gully face, and road-cut

observations of the roots of woody shrubs penetrating into the regolith and bedrock fractures. If it is assumed that the effective vegetation type LAI is sufficiently known from remote sensing, only the canopy interception coefficient needs calibration. This gives 48 parameters, which can be further reduced to 36 if internal relationships between soil properties, essentially a soil moisture retention curve shape, are assumed for each soil type.

Model soil infiltration rate values were set significantly lower than values that would be estimated from soil texture. This is necessary in the case of a daily time-step model when information about sub-daily rainfall intensity is not available. The 'infiltration rate' parameter is not purely a property of the soil surface, but rather a combination of soil and average storm intensity characteristics to allow the calculation of infiltration in a 24 hour period given daily rainfall. In addition these landscape units have considerable rock cover on the soil and bare rock outcrops. In dry conditions surface runoff was seen on hillslopes after storms of over 15mm, while 30-50mm was needed to initiate surface flow at the tributary catchment outlet. Using these values as guides for parameter value ranges, the model would produce hillslope surface runoff in dry conditions given 12-28mm of rain, while 35-180 mm would be needed to have surface outflow from the average tributary catchment based on an area weighted average for the component land units (Table 1-7).

Patterns in the groundwater data gave indication of the magnitude of horizontal drainage time constants for the linear reservoir model components as described previously: days to weeks for lateral outflow from the interflow reservoir and months to years for outflow from the mountain bedrock aquifer. Little is known about the rate of vertical percolation into the

mountain bedrock aquifer and as such a wider potential value range is given for this property (Table 1-8). Horizontal, or lateral, conductivity in the interflow zone is assumed to be faster than in the vertical direction into the bedrock, because of the higher fracture density and porosity along the lateral path. However, the average length of the lateral flow path to reach the outlet of the tributary catchment is much longer than the vertical distance water would need to travel to leave the interflow zone, on the order of kilometers versus meters. Water percolating downwards out of the interflow zone may then have to travel a significant distance to reach the effective mountain bedrock water table, however this additional lag should be captured in the drainage constant of the mountain bedrock aquifer rather than in the vertical outflow of the interflow reservoir. Otherwise there may be too much water estimated in the interflow reservoir for accurate estimation of the lateral outputs.

Table 1-7 A-priori vegetation and soil parameter ranges and resulting runoff thresholds

F – floodplain, C – channel, T – topsoil, A – alluvium, infilt. - infiltration

Parameter	Landscape unit				
	Plateau	**Hillslope**	**Cliff**	**Canyon**	**Floodplain & fan**
Dominant vegetation	fynbos	thicket	thicket	forest	savanna
Fraction of subcatchment	30%	42%	18%	10%	
Leaf area index, LAI	1 - 3	0.4 - 1	0.2 - 0.6	3 - 5	1 - 3
Manning's n ($m^{1/3}/s$)	0.1 - 0.8	0.1 - 0.8	*same as hillslope*	0.1 - 0.8	0.05 - 0.7 F 0.02 - 0.05 C
ET coefficient	0.4 - 0.6	0.3 - 0.5	0.2 - 0.4	0.7 - 0.9	0.8 - 1.0
Root depth (mm)	500 - 1,000	300 - 800	100 - 500	5,000 - 10,000	10,000 - 35,000
Soil depth (mm), *SD*					600 - 1,000 T
Saturated water content, *SWC*	0.3 - 0.5	0.3 - 0.5		0.4 - 0.6	0.4 - 0.6 T 0.3 - 0.5 A
Field capacity, *FC*	0.1 - 0.2	0.1 - 0.2	*same as hillslope*	0.2 - 0.4	0.2 - 0.4 T 0.1 - 0.2 A
Wilting point, *WP*	0.07 - 0.1	0.07 - 0.1		0.08 - 0.1	0.08 - 0.1 T 0.06 - 0.1 A
Maximum infiltration rate (mm/hr)	1.0 - 3.5	1.0 - 2.0		35 - 350	K_{sat} 50 - 300 T K_{sat} 10 - 1,700 A
Estimation of average thresholds for model surface runoff using a one day time-step					
Max. 1 day interception (mm)	*0.3 - 3*	*0.3 - 4*	*0.3 - 4*	*2 - 10*	*0.7 - 6*
Max. soil storage (mm); SD(SWC – WP)*	*50 - 500*	*50 - 500*	*4.5 - 95*	*160 - 1650*	*228 - 450*
Max. infilt. rate (mm/day)	*12 - 72*	*12 - 24*	*12 - 240*	*240 - 1200*	*1200 - 7200*
Max. 1 day infilt. (mm); *MIN(storage, rate)*	***12 - 72***	***12 - 24***	***4.5 - 95***	***160 - 1200***	***228 - 450***

Table 1-8 Time constants for linear reservoirs representing tributary catchment groundwater flow

Parameter	Linear reservoir	
	Interflow	Mountain bedrock
Lateral outflow time constant (days)	5 - 50	100 - 30,000
Vertical percolation time constant (days)	1 - 50	

1.5 Discussion

This study employed a variety of diagnostic pattern analyses to streamflow, groundwater, soil moisture, and surface runoff data to guide the development of a conceptual and numeric hydrologic model for a semi-arid, meso-scale catchment. Ideally the result of this method of model development should be a model with minimal structural error in its internal process representation for which calibration yields accurate outputs within a narrow range of parameter values. To assess the degree to which this was achieved, multi-criteria calibration of the resulting numeric model will be addressed in a subsequent paper. The scale of the catchment area, the need to design a model capable of being used for specific scenario analyses, and the available hydrometric data all influenced the choice of diagnostics and structure decisions. Data collection is always limited by resources and time. The semi-arid environment further limits the locations and times when surface flows occur, while groundwater data can be costly to obtain where wells do not already exist. For most of the data, only a two year time-series was available. However, patterns evident across multiple different types of data and data from different locations, even over this relatively

short time span, provided significant guidance on the dominance of different flow paths, the connectivity between discretized land units, and reasonable parameter ranges.

Unlike micro-scale catchments, for which spatially lumped, parsimonious, models of dominant processes can be identified through downward model development procedures and can sufficiently recreate streamflow patterns (Fenicia et al., 2008a; McMillan et al., 2011; Vaché and McDonnell, 2006; Young, 2003), a more spatially distributed approach at the level of landscape topographic units was assumed to be necessary for the meso-scale, supported by the experience of Clark et al. (2009), Fenicia et al. (2014), Gao et al. (2014), McGlynn et al. (2004), Savenije (2010), and Uhlenbrook et al. (2004). This discretization was also necessary to allow parameterization of the different land cover scenarios. Given this, both the processes within each land unit as well as the nature of connectivity between them needed to be conceptualized to develop the model. To assist in these model decisions, patterns in hydrometric data that could yield information about surface and subsurface connectivity between land units were assessed, adding another layer of analyses compared to lumped model development for smaller catchments.

Diagnostics of connectivity were mostly in the form of comparative runoff and groundwater response thresholds, magnitudes, and timing between different locations within the catchment, capturing inputs of different land units. For example, looking at both the magnitude of rainfall needed to initiate surface flows out of mountain tributary subcatchments and the magnitude and timing of the floodplain alluvial aquifer response to rainfall events below this threshold, it was concluded that there was significant subsurface

flow from the tributary subcatchments to the alluvial aquifer. As has been suggested by others for semi-arid catchments and those with low lying areas of high conductivity alluvium (Maneta et al., 2008; Savenije, 2010; Winsemius et al., 2006), data analyses showed evidence of dynamic, threshold controlled, surface and subsurface connectivity between land units, indicating that flows generated at the scale of each land unit should be connected in series along a flow path catena rather than in parallel. The relative importance of delayed subsurface flow to the total catchment yield and evidence of the dynamic connection between the alluvial aquifer and streamflow and the impact of ET on the alluvial aquifer levels and flow recessions, supported the decision to dynamically model flows between the alluvial aquifer and the river channel.

Consideration of the desired end use of the model increased the complexity of process representation included for surface and near surface processes, perhaps leading to the use of more parameters than can be resolved with the available hydrometric data. To parameterize scenarios of vegetation change, lacking streamflow data under the changed conditions, it was decided to explicitly model interception, infiltration, percolation, AET, and surface runoff routing for each vegetation and soil type based on measurable vegetation and soil properties. A simpler alternative could have been to represent these surface processes through one or more reservoirs represented by fewer coefficients whose values could be found through calibration, the method chosen for the subsurface flows leaving the tributary catchments. Nevertheless, the resulting parameterization effectively has eight parameters for each land unit in the tributary catchment, not substantially more than the six parameter models (Savenije, 2010) proposed for similar topographic units based on their dominant

processes. In an step-wise top-down model development exercise for a meso-scale catchment, calibrating and evaluating successively more complex model structures against streamflow data, Fenicia et al. (2008b) found that more accuracy was gained in spatial discretization of surface processes with fast runoff response times than for discretizing slower subsurface processes. This supports the structure applied here to the tributary catchments.

Despite the high number of potential calibration parameters in the resulting structure, indications of dominant processes gained from the field data diagnostics, and from observations of similar topographic units elsewhere, can indicate which parameters are likely to be the most sensitive. Parameters to which the desired outputs are not very sensitive can be assigned fixed values to reduce the dimensionality of the calibration problem. For example, surface runoff connectivity from the tributary catchment land units all the way to the catchment outlet was only seen extreme rainfall events during high flows and only persisted for a few days. The short, steep flow paths out of the tributary subcatchments would mean that surface runoff would reach their outlet within the day timestep in these cases. As such variations in Manning's roughness values for these land units within the a-priori ranges are likely to have little effect on model outputs. Similarly, lower slope plateau areas are Sensitive parameters for which there was little or no field data to constrain are those for which further field research is recommended. These will be explored further in the follow-up paper on model calibration and evaluation.

The suggested model structure for the Baviaanskloof catchment contains a mixture of different spatial and process resolutions, from a gridded groundwater and channel model of the floodplain to a simple linear reservoir representation of the mountain bedrock outflow. The highly fractured geologies and coarse alluvial floodplain fills of the catchment are likely to be characteristic of other meso-scale, semi-arid, mountainous catchments. These features appeared to buffer some of the high flows and prolong elevated baseflow periods through processes that are not typically explicitly considered in many pre-existing catchment scale hydrologic modelling programs, such as dynamic two-way interaction between floodplain channels and the floodplain aquifer, aquifer recharge during to overbank flooding, and both lateral and longitudinal flow in the floodplain aquifer (Hammersmark et al., 2008; Loheide and Booth, 2011). The MIKE-SHE/MIKE-11 (DHI) modeling system was found to be one of the few available platforms offering this range of process representation options and the capacity to model river channel and floodplain aquifer as a dynamically coupled hydraulic-hydrologic system. In this program the described numeric model could be built as two coupled models: a model of the tributary subcatchments and mountain block providing boundary condition outputs for a separate alluvial aquifer and channel network model. The need for dual-scale modeling to look at floodplain-scale processes affected by the broader catchment context was similarly recognized by Hipsey et al. (2011) when modeling vegetation and channel change in a semi-arid catchment in Australia.

1.6 Conclusion

This study demonstrates how hydrometric field data collected at different spatial scales can be used to inform the development of a conceptual and numeric catchment model for a complex, semi-arid, meso-scale catchment. Catchments of this scale have been less subject to data-based downward model development approaches, particularly those in semi-arid regions. As such, this study contributes to the ongoing effort to be able to link catchment form to appropriate model structure in order to better model data poor or ungauged catchment areas (Gupta et al 2008). To deal with the number of processes likely to be dominant at different scales and times in a large catchment, the area was discretized into topographic land units. Patterns in streamflow and groundwater responses at scales ranging from tributary subcatchments to the main valley floodplain to the catchment outlet were compared to indicate the nature of connectivity between units. At more local scales, soil moisture data and the detection of surface runoff on a sample hillslope gave information on hillslope runoff processes and comparative water surface elevations between the alluvial aquifer and the river channel indicated the dynamic connectivity between channel flow and the aquifer. Despite the relatively short data series, the variety of data types and scales provided significant information about catchment processes with which to structure and parameterize the model. The resulting suggested model structure for the Baviaanskloof catchment included calculation of recharge and surface flow at the scale of broad topographic land units in the tributary subcatchments of the mountain block, simple linear reservoirs for subsurface flows out of the fractured bedrock reaching the central floodplain,

and a gridded groundwater and channel model for the alluvial fans and main valley floodplain allowing for dynamic exchange of water between the aquifer and channel.

In practical contexts, hydrologic models are typically built with a desired end use in mind, requiring certain processes to be explicitly considered and outputs produced, regardless of the data available to inform them. In the model development process applied here, structural decisions were additionally guided and constrained by an explicit planned end use: to assess the impacts of hillslope vegetation and floodplain and alluvial fan channel property scenarios on floodplain groundwater and catchment outlet surface water supplies. In some cases this application required additional complexity in process conceptualization than may have been warranted by the available data against which process parameters can be calibrated. This will be evaluated further in a follow-up paper on the multi-criteria calibration of the resulting model structure. Comparing the level of process representation in a model to that warranted by the information used to inform it through a process of downward model development can help indicate the levels and sources of uncertainty in the model structure and target further research.

1.7 References

Arnold, J.G., Srinivasan, R., Muttiah, R.S., and Williams, J.R. (1998). Large area hydrologic modeling and assessment - Part 1: Model development. J. Am. Water Resour. Assoc. *34*, 73–89.

Banks, E.W., Simmons, C.T., Love, A.J., and Shand, P. (2011). Assessing spatial and temporal connectivity between surface water and groundwater in a regional catchment: Implications for regional scale water quantity and quality. J. Hydrol. *404*, 30–49.

Beven, K., and Freer, J. (2001). Equifinality, data assimilation, and uncertainty estimation in mechanistic modelling of complex environmental systems using the GLUE methodology. J. Hydrol. *249*, 11–29.

Bicknell, B.R., Imhoff, J.C., Kittle Jr, J.L., Donigian, A.S., and Johanson, R.C. (1993). Hydrologic Simulation Program-FORTRAN (HSPF): User's Manual for Release 10 (Athens, Ga: U.S. EPA Environmental Research Lab).

Bobbins, K.L. (2011). Developing a form-process framework to describe the functioning of semi-arid alluvial fans in the Baviaanskloof Valley, South Africa (S.l.: s.n.]).

Clark, M.P., Slater, A.G., Rupp, D.E., Woods, R.A., Vrugt, J.A., Gupta, H.V., Wagener, T., and Hay, L.E. (2008). Framework for Understanding Structural Errors (FUSE): A modular framework to diagnose differences between hydrological models. Water Resour. Res. *44*, W00B02.

Clark, M.P., Rupp, D.E., Woods, R.A., Tromp-van Meerveld, H.J., Peters, N.E., and Freer, J.E. (2009). Consistency between hydrological models and field observations: linking processes at the hillslope scale to hydrological responses at the watershed scale. Hydrol. Process. *23*, 311–319.

Clark, M.P., McMillan, H.K., Collins, D.B.G., Kavetski, D., and Woods, R.A. (2011). Hydrological field data from a modeller's perspective: Part 2: process-based evaluation of model hypotheses. Hydrol. Process. *25*, 523–543.

Consoli, S., Inglese, G., and Inglese, P. (2013). Determination of Evapotranspiration and Annual Biomass Productivity of a Cactus Pear [Opuntia ficus-indica L. (Mill.)] Orchard in a Semiarid Environment. J. Irrig. Drain. Eng. *139*, 680–690.

Das, T., Bárdossy, A., Zehe, E., and He, Y. (2008). Comparison of conceptual model performance using different representations of spatial variability. J. Hydrol. *356*, 106–118.

DHI (2014a). MIKE SHE User Manual, Volume 2: Reference Guide (Hørsholm, Denmark: Danish Hydrologic Institute (DHI)).

DHI (2014b). MIKE 11 A Modelling System for Rivers and Channels: Reference Manual (Hørsholm, Denmark: Danish Hydrologic Institute (DHI)).

Dilts, T. (2010). Topography Tools 9.3.

Essaid, H.I., and Hill, B.R. (2014). Watershed-scale modeling of streamflow change in incised montane meadows. Water Resour. Res. *50*, 2657–2678.

Euston-Brown, D.I.W. (2006). Baviaanskloof Mega-Reserve Project: Vegetation mapping contract report on methodology, vegetation classification and short descriptions of habitat units (South Africa: Eastern Cape Parks & Tourism Agency).

Fenicia, F., McDonnell, J.J., and Savenije, H.H.G. (2008a). Learning from model improvement: On the contribution of complementary data to process understanding. Water Resour. Res. *44*, W06419.

Fenicia, F., Savenije, H.H.G., Matgen, P., and Pfister, L. (2008b). Understanding catchment behavior through stepwise model concept improvement. Water Resour. Res. *44*, W01402.

Fenicia, F., Kavetski, D., Savenije, H.H.G., Clark, M.P., Schoups, G., Pfister, L., and Freer, J. (2014). Catchment properties, function, and conceptual model representation: is there a correspondence? Hydrol. Process. *28*, 2451–2467.

Ganguly, S., Anav, A., Liang Xu, Samanta, A., Shilong Piao, Nemani, R.R., Myneni, R.B., Zaichun Zhu, Jian Bi, and Yaozhong Pan (2013). Global Data Sets of Vegetation Leaf Area Index (LAI)3g and Fraction of Photosynthetically Active Radiation (FPAR)3g Derived from Global Inventory Modeling and Mapping Studies (GIMMS) Normalized Difference Vegetation Index (NDVI3g) for the Period 1981... Remote Sens. *5*, 927–948.

Gao, H., Hrachowitz, M., Fenicia, F., Gharari, S., and Savenije, H.H.G. (2014). Testing the realism of a topography-driven model (FLEX-Topo) in the nested catchments of the Upper Heihe, China. Hydrol Earth Syst Sci *18*, 1895–1915.

Graham, D.N., and Butts, M.B. (2005). Flexible, integrated watershed modelling with MIKE SHE. In Watershed Models, V.P. Singh, and D.K. Frevert, eds. (Boca Raton, FL, USA: Taylor and Francis Group), pp. 245–272.

Gupta, H.V., Wagener, T., and Liu, Y. (2008). Reconciling theory with observations: elements of a diagnostic approach to model evaluation. Hydrol. Process. *22*, 3802–3813.

Gupta, H.V., Clark, M.P., Vrugt, J.A., Abramowitz, G., and Ye, M. (2012). Towards a comprehensive assessment of model structural adequacy. Water Resour. Res. *48*, W08301.

Hammersmark, C., Rains, M., and Mount, J. (2008). Quantifying the hydrological effects of stream restoration in a montane meadow, northern California, USA. RIVER Res. Appl. *24*, 735–753.

Hargreaves, G., and Samani, Z. (1982). Estimating potential evapotranspiration. J. Irrig. Drain. Div.-Asce *108*, 225–230.

Herr, J.W., and Chen, C.W. (2012). Warmf: Model Use, Calibration, and Validation. Trans. Asabe *55*, 1385–1394.

Hipsey, M.R., Vogwill, R., Farmer, D., and Busch, B.D. (2011). A multi-scale ecohydrological model for assessing floodplain wetland response to altered flow regimes (Christchurch: Modelling & Simulation Soc Australia & New Zealand Inc).

Holmes, P.J. (2012). Southern African Geomorphology: Recent Trends and New Directions (AFRICAN SUN MeDIA).

Hughes, D.A., Hannart, P., and Watkins, D. (2004). Continuous baseflow separation from time series of daily and monthly streamflow data. Water SA *29*, 43–48.

Jansen, H.C. (2008). Water for Food and Ecosystems in the Baviaanskloof Mega Reserve: Land and water resources assessment in the Baviaanskloof (Wageningen, The Netherlands: Alterra).

Jencso, K.G., and McGlynn, B.L. (2011). Hierarchical controls on runoff generation: Topographically driven hydrologic connectivity, geology, and vegetation. Water Resour. Res. *47*, W11527.

Jencso, K.G., McGlynn, B.L., Gooseff, M.N., Bencala, K.E., and Wondzell, S.M. (2010). Hillslope hydrologic connectivity controls riparian groundwater turnover: Implications of catchment structure for riparian buffering and stream water sources. Water Resour. Res. *46*, 18 PP.

Jenness, J. (2006). Topographic Position Index (tpi_jen.avx) extension for ArcView 3.x, v. 1.3a (Jenness Enterprises).

Kao, Y.-H., Liu, C.-W., Wang, S.-W., and Lee, C.-H. (2012). Estimating mountain block recharge to downstream alluvial aquifers from standard methods. J. Hydrol. *426–427*, 93–102.

Karen, I. (2009). A top–down approach to characterise aquifer–river interaction processes. J. Hydrol. *365*, 145–155.

Katsuyama, M., Tani, M., and Nishimoto, S. (2010). Connection between streamwater mean residence time and bedrock groundwater recharge/discharge dynamics in weathered granite catchments. Hydrol. Process. *24*, 2287–2299.

Knudsen, J. (1985). WATBAL User's Guide (Hørsholm, Denmark: Danish Hydrologic Institute (DHI)).

Loheide, S.P., and Booth, E.G. (2011). Effects of changing channel morphology on vegetation, groundwater, and soil moisture regimes in groundwater-dependent ecosystems. Geomorphology *126*, 364–376.

Loheide, S.P.I., and Gorelick, S.M. (2007). Riparian hydroecology: A coupled model of the observed interactions between groundwater flow and meadow vegetation patterning. Water Resour. Res. *43*, 16 PP.

van Luijk, G., Cowling, R.M., Riksen, M.J.P.M., and Glenday, J. (2013). Hydrological implications of desertification: Degradation of South African semi-arid subtropical thicket. J. Arid Environ. *91*, 14–21.

Lynch, S.D. (2003). Development of a Raster Database of Annual, Monthly and Daily Rainfall for Southern Africa (Pretoria, South Africa: Water Research Commission (WRC)).

Magruder, I.A., Woessner, W.W., and Running, S.W. (2009). Ecohydrologic Process Modeling of Mountain Block Groundwater Recharge. Ground Water *47*, 774–785.

Mander, M., Blignaut, J., van Niekerk, M., Cowling, R.M., Horan, M., Knoesen, D., Mills, A.J., Powell, M., and Schulze, R.E. (2010). Baviaanskloof-Tsitsikamma Payment for Ecosystem Services:

A Feasibility Assessment (South Africa: FutureWorks report for South African National Biodiversity Institute (SANBI)).

Maneta, M., Schnabel, S., and Jetten, V. (2008). Continuous spatially distributed simulation of surface and subsurface hydrological processes in a small semiarid catchment. Hydrol. Process. *22*, 2196–2214.

McDonald, M.C., and Harbaugh, A.W. (1988). A modular three dimensional finite difference groundwater flow model. In U.S. Geological Survey Techniques of Water Resources Investigations, (USA: USGS),.

McGlynn, B.L., McDonnell, J.J., Seibert, J., and Kendall, C. (2004). Scale effects on headwater catchment runoff timing, flow sources, and groundwater-streamflow relations. Water Resour. Res. *40*, W07504.

McGrane, S.J., Tetzlaff, D., and Soulsby, C. (2014). Influence of lowland aquifers and anthropogenic impacts on the isotope hydrology of contrasting mesoscale catchments. Hydrol. Process. *28*, 793–808.

McMichael, C.E., Hope, A.S., and Loaiciga, H.A. (2006). Distributed hydrological modelling in California semi-arid shrublands: MIKE SHE model calibration and uncertainty estimation. J. Hydrol. *317*, 307–324.

McMillan, H.K., Clark, M.P., Bowden, W.B., Duncan, M., and Woods, R.A. (2011). Hydrological field data from a modeller's perspective: Part 1. Diagnostic tests for model structure. Hydrol. Process. *25*, 511–522.

Midgley, J.J., and Scott, D.F. (1994). Use of stable isotopes of water (d and o-18) in hydrological studies in the Jonkershoek valley.

Mills, A., and Fey, M. (2004). Transformation of thicket to savanna reduces soil quality in the Eastern Cape, South Africa. Plant Soil *265*, 153–163.

Mills, A.J., and Cowling, R.M. (2006). Rate of Carbon Sequestration at Two Thicket Restoration Sites in the Eastern Cape, South Africa. Restor. Ecol. *14*, 38–49.

Mills, A.J., and Cowling, R.M. (2010). Below-ground carbon stocks in intact and transformed subtropical thicket landscapes in semi-arid South Africa. J. Arid Environ. *74*, 93–100.

Mills, A.J., Cowling, R.M., Fey, M.V., Kerley, G.I.H., Donaldson, J.S., Lechmere-Oertel, R.G., Sigwela, A.M., Skowno, A.L., and Rundel, P. (2005). Effects of goat pastoralism on ecosystem carbon storage in semiarid thicket, Eastern Cape, South Africa. Austral Ecol. *30*, 797–804.

Nathan, R.J., and McMahon, T.A. (1990). Evaluation of automated techniques for base flow and recession analyses. Water Resour. Res. *26*, 1465–1473.

Ohara, N., Kavvas, M.L., Chen, Z.Q., Liang, L., Anderson, M., Wilcox, J., and Mink, L. (2014). Modelling atmospheric and hydrologic processes for assessment of meadow restoration impact on flow and sediment in a sparsely gauged California watershed. Hydrol. Process. *28*, 3053–3066.

Ophori, D., and Tóth, J. (1990). Relationships in regional groundwater discharge to streams: An analysis by numerical simulation. J. Hydrol. *119*, 215–244.

Phillips, R.W., Spence, C., and Pomeroy, J.W. (2011). Connectivity and runoff dynamics in heterogeneous basins. Hydrol. Process. *25*, 3061–3075.

Powell, R. (2015). Recent degradation along the upper-middle reaches of the Baviaanskloof River-floodplain: An examination of drivers of change and best rehabilitation practices. PhD dissertation. Rhodes University.

Refsgaard, J.C., and Storm, B. (1995). MIKE SHE. In Computer Models of Watershed Hydrology, V.P. Singh, ed. (Water Resources Publications), pp. 809–846.

Roets, W., Xu, Y., Raitt, L., and Brendonck, L. (2008). Groundwater discharges to aquatic ecosystems associated with the Table Mountain Group (TMG) aquifer: A conceptual model. Water SA *34*, 77–88.

Ross, M.A., Tara, P.D., Donaldson, J.S., and Stewart, M.T. (1997). FIPR Hydrologic Model Users Manual and Technical Documentation. (Tampa, Florida: Center for Modeling Hydrologic and Aquatic Systems, University of South Florida).

Rupp, D.E., and Selker, J.S. (2006). Information, artifacts, and noise in dQ/dt − Q recession analysis. Adv. Water Resour. *29*, 154–160.

Savenije, H.H.G. (2010). HESS Opinions "Topography driven conceptual modelling (FLEX-Topo)." Hydrol. Earth Syst. Sci. *14*, 2681–2692.

Schulze, R.E. (1995). Hydrology and Agrohydrology: A Text to Accompany the ACRU 3.00 Agrohydrological Modelling System (Pretoria, South Africa: Water Research Commission (WRC)).

Seibert, J., and McDonnell, J.J. (2002). On the dialog between experimentalist and modeler in catchment hydrology: Use of soft data for multicriteria model calibration. Water Resour. Res. *38*, 1241.

Selaolo, E.T. (1998). Tracer studies and groundwater recharge assessment in the eastern fringe of the Botswana Kalahari, The Letlhakeng-Botlhapatlou Area. PhD dissertation. Vrije Universiteit.

Shen, C., and Phanikumar, M.S. (2010). A process-based, distributed hydrologic model based on a large-scale method for surface–subsurface coupling. Adv. Water Resour. *33*, 1524–1541.

Sigwela, A.M., Kerley, G.I.H., Mills, A.J., and Cowling, R.M. (2009). The impact of browsing-induced degradation on the reproduction of subtropical thicket canopy shrubs and trees. South Afr. J. Bot. *75*, 262–267.

Sivakumar, B. (2004). Dominant processes concept in hydrology: moving forward. Hydrol. Process. *18*, 2349–2353.

Sivapalan, M., Blöschl, G., Zhang, L., and Vertessy, R. (2003). Downward approach to hydrological prediction. Hydrol. Process. *17*, 2101–2111.

Smakhtin, V.U. (2001). Low flow hydrology: a review. J. Hydrol. *240*, 147–186.

Smit, S. (2013). Observation of changes in vegetation cover density in the Baviaanskloof catchment using field sampling and remotely sensed NDVI (Normalized Difference Vegetation Index). BSc Thesis. University of Applied Science Van Hall Larenstein.

Smith, T., Marshall, L., McGlynn, B., and Jencso, K. (2013). Using field data to inform and evaluate a new model of catchment hydrologic connectivity. Water Resour. Res. *49*, 6834–6846.

Soltau, L., Smith-Adao, L., and Bugan, R. (2011). Baviaanskloof resistivity survey to define water level and depth to bedrock (Stellenbosch, South Africa: Center for Scientific and Industrial Research (CSIR)).

Sophocleous, M.A., Koelliker, J.K., Govindaraju, R.S., Birdie, T., Ramireddygari, S.R., and Perkins, S.P. (1999). Integrated numerical modeling for basin-wide water management: The case of the Rattlesnake Creek basin in south-central Kansas. J. Hydrol. *214*, 179–196.

Steinwand, A.L., Harrington, R.F., and Groeneveld, D.P. (2001). Transpiration coefficients for three Great Basin shrubs. J. Arid Environ. *49*, 555–567.

Tague, C., and Band, L. (2004). RHESSys: Regional Hydro-Ecologic Simulation System-An Object-Oriented Approach to Spatially Distributed Modeling of Carbon, Water, and Nutrient Cycling. EARTH Interact. *8*.

Tague, C., McMichael, C., Hope, A., Choate, J., and Clark, R. (2004). Application of the RHESSyS model to a California semiarid shrubland watershed. JAWRA J. Am. Water Resour. Assoc. *40*, 575–589.

Tague, C., Valentine, S., and Kotchen, M. (2008). Effect of geomorphic channel restoration on streamflow and groundwater in a snowmelt-dominated watershed. Water Resour. Res. *44*, 10 PP.

Tetzlaff, D., McDonnell, J.J., Uhlenbrook, S., McGuire, K.J., Bogaart, P.W., Naef, F., Baird, A.J., Dunn, S.M., and Soulsby, C. (2008). Conceptualizing catchment processes: simply too complex? Hydrol. Process. *22*, 1727–1730.

Tetzlaff, D., Carey, S.K., Laudon, H., and McGuire, K. (2010). Catchment processes and heterogeneity at multiple scales—benchmarking observations, conceptualization and prediction. Hydrol. Process. *24*, 2203–2208.

Tromp-van Meerveld, H.J., and McDonnell, J.J. (2006). Threshold relations in subsurface stormflow: 2. The fill and spill hypothesis. Water Resour. Res. *42*, W02411.

Tromp-van Meerveld, H.J., Peters, N.E., and McDonnell, J.J. (2007). Effect of bedrock permeability on subsurface stormflow and the water balance of a trenched hillslope at the Panola Mountain Research Watershed, Georgia, USA. Hydrol. Process. *21*, 750–769.

Uhlenbrook, S., Roser, S., and Tilch, N. (2004). Hydrological process representation at the meso-scale: the potential of a distributed, conceptual catchment model. J. Hydrol. *291*, 278–296.

Vaché, K.B., and McDonnell, J.J. (2006). A process-based rejectionist framework for evaluating catchment runoff model structure. Water Resour. Res. *42*, W02409.

Van den Bos, R., Hoffman, L., Juilleret, J., Matgen, P., and Pfister, L. (2006). Regional runoff prediction through aggregation of first-order hydrological process knowledge: a case study. Hydrol. Sci. J. *51*, 1021–1038.

Wagener, T., Boyle, D.P., Lees, M.J., Wheater, H.S., Gupta, H.V., and Sorooshian, S. (2001). A framework for development and application of hydrological models. Hydrol Earth Syst Sci *5*, 13–26.

Welch, L.A., and Allen, D.M. (2012). Consistency of groundwater flow patterns in mountainous topography: Implications for valley bottom water replenishment and for defining groundwater flow boundaries. Water Resour. Res. *48*, n/a – n/a.

Winsemius, H.C., Savenije, H.H.G., Gerrits, A.M.J., Zapreeva, E.A., and Klees, R. (2006). Comparison of two model approaches in the Zambezi river basin with regard to model reliability and identifiability. Hydrol Earth Syst Sci *10*, 339–352.

Winsemius, H.C., Schaefli, B., Montanari, A., and Savenije, H.H.G. (2009). On the calibration of hydrological models in ungauged basins: A framework for integrating hard and soft hydrological information. Water Resour. Res. *45*, W12422.

Wittenberg, H. (2003). Effects of season and man-made changes on baseflow and flow recession: case studies. Hydrol. Process. *17*, 2113–2123.

Xu, Y., Titus, R., Holness, S.D., Zhang, J., and Tonder, G.V. (2002). A hydrogeomorphological approach to quantification of groundwater discharge to streams in South Africa. Water SA *28*, 375–380.

Xu, Y., Wu, Y., and Beekman, E.H. (2003). The role of interflow in estimating recharge in mountainous catchments. In Groundwater Recharge Estimation in Southern Africa, Y. Xu, and E.H. Beekman, eds. (Paris, France: UNESCO),.

Xu, Y., Lin, L., Jia, H., South Africa., and Water Research Commission. (2009). Groundwater flow conceptualization and storage determination of the Table Mountain group (TMG) aquifers: report to the Water Research Commission (Gezina, Pretoria: Water Research Commission]).

Young, P. (2003). Top-down and data-based mechanistic modelling of rainfall–flow dynamics at the catchment scale. Hydrol. Process. *17*, 2195–2217.

Young, P., Parkinson, S., and Lees, M. (1996). Simplicity out of complexity in environmental modelling: Occam's razor revisited. J. Appl. Stat. *23*, 165–210.

Yu, Z.B. (1997). Application of vector and parallel supercomputers to ground-water flow modeling. Comput. Geosci. *23*, 917–927.

Chapter 2 Multi-criteria calibration of a hydrologic model for a semi-arid, mountainous, meso-scale catchment

2.1 Introduction

Multi-criteria calibration procedures for hydrologic models provide means of making full use of available data and information about a catchment during calibration, and as a result can improve parameter identifiability and increase the resulting model's realism (Fenicia et al., 2008a, 2008b; Gupta et al., 2008; McMillan et al., 2011; Seibert and McDonnell, 2002; Vaché and McDonnell, 2006; Wöhling et al., 2013). In multi-criteria evaluation, model outputs are assessed against multiple performance measures, which can be derived from various types of data and can be chosen to target model's representation of different hydrologic processes. Such methods provide a formalized way to include 'soft data', referring to less quantitative information about catchment behavior and/or data that is less directly commensurable with model outputs than a gaged streamflow time-series, for example, in model evaluation (Seibert and McDonnell, 2002).

The use of multiple criteria and multiple data types in calibration becomes increasingly beneficial the more complex the model and the shorter or sparser the available time-series of hydrometric measurements. Hence, the use of additional data sources should be helpful in constraining parameterization for large, arid catchments, which often require complex

models because of their diverse and variable processes and flow paths (Maneta and Wallender, 2013; Maneta et al., 2008). The use of model performance criteria based on additional data types can assist model development and calibration for areas with relatively short or poor streamflow gage records. However the bulk of multi-criteria calibration studies have focused on demonstration and evaluation of the technique for small, well-instrumented catchments, focusing on the value of including particular data types or performance measures, often using a lumped model and two to three criteria (Efstratiadis and Koutsoyiannis, 2010).

My study quantified the benefits of the multi-criteria calibration in terms of improving model performance and parameter identifiability when applied to a semi-distributed model of a semi-arid, meso-scale catchment, the Baviaanskloof, South Africa. The catchment model was developed for the purpose of aiding catchment management decisions about land management and river restoration. The model performance criteria applied in calibration were selected to account for the conceptual model of the catchment's dominant flow pathways and the level of accuracy needed for the desired uses of the model output. It was hypothesized that the use of additional data types and criteria in calibration of the Baviaanskloof model would improve parameter identifiability and model performance compared to that which would be achieved using a single standard metric of model output fit to the short gaged streamflow record.

The catchment of the Baviaanskloof River is data poor, particularly in relation to its large size, topographic complexity, and variability of climate and streamflow. Accurate

catchment models would be a boon to catchment management efforts, particularly as this area supplies an important regional water supply reservoir. In order to address local catchment management questions around the impacts of land cover change and river restoration interventions, models would need to be semi-distributed in their representation of internal catchment processes. However, the catchment has only been gauged since 2012 and has a relatively short streamflow record against which a model could be assessed. Additional data sources, such as regional flow records, monthly groundwater records from farm irrigation systems, and surface flow presence-absence observations, do exist and could potentially be used to evaluate model accuracy. This study used all available data on streamflow and floodplain water table fluctuations, with multiple spatial and temporal scales, in the calibration of a semi-distributed model of the catchment. The utility of the additional information beyond the short-term gauged streamflow record was assessed in terms of additionally constraining model parameter values considered physically reasonable and improving calibrated model performance. This was done by comparing calibrated model performance measures and parameter ranges when using different calibration methods: (a) using only the Nash-Sutcliffe efficiency (NSE) of daily streamflow outputs, (b) using multiple criteria based only on the daily streamflow record, and (c) using criteria based onstreamflow, groundwater, and surface runoff data to determine model acceptability.

With highly parameterized, distributed models that use complex mechanistic algorithms to represent internal catchment processes, solely calibrating against a single goodness-of-fit measure, such as the root mean square error (RMSE) or the NSE of modeled catchment outlet streamflow, allows for potential acceptance of models that recreate catchment-scale

streamflow output for the calibration period reasonably well despite having physically inaccurate representations of internal processes (Gupta et al., 2008). For example, a model predicting high run-off production on hillslopes with high infiltration and evapotranspiration from a valley bottom, may predict similar catchment scale streamflow as a model in which there is little hillslope runoff but far less ET loss in the valley bottom. This may become a problematic source of unquantified uncertainty when the model structure is applied further in scenario modeling and/or if model outputs of internal processes or states are to be used for decision-making. Multi-criteria calibration can help to address this issue by including performance criteria that test realism of modeled internal processes to the degree that these are understood. The selection of criteria and thresholds of acceptability necessarily varies with the type of catchment and its dominant processes, the model structure being applied, data availability, and the purpose of the modeling exercise. Previous studies have used multiple model performance measures based on derived streamflow indices, streamflow data from different sub-catchment scales, groundwater fluctuations, soil moisture patterns, and isotope-derived water residence times and/or runoff source information, often tailored to test the accuracy of different internal model process representations and different scales of interest (Fenicia et al., 2008b, 2008b; Seibert and McDonnell, 2002; Tekleab et al., 2011; Vaché and McDonnell, 2006; Wöhling et al., 2013).

Employing multiple types of data to assess model performance should be particularly useful in constraining parameter values when modeling drier environments and larger catchment areas, both conditions that warrant more complex model structures (Maneta and Wallender, 2013; Maneta et al., 2008). In arid and semi-arid environments surface flows

may be discontinuous and runoff producing rainfall events have low frequencies. As such, the time-series of streamflow data required to characterize runoff responses to a range of weather events in a more arid environment, and to then test a model's re-creation of this, would need to be longer than for wetter catchments that have more frequent runoff-causing events. Other data types, such as groundwater and soil moisture fluctuation data, can compensate for this, yielding information about catchment processes in periods during which there is little measurable streamflow response. Larger catchment areas are more likely to encompass a wider variety of topographic units with more distinct slope, soil, and vegetation properties than smaller catchments, and hence have more heterogeneity in dominant hydrologic processes. Further adding to model dimensionality for large catchments, deep groundwater outflows and channel routing also become more important determinants of streamflow with increasing catchment size, and their explicit inclusion in meso-scale catchment models can increase accuracy (McGrane et al., 2014; Ophori and Tóth, 1990; Uhlenbrook et al., 2004).

As pointed out by Seibert and McDonnell (2002) and Freer et al. (2004), the relative uncertainty and commensurability of the available observational data and the model structure need to be considered to determine what kind of goodness-of-fit measures can be reasonably applied to the model's outputs. For example, observations such as localized point soil moisture or groundwater levels may be of different spatial or temporal scales than the model's outputs. Data and/or model outputs may need to be aggregated and in some cases only trends and patterns can be reasonably compared to model output, as opposed to absolute values. The relative uncertainty of different observational data can be considered

using wider thresholds of acceptability or lower weightings for certain criteria compared to those derived from data thought to be more accurate and directly commensurable. When more subjective decision-making is required to establish the points for comparison, the data and derived criteria are considered 'soft' (Seibert and McDonnell, 2002).

The choice of which and how many model performance criteria to use is often subjective (Seibert and McDonnell, 2002; Zheng and Keller, 2007a). Seibert and McDonnell (2002) used 27 criteria while Vaché and McDonnell (2006) used three to guide calibration of models of similar levels of complexity for the same micro-scale study catchment, albeit with different goals: the former to demonstrate usefulness of the available soft data in calibration, and the later the usefulness of isotope derived mean residence time data. Even if only catchment-scale streamflow data are available, there are multiple streamflow diagnostics, such as model fit to seasonal flow distribution, dry period flow, or recession characteristics, that can help constrain parameters relevant to baseflow production processes and be used as additional criteria to those that favor good fits to high flows, such as NSE and RMSE (e.g. Fenicia et al., 2008b; Tekleab et al., 2011; Wöhling et al., 2013). Gupta et al. (2008) suggest that a model should be evaluated against a number of diagnostics equal to the number of degrees of freedom in the model structure, matching the number and complexity of processes being explicitly considered. This would be the natural outcome of a model structure that has been derived from process diagnostics in the available data, under a 'top-down' model development approach (Sivapalan et al., 2003). However, this method of model development is not generally adhered to or even feasible in many applied modelling exercises. There is rarely sufficient data for this level of evaluation for semi-distributed and

distributed model structures. In my study, a selection of performance measures based on the available data were chosen to assess model representation of processes thought to be dominant according to the conceptual model of the catchment and of those presumed to change under the vegetation and river channel scenarios of interest. Measures were also selected to assess model accuracy in reproducing outputs of interest for water supply management.

Various techniques have been applied to select optimum or acceptable/behavioral models and parameter sets in a multi-criteria calibration procedure: accepting only parameter sets that lie on the Pareto optimum front for all the goodness-of-fit measures (Fenicia et al., 2008a, 2008b), setting thresholds of acceptability for each of the goodness-of-fit measures (Seibert and McDonnell, 2002), and/or scaling and weighting measures for combination into one objective function in a GLUE-based method (Generalized Likelihood Uncertainty Estimation - Beven and Freer, 2000; Winsemius et al., 2009). Thresholds of acceptability for performance measures or objective functions are generally arbitrarily chosen (Siebert & McDonnel 2002, Fenicia et al 2008). In my study the desired use of the model output was explicitly considered in the criteria and threshold selection, similar to the uncertainty assessment procedure suggested by Zheng and Keller (2007b). This was done by estimating a minimum level of accuracy needed for different model outputs to be of practical assistance to decision-making to determine if the model is 'fit-for-purpose.' Ideally this would be done through stakeholder engagement with formal risk and value assessment, but here thresholds were chosen by the researcher.

2.2 Methods

2.2.1 Conceptual numeric model of the Baviaanskloof catchment

Based on catchment characteristics, available data, and the desired use of the model to estimate the impacts of changes in vegetation and river channel change, a conceptual and numeric model structure was built for the Baviaanskloof catchment, as described in Chapter 1. This model uses different scales of representation for broad topographic units based on the information available about the process and the need to change its parameterization in scenario modeling. The topographic units considered were plateaus, hillslopes, cliffs, canyon floors, alluvial fans, and the main valley floodplain. Surface and subsurface flows for mountain tributary subcatchments, made up of plateaus, hillslopes, cliffs, and canyon floors, were modeled more simply than for alluvial fans and floodplains. More is known about the dynamics and connectivity of the surface-subsurface flows and interactions in the floodplain than about the flow paths in the surrounding mountains and groundwater levels within the floodplain are of interest for local water supply. As such, the model was constructed in two parts. The first sub-model calculates the surface and subsurface flows leaving tributary subcatchments. The second sub-model routes these surface and subsurface inputs, plus direct rainfall inputs, across and through the alluvial fans and floodplain of the central valley, accounting for ET and channel-aquifer flow interaction (see Chapter 1, Figure 1-18 to Figure 1-20).

The MIKE-SHE/MIKE 11 modeling system (Refsgaard and Storm, 1995) was chosen for model construction as it allows for the multiple levels and spatial scales of process representation called for in the conceptualization of the catchment and can include coupled hydraulic-hydrologic modeling needed in order to consider the floodplain aquifer-channel flow interaction. External code written in MATLAB was used to link the outputs of the mountain tributary sub-model to the floodplain sub-model. Models were run at a daily time-step. Precipitation and PET time-series for each land unit were estimated by scaling the time-series of the nearest station using monthly precipitation and PET surfaces derived by (Lynch, 2003) and (Schulze, 2007).

A detailed description of the numeric model is given in Chapter 1 Section 1.1.4 and a more abridged account is given here. In the model of the mountain tributary subcatchments, canopy interception, infiltration, soil moisture storage, actual evapotranspiration (AET), vertical percolation, and surface runoff routing were calculated for each of the four land units in each tributary sub-catchment, while interflow and slow mountain bedrock groundwater flow were modeled as lumped linear reservoirs at the sub-catchment scale (see Chapter 1, Figure 1-19). Canopy interception was calculated using a canopy storage threshold value determined based on vegetation type average leaf area index (LAI). Through-fall to the soil surface in excess of the maximum infiltration rate was assumed to become surface runoff. Infiltration was limited by the available soil storage space such that saturation excess surface runoff was also possible. Routing of available surface water across each unit was calculated based on Manning's equation using the average slope and slope-length of the land unit and a vegetation type roughness coefficient. Surface runoff was

routed across land units in a catena from plateau through to canyon floor. Flow entering from an upslope unit was added to the surface pool available for infiltration and routing. ET withdrawal from soil was calculated based on the remaining PET demand after canopy interception limited by the vegetation type ET coefficient and available soil storage above wilting point, with ET rates being linearly curtailed below field capacity. Soil moisture in excess of field capacity percolates into the interflow reservoir. Interflow, presumably occurring at the rock-soil interface and/or in the highly fractured surface layer of the bedrock, was modeled as a simple linear reservoir with two outlets representing lateral flow into the alluvial aquifer and vertical percolation into the deeper mountain bedrock groundwater store. Slower outflow from the mountain bedrock aquifer to the alluvial aquifer was modeled using a linear reservoir with a single output constant.

Flows across and through the central valley alluvial fill were modeled with a coupled hydraulic-hydrologic model system in which groundwater flow was modeled through a 50 m resolution finite element grid governed by Darcy's Law, channel flow was modeled using a kinematic wave approximation, and exchange of flow between the river channel and the aquifer was calculated at riparian grid cells based on the difference in water surface elevation and the conductivity of the alluvium. Surface flow leaving the canyon floor units of tributary subcatchments was either input as a point source to the channel network or input as dispersed surface flow onto the alluvial fan surface, depending on whether or not the alluvial fan had been channelized. Interflow and mountain bedrock outflows were added as inputs to the alluvial aquifer boundary. The floodplain material was generalized as a loamy sand topsoil layer overlying a sand and cobble layer. Canopy interception of precipitation,

infiltration or runoff of through-fall, soil moisture storage and percolation to the water table, and AET were calculated by grid cell, however parameterization was uniform across the floodplain. If withdrawal from the unsaturated zone cannot meet remaining PET demand, vegetation ET withdrawals were permitted from the saturated zone when the water table occurred within the rooting zone.

In the diffusive wave hydraulic model, surface flows were routed through a channel network defined by cross-sections and channel slopes specified at 500m spacing. Model cross-sections span the floodplain such that overbank flows can be considered, with separate roughness values specified for the channel and the floodplain. Channel cross sections and slopes were obtained through topographic survey while a 30 m DEM (NASA Shuttle Radar Topography Mission data) was smoothed and aggregated to 50 m resolution to specify the floodplain topography. Measured channel cross sections were interpolated to stream network nodes matching the groundwater grid cells. Average daily channel water surface elevations at these nodes in the hydraulic model were compared to the groundwater table elevation to calculate the direction and magnitude of the exchange of water between the two and both models were then updated. Overbank flows in the hydraulic model were made available for infiltration on the hydrologic model grid cells they would cover, after which the channel flow model volume was updated.

Table 2-1 A-priori and calibrated values ranges for vegetation and soil parameters *(calibrated values italicized)*

Parameter	Landscape unit				
	Plateau	**Hillslope**	**Cliff**	**Canyon**	**Floodplain and fan**
Dominant vegetation	fynbos	thicket	thicket	forest	savanna
Percent of catchment	29%	40%	17%	10%	5%
Leaf area index, LAI	1 - 3 *1.3 - 3*	0.4 - 1 *0.44 - 0.68*	0.2 - 0.6 *0.2 - 0.53*	3 - 5 *3 - 4.8*	1 - 3 *1.5 - 2.8*
Manning's n ($m^{1/3}/s$)	0.05 - 0.80 *0.07 - 0.80*	0.05 - 0.80 *0.07 - 0.80*	*same as hillslope*	0.10 - 0.80 0.35 - 0.80	0.050 - 0.70 F *0.050 - 0.46* 0.020 - 0.050 C *0.026 - 0.038*
ET coefficient	0.40 - 0.60 *0.43 - 0.59*	0.30 - 0.50 *0.34 - 0.47*	0.20 - 0.40 *0.22 - 0.36*	0.70 - 0.90 *0.71 - 0.90*	0.80 - 1.0 *0.90 - 1.0*
Root depth (mm)	500 - 1,000 *610 - 1,000*	300 - 800 *560 - 800*	*200*	5,000 - 10,000 *6,000 - 10,000*	10,000 - 35,000 R *15,000 - 29,800*
Soil depth (mm)					600 - 1,000 T *650 - 916*
Saturated water content	0.30 - 0.50 *0.35 - 0.49*	0.30 - 0.50 *0.31 - 0.49*		0.40 - 0.60 *0.41 - 0.50*	0.40 - 0.55 T *0.42 - 0.55* 0.30 - 0.45 A *0.30 - 0.37*
Field capacity	0.14 - 0.24 *0.16 - 0.22*	0.14 - 0.24 *0.14 - 0.22*	*same as hillslope*	0.24 - 0.36 *0.25 - 0.30*	0.25 - 0.38 T *0.28 - 0.36* 0.12 - 0.18 A *0.12 - 0.15*
Wilting point	0.075 - 0.12 *0.087 - 0.12*	0.075 - 0.12 *0.078 - 0.12*		0.080 - 0.12 *0.082 - 0.10*	0.085 - 0.12 T *0.092 - 0.12* 0.060 - 0.090 A *0.060 - 0.073*
Maximum infiltration rate (mm/hr)	1.0 - 3.5 *2.9 - 3.4*	1.0 - 1.6 *1.4 - 1.6*		35 - 350 *175 - 342*	K_{sat} 50 - 300 T *82 - 241* K_{sat} 10 - 1,700 A *51 - 400*

Table 2-2 A-priori and calibrated value ranges for the time constants of the linear reservoirs representing subcatchment groundwater flows *(calibrated values italicized)*

Parameter	Linear reservoir	
	Interflow	**Mountain bedrock**
Lateral outflow time constant (days)	10 - 150 *35 - 56*	10,000 - 150,000 *100,300 - 114,910*
Vertical percolation time constant (days)	1 - 300 *61 - 188*	

The resulting combined model for the entire catchment area had 42 calibration parameters and the a-priori ranges of these are listed in Table 2-1 and Table 2-2. These value ranges were informed by the flow and groundwater data patterns (Chapter 1), local sampling and remote sensing of vegetation and soil properties (van Luijk et al., 2013; Mills and Cowling, 2006, 2010; Mills and Fey, 2004; Mills et al., 2005; Smit, 2013), and review of parameter values estimated for similar vegetation types and geomorphological settings (Consoli et al., 2013; Ganguly et al., 2013; Hammersmark et al., 2008; McMichael et al., 2006; Schulze, 1995, 2007; Steinwand et al., 2001; Tague et al., 2004). Several parameters (roughness, soil physical properties, excluding soil depth) for the cliff areas were assumed to be similar enough to those on the hillslopes to warrant assignment of the same parameter values in the model, thereby reducing dimensionality of the calibration. Field observations of surface flows and groundwater levels in the Baviaanskloof suggested significant recharge of the alluvial aquifer via mountain slope interflow and sizable contributions of subsurface flow via the alluvial aquifer to the total water yield (20-50%), as in Chapter 1.

2.2.2 Model performance criteria and calibration procedure

The parameter value ranges were constrained through the calibration process by selecting parameter sets for which model outputs were considered acceptable in terms of multiple 'goodness-of-fit' performance criteria (Table 2-3). Four hard data criteria were applied based on the gaged streamflow record, while six additional soft data criteria were considered based on other available information. Simple thresholds of acceptability were applied for each criterion, such that all parameter sets for which model output met all the criteria were considered equally acceptable. Given likely uncertainties in the observational data, improved goodness-of-fit of model outputs to the observational dataset beyond a certain threshold may not actually represent a true improvement in model realism. The calibration criteria and their limits of acceptability were selected based on the available data, dominant processes in the catchment, and processes and model outputs of particular importance for the desired end use of the model, as described further below. The measured daily streamflow at the catchment outlet from 2012-2013 was considered hard data, being directly commensurable with model outputs. The estimated monthly long-term streamflow record (1991-2013) was based on combined reservoir inflow and regional gage data, rather than local measurement in the Baviaanskloof River, and was therefore considered soft data. Due to spatial and temporal commensurability and process representation simplifications in the model, the measured groundwater data and tributary outflow presence were also considered soft data. Data regarding hillslope surface run-off presence was directly used to constrain the allowable value range for hillslope vegetation and soil parameters prior to

calibration (Chapter 1) and so was not used to evaluate model output as all parameter sets would necessarily meet this criterion.

The groundwater linear reservoir time constants were predicted to have a large impact on model output in relation to the a-priori uncertainty in their values. This was confirmed through initial exploratory model testing using the minimum and maximum parameter values of the a-priori ranges. As such, an initial set of 5,000 calibration model runs were performed in which only the three groundwater linear reservoir parameters (Table 2-2-2) were varied, while all other parameters were held at the mean values of their a-priori ranges. This was done to constrain the value ranges for these parameters to be used in the full calibration exercise in which all 42 parameters were varied, allowing for a more thorough exploration of the more constrained input parameter space with fewer model runs. Given that the other parameters were not varied in these runs, a generous streamflow NSE acceptability threshold of 0.5 was applied to do this initial reduction of value ranges for these three parameters.

In the full calibration exercise, 10,000 parameter sets were tested over the revised a-priori parameter space. Parameter value probability distributions within the a-priori ranges were considered uniform and the trialed parameter sets were selected from the a-priori parameter space using Latin Hypercube sampling (McKay et al., 1979). Model outputs for each parameter set were compared to the limits of acceptability for each model performance measure to determine its inclusion or exclusion from the calibrated set. To assess the impact of the inclusion of the different types of data and criteria in the calibration, acceptable

parameter set selection was done separately for three different levels of calibration: (a) using a single hard data criterion, the NSE of modeled streamflow; (b) using all four hard data criteria; and (c) using all ten hard and soft criteria. The resulting parameter value ranges and model output performance measures for accepted sets were compared between these three cases.

The calibrated model of the Baviaanskloof catchment is to be used in assessing likely impacts of different management scenarios on both local and regional water supplies. Water users within the catchment rely on groundwater in the floodplain aquifer while downstream users rely on streamflow water yield reaching the catchment outlet which feeds a major water supply reservoir. Model evaluation criteria were therefore selected to assess model performance in capturing fluctuations in both floodplain aquifer levels and catchment outflow. As described below, modeled water levels in the floodplain aquifer were not expected to be directly commensurable to water table measurements at specific locations; however the magnitude of spatially average water table fluctuation in the model can be expected to fit the averaged fluctuation of the observed values. Being able to predict the range of this fluctuation to within 0.5 m accuracy was assumed to be a reasonable threshold of acceptability to assess impacts on groundwater availability. Ideally this threshold value would be selected by stakeholders, based, for example, on the magnitude of fluctuation and duration of low levels that would cause a significant increase in pumping costs.

Table 2-3 Model performance criteria and limits of acceptability

Type	Data	Time period	Model performance measure	Limit of acceptability
Hard	Streamflow (daily)	2012-2013	NSE of daily flow	≥0.7
	Streamflow (daily)	2012-2013	NSE of log daily flow	≥0.6
	Streamflow (daily)	2012-2013	Absolute error in average daily flow (m^3/s)	≤0.5
	Streamflow (daily)	2012-2013	Absolute error in annual maximum monthly flow (m^3/s)	≤1
Soft	Streamflow (monthly)	1991-2013	NSE of monthly flow	≥0.7
	Streamflow (monthly)	1991-2013	NSE of log flow monthly flow	≥0.6
	Tributary catchment outflow presence	2012-2013	Absolute error in duration of flow per month (days)	≤3
	Streamflow connectivity across wide floodplain reach	2012-2013	Absolute error in duration of channel flow connectivity (weeks)	≤1
	Floodplain water table depth (monthly)	2012-2013	R^2	≥0.7
	Floodplain water table depth (monthly)	2012-2013	Error in min-max value range (m)	≤0.5

For downstream water users, the reservoir storage buffers supply availability against shorter-term streamflow fluctuation on the orders of days to months. However, prolonged dry periods of several months to years have resulted in shortages and water-use rationing in the past, and high flood flows during relatively wet periods have resulted in significant uncontrolled reservoir overflow volumes, which could be considered a loss of potential supply (Jansen, 2008). Therefore, while the accuracy of daily streamflow inputs to the

reservoir is not critical to water supply management if longer term yields are accurate, estimating magnitudes of seasonal highs and long duration low flow periods is important for the model's applied use. These were considered based on the accuracy of the monthly averaged flow for the highest flow month in the record and of the annual average flow. A 1 m^3/s accuracy for peak month averaged flow was assumed acceptable based on the estimated order of magnitude of the monthly inflow likely to result in uncontrolled spillage. On average the Kouga Dam has 32 million m^3 of available storage space. From this average starting state, a month with a mean inflow of 12 m^3/s would completely fill the storage, accounting for average rates of controlled outflow and dam surface evaporation. The Baviaanskloof River contributes roughly a third of the incoming flow to the dam on average during high flow events, meaning a 4 m^3/s mean monthly flow rate in the Baviaanskloof is likely to be associated with overflow. A 0.5 m^3/s accuracy was assumed acceptable for annual averaged daily flow, being 10% of the maximum daily water demand from the reservoir, reflecting the need to ascertain whether long term average inflows are less than average water demand. Again, these thresholds should ideally be selected by those managing the water supply systems and these values are proposed for demonstration.

Other than model fit to observed outputs that are of direct interest to water users, additional indicators of accuracy and internal process realism were also applied. The NSE of catchment outlet streamflow and of logged flow values were used to assess overall model fit to both high and low flows. While the accuracy of modeled daily streamflow may be of less direct importance for water supply management, the model is to be used to investigate scenarios with different floodplain channel properties, which can impact overbank flooding

during peak flows occurring at daily or sub-daily time-steps, and also impact groundwater-channel interactions during low flows, observed to change notably over periods of weeks. Although the time-series of daily streamflow values for this assessment was relatively short, 2 years, these measures were also applied to monthly estimated flows for the 22 year period from 1991-2013. Thresholds of acceptability for NSE were set at 0.7, based on commonly achieved NSE values for semi-distributed models in literature, and cognizant of likely uncertainties in the observational data to which model outputs are compared. The thresholds for the NSE of logged streamflow was set at 0.6 because of the greater difficulty in capturing low flows, which are controlled by less well described subsurface processes, and the lower need for daily accuracy in daily low flow estimation. The estimated 22 year time-series was considered to have greater uncertainty than the more directly measured 2 year series, however if possible errors in the longer term data were not consistently above or below the actual streamflow, monthly accumulated output can be expected to be more accurate than the daily values. Hence the same NSE thresholds were applied when comparing model outputs to the long-term, monthly estimated values as for the short-term daily observed data.

A significant portion of the catchment outflow, as much as 50%, is likely to pass through subsurface pathways via the floodplain alluvial aquifer (Chapter 1). As such, representation of processes affecting flow through the aquifer is predicted to be important to both capturing low flows and long-term yields. In addition, to examine floodplain channel change scenarios that impact the alluvial aquifer-channel exchange, accuracy in modeling the water level fluctuations in the alluvial aquifer are important. However, the level of information on

the spatial variability and distribution of aquifer material properties is limited and the time-series of groundwater level observations are too sparse to compare to detailed, spatially variable modeling of the floodplain aquifer. Given a spatially uniform set of aquifer material properties applied in the model, assumed to represent the effective average, and a 50 m grid size, comparison of point groundwater table observations to corresponding grid cell outputs would be inappropriate. The pattern of fluctuation in the average groundwater depth over monitored sites in the central floodplain was therefore compared to that of the average floodplain groundwater level in the model using the R^2 correlation coefficient. This accounts for the fit of the pattern of fluctuation, allowing for differences in absolute value and amplitude. The need for accuracy in fluctuation amplitude was considered in a separate criterion. The connectivity of the aquifer to the stream is captured in a criterion looking at the connectivity of flow across the gauged wide floodplain reach that has surface flow quasi-seasonally. When streamflow ceases along this reach, the average groundwater table in the floodplain must sit below the channel depth. Because of the simplified representation of the aquifer and the channel and the spatial variability of their connectivity, model accuracy of exceedance of a specified threshold aquifer depth for channel connectivity was not used as a criterion, rather a general match to the amount of time the channel was dry was used.

Data on the presence of surface runoff at the scale of tributary catchments and the duration of streamflow connectivity across the floodplain were used as additional soft data checks on process representation. The available data on these processes are limited in duration and spatial extent and so relatively generous limits of acceptability were applied. Capturing the frequency and magnitude of flows reaching alluvial fans from the tributary

catchments is important for assessing the impact of the fan channel property scenarios. Similarly capturing the general patterns of connectivity between the floodplain channel and the alluvial aquifer is important for assessing the impact of floodplain channel incision scenarios. During 2012-2013 surface flow was detected for 5 days in a single event (October 2012) at an instrumented tributary catchment during the observation period, with no flow in the channel for the remainder. Catchment residents observed 3-7 days of tributary surface flow at other locations during this event, and 2-5 days of flow during the July 2012 flood event. The number of days per month with modeled surface outflow leaving any tributary catchment was compared to these observations, accepting a 3 day margin of error for the presence of surface flow in both months. In the floodplain, streamflow was detected at all monitored points for 94 out of the 104 weeks in the monitoring period, with channel reaches in the middle of the wide floodplain areas being dry for 10 weeks prior to the July 2012 floods. Given that model topography, bed infiltration rates, and spatial distributions of groundwater levels are generalized and small changes could make a difference between a low flow and zero flow, a one week margin of error was considered acceptable for model output of non-zero streamflow at nodes in the central floodplain.

2.2.3 Parameter sensitivity and uncertainty analyses

Model sensitivity to different parameters was assessed using an adjusted regional sensitivity analysis advocated by Fenicia et al. (2008a), in which the spread of parameter

values in the acceptably behavioral parameter sets (those for which model output met all criteria) is used as an indicator of sensitivity. Cumulative density plots were made for the values of each parameter in the accepted sets for visual analyses. Ranges of values having steeper slopes in the cumulative density plot are regions of identifiability, being the value ranges where the majority of behavioral model outputs were produced. In addition, two numeric sensitivities indices (SI) were calculated for each parameter. The first, referred to here as SI_1, looked at the relative spread of values of a parameter within the accepted parameter sets, as in Seibert and McDonnell (2002):

$$SI_{1X} = \frac{X_{Ap90} - X_{Ap10}}{X_{Amed}}$$

Equation 1

SI_{1X} is the sensitivity index 1 value for parameter X, X_{Ap90} is the value of parameter X that is the ninetieth percentile of all values of X in the accepted parameter sets, X_{Ap10} is the tenth percentile value of X in the accepted sets, and X_{Amed} is the median value of X in the accepted sets. Lower values of SI_1 indicate a narrower range of acceptable values compared to the median, hence a greater sensitivity of model acceptability to a change in value of this parameter.

SI_1 does not include any consideration of the magnitude of a-priori uncertainty in the value of the parameter, which represents the understanding of the catchment properties and processes gleaned from initial field observations and literature. A second sensitivity index,

SI_2, was also calculated for each parameter to take this into account. This index compared the magnitude of the accepted range of values to the magnitude of the a-priori value range:

$$SI_{2X} = \frac{X_{Amin} - X_{Amax}}{X_{min} - X_{max}}$$

Equation 2

SI_{2X} is the sensitivity index 2 value for parameter X, X_{min} is the minimum and X_{max} is the maximum value of parameter X in the a-priori range of values of X tested in the calibration exercise, and X_{Amin} is the minimum and X_{Amax} is the maximum of all values of parameter X in the accepted parameter sets when the calibration criteria have been applied. Lower values of SI_2 therefore indicate a greater sensitivity of model acceptability to the choice of a parameter value within the range of values originally considered possible (the a-priori range).

Sensitivity analyses were done for parameter sets selected in the different levels of calibration: applying only the threshold of acceptability for streamflow NSE, applying all hard data criteria, and applying all hard and soft data criteria. This allowed assessment of any increase in parameter identifiability gained by including additional criteria types in the calibration. This would be seen as a region of increased slope in the cumulative density plots and a decrease in SI_1 and SI_2 values. The ranking of different parameters in terms of model sensitivity was compared between calibration levels. A change in sensitivity values and rankings of parameter can highlight catchment processes that are better evaluated by inclusion of the additional criteria.

If model performance is insensitive to the value of a parameter within the tested value range this can suggest that the model structure is too highly parameterized relative to the data being used to discern appropriate parameter values. However, if the range of parameter values tested in the calibration exercise is relatively small, for example if values are well constrained a-priori by commensurable field data or other information, insensitivity over a small tested range of values for a parameter may not pose a significant problem for uncertainty and further application of the model. This could be tested by subsequently widening the range of parameter values tested for those with little sensitivity over the initial range, in order to see if sensitivity does or does not increase over the widened range. There is also the possibility that more realistic values lie outside the tested range. This was not explored here and it was assumed that the tested parameter value ranges were sufficiently wide.

2.3 Results

2.3.1 Model performance

Calibration of the proposed Baviaanskloof catchment model was successful in that parameter sets were found within the a-priori parameter space which satisfied all the model performance criteria applied for various streamflow and groundwater patterns (criteria listed in Table 2-3). Of the 10,000 parameter sets tested, 55% met the NSE threshold, 8% met all four hard criteria, and 7% met all hard and soft criteria. The ranges of model output

performance measures for the different calibrated sets, those accepted using the streamflow NSE threshold, those accepted using all the hard data criteria, and those accepted using all hard and soft data criteria, are shown in Figure 2-1. Eight out of the ten calibration criteria applied constrained the accepted parameter space, while for two criteria, thresholds for error in duration of tributary catchment surface flow and the R^2 of floodplain water table fluctuation, all of the tested parameter sets produced acceptable output. Therefore the inclusion of these two criteria had no bearing on the calibration within the a-priori parameter space. As Figure 2-1 illustrates, only applying a NSE threshold for 2012-2013 daily streamflow did not select for models with acceptable low flows (seen as below-threshold values for the NSE of logged streamflow, Figure 2-1 B), long-term monthly streamflows (Figure 2-1 E), floodplain channel connectivity (Figure 2-1 G), or floodplain groundwater fluctuation patterns (Figure 2-1 H& I). Only models selected by directly applying all the effective hard and soft criteria ended up meeting all the performance measure criteria.

In general, the inclusion of additional criteria in the calibration improved model performance across the indicators used for the various patterns and processes, improving the means and/or the ranges of performance measure values for the selected set. This indicates that the additional hard and soft criteria did not require major performance trade-offs in order for the model to achieve acceptable results for the additional scales and processes being assessed by the extra criteria. If this had been the case, average calibrated model performance for some indicators would have decreased with the addition of extra calibration criteria. For example, the mean of streamflow NSE values for the calibrated set could have decreased when additionally selecting for models that recreated the groundwater level

fluctuation acceptably well. This did not occur (Figure 2-1). Across most performance measures, the inclusion of the additional hard data criteria beyond the NSE threshold resulted in a bigger gain in performance than the subsequent performance gains from the additional inclusion of the soft criteria. Nevertheless, applying the four hard data criteria alone was not sufficient to achieve adequate performance on all measures considered, resulting in inclusion of some parameter sets producing unacceptable errors in modeled channel flow duration and range in groundwater fluctuation (Figure 2-1 G&I).

The observed hydrographs, ranges of model streamflow output for the three different calibrated sets, and the mean of modeled flow for the hard and soft criteria calibrated set, are shown for 2012-2013 and 1991-2013 in Figure 2-2 and Figure 2-4. These figures illustrate the decreasing range in output values, or increase in model precision, as additional criteria were included into the calibration, particularly for peak flows. The variation in predicted mean 2012-2013 streamflows for all the models with acceptable NSEs spanned a range with a width that was 61% of the average value. The range of modeled mean flows was reduced to 15% of the average when applying the other hard data criteria and 13% when adding the soft.

Inspection of the 2012-2013 daily hydrographs showed that the additional hard and soft criteria served to improve both calibrated model accuracy and precision in prediction of the peak flows for the two major flood events in this period (July and October of 2012). This was also true for the recession of flow during the first few days after these peaks and for baseflow levels several months after each peak (i.e., September and December of 2012).

However, all models over-predicted streamflow during a period of about two weeks immediately following the July 2012 flood event and under-predicted flows over three weeks following the October 2012 flood event, regardless of the calibration method (Figure 2-2). This could indicate a failure of the model to adequately represent some storage of water, either in hillslope soils, the interflow zone at the bedrock surface, and/or the floodplain alluvium, which was replenished by the July 2012 rainfall, potentially persisting and creating antecedent conditions that resulted in a higher event runoff ratio in the October event and higher than modeled flows in its recession (Chapter 1). Predicted streamflow in all models was too responsive to smaller rainfall events, showing several small spikes in daily flow when the observed data showed little change (Figure 2-2). As would be expected, the effects of this were less pronounced when the data was aggregated monthly for comparison to the 1991-2013 estimated monthly time-series (Figure 2-4). There was some over-prediction of smaller peaks in monthly flow (those with month average flows under 2 m^3/s) and under-prediction of the higher monthly peaks; however, notable exceptions, such as over-predicting the late 1996 and the 2011 high flow months, indicate the error is not completely systematic.

The resulting mean NSE of modeled daily streamflow for 2012-2013 was 0.83 (range 0.70-0.92) for calibrated models when using the single NSE criteria calibration. Additionally applying the three other hard data criteria based on the observed daily streamflow time-series (NSE of logged streamflow, error in the mean, and error in maximum monthly flow) increased the mean NSE of calibrated models to 0.89 (range 0.76-0.92). Further applying the soft data criteria, which tested model capability to recreate monthly flows for 1991-2013, the

duration of tributary subcatchment surface flows, floodplain channel surface flow, and fluctuations in the floodplain aquifer water table, further constrained the accepted parameter sets such that the mean daily flow NSE of accepted models was 0.90 (range 0.87-0.92).

Model NSE values for the 22-year (1991-2013) estimated monthly streamflow time-series were generally lower than those for the short-term (2012-2013) daily gaged streamflow series (Figure 2-1 A vs E). The additional inclusion of the hard and soft criteria had a relatively small effect on the mean performance of calibrated sets for this indicator; however, they did constrain the range, excluding poorer performing sets. The mean 1991-2013 monthly flow NSE value was 0.80 (range 0.63-0.85) for models calibrated with the NSE threshold for 2012-2013 daily flow, while the mean was 0.81 (range 0.74-0.85) for those meeting all of the hard data criteria and 0.81 (range 0.79-0.85) for those meeting all hard and soft criteria. Although the fit of the model output to the estimated long-term monthly flow time-series was considered a soft data criterion, all models selected in the hard criteria only calibration also met the threshold of acceptability for this soft data performance measure (NSE≥0.7). This was not true for the short-term NSE criteria selected set, which included models producing unacceptable 1991-2013 monthly modeled flow NSE values (Figure 2-1 E).

As expected, values of model NSE for logged streamflow, in which low flow values have more weight in determining the NSE than they do in when using raw flow data, were lower than untransformed flow NSE values. The mean logged daily streamflow NSE for 2012-2013 was 0.58 (range 0.20-0.68) for the NSE criteria calibrated models, 0.64 (range

0.60-0.68) for the hard criteria calibrated models, and 0.62 (range 0.61-0.67) for the hard and soft criteria calibrated models. In this case, the addition of the soft data criteria slightly reduced model performance for the indicator. Opposite to the trend seen for the untransformed streamflow NSE values, the NSE values for 1991-2013 logged monthly flows were greater than those for the 2012-2013 logged daily flows: mean model NSE of logged monthly streamflow for 1991-2013 was 0.67 (range 0.56-0.70) for the daily flow NSE criteria calibrated models, 0.68 (range 0.62-0.70) for the hard criteria calibrated models, and 0.68 (range 0.66-0.70) for the hard and soft criteria calibrated models. Again all hard criteria calibrated models met the soft data criteria for long-term monthly logged flow NSE, which was not true for all the models selected using only the short-term daily NSE criteria.

Thresholds of acceptable error in the mean flow and in maximum monthly flow for 2012-2013 were used as additional hard data criteria and their inclusion improved the performance of the calibrated sets for these measures over that of the set selected only based on NSE of daily flow. The average error in mean flow for models selected based on NSE was 0.40 m^3/s (range 0.01-1 m^3/s), while it was reduced to 0.34 m^3/s in both the hard criteria (range 0.18-0.47 m^3/s) and hard and soft criteria (range 0.20-0.45 m^3/s) selected sets. The average error in maximum monthly flow was 1.54 m^3/s (range 0.01-5.1 m^3/s) in the NSE selected set, 0.49 m^3/s (range 0.01-0.97 m^3/s) in the hard criteria set, and 0.51 m^3/s (range 0.01-0.94 m^3/s) in the hard and soft criteria set. The addition of the soft data criteria did not improve the calibrated model set's performance on these measures, but did not reduce mean performance either. Adding the soft criteria reduced the number of models accepted,

reducing the range in flow error values by exclusion of both models with worse and those with better performance on these measures.

Figure 2-4 shows observed groundwater levels averaged across monitored sites in the central floodplain and the ranges of relative modeled groundwater elevations averaged over these locations in the model grid for the different calibrated sets. Groundwater depth data was transformed into relative elevation compared to the level on the date of the first observation point (15/01/2012) to allow for averaging across sites and comparison of fluctuation patterns between observed and modeled data. In general all models under-predicted the fluctuation of the floodplain groundwater table, having lower and less delayed peaks and smaller water table recessions in dry periods than observed. Model outputs from 50 m resolution grid cells with uniform soil and aquifer properties were not expected to be directly commensurable to point observations from a heterogeneous environment and so acceptability thresholds were purposefully relatively loose. However, all parameter sets tested had a floodplain groundwater fluctuation R^2 correlation coefficient of over 0.7 (Figure 2-1), therefore this soft data criteria did not constrain accepted parameter values within the a-priori parameter space. Other criteria, such as the error in the range of water table depths, duration of floodplain channel flow, fit to the estimated long-term month streamflow series, did constrain the calibrated sets such that the range of the modeled groundwater depths did narrow when more criteria were added (Figure 2-4). However there was no improvement in sets' mean groundwater pattern correlation to the observed data when additionally applying the hard and soft criteria to the NSE threshold selected set: the mean R^2 was 0.8 for all three calibrated sets. Application of the other three hard criteria resulted in rejection of both

better and worse performing models for this measure, while the other five soft criteria generally resulted in rejection of sets with lower R^2 values, such that the final range was 0.79-0.81 (Figure 2-1 H). Unlike the correlation threshold, the threshold of accepted error in the range of groundwater depth over the modeled period did restrict the parameter sets accepted. It reduced the range of outputs for this measure, rejecting poorer performing sets, but not making much change to the mean performance of the calibrated set (Figure 2-1 I). The mean error in the range of water table depths in the hard and soft criteria calibrated set was 0.35m (range 0.16-0.48m).

There was a wide range in the number of weeks of predicted channel flow across the central floodplain in the uncalibrated model and all three calibration levels reduced the error in the flow duration of the accepted model set. The hard and soft criteria did much more to improve performance on this measure than applying the daily streamflow NSE criterion alone (Figure 2-1): mean error for the set selected using only the NSE was 1.3 weeks (range 0.1-11.6 weeks), 0.2 weeks for the hard criteria set (range 0.1-1.4 weeks), and 0.1 for the hard and soft criteria selected set (range 0.13-0.14 weeks). As with some of the other soft data based performance measures, the inclusion of the additional hard data based criteria in calibration served to improve the calibrated model set's performance on this measure without directly selecting for models based on the measure.

Because the inclusion of the additional hard and soft data criteria resulted in an improved mean and reduced range of calibrated model NSE values, it appeared possible that simply increasing the stringency of the NSE acceptability threshold could produce similar

resulting performance of the calibration set as the application of the other hard and soft data criteria. This was tested by re-calibrating using a 2012-2013 daily streamflow NSE acceptability threshold of 0.87 instead of 0.70. The value 0.87 was selected because it was the minimum NSE value of models selected when using all the hard and soft data criteria. This higher NSE threshold reduced the percentage of accepted parameter sets from 55% to 22%. The greater selection stringency did serve to improve mean performance for several of the measures when compared to the NSE≥0.70 set, however models selected with the NSE≥0.87 threshold still included parameter sets with unacceptable performance against both some of the hard and some of the soft criteria, namely the NSE of logged 2012-2013 daily flow, maximum monthly flow, the NSE of raw and logged monthly 1991-2013 flow, and floodplain channel flow duration (Supplementary information, Figure 2-6).

Figure 2-1 Distribution of model performance measures used as calibration criteria for different sets of model runs: all parameter sets tested (All), those exceeding the NSE threshold (NSE), those meeting all hard criteria (H), and those meeting all hard and soft criteria (H&S).

Dotted lines show the threshold applied for the criterion. Thresholds for measures shown in graphs A-D were hard-data based criteria while those in E-I were soft-data based. 'Error' values are absolute values.

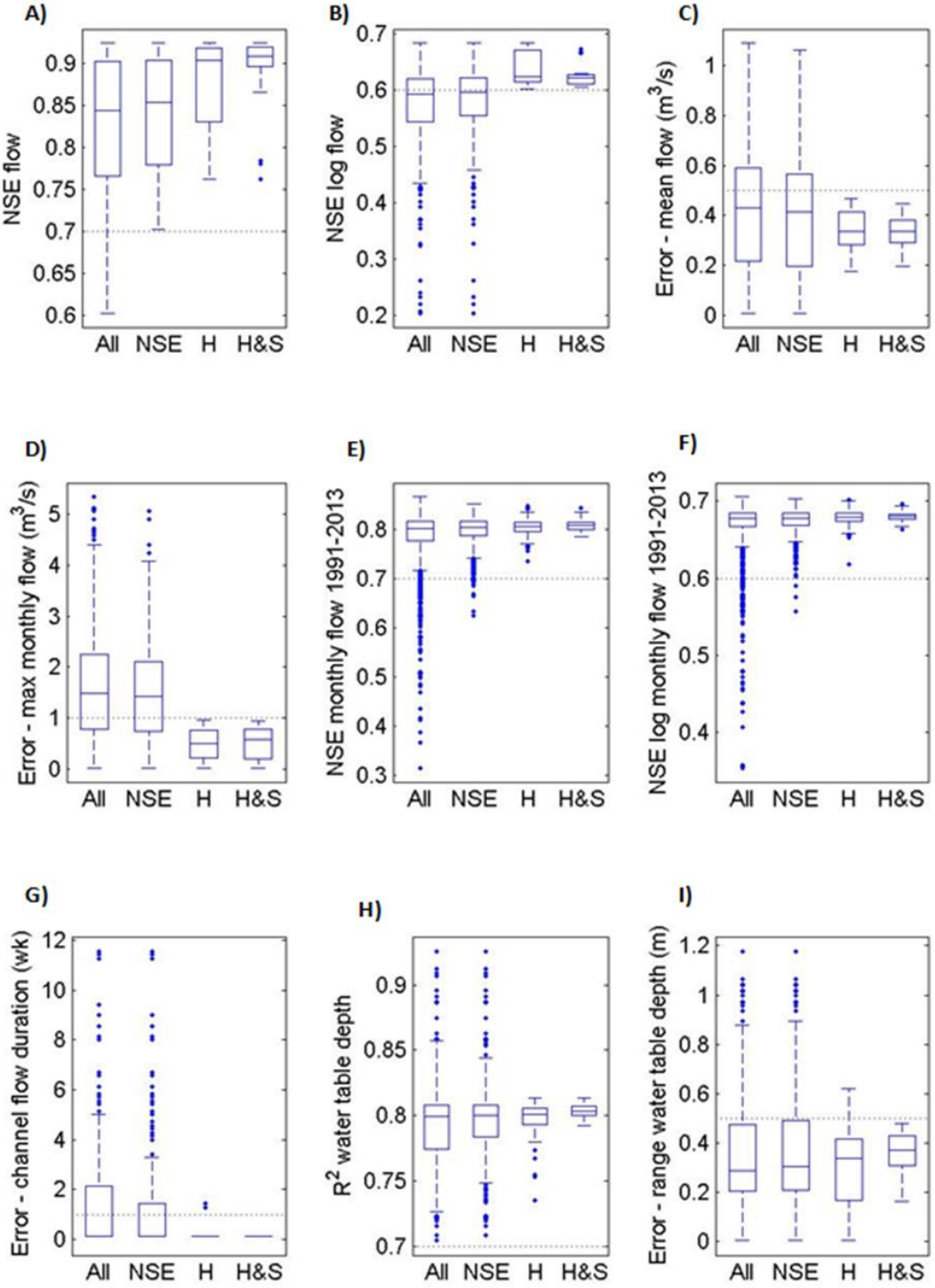

Figure 2-2 Observed and modelled daily streamflow for 2012-2013, showing the range of model output values for parameter sets selected using different performance measure criteria: NSE only, hard data criteria (H), and hard and soft data criteria (H&S) .

The period from 1/7/2012 to 1/1/2013 is shown at higher resolution below, including the major flood events of the observation period.

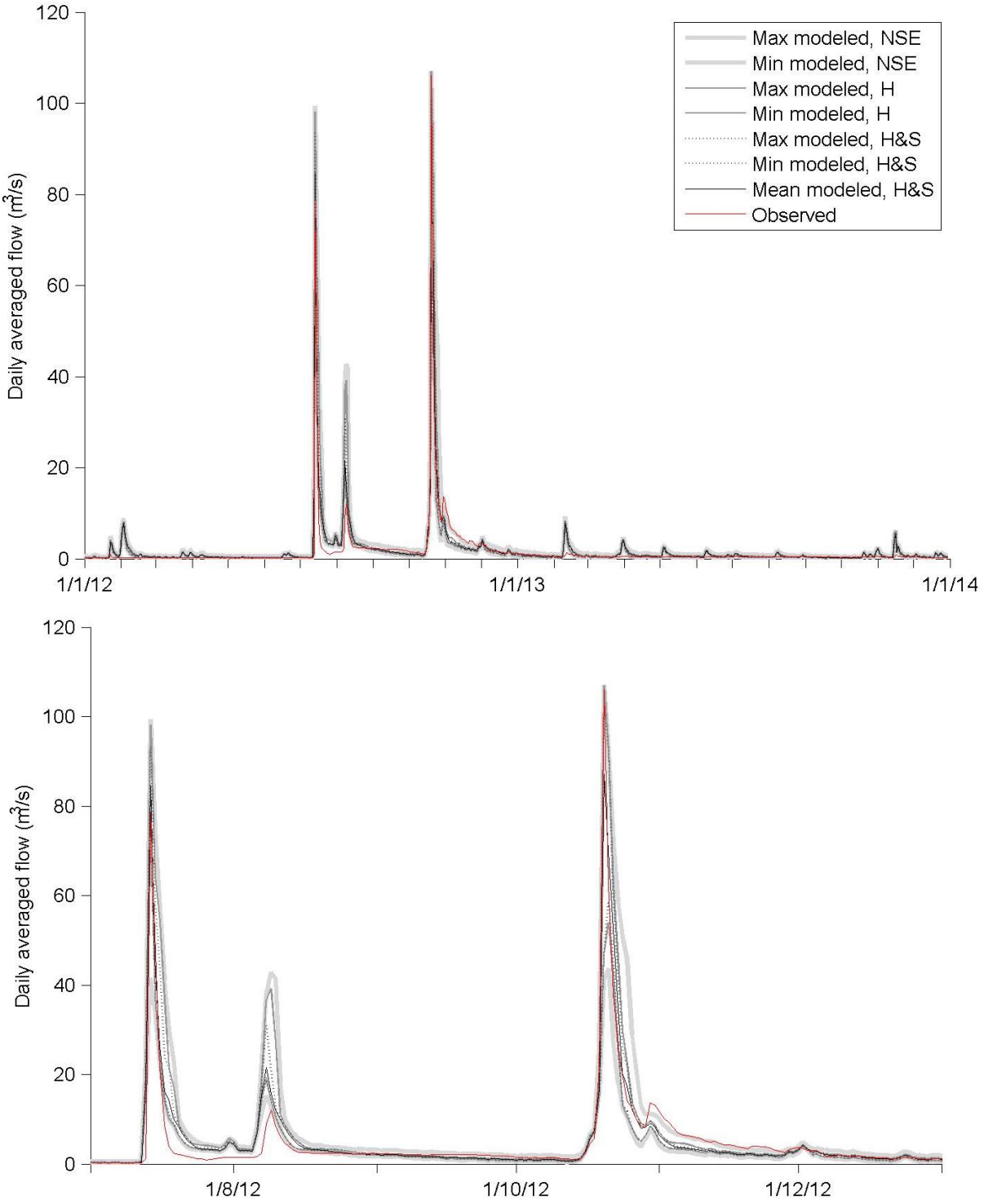

Figure 2-3 Monthly average streamflow for 1991-2013 as estimated from regional gages and as modelled using parameter sets for which output met hard (H) or both hard and soft (H&S) criteria

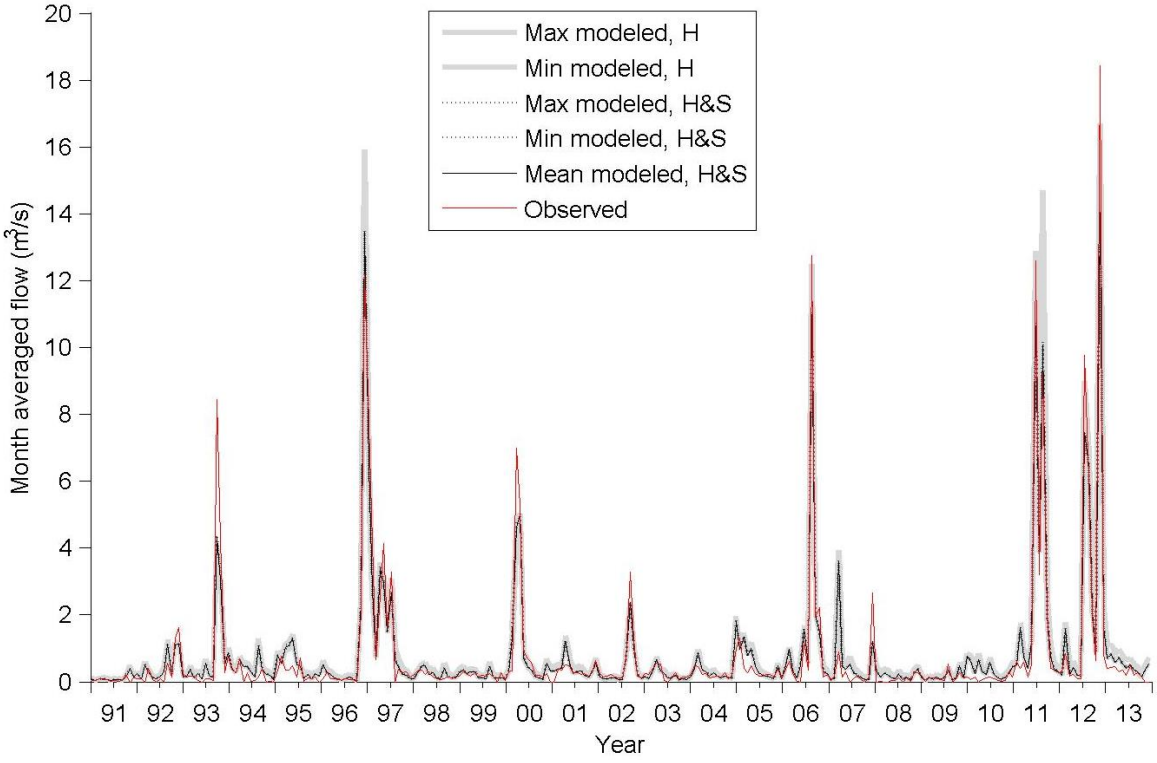

Figure 2-4 Observed and modelled average groundwater level (relative to first observed water table depth, 24/01/2012) at central locations in the alluvial floodplain for 2012 – 2013. The range of model output is shown for parameter sets selected using

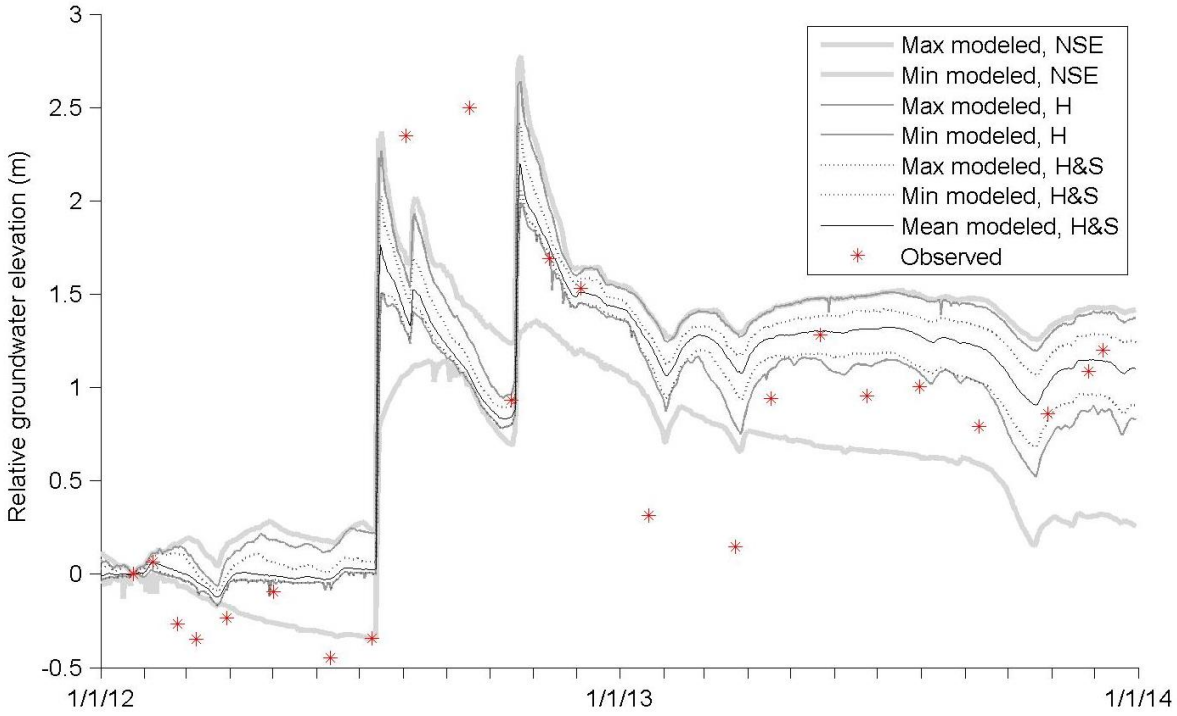

2.3.2 Parameter sensitivity and uncertainty

The parameters for which model acceptability was most sensitive to changes in parameter value, as indicated by sensitivity index 1 (SI1, Equation 1), differed somewhat with the calibration criteria applied. However, sensitivity to the values of the hillslope and plateau infiltration rates, the mountain bedrock aquifer outflow constant, and the evapotranspiration coefficient (ET_k) of the floodplain vegetation, were consistently high (Table 2-4 below and Table 2-7 in Supplementary Information). One or more of the floodplain material water retention properties (saturated soil moisture, field capacity, wilting point) were also consistently amongst the highest sensitivity parameters. The average parameter SI1 value for the calibrated set decreased by 12% from 0.55 to 0.48 when additionally including the extra hard data criteria beyond just using NSE threshold, and decreased by another 13% (to 0.42) when including the soft data criteria, showing a progressive increase in overall ability to constrain acceptable parameter values. The 0.42 mean SI1 value for the hard and soft calibrated set, was still relatively high, meaning that the average width of the value range from the 10^{th} to 90^{th} percentile of accepted parameter values is 42% of the median; however, there was a wide range in sensitivities between parameters with SI1 values ranging from 0.02 to 2.6. The parameters with the lowest sensitivity as measured by SI1 were the surface roughness (Manning's n) values for all land units, hydrologic conductivities (K_{sat}) of floodplain topsoil and cobble aquifer, and plateau and cliff vegetation LAI (Table 2-7). Low sensitivity to surface roughness was expected as much of the flow through the catchment was found to be subsurface and because the relatively high terrain slopes and use of a daily time-step would make roughness values less

significant in estimating the quantity and timing of surface runoff in the model when it did occur. Floodplain K_{sat} values were notably constrained in calibration, as described further below, however acceptable values still had a relatively wide range compared to the median, hence the high SI1 values compared to other parameters.

The additional hard criteria, which selected for model prediction of 2012-2013 low flows, high monthly flows, and the annual average, increased sensitivity to the values used for properties of the floodplain aquifer material, particularly the floodplain aquifer K_{sat} (SI1 decreased 31% from 1.9 to 1.3 for this parameter), and the interflow reservoir outflow time constant (SI1 decreased 37% from 0.9 to 0.5). Subsequent inclusion of the soft criteria, which selected for better fit to long term monthly flow patterns, groundwater level patterns, and floodplain channel connectivity, notably increased sensitivity to floodplain aquifer K_{sat}, floodplain material water holding properties, interflow time constants, and river channel roughness (Table 2-7). These criteria also resulted in increased sensitivity to soil water holding properties of the canyon floors in tributary catchments such that these were amongst the highest ranked parameters in terms of SI1 (Table 2-4). Although this a minor land unit in terms of area, all surface runoff from the plateau, hillslope, and cliff units passes through the canyons which have high infiltration capacities. Comparable to the role of the central valley floodplain at the scale of the entire meso-scale catchment, the canyons' capacity to hold water plays a role in determining the amount of surface and groundwater leaving the tributary sub-catchments, which appears to be notable in determining patterns of floodplain groundwater and/or long-term streamflow captured, as assessed by the soft data criteria.

Examining the change in range of accepted parameter values in the different calibration sets versus the parameters' a-priori ranges, as indicated by SI2 values (see Equation 2), highlighted several of the same key parameter sensitivities as SI1. SI2 additionally shows the calibration procedures' impact on constraining values of parameters for which relatively little prior information was available. The mountain bedrock outflow constant, the interflow constants, hillslope and plateau infiltration, and river channel roughness consistently were among the parameters with the lowest SI2 values, meaning that calibration most significantly limited the value ranges of these parameters compared to their a-priori ranges (see Table 2-5 and Table 2-8 in Supplementary Information). NSE threshold and hard data criteria calibration limited the ranges of parameter values related to hillslope and cliff thicket vegetation (ET_k , LAI, and root depth) more so than for some of other parameters that were ranked as more sensitive using SI1 (Table 2-4, Table 2-5). These parameters were not considered highly sensitive when ranked using SI1 because, even when constrained, the accepted value range was wide relative to the median value.

The change in SI2 values between calibration levels showed the effectiveness of the additional calibration criteria in constraining the parameter value ranges. The average SI2 value for the NSE only calibrated set was 0.87, meaning that the range of accepted values was 87% of the a-priori value range for the average parameter. Adding the hard criteria reduced the average SI2 by 13% to 0.76, while adding the soft criteria further reduced it by 20% to 0.61. The parameters for which the additional hard data criteria had the biggest effect on constraining the value range compared to the initial set were floodplain aquifer K_{sat} and the infiltration rates of the hillslopes and plateaus. The additional hard criteria did little

to further constrain the mountain bedrock outflow constant, already highly constrained by the NSE criteria, and less sensitive parameters such as the surface roughness of plateaus, hillslopes, and canyon floors. The subsequent inclusion of the soft data criteria had the biggest additional value-constraining effect on the interflow constant, the soil water retention properties of the canyon floors, and the floodplain aquifer K_{sat} (Table 2-5 and Table 2-8). This indicates that the values selected for these parameters influenced the long term flow patterns, groundwater fluctuations, and/or floodplain channel flow connectivity, and that these processes were not as well assessed using the calibration criteria for the hard data, meaning the short-term streamflow data, alone. The parameters for which the calibration procedures were the least effective in constraining the acceptable value ranges beyond their a-priori limits were surface roughnesses for the various landscape units, excluding the river channel, and LAI and ET_k parameters for the canyon floors and plateaus (Table 2-8, Supplementary Information).

Cumulative density plots for the nine parameters with the greatest sensitivities, looking at both SI1 and SI2 across the different calibration trials, are presented in Figure 2-5. These plots illustrate the regions of greatest value likelihood out of the range of values tested (plot x-axes span the a-priori range), seen as ranges with high slopes, and illustrate the increase in identifiability when calibrating with the additional hard and soft criteria, seen as increases in slope in the plots between different calibration sets. For example, the mountain bedrock outflow constant was highly constrained at a value close to 100,000 days in the NSE threshold calibration and the additional criteria did relatively little to further constrain the acceptable value. By comparison, values of the interflow reservoir vertical outflow

(percolation) time constant were noticeably more constrained to a region around 100-150 days when the additional hard criteria were included compared to calibration with just the NSE criterion. The calibrated values of infiltration rates for the hillslope and plateaus were concentrated close to the upper limit of the range of values tested, while the accepted floodplain aquifer K_{sat} values were clustered close to the lower end of the range. This could indicate that widening the ranges of values tested for these parameters may yield more models with improved performance. In both cases the value ranges for these parameters were limited a-priori by field observations, direct property measurements and plot scale surface runoff presence data, as described in Chapter 1. For the other parameters, the value ranges more frequently producing acceptable model outputs were located further from the limits of the range tested.

Table 2-4 Top ten parameters to which model acceptability was most sensitive, as assessed by Sensitivity Index 1, using different sets of model performance acceptability criteria

(PLT – plateau, HL – hillslope, CLF – cliff, CYN – canyon, FP – floodplain, MBR – mountain bedrock, SWC – saturated water content, SM – soil moisture, FC – field capacity, WP – wilting point, ET_k - evapotranspiration coefficient)

Parameter	**NSE threshold**		Hard criteria		Hard & soft	
	SI 1	**Rank**	*SI 1*	Rank	*SI 1*	Rank
Infilt. rate - HL (mm/hr)	***0.04***	**1**	*0.03*	1	*0.02*	1
MBR outflow constant (days)	***0.10***	**2**	*0.10*	3	*0.10*	4
ET_k - FP savanna	***0.10***	**3**	*0.10*	4	*0.08*	3
Infilt. rate - PLT (mm/hr)	***0.10***	**4**	*0.09*	2	*0.07*	2
ET_k - CYN forest	***0.20***	**5**	*0.19*	5	*0.19*	11
SM-FC - FP topsoil	***0.23***	**6**	*0.23*	11	*0.22*	18
SWC - FP topsoil	***0.24***	**7**	*0.23*	12	*0.21*	16
SM-WP - FP topsoil	***0.24***	**8**	*0.24*	14	*0.20*	12
SWC - HL	***0.26***	**9**	*0.21*	6	*0.21*	13
SM-FC - HL	***0.26***	**10**	*0.21*	7	*0.21*	14

Parameter	NSE threshold		**Hard criteria**		Hard & soft	
	SI 1	Rank	***SI 1***	**Rank**	*SI 1*	Rank
Infilt. rate - HL (mm/hr)	*0.04*	1	***0.03***	**1**	*0.02*	1
Infilt. rate - PLT (mm/hr)	*0.10*	4	***0.09***	**2**	*0.07*	2
MBR outflow constant (days)	*0.10*	2	***0.10***	**3**	*0.10*	4
ET_k - FP savanna	*0.10*	3	***0.10***	**4**	*0.08*	3
ET_k - CYN forest	*0.20*	5	***0.19***	**5**	*0.19*	11
SWC - HL	*0.26*	9	***0.21***	**6**	*0.21*	13
SM-FC - HL	*0.26*	10	***0.21***	**7**	*0.21*	14
SM-WP - HL	*0.26*	11	***0.21***	**8**	*0.21*	15
SWC - FP cobble	*0.29*	18	***0.22***	**9**	*0.14*	8
SM-WP - FP cobble	*0.28*	16	***0.23***	**10**	*0.16*	9

Parameter	NSE threshold		Hard criteria		**Hard & soft**	
	SI 1	Rank	*SI 1*	Rank	***SI 1***	**Rank**
Infilt. rate - HL (mm/hr)	*0.04*	1	*0.03*	1	***0.02***	**1**
Infilt. rate - PLT (mm/hr)	*0.10*	4	*0.09*	2	***0.07***	**2**
ET_k - FP savanna	*0.10*	3	*0.10*	4	***0.08***	**3**
MBR outflow constant (days)	*0.10*	2	*0.10*	3	***0.10***	**4**
SM-WP - CYN	*0.27*	12	*0.24*	15	***0.12***	**5**
SWC - CYN	*0.27*	13	*0.24*	16	***0.12***	**6**
SM-FC - CYN	*0.27*	14	*0.24*	17	***0.12***	**7**
SWC - FP cobble	*0.29*	18	*0.22*	9	***0.14***	**8**
SM-WP - FP cobble	*0.28*	16	*0.23*	10	***0.16***	**9**
SM-FC - FP cobble	*0.28*	15	*0.23*	13	***0.17***	**10**

Table 2-5 Top ten parameters to which model acceptability was most sensitive compared to a-priori value uncertainty, as assessed by Sensitivity Index 2, using different criteria sets

(PLT – plateau, HL – hillslope, CLF – cliff, CYN – canyon, FP – floodplain, MBR – mountain bedrock, SWC – saturated water content, SM – soil moisture, FC – field capacity, WP – wilting point, ET_k - evapotranspiration coefficient)

Parameter	**NSE threshold**		Hard criteria		Hard & soft	
	SI 2	**Rank**	*SI 2*	Rank	*SI 2*	Rank
MBR outflow constant (days)	***0.11***	**1**	*0.11*	1	*0.10*	1
Interflow horiz. constant (days)	***0.49***	**2**	*0.37*	4	*0.15*	3
Infilt. rate - HL (mm/hr)	***0.51***	**3**	*0.23*	2	*0.11*	2
LAI - HL thicket	***0.53***	**4**	*0.49*	6	*0.45*	14
ET_k - FP savanna	***0.60***	**5**	*0.59*	9	*0.47*	16
Manning's n - FP river channel	***0.66***	**6**	*0.56*	7	*0.40*	6
ET_k - CLF thicket	***0.70***	**7**	*0.69*	15	*0.67*	24
Infilt. rate - PLT (mm/hr)	***0.73***	**8**	*0.30*	3	*0.19*	4
Soil/root depth - HL thicket (mm)	***0.82***	**9**	*0.60*	10	*0.45*	13
SM-WP - FP cobble	***0.87***	**10**	*0.66*	13	*0.45*	12

Parameter	NSE threshold		**Hard criteria**		Hard & soft	
	SI 2	Rank	***SI 2***	**Rank**	*SI 2*	Rank
MBR outflow constant (days)	*0.11*	1	***0.11***	**1**	*0.10*	1
Infilt. rate - HL (mm/hr)	*0.51*	3	***0.23***	**2**	*0.11*	2
Infilt. rate - PLT (mm/hr)	*0.73*	8	***0.30***	**3**	*0.19*	4
Interflow horiz. constant (days)	*0.49*	2	***0.37***	**4**	*0.15*	3
Ksat - FP cobble (mm/hr)	*1.00*	41	***0.44***	**5**	*0.20*	5
LAI - HL thicket	*0.53*	4	***0.49***	**6**	*0.45*	14
Manning's n - FP river channel	*0.66*	6	***0.56***	**7**	*0.40*	6
Interflow vert. constant (days)	*0.88*	14	***0.57***	**8**	*0.42*	7
ET_k - FP savanna	*0.60*	5	***0.59***	**9**	*0.47*	16
Soil/root depth - HL thicket (mm)	*0.82*	9	***0.60***	**10**	*0.45*	13

Parameter	NSE threshold		Hard criteria		**Hard & soft**	
	SI 2	Rank	*SI 2*	Rank	***SI 2***	**Rank**
MBR outflow constant (days)	*0.11*	1	*0.11*	1	***0.10***	**1**
Infilt. rate - HL (mm/hr)	*0.51*	3	*0.23*	2	***0.11***	**2**
Interflow horiz. constant (days)	*0.49*	2	*0.37*	4	***0.15***	**3**
Infilt. rate - PLT (mm/hr)	*0.73*	8	*0.30*	3	***0.19***	**4**
Ksat - FP cobble (mm/hr)	*1.00*	41	*0.44*	5	***0.20***	**5**
Manning's n - FP river channel	*0.66*	6	*0.56*	7	***0.40***	**6**
Interflow vert. constant (days)	*0.88*	14	*0.57*	8	***0.42***	**7**
SWC - CYN	*1.00*	29	*0.98*	36	***0.44***	**8**
SM-FC - CYN	*1.00*	28	*0.98*	38	***0.44***	**9**
SM-WP - CYN	*1.00*	30	*0.98*	37	***0.44***	**10**

Figure 2-5 Cumulative density plots of parameter value occurrence in the sets selected as acceptable using different model performance criteria: streamflow NSE threshold (NSE), all hard data criteria (H), all hard and soft data criteria (HSE).

Plots shown for parameters to which model acceptability was most sensitive within tested value ranges. Plot x-axes span the range of values tested. A density line slope of 1 indicates no sensitivity over the range. (PLT – plateau, HL – hillslope, CLF – cliff, CYN – canyon, FP – floodplain, MBR – mountain bedrock, SWC – saturated water content, ET_k - evapotranspiration coefficient)

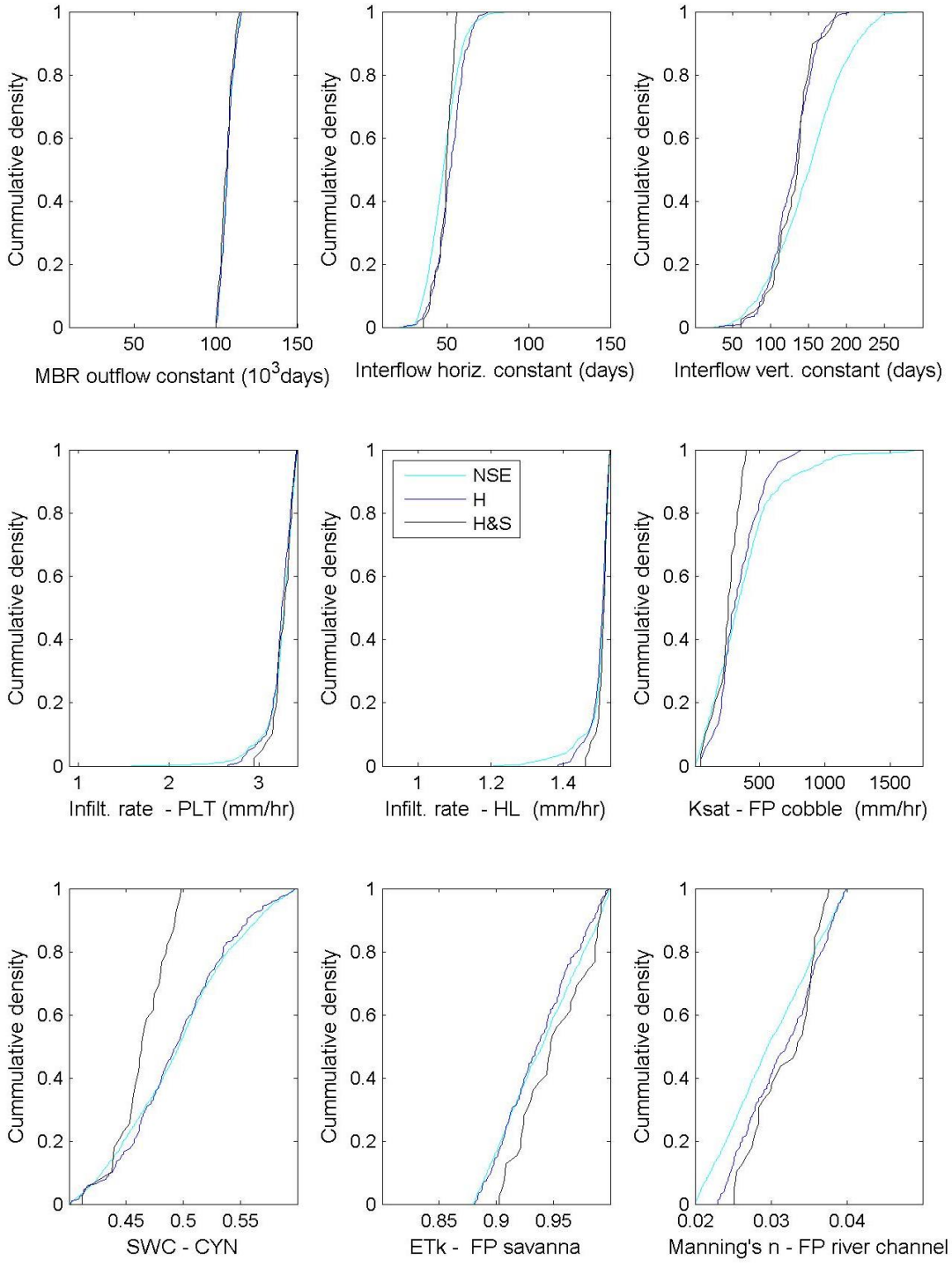

2.4 Discussion

Applying a high dimensionality model to a catchment with relatively little streamflow data is not unusual in practical catchment management contexts (Efstratiadis and Koutsoyiannis, 2010). Complex, physically-based hydrologic models are often advocated as decision making tools even in data poor areas. This case study demonstrated the value of using additional model performance criteria and data types to supplement the widely used streamflow NSE in the calibration of a relatively complex catchment model with a short streamflow record. Because of the size and topographic complexity of the catchment, and the desired use of the model to assess land and river management scenarios, the proposed model of the Baviaanskloof was necessarily highly dimensional, having 42 parameter values to be calibrated. In contrast, only two years of gaged streamflow data was available with which to evaluate the model. This is a very short time period given the semi-arid climate and highly variable rainfall patterns. Fortunately the observation period included two major flood events and recessions which could shed light on catchment processes; however, the information in this record can still be considered limited in relation to the dimensionality of the model. It was found that attempting to calibrate this model using only the NSE to measure its goodness-of-fit to the short streamflow time-series resulted in large parameter uncertainty and hence low output precision, and acceptance of parameter values that produced unacceptably inaccurate groundwater level fluctuations and short and long-term streamflow pattern predictions. Use of additional model performance measures based on this streamflow record as criteria in calibration increased both parameter identifiability and model accuracy for most measures applied. Further improvement was achieved when adding

criteria based on the available soft data: floodplain groundwater table fluctuations, channel flow presence, and estimated long term monthly flows, with notable gains in parameter identifiability, but more minor improvements in calibrated model performance and precision.

A valuable outcome in this study for areas in which only streamflow data is available was the improvement in calibrated model performance achieved with the additional calibration criteria that were based only on the streamflow record. The availability of supplementary groundwater and surface flow data for the Baviaanskloof catchment allowed for evaluation of the model against more targeted measures of the realism of its representation of internal catchment processes. If this data had not been available there would have been no way to directly evaluate the short-comings of the NSE calibrated model in recreating patterns in floodplain groundwater levels or channel connectivity, and no way to directly select for parameter values that resulted in acceptable model performance on these fronts. It was found that making more complete use of information in the available streamflow record through additional hard data indices can be of use in this situation. Particular patterns in the catchment-scale streamflow hydrograph can be used to assess selected aspects of the model's representation of catchment processes, such as the flow paths resulting in baseflow, for example. In this case, to the degree that baseflow is controlled by floodplain groundwater levels, both in reality and in the model structure, criteria selecting for models with more accurate low flow prediction can indirectly select for those that more accurately predict floodplain groundwater levels. For the Baviaanskloof, it was seen that inclusion of additional hard data based calibration criteria, such as the NSE of logged

streamflow which increases the weight of low flow values, was able to exclude many parameter sets with unacceptable performance in capturing observed groundwater and floodplain channel patterns.

It is possible that this improvement in performance with the additional streamflow-based criteria could be a coincidental result of reducing the number of acceptable parameter sets, but this was found not to be the case. When a more stringent untransformed streamflow NSE threshold was applied in a single criteria calibration, the number of accepted parameter sets was reduced, but still included sets with unacceptable performance in capturing groundwater and surface flow patterns, sets which were excluded when instead applying the other hard data criteria. This demonstrated that maximizing streamflow NSE does not always optimize the realism achievable with a given model structure. Improved model realism in representing internal processes through the inclusion of additional streamflow indices has been observed in other studies (Freer et al., 2004; Seibert and McDonnell, 2002; Wöhling et al., 2013); however these were for smaller, less heterogeneous catchments with more data and wetter conditions.

Multi-criteria calibration can also provide a means of highlighting limitations in the model structure and parameterization, and potentially the suitability of the observational data and criteria, through the identification of performance trade-offs between different criteria (Efstratiadis and Koutsoyiannis, 2010; Kollat et al., 2012). The proposed model structure of the Baviaanskloof catchment was validated in the sense that parameter sets were found, within the parameter value space deemed reasonable a-priori, which could produce

streamflow and groundwater outputs that were considered acceptably accurate when compared to available observational data. In addition, the calibrated model average NSE values for raw and log-transformed catchment outlet streamflow improved with additional inclusion of criteria selecting for better representation of floodplain groundwater and channel flow patterns. This provides support for the model's linkages between the floodplain sub-surface and surface flows and the catchment scale outflow. Nevertheless, there were some trade-offs signaling potential areas for improvement. Some of the parameter sets with the best performance in the NSE of log transformed 2012-2013 daily flow and the R^2 of floodplain groundwater table that were accepted against the hard criteria were rejected with the addition of the soft data criteria. In particular these models were rejected due to their higher level of error in predicting the magnitude of the range of groundwater depth fluctuation over the observation dates. This may be a function of the model's simplified representation of the floodplain aquifer material and processes and of issues of unaccounted for spatial heterogeneity of processes present in the observational data.

The lower log-transformed streamflow NSE for the hard and soft criteria calibrated model set (mean 0.62, range 0.61-0.67) compared to the raw streamflow NSE (mean 0.90, range 0.87-0.92) indicated the calibrated model was better able to reproduce peak flows than low flows. This indicates greater relative inaccuracies in model representation of processes controlling low flows, such as percolation, groundwater flow, ET, and the channel-aquifer interaction. Greater uncertainties about these processes were acknowledged a-priori with wide parameter ranges. Because the daily fluctuation in low flows was considered less

important for water supply management in this context compared to long term averages, a looser threshold of acceptability was applied for the NSE of log-transformed flow.

Further calibration of the applied model structure would be unlikely to improve the low flow prediction, as all the parameter sets considered over-predicted streamflow response to small rainfall events, over-predicted flow during the weeks immediately following the July 2012 flood, and under-predicted flow during the weeks following the October 2012 flood. This may indicate misrepresentation of water storage in one or more landscape units, potentially addressable by increasing soil depth and/or water holding capacity, reducing root depth or ET, and/or changing interflow reservoir or floodplain aquifer properties. These errors could also be linked to unquantified inaccuracies in spatially distributed rainfall in the catchment, which was estimated based on relatively sparsely distributed gages and a regionally calibrated monthly precipitation surface (Lynch, 2003). Possible systematic errors in rainfall estimation would have been implicitly adjusted for in the selection of process parameter values resulting in outputs better fitting the observations. For example systematic over estimation of catchment scale precipitation could result in selection of higher infiltration and ET parameters to effectively remove this added water from the simulation. This is one possible explanation for calibrated hillslope infiltration parameters being at the upper extreme of the a-priori range and the alluvial aquifer conductivity values at the lower end (Figure 2-5). Precipitation adjustment factors could have be included as additional calibration parameters, however that was not considered here as it was considered unlikely that there was enough observational data to additionally resolve these parameter values given that relatively similar effects could be achieved by changing other process parameters.

Precipitation estimation errors that are not systematic, varying between events or seasons, could limit the ability of the model to recreate the observations setting a limit to the improvements to be gained with further calibration attempts.

The lower performance for the NSE of monthly streamflow for 1991-2013 (calibrated model mean 0.81, range 0.79-0.85) compared to that for daily streamflow for 2012-2013 (mean 0.90 range 0.87-0.92) was somewhat surprising as monthly accumulation of flow was expected to absorb some process inaccuracies manifest at smaller timescales. Model under and over-prediction of certain flow periods did not appear systematic in the long-term record, perhaps pointing to errors in observational data and climate input data. The long-term data-set of monthly flows from the Baviaanskloof was estimated based on reservoir volume change in the Kouga Dam and gaged streamflow on the Kouga River and therefore assumed to have greater uncertainty than the 2012-2013 gaged record. Use of this dataset in the soft data criteria did not actually change the calibration results as the hard data criteria had already indirectly selected only parameter sets that met the threshold of acceptability for goodness-of-fit to the long-term estimated monthly flows. The acceptable fit of the model to this estimated long-term flow dataset acts as validation of the model's streamflow performance, given that the 2012-2013 gaged data record was deemed too short to reasonably divide into separate calibration and validation periods.

Models cannot be perfect representations of reality and so the goal of the model building and calibration exercise is to arrive at a model that is fit-for-purpose to the degree possible given the limitations of available data, conceptual understanding of catchment processes,

time, and computing resources. Calibration criteria used for acceptance of models are often arbitrary (Seibert and McDonnell, 2002) and can notably influence the resulting uncertainty in prediction of events of management concern (Zheng and Keller, 2007b). This study demonstrated the inclusion of calibration criteria that represent the level of accuracy needed for the model's application. In the Baviaanskloof, a catchment model is to be used to look at likely impacts of management scenarios on water supply, and so should achieve levels of accuracy in predicting change in floodplain groundwater levels that is meaningful to irrigating farmers and surface water yields to the downstream reservoir meaningful to downstream users. In this case study the performance measures and acceptable accuracy levels were chosen by the researcher using available basic information about water supply access and management, but should ideally be agreed upon by the group of end users of model output. Zheng and Keller (2007b) provide a method for calculating a model's uncertainty in predicting attainment of specific management objectives and using this for assessment and calibration. In this study both management objectives and indicators of internal catchment processes about which data exists were included.

An effort was made to make full use of available information on catchment processes during calibration by using multiple measures to assess model fit to different patterns in the streamflow record and assessing model fit to observed patterns in surface flows at different landscape scales, floodplain groundwater levels, and estimated long-term streamflows. Acknowledgement was given to the limitations of the observational data in terms of uncertainty and commensurability to model output in order to prevent over-fitting the model to data which also contains inaccuracies. Selecting for models with better performance

against multiple types of data should help to offset the effects of inaccuracies in each individual data-set on the resulting realism of the calibrated model. The same sets of observational data had already been used to inform the model structure and a-priori parameter ranges through identification of patterns indicative of the dominance of different processes and flow paths and their linkages (Chapter 1). The degree to which the information in a dataset had already been fully incorporated in the model in this initial step was demonstrated when all parameter sets tested during calibration met criteria based on this data. This was the case for the criteria regarding duration of surface flow from the tributary catchments in 2012-2013. Observations of the conditions needed to initiate surface flows on hillslopes and from tributary catchments had already been used in deciding upon flow path connectivity between land units in tributary subcatchments and the likely ranges of values for their soil properties in the model.

The model of the Baviaanskloof resulting from the model development and calibration process applied can be considered an adequate representation of existing knowledge about the catchment and fit-for-purpose, to the degree to which the acceptability criteria applied measured this sufficiently. Further improvements in model realism, accuracy, and precision could be made given longer accurate hydrometric and climate datasets and/or land unit physical property data, when the latter is commensurable to model parameterization. It is also possible that further improvements could be made using only the existing data, given additional time investment in model development. Additional attention could be given to the criteria derived from the data, for example better accounting for heterogeneity in the floodplain aquifer when finding measures to compare model outputs to observations. A

wider range of criteria could be tested to further plumb the data for catchment process information, and more parameter sets could be tested within a parameter space that was refined based on the results of initial calibration work done in this study.

The currently remaining uncertainties around the understanding of catchment processes and their model representation, given the complexity of the Baviaanskloof catchment and limitations of the available data, make it unreasonable to attempt to apply the present model structure further using a single best-fitting parameter set, hence the threshold of acceptability calibration approach used here. To use the resulting calibrated model for scenario assessment therefore entails that it be run over the range of accepted parameter values resulting in an output value range for each scenario. The degree to which this results in a detectable difference in output between scenarios will also be a measure of whether or not the calibrated model is indeed fit-for-purpose to assist in decision making without further data collection or refinements in the calibration procedure. This will be explored through scenario modeling in a further study.

2.5 Conclusion

This study demonstrated that multi-criteria calibration can make notable improvement to the realism, accuracy, and precision of a complex model of a semi-arid catchment with a short streamflow record. In the case of the Baviaanskloof catchment, additional to the short gaged streamflow record, soft data on floodplain groundwater levels and surface flows at different locations within the catchment were available and put to use in the calibration and

evaluation procedure. Similar kinds of soft data are likely to be available in many other catchments, particularly in inhabited areas where residents make use of local ground and surface water resources, and could be consulted when developing and testing catchment models. Calibration using only the NSE of the streamflow record would have resulted in acceptance of models with poor performance against several indicators considered relevant for catchment management, such as prediction of floodplain groundwater fluctuations. However, even had the additional soft data not been available, the use of additional hard data criteria, which selected for goodness-of-fit to different patterns in the streamflow record beyond the typically used NSE measure, was already seen to significantly improve performance on indicators of internal catchment process representation. Indeed, after these other streamflow indices were incorporated in the calibration, the subsequent further addition of the soft data criteria did relatively little to improve model performance and parameter identifiability. The number of selected parameter sets was reduced and performance was improved, but the difference was small compared to the differences between the NSE only selection and that using all four hard data criteria. This indicated correlation between the signals evident in the hard streamflow data, such as patterns in low flows, and the patterns being selected for by the soft data criteria, such as floodplain groundwater levels, showing that making more complete use of even limited streamflow data records can help enhance model realism.

This study also aimed to demonstrate a calibration procedure aimed at producing a model that is fit-for-purpose – in this instance as catchment management decision support for those concerned about local and regional water supply. In the case of the Baviaanskloof,

parameter sets producing acceptable model outputs against desired minimum accuracy levels for this application were found. Significant parameter uncertainty remained even after the calibration procedure due to high dimensionality of the model structure and the data available, however the likely ranges of several key variables such as those controlling mountain block aquifer and interflow zone outflows, were considerably constrained compared to the a-priori uncertainty in their values. There will always be room for improvement, however applying a model development and testing procedure which attempted to make full use of all available data, with consideration for its uncertainty, means that the resulting model represents the existing knowledge and the uncertainties about catchment processes upon which to base decisions

2.6 References

Beven, K., and Freer, J. (2001). Equifinality, data assimilation, and uncertainty estimation in mechanistic modelling of complex environmental systems using the GLUE methodology. J. Hydrol. *249*, 11–29.

Consoli, S., Inglese, G., and Inglese, P. (2013). Determination of Evapotranspiration and Annual Biomass Productivity of a Cactus Pear [Opuntia ficus-indica L. (Mill.)] Orchard in a Semiarid Environment. J. Irrig. Drain. Eng. *139*, 680–690.

Efstratiadis, A., and Koutsoyiannis, D. (2010). One decade of multi-objective calibration approaches in hydrological modelling: a review. Hydrol. Sci. J.-J. Sci. Hydrol. *55*, 58–78.

Euston-Brown, D.I.W. (2006). Baviaanskloof Mega-Reserve Project: Vegetation mapping contract report on methodology, vegetation classification and short descriptions of habitat units (South Africa: Eastern Cape Parks & Tourism Agency).

Fenicia, F., Savenije, H.H.G., Matgen, P., and Pfister, L. (2008a). Understanding catchment behavior through stepwise model concept improvement. Water Resour. Res. *44*, W01402.

Fenicia, F., McDonnell, J.J., and Savenije, H.H.G. (2008b). Learning from model improvement: On the contribution of complementary data to process understanding. Water Resour. Res. *44*, W06419.

Freer, J.E., McMillan, H., McDonnell, J.J., and Beven, K.J. (2004). Constraining dynamic TOPMODEL responses for imprecise water table information using fuzzy rule based performance measures. J. Hydrol. *291*, 254–277.

Ganguly, S., Anav, A., Liang Xu, Samanta, A., Shilong Piao, Nemani, R.R., Myneni, R.B., Zaichun Zhu, Jian Bi, and Yaozhong Pan (2013). Global Data Sets of Vegetation Leaf Area Index (LAI)3g and Fraction of Photosynthetically Active Radiation (FPAR)3g Derived from Global Inventory Modeling and Mapping Studies (GIMMS) Normalized Difference Vegetation Index (NDVI3g) for the Period 1981... Remote Sens. *5*, 927–948.

Gupta, H.V., Wagener, T., and Liu, Y. (2008). Reconciling theory with observations: elements of a diagnostic approach to model evaluation. Hydrol. Process. *22*, 3802–3813.

Hammersmark, C., Rains, M., and Mount, J. (2008). Quantifying the hydrological effects of stream restoration in a montane meadow, northern California, USA. RIVER Res. Appl. *24*, 735–753.

Hargreaves, G., and Samani, Z. (1982). Estimating potential evapotranspiration. J. Irrig. Drain. Div.-Asce *108*, 225–230.

Jansen, H.C. (2008). Water for Food and Ecosystems in the Baviaanskloof Mega Reserve: Land and water resources assessment in the Baviaanskloof (Wageningen, The Netherlands: Alterra).

Kollat, J.B., Reed, P.M., and Wagener, T. (2012). When are multiobjective calibration trade-offs in hydrologic models meaningful? Water Resour. Res. *48*, W03520.

van Luijk, G., Cowling, R.M., Riksen, M.J.P.M., and Glenday, J. (2013). Hydrological implications of desertification: Degradation of South African semi-arid subtropical thicket. J. Arid Environ. *91*, 14–21.

Lynch, S.D. (2003). Development of a Raster Database of Annual, Monthly and Daily Rainfall for Southern Africa (Pretoria, South Africa: Water Research Commission (WRC)).

Maneta, M.P., and Wallender, W.W. (2013). Pilot-point based multi-objective calibration in a surface-subsurface distributed hydrological model. Hydrol. Sci. J.-J. Sci. Hydrol. *58*, 390–407.

Maneta, M.P., Schnabel, S., Wallender, W.W., Panday, S., and Jetten, V. (2008). Calibration of an evapotranspiration model to simulate soil water dynamics in a semiarid rangeland. Hydrol. Process. *22*, 4655–4669.

McGrane, S.J., Tetzlaff, D., and Soulsby, C. (2014). Influence of lowland aquifers and anthropogenic impacts on the isotope hydrology of contrasting mesoscale catchments. Hydrol. Process. *28*, 793–808.

McKay, M.D., Beckman, R.J., and Conover, W.J. (1979). Comparison of Three Methods for Selecting Values of Input Variables in the Analysis of Output from a Computer Code. Technometrics *21*, 239–245.

McMichael, C.E., Hope, A.S., and Loaiciga, H.A. (2006). Distributed hydrological modelling in California semi-arid shrublands: MIKE SHE model calibration and uncertainty estimation. J. Hydrol. *317*, 307–324.

McMillan, H.K., Clark, M.P., Bowden, W.B., Duncan, M., and Woods, R.A. (2011). Hydrological field data from a modeller's perspective: Part 1. Diagnostic tests for model structure. Hydrol. Process. *25*, 511–522.

Midgley, J.J., and Scott, D.F. (1994). Use of stable isotopes of water (d and o-18) in hydrological studies in the Jonkershoek valley.

Mills, A., and Fey, M. (2004). Transformation of thicket to savanna reduces soil quality in the Eastern Cape, South Africa. Plant Soil *265*, 153–163.

Mills, A.J., and Cowling, R.M. (2006). Rate of Carbon Sequestration at Two Thicket Restoration Sites in the Eastern Cape, South Africa. Restor. Ecol. *14*, 38–49.

Mills, A.J., and Cowling, R.M. (2010). Below-ground carbon stocks in intact and transformed subtropical thicket landscapes in semi-arid South Africa. J. Arid Environ. *74*, 93–100.

Mills, A.J., Cowling, R.M., Fey, M.V., Kerley, G.I.H., Donaldson, J.S., Lechmere-Oertel, R.G., Sigwela, A.M., Skowno, A.L., and Rundel, P. (2005). Effects of goat pastoralism on ecosystem carbon storage in semiarid thicket, Eastern Cape, South Africa. Austral Ecol. *30*, 797–804.

Ophori, D., and Tóth, J. (1990). Relationships in regional groundwater discharge to streams: An analysis by numerical simulation. J. Hydrol. *119*, 215–244.

Refsgaard, J.C., and Storm, B. (1995). MIKE SHE. In Computer Models of Watershed Hydrology, V.P. Singh, ed. (Water Resources Publications), pp. 809–846.

Roets, W., Xu, Y., Raitt, L., and Brendonck, L. (2008). Groundwater discharges to aquatic ecosystems associated with the Table Mountain Group (TMG) aquifer: A conceptual model. Water SA *34*, 77–88.

Schulze, R.E. (1995). Hydrology and Agrohydrology: A Text to Accompany the ACRU 3.00 Agrohydrological Modelling System (Pretoria, South Africa: Water Research Commission (WRC)).

Schulze, R.E. (2007). South African Atlas of Climatology and Agrohydrology. (Pretoria, South Africa: Water Research Commission).

Schulze, R.E., and Maharaj, M. (2004). Development of Database of Gridded Daily Temperature for Southern Africa (Pretoria, South Africa: Water Research Commission (WRC)).

Seibert, J., and McDonnell, J.J. (2002). On the dialog between experimentalist and modeler in catchment hydrology: Use of soft data for multicriteria model calibration. Water Resour. Res. *38*, 1241.

Selaolo, E.T. (1998). Tracer studies and groundwater recharge assessment in the eastern fringe of the Botswana Kalahari, The Letlhakeng-Botlhapatlou Area. PhD dissertation. Vrije Universiteit.

Sigwela, A.M., Kerley, G.I.H., Mills, A.J., and Cowling, R.M. (2009). The impact of browsing-induced degradation on the reproduction of subtropical thicket canopy shrubs and trees. South Afr. J. Bot. *75*, 262–267.

Sivapalan, M., Blöschl, G., Zhang, L., and Vertessy, R. (2003). Downward approach to hydrological prediction. Hydrol. Process. *17*, 2101–2111.

Smit, S. (2013). Observation of changes in vegetation cover density in the Baviaanskloof catchment using field sampling and remotely sensed NDVI (Normalized Difference Vegetation Index). BSc Thesis. University of Applied Science Van Hall Larenstein.

Soltau, L., Smith-Adao, L., and Bugan, R. (2011). Baviaanskloof resistivity survey to define water level and depth to bedrock (Stellenbosch, South Africa: Center for Scientific and Industrial Research (CSIR)).

Steinwand, A.L., Harrington, R.F., and Groeneveld, D.P. (2001). Transpiration coefficients for three Great Basin shrubs. J. Arid Environ. *49*, 555–567.

Tague, C., McMichael, C., Hope, A., Choate, J., and Clark, R. (2004). Application of the RHESSyS model to a California semiarid shrubland watershed. JAWRA J. Am. Water Resour. Assoc. *40*, 575–589.

Tekleab, S., Uhlenbrook, S., Mohamed, Y., Savenije, H.H.G., Temesgen, M., and Wenninger, J. (2011). Water balance modeling of Upper Blue Nile catchments using a top-down approach. Hydrol Earth Syst Sci *15*, 2179–2193.

Uhlenbrook, S., Roser, S., and Tilch, N. (2004). Hydrological process representation at the meso-scale: the potential of a distributed, conceptual catchment model. J. Hydrol. *291*, 278–296.

Vaché, K.B., and McDonnell, J.J. (2006). A process-based rejectionist framework for evaluating catchment runoff model structure. Water Resour. Res. *42*, W02409.

Winsemius, H.C., Schaefli, B., Montanari, A., and Savenije, H.H.G. (2009). On the calibration of hydrological models in ungauged basins: A framework for integrating hard and soft hydrological information. Water Resour. Res. *45*, W12422.

Wöhling, T., Samaniego, L., and Kumar, R. (2013). Evaluating multiple performance criteria to calibrate the distributed hydrological model of the upper Neckar catchment. Environ. Earth Sci. *69*, 453–468.

Xu, Y., Titus, R., Holness, S.D., Zhang, J., and Tonder, G.V. (2002). A hydrogeomorphological approach to quantification of groundwater discharge to streams in South Africa. Water SA *28*, 375–380.

Xu, Y., Wu, Y., and Beekman, E.H. (2003). The role of interflow in estimating recharge in mountainous catchments. In Groundwater Recharge Estimation in Southern Africa, Y. Xu, and E.H. Beekman, eds. (Paris, France: UNESCO),.

Zheng, Y., and Keller, A.A. (2007a). Uncertainty assessment in watershed-scale water quality modeling and management: 1. Framework and application of generalized likelihood uncertainty estimation (GLUE) approach. Water Resour. Res. *43*, W08407.

Zheng, Y., and Keller, A.A. (2007b). Uncertainty assessment in watershed-scale water quality modeling and management: 2. Management objectives constrained analysis of uncertainty (MOCAU). Water Resour. Res. *43*, W08408.

2.7 Supplementary Information

Table 2-6 Minimum and maximum parameter values for all parameter sets tested

Parameter	All sets		NSE threshold		Hard criteria		Hard and soft	
	Min	Max	Min	Max	Min	Max	Min	Max
MBR outflow constant (days)	10,000	150,000	100,010	115,730	100,130	115,700	100,290	114,910
Interflow horiz. constant (days)	10	150	21	89	24	76	35	56
Interflow vert. constant (days)	1	300	25	287	33	204	61	188
LAI - PLT fynbos	1.0	3.0	1.1	3.0	1.2	3.0	1.3	3.0
LAI - HL thicket	0.4	1.0	0.4	0.7	0.4	0.7	0.4	0.7
LAI - CLF thicket	0.2	0.6	0.2	0.5	0.2	0.5	0.2	0.5
LAI - CYN forest	3.0	5.0	3.0	5.0	3.0	5.0	3.0	4.8
LAI - FP savanna	1.0	3.0	1.1	3.0	1.2	3.0	1.5	2.8
Manning's n - HL & PLT	0.04	0.83	0.04	0.83	0.04	0.83	0.07	0.83
Manning's n - CYN	0.08	0.83	0.08	0.83	0.08	0.82	0.35	0.82
Manning's n - FP surface	0.05	0.70	0.05	0.70	0.05	0.46	0.05	0.46
Manning's n - FP river channel	0.020	0.050	0.020	0.040	0.023	0.040	0.026	0.038
ET_k - PLT fynbos	0.40	0.60	0.42	0.60	0.42	0.60	0.43	0.59
ET_k - HL thicket	0.30	0.50	0.32	0.50	0.32	0.48	0.34	0.47
ET_k - CLF thicket	0.20	0.40	0.22	0.36	0.22	0.36	0.22	0.36
ET_k - CYN forest	0.70	0.90	0.70	0.90	0.70	0.90	0.71	0.90
ET_k - FP savanna	0.80	1.00	0.88	1.00	0.88	1.00	0.90	1.00
Soil/root dpt - PLT fynbos (mm)	500	1,000	550	1,000	601	996	611	996
Soil/root dpt - HL thicket (mm)	300	800	390.1	799.8	500.0	799.4	573.4	799.0
Soil/root dpt - CYN forest (mm)	5,000	10,000	5,054	9,993	5,815	9,962	6,026	9,961
Topsoil depth - FP (mm)	600	1,000	640.3	999.9	642.2	947.5	650.3	916.2
Root depth - FP savanna (mm)	10,000	29,998	11,010	29,993	15,089	29,872	15,089	29,767
SWC - PLT	0.30	0.50	0.30	0.50	0.31	0.50	0.35	0.49
SWC - HL	0.30	0.50	0.30	0.50	0.31	0.50	0.31	0.49
SWC - CYN	0.40	0.60	0.40	0.60	0.40	0.60	0.41	0.50
SWC - FP topsoil	0.40	0.55	0.41	0.55	0.41	0.55	0.42	0.55
SWC - FP cobble	0.30	0.45	0.30	0.43	0.31	0.41	0.30	0.37
SM-FC - PLT	0.14	0.22	0.14	0.22	0.14	0.22	0.16	0.22
SM-FC - HL	0.14	0.23	0.14	0.22	0.14	0.22	0.14	0.22
SM-FC - CYN	0.24	0.36	0.24	0.36	0.24	0.36	0.25	0.30
SM-FC - FP topsoil	0.27	0.37	0.27	0.37	0.27	0.37	0.28	0.36
SM-FC - FP cobble	0.12	0.18	0.12	0.17	0.12	0.16	0.12	0.15
SM-WP - PLT	0.075	0.125	0.075	0.125	0.076	0.125	0.087	0.123
SM-WP - HL	0.075	0.125	0.075	0.125	0.078	0.125	0.078	0.123
SM-WP - CYN	0.080	0.120	0.080	0.120	0.080	0.120	0.082	0.100
SM-WP - FP topsoil	0.086	0.119	0.088	0.119	0.088	0.119	0.092	0.118
SM-WP - FP cobble	0.060	0.090	0.060	0.086	0.062	0.082	0.060	0.073
Infilt. rate - PLT (mm/hr)	0.9	3.4	1.6	3.4	2.7	3.4	2.9	3.4
Infilt. rate - HL (mm/hr)	0.9	1.5	1.2	1.5	1.4	1.5	1.46	1.53
Infilt. rate - CYN (mm/hr)	36	342	39	342	59	342	175	342
Ksat - FP topsoil (mm/hr)	50	300	60	280	78	255	83	241
Ksat - FP cobble (mm/hr)	9	1,746	9	1,746	51	824	51	400

Table 2-7 Median, 10th to 90th percentile range (P.range), and the resulting sensitivity index (SI 1) by parameter for sets selected by different criteria.

(Parameters listed by declining sensitivity in the final hard and soft criteria selected set)

Parameter	NSE threshold			Hard criteria			Hard and soft criteria		
	Median	P.Rng	*SI 1*	Median	P.Rng	*SI 1*	Median	P.Rng	*SI 1*
Infilt. rate - HL (mm/hr)	1.51	0.06	***0.04***	1.51	0.05	***0.03***	1.51	0.03	***0.02***
Infilt. rate - PLT (mm/hr)	3.28	0.34	***0.10***	3.25	0.30	***0.09***	3.28	0.23	***0.07***
ET_k FP savanna	0.94	0.09	***0.10***	0.94	0.10	***0.10***	0.94	0.08	***0.08***
MBR outflow constant (days)	106,900	10,514	***0.10***	107,150	10,686	***0.10***	106,740	10,400	***0.10***
SM-WP - CYN	0.099	0.027	***0.27***	0.099	0.024	***0.24***	0.093	0.011	***0.12***
SWC - CYN	0.50	0.14	***0.27***	0.49	0.12	***0.24***	0.46	0.06	***0.12***
SM-FC - CYN	0.30	0.08	***0.27***	0.30	0.07	***0.24***	0.28	0.03	***0.12***
SWC - FP cobble	0.36	0.11	***0.29***	0.36	0.08	***0.22***	0.33	0.05	***0.14***
SM-WP - FP cobble	0.073	0.020	***0.28***	0.071	0.016	***0.23***	0.068	0.011	***0.16***
SM-FC - FP cobble	0.15	0.04	***0.28***	0.15	0.03	***0.23***	0.13	0.02	***0.17***
ET_k CYN forest	0.80	0.16	***0.20***	0.80	0.15	***0.19***	0.80	0.15	***0.19***
SM-WP - FP topsoil	0.103	0.025	***0.24***	0.103	0.025	***0.24***	0.104	0.021	***0.20***
SWC - HL	0.42	0.11	***0.26***	0.43	0.09	***0.21***	0.43	0.09	***0.21***
SM-FC - HL	0.19	0.05	***0.26***	0.19	0.04	***0.21***	0.19	0.04	***0.21***
SM-WP - HL	0.106	0.028	***0.26***	0.107	0.023	***0.21***	0.107	0.022	***0.21***
SWC - FP topsoil	0.48	0.11	***0.24***	0.48	0.11	***0.23***	0.50	0.11	***0.21***
ET_k PLT fynbos	0.51	0.14	***0.28***	0.51	0.14	***0.28***	0.50	0.11	***0.22***
SM-FC - FP topsoil	0.32	0.07	***0.23***	0.32	0.07	***0.23***	0.33	0.07	***0.22***
SWC - PLT	0.42	0.12	***0.30***	0.40	0.12	***0.29***	0.43	0.11	***0.25***
SM-FC - PLT	0.19	0.06	***0.30***	0.18	0.05	***0.29***	0.19	0.05	***0.25***
SM-WP - PLT	0.104	0.031	***0.30***	0.100	0.029	***0.29***	0.108	0.027	***0.25***

Parameter	NSE threshold			Hard criteria			Hard and soft criteria		
	Median	**P.Rng**	***SI 1***	**Median**	**P.Rng**	***SI 1***	**Median**	**P.Rng**	***SI 1***
ET_k HL thicket	0.41	0.14	***0.35***	0.39	0.12	***0.32***	0.40	0.10	***0.26***
Topsoil depth - FP (mm)	823	289	***0.35***	804	244	***0.30***	796	209	***0.26***
Soil & root depth - HL thicket (mm)	598	328	***0.55***	655	237	***0.36***	650	175	***0.27***
Interflow horizontal constant (days)	47	24	***0.52***	52	23	***0.45***	49	15	***0.30***
Soil & root depth - PLT fynbos (mm)	776	362	***0.47***	812	306	***0.38***	827	277	***0.33***
Manning's n - FP river channel	0.030	0.016	***0.54***	0.032	0.014	***0.44***	0.031	0.010	***0.34***
Soil & root depth - CYN forest (mm)	7,567	4,023	***0.53***	8,130	3,439	***0.42***	8,476	2,889	***0.34***
LAI CYN forest	4.03	1.62	***0.40***	4.12	1.68	***0.41***	4.03	1.49	***0.37***
ET_k CLF thicket	0.29	0.11	***0.38***	0.29	0.11	***0.38***	0.27	0.11	***0.39***
LAI HL thicket	0.56	0.26	***0.46***	0.56	0.24	***0.43***	0.55	0.22	***0.40***
LAI FP savanna	2.09	1.55	***0.74***	2.07	1.45	***0.70***	2.29	1.10	***0.48***
Interflow vertical constant (days)	151	129	***0.85***	132	71	***0.54***	135	68	***0.50***
Infilt. rate - CYN (mm/hr)	216	182	***0.84***	219	172	***0.79***	253	143	***0.56***
Root depth - FP savanna (mm)	20,190	15,469	***0.77***	21,639	12,917	***0.60***	22,803	13,365	***0.59***
Manning's n - CYN	0.52	0.47	***0.90***	0.50	0.45	***0.89***	0.55	0.33	***0.61***
LAI CLF thicket	0.38	0.29	***0.76***	0.35	0.27	***0.76***	0.34	0.21	***0.63***
Ksat - FP topsoil (mm/hr)	168.6	173.0	***1.03***	163.1	142.6	***0.87***	172.7	119.7	***0.69***
LAI PLT fynbos	2.05	1.51	***0.74***	2.09	1.48	***0.71***	2.22	1.55	***0.70***
Ksat - FP cobble (mm/hr)	329	622	***1.89***	313	406	***1.30***	263	265	***1.01***
Manning's n - FP surface	0.09	0.22	***2.48***	0.09	0.21	***2.32***	0.09	0.22	***2.45***
Manning's n - HL & PLT	0.18	0.45	***2.57***	0.15	0.36	***2.37***	0.14	0.37	***2.60***

Table 2-8 Value ranges by parameter for all parameter sets tests and for sets selected by different model performance criteria and the resulting range change sensitivity index (SI 2).

(Parameters listed by declining sensitivity in the final hard and soft criteria selected set)

Parameter	All sets	NSE threshold		Hard criteria		Hard and soft	
	Range	Range	*SI 2*	Range	*SI 2*	Range	*SI 2*
MBR outflow constant (days)	140,000	15,720	***0.11***	15,570	***0.11***	14,620	***0.10***
Infilt. rate - HL (mm/hr)	0.63	0.32	***0.51***	0.14	***0.23***	0.07	***0.11***
Interflow horiz. constant (days)	140	68	***0.49***	52	***0.37***	21	***0.15***
Infilt. rate - PLT (mm/hr)	2.52	1.84	***0.73***	0.77	***0.30***	0.47	***0.19***
Ksat - FP cobble (mm/hr)	1,737	1,737	***1.00***	773	***0.44***	348	***0.20***
Manning's n - FP river channel	0.030	0.020	***0.66***	0.017	***0.56***	0.012	***0.40***
Interflow vert. constant (days)	299	262	***0.88***	171	***0.57***	127	***0.42***
SM-FC - CYN	0.12	0.12	***1.00***	0.12	***0.98***	0.05	***0.44***
SM-WP - CYN	0.040	0.040	***1.00***	0.039	***0.98***	0.017	***0.44***
SWC - CYN	0.20	0.20	***1.00***	0.20	***0.98***	0.09	***0.44***
SM-FC - FP cobble	0.06	0.05	***0.87***	0.04	***0.66***	0.03	***0.45***
SM-WP - FP cobble	0.030	0.026	***0.87***	0.020	***0.66***	0.013	***0.45***
Soil/root depth - HL thicket (mm)	500	409.7	***0.82***	299.4	***0.60***	225.6	***0.45***
LAI - HL thicket	0.6	0.3	***0.53***	0.3	***0.49***	0.3	***0.45***
SWC - FP cobble	0.15	0.13	***0.87***	0.10	***0.67***	0.07	***0.45***
ET_k - FP savanna	0.20	0.12	***0.60***	0.12	***0.59***	0.09	***0.47***
Infilt. rate - CYN (mm/hr)	306	303	***0.99***	283	***0.92***	166	***0.54***
LAI - FP savanna	2.0	1.9	***0.95***	1.8	***0.89***	1.2	***0.62***
Manning's n - FP surface	0.65	0.65	***1.00***	0.41	***0.63***	0.41	***0.62***
Ksat - FP topsoil (mm/hr)	250	219.9	***0.88***	176.7	***0.71***	158.6	***0.63***
Manning's n - CYN	0.75	0.75	***1.00***	0.74	***0.99***	0.48	***0.64***
ET_k - HL thicket	0.20	0.18	***0.90***	0.16	***0.78***	0.13	***0.66***
Topsoil depth - FP (mm)	400	359.5	***0.90***	305.3	***0.76***	266.0	***0.66***
ET_k - CLF thicket	0.20	0.14	***0.70***	0.14	***0.69***	0.13	***0.67***
SM-FC - PLT	0.09	0.09	***1.00***	0.09	***0.97***	0.07	***0.73***
SM-WP - PLT	0.050	0.050	***1.00***	0.048	***0.97***	0.036	***0.73***
SWC - PLT	0.20	0.20	***1.00***	0.19	***0.97***	0.15	***0.73***
Root depth - FP savanna (mm)	19,997	18,983	***0.95***	14,783	***0.74***	14,678	***0.73***
Soil/root dpt - PLT fynbos (mm)	500	450	***0.90***	395	***0.79***	386	***0.77***
Soil/root dpt - CYN forest (mm)	5,000	4,939	***0.99***	4,147	***0.83***	3,935	***0.79***
ET_k - PLT fynbos	0.20	0.18	***0.90***	0.18	***0.90***	0.16	***0.80***
SM-FC - FP topsoil	0.10	0.09	***0.94***	0.09	***0.93***	0.08	***0.81***
SM-WP - FP topsoil	0.033	0.031	***0.94***	0.031	***0.93***	0.027	***0.81***
LAI - CLF thicket	0.4	0.3	***0.87***	0.3	***0.82***	0.3	***0.81***
SWC - FP topsoil	0.15	0.14	***0.93***	0.14	***0.92***	0.12	***0.83***
LAI - PLT fynbos	2.0	1.9	***0.95***	1.8	***0.89***	1.7	***0.87***
SM-FC - HL	0.09	0.09	***1.00***	0.08	***0.93***	0.08	***0.89***
SM-WP - HL	0.050	0.050	***1.00***	0.046	***0.93***	0.044	***0.89***
SWC - HL	0.20	0.20	***1.00***	0.19	***0.93***	0.18	***0.89***
LAI - CYN forest	2.0	2.0	***1.00***	2.0	***0.99***	1.8	***0.91***
ET_k - CYN forest	0.20	0.20	***1.00***	0.20	***0.98***	0.19	***0.94***
Manning's n - HL & PLT	0.79	0.79	***1.00***	0.79	***1.00***	0.77	***0.97***

Figure 2-6 Distribution of model performance measures used as calibration criteria for different sets of model runs: all parameter sets tested (All), those exceeding an NSE threshold of 0.70 (N0.70), and those exceeding an NSE threshold of 0.87 (N0.87).

Dotted lines in each plot show the threshold value applied for each criterion. Thresholds for measures shown in graphs A-D were hard-data based criteria while those in E-I were soft-data based. 'Error' values are absolute values.

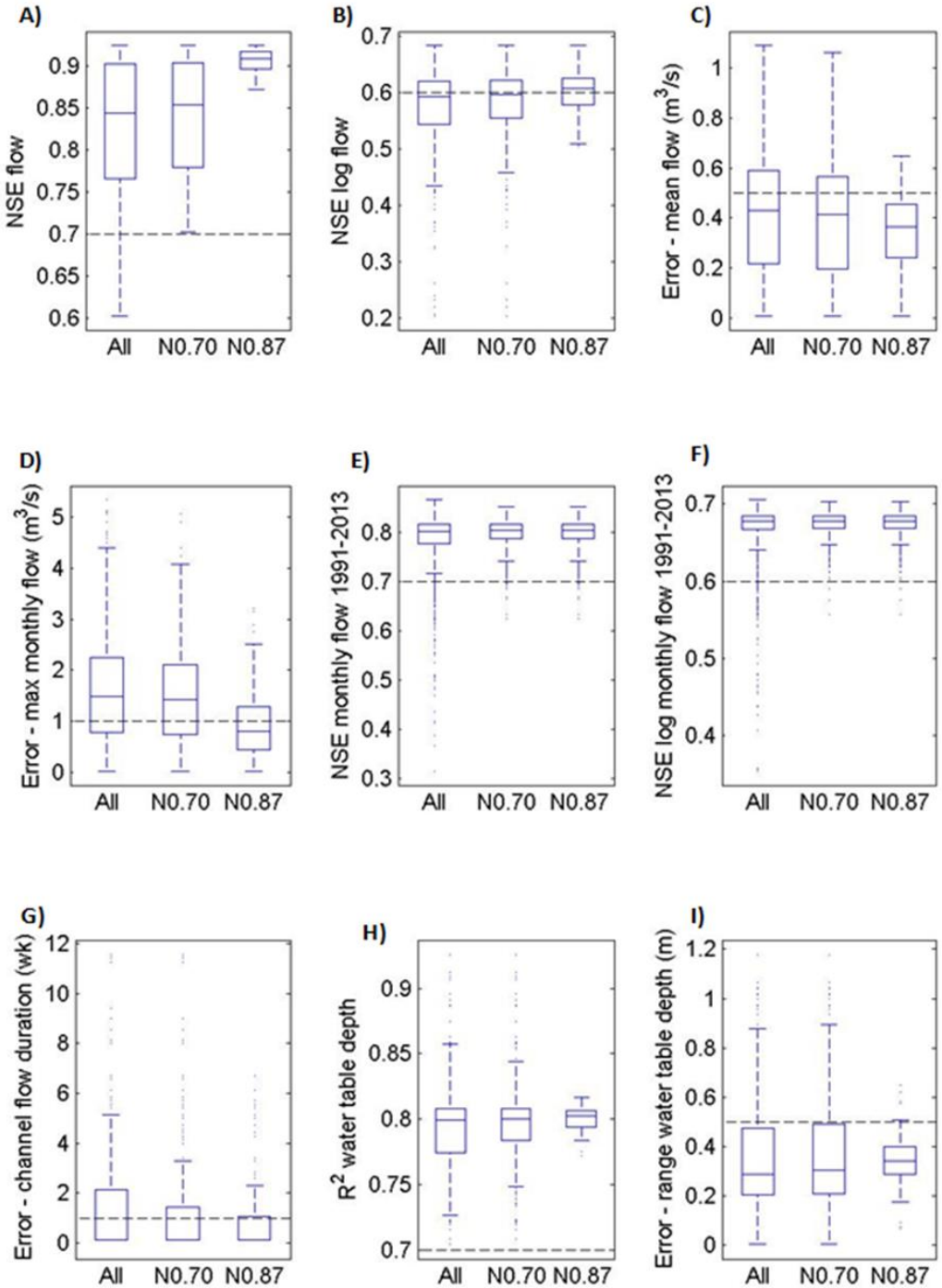

Chapter 3 Impacts of subtropical thicket degradation and restoration on streamflow and groundwater in a semi-arid meso-scale catchment

3.1 Introduction

Understanding the impacts of changes in vegetative cover on streamflow and groundwater is a key part of catchment management in areas where large-scale changes are occurring. This is the case for catchment areas throughout the subtropical thicket biome in South Africa's Eastern and Western Cape Provinces, a water-stressed region with a fast growing human population. The subtropical thicket form that is dominated by the succulent *Portulacaria afra* is highly vulnerable to canopy cover loss when subjected to livestock grazing (Lechmere-Oertel et al., 2005a; Mills et al., 2005). This vegetation naturally occurs across an area of about 17,000 km^2 and approximately half of this area, including significant portions of catchments providing regional water supplies, has been classified as significantly degraded due to high density livestock farming (Lloyd et al., 2002). In recent years, recognition of the loss of biodiversity, agricultural productivity, carbon storage, and watershed services resulting from severe thicket degradation has been motivation for large-scale restoration proposals (Mills et al., 2007). The impacts of thicket canopy loss on rainfall interception, soil infiltration, and runoff production have been measured at the plot scale (Mills and Fey, 2004b, 2004a; Mills and Cowling, 2010; Cowling and Mills, 2011; van Luijk et al., 2013), but hydrologic impacts of subtropical thicket degradation and restoration at the catchment scale have not been well explored. This study uses hydrologic modeling to

assess likely impacts of changes in thicket canopy cover on long-term streamflow and groundwater in a meso-scale catchment. The catchment of the Baviaanskloof River was used as a case study, a 1,234 km^2 area which feeds a major water supply reservoir and in which 32% of the vegetation cover is degraded thicket.

Catchment scale impacts of vegetation cover changes on water yield, flood flows, and baseflows have been monitored and modeled for a variety of environments and scales globally, showing that trends can differ in direction and magnitude between different climate regimes, vegetation types, catchment geomorphologies, and the topographic location and extent of the change (Bosch and Hewlett, 1982; Brown et al., 2005; Price, 2011; Stednick, 1996). A loss of vegetation cover will change local interception of rainfall, infiltration, and evapotranspiration (ET), impacting both surface runoff and percolation to groundwater. The net impacts of these changes on resulting streamflow patterns will depend on the balance of the different processes affected, and this balance is location specific. Conversion of closed canopy vegetation to open canopies generally result in greater storm runoff and less infiltration due to decreased canopy interception, lower surface roughness, and potentially lower soil infiltration rates (Bhark and Small, 2003; Dunjó et al., 2004; Bautista et al., 2007; Turnbull et al., 2010; Peña-Arancibia et al., 2012). The magnitude of this impact is moderated by climate, soil type, slope, and landscape flow path context. However, while vegetation cover loss increases storm event surface runoff, and hence streamflow peaks to varying degrees, impacts on low flows can be in either direction. Lower vegetation densities results in decreased transpiration, and often decreased total ET, but increases in evaporation from wind exposed and unshaded soils and/or snowpacks has also been observed to result in

increased total ET with vegetation losses in certain locations (Biederman et al., 2014). Even if ET does decrease with vegetation loss, this may or may not be countered by simultaneous decreases in infiltration, reducing percolation, interflow, and/or groundwater flows that also impact baseflow (Price, 2011).

Large-scale loss of vegetation cover, or conversion of one vegetation type to another having lower transpiration rates, can result in increased overall catchment water yield due to a decrease in ET (Bosch and Hewlett, 1982; Le Maitre et al., 2002; Brown et al., 2005; Stednick, 1996). However, in addition to the percent cover and species present, vegetation water use is moderated by the plants' access to water, often impacted by topographic position. Deep-rooted vegetation in riparian zones that can perennially access groundwater can have significantly greater annual total ET than stands of the same species located in uplands, with observed differences in the range of 30-100% (Dzikiti et al., 2013, 2014). Changes in riparian vegetation cover can be expected to produce greater ET-driven impacts on water yield than proportional changes in upland vegetation. There is potential for increased vegetation cover, particularly in uplands with shallow and/or well drained soils, to result in increased infiltration of rainfall and hence interflow and/or groundwater recharge, without significantly increasing ET withdrawals from subsurface pathways feeding baseflow. This can account for increased baseflow observed with increased vegetation cover in some cases (e.g. Bruijnzeel, 2004; Line and White, 2007; Ma et al., 2009; Price, 2011; Peña-Arancibia et al., 2012).

South African subtropical thicket occurs primarily on the semi-arid hillslopes of the coastal forelands of the Eastern Cape Province. Intact, it is characterized by a closed, dense, low (<3 m) canopy of evergreen trees and shrubs, many of which are succulents. Full thicket canopy cover can occur on steep slopes (close to 60%) with thin (100 mm) rocky soils. Drier forms of thicket (>450 mm mean annual precipitation) have canopies dominated by the succulent shrub *P.afra,* commonly known as 'spekboom', and this form will hereafter be referred to as 'spekboom thicket' (Vlok et al., 2003). Spekboom is relatively resilient to the browsing patterns of large indigenous herbivores eating from the top of the canopy (Stuart-Hill, 1992), but can be completely removed when subjected to consistent grazing by domestic goats (Lechmere-Oertel et al., 2005a; Mills et al., 2005). The result is a transformation of closed canopy spekboom thicket into an open community with low densities of isolated small trees and remnant thicket clumps surrounded by ephemeral herbs and bare ground (Hoffman and Cowling, 1990; Stuart-Hill, 1992; Moolman and Cowling, 1994; Lechmere-Oertel et al., 2005a, 2005b).

When grazing pressure is removed, canopy regeneration on severely degraded areas is slow or non-existent over multi-decadal timescales, likely due to changes in soil and microclimate conditions, thicket species' reproductive strategies that limit recolonization to the margins of remnant clumps, sparse remnant clump source populations, and slow growth in semi-arid conditions (Kerley et al., 1995; Vlok et al., 2003; Lechmere-Oertel et al., 2005a; van der Vyver et al., 2013). However, active restoration through planting spekboom truncheons and protection from herbivory has been met with success, with the planted spekboom establishing in open areas lacking organic topsoil and subsequently fostering

recolonization by the other thicket species (Mills and Cowling, 2006; van der Vyver et al., 2013). Therefore the return of a full thicket canopy on currently degraded areas is not a physically unreasonable scenario for the long-term future (30-50 years).

Effects of the loss of spekboom thicket canopy cover on rainfall interception, soil properties and soil moisture, and storm runoff and sheet erosion have been measured at different scales by previous studies (Mills and Fey, 2004b, 2004a; Mills and Cowling, 2010; Cowling and Mills, 2011; van Luijk et al., 2013). Van Luijk et al (2013) and Cowling and Mills (2011) both measured canopy interception and throughfall in spekboom thicket, recording interception rates of 31-46% of the net rainfall over a season and a halving of the maximum intensity measured in the throughfall compared to the rainfall. Mills and Fey, 2004b sampled soils at paired grazed degraded and ungrazed intact thicket sites along fenceline contrasts and found degraded sites had less than half the laboratory infiltration rate of those with canopy cover and had greater capacity to crust. Van Luijk et al. (2013) sampled soils along a fenceline contrast finding over a 100 fold decrease in field measured infiltration rates and a 20% decline in saturated soil moisture content. These results are consistent with observations of declining soil organic matter with thicket loss: a 90% decrease in litter input (Lechmere-Oertel and Kerley, 2008) and a 50-70% decrease in topsoil carbon (Mills and Cowling, 2010; Mills et al 2005). Using paired transects of Gerlach troughs, (van Luijk et al., 2013) observed a doubling in runoff and near six-fold increase in sediment transport on the grazed, open canopy side of the fence compared to the intact thicket side. In the same study, despite higher canopy interception and potentially higher ET, the soil moisture under the spekboom canopy was seen to reach and maintain

higher levels than the open site, likely due to increased infiltration, soil water holding capacity, and shading and wind buffering effects (van Luijk et al., 2013).

Given these observations it is expected that large scale loss of spekboom canopy cover would result in increased streamflow peaks following sizeable rainfall events. This is predicted to be evident in small headwater catchments lacking significant floodplain areas. It is hypothesized that at larger catchment scales, such as for the entire Baviaanskloof catchment, the effects of hillslope canopy cover loss on increasing flow peaks will be buffered by the presence of larger floodplains. In addition to the lower gradient generally slowing flow, floodplains in this region are characterized by transmissive coarse alluvial deposits and deep-rooted vegetation such as savannah or riparian forest. Channel roughness, overbank flooding, and channel and floodplain infiltration would reduce the intensity of flood peaks, particularly those occurring in periods when the floodplain aquifer water table lies below the river channel allowing for high channel infiltration losses.

In this context, the decrease in soil infiltration observed with the loss of thicket canopy cover could also reasonably be expected to result in a decrease in river baseflow. In the mountainous Baviaanskloof catchment, as seen elsewhere in the Table Mountain Group geologic region, interflow at the soil-rock interface and in the highly fractured surface rock layer of the hillslopes is a significant source of water feeding streams, wetlands, and floodplain aquifers (Midgley and Scott, 1994; Roets et al., 2008; Xu et al., 2002, 2003; Chapter 1). Steep slopes and coarse grained thin soils may facilitate interflow even when the vegetation increases soil water holding capacity and ET. With less water infiltrating on

hillslopes after thicket degradation, less interflow is expected. Less recharge to deep groundwater is expected, potentially decreasing baseflow sourced from the mountain bedrock aquifer over longer timescales. In a larger catchment area the impact of hillslope changes on catchment outlet flows will be buffered by the floodplain. Some of the additional surface runoff expected from degraded hillslopes, taking the place of interflow, could infiltrate into the floodplain and may still feed downvalley baseflow. In the case of intact thicket, it is also possible that additional hillslope interflow quantities expected to recharge floodplain alluvium may be lost to ET by deep rooted floodplain vegetation.

Published field measurements of transpiration rates in spekboom thicket are not currently available; however, it can be assumed that transpiration from intact thicket will be higher than that of degraded open canopy communities. This means the loss of thicket could potentially result in an overall increase in catchment water yield through a decline in ET. Evergreen shrubs and trees typically use more water than seasonally dormant grasses (Calder and Dye, 2001). Actual evapotranspiration (AET) by spekboom thicket and other regional vegetation types was estimated by (Meijninger and Jarmain, 2014) at the scale of the entire Western Cape Province by applying the SEBAL model to satellite data for wet, dry, and average years. In this study, average annual thicket AET was similar to mountain fynbos (515 vs. 555 mm) and greater than escarpment renosterveld (95mm) and central mountain renosterveld (385mm), characterized by shorter vegetation and sparser cover in rocky soils (Meijninger and Jarmain, 2014).

Despite the plot-scale observations of large hydrologic impacts, the impacts of spekboom thicket loss on streamflow patterns at the meso-catchment scale will be the product of many affected processes, the flow path between hillslopes and the catchment outlet, and weather patterns. The observed decrease in hillslope interception, infiltration, transpiration, and potentially ET, and increase in surface runoff, will likely result in increased flood peaks from large events, when surface flows exceed the buffering capacity of downslope alluvial fans and floodplains. However, the effects on baseflow will be determined by the balance of changes in ET on the hillslopes, recharge to the interflow zone and the bedrock aquifer, and ET along flow paths through the central valley alluvial floodplain to reach the catchment outlet. The overall effects on average outflow will be influenced by the proportion and pattern of large and small rainfall events. A catchment model that realistically conceptualizes all of these linked processes and pathways is needed to predict catchment scale outputs.

A model of the Baviaanskloof catchment built using MIKE-SHE/MIKE-11 hydrologic modeling software (Refsgaard and Storm, 1995) was used to examine hydrologic impacts of thicket loss. The numeric model was structured to represent a conceptual model of surface and subsurface flow patterns in the catchment informed by streamflow and groundwater observations (Chapters 1 and 2). This semi-distributed model allowed targeted analyses of the likely influence of thicket vegetation cover properties on surface flow, hillslope interflow, mountain bedrock groundwater flow, and floodplain alluvial aquifer flow. Different hillslope vegetation cover scenarios were modeled to explore impacts on total

water yield, flood peaks, and baseflows over 38 years of historic temperature and rainfall variability.

Figure 3-1 Vegetation cover change in the Baviaanskloof catchment along a fence-line between a continuously grazed area and a recovering subtropical thicket area with 40 years of livestock exclusion

As seen in 2009 aerial photography (left) (source: South Africa NGIS), and estimated canopy cover (right) as calculated from NDVI based on Landsat imagery for March 2013 (Smit 2013). (Site used for field sampling by van Luijk et al 2013 and is further described there.)

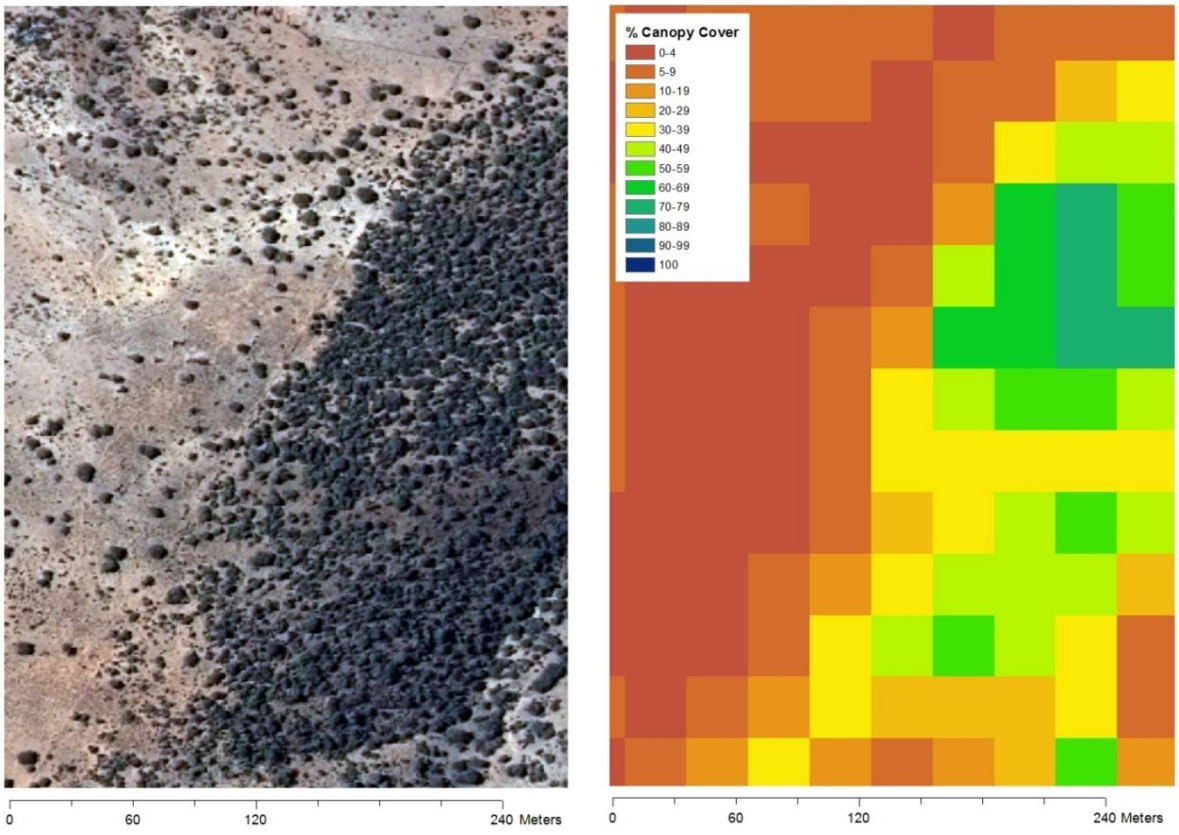

Figure 3-2 Estimated canopy cover as calculated from NDVI based on Landsat imagery for March 2013 and field surveys (Smit 2013) – blank areas occur where shade precluded analyses

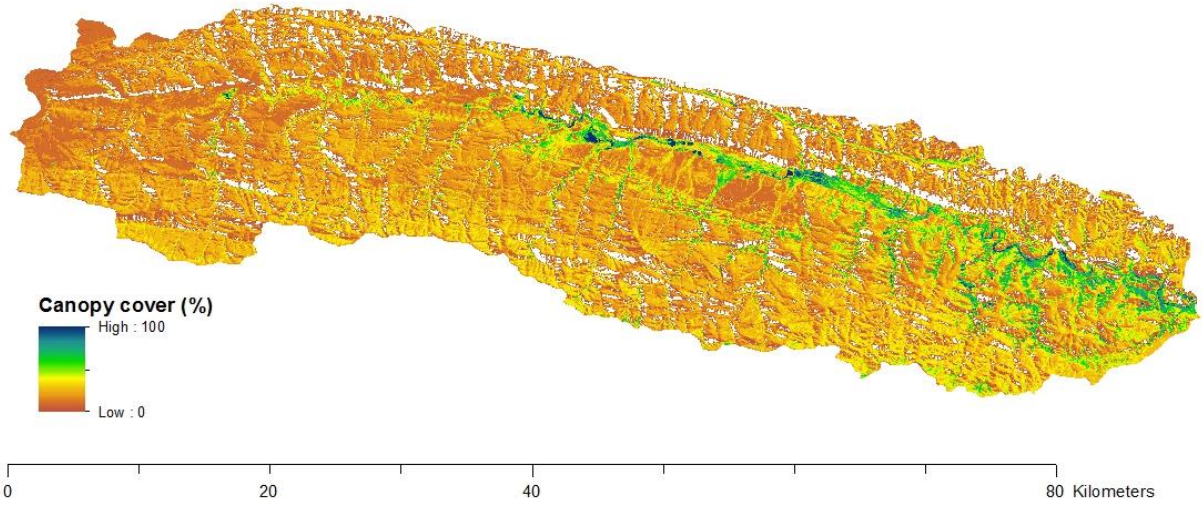

Figure 3-3 Vegetation type distribution and degradation class in the Baviaanskloof catchment based on Euston-Brown 2006

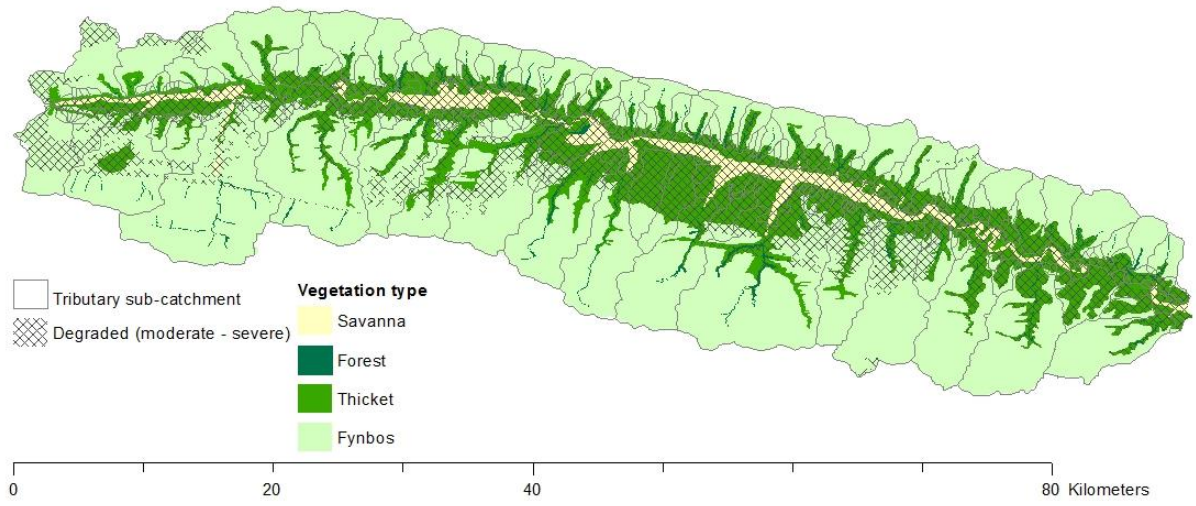

3.2 Methods

3.2.1 Vegetation description

The Baviaanskloof catchment is described in detail in Chapter 1, Section 1.2.1. The hillslopes over much of the catchment have been used for goat grazing for well over a century. Favorable wool prices in the 1940s and 1970s led to particularly high stocking rates with Angora goats in these periods. This has significantly reduced vegetation cover in areas which would otherwise have had a dense spekboom thicket canopy, as supported by the location, climate, soil, remnant vegetation clumps, cover at comparable ungrazed sites, and cover contrasts along fencelines between differently managed properties (Euston-Brown, 2006; Sigwela et al., 2009). Based on these observations, it has been suggested that 40% of the catchment area would support spekboom thicket, of which 82% has been classified as significantly degraded based on aerial photography and ground-truthing (Euston-Brown, 2006). The fynbos vegetation found at higher elevations has far fewer palatable species and was largely not farmed.

Current LAI and canopy cover have been estimated for the Baviaanskloof catchment at a 30 m resolution (Figure 3-1 and Figure 3-2) based on Landsat derived NDVI for March 2013 (Smit, 2013). Relationships between NDVI and canopy cover (R^2=0.8-0.9) and LAI (R^2=0.7-0.8) were derived based on sample site field canopy measurements and septometer readings in the main vegetation types (Gwate et al., 2015; Smit, 2013). Based on the resulting maps, hillslopes that would support spekboom thicket in the Baviaanskloof have an estimated average canopy cover of 20% and LAI of 0.6. Areas classified as intact thicket

had an estimated average canopy cover of 65%, consistent with the 60% observed in intact thicket field plots in other regions (Lechmere-Oertel et al., 2005a), and an LAI of 2, similar to other semi-arid shrublands (Steinwand et al., 2001). The average estimated canopy cover for extremely degraded thicket sites was 8% with an LAI of 0.2. These values are only slightly lower than what would be predicted using a linear relationship between canopy cover and LAI found for semi-arid shrublands in California by (Steinwand et al., 2001) which would predict LAI of 2.6, 0.8, and 0.3 given the canopy cover values found for intact, current, and degraded thicket.

3.2.2 Scenario modeling

A daily time-step, semi-distributed model was constructed and calibrated for the Baviaanskloof catchment given its current land cover. This model was built using the MIKE-SHE/MIKE-11 modeling system (Refsgaard and Storm, 1995) as described below and in Chapters 1 and 2, based on a conceptual model informed by field observations of surface and groundwater flows, soil and vegetation properties, and topography, and spatially discretized in order to give separate consideration to thicket areas in the landscape. In this model, the catchment area was discretized into mountain tributary subcatchments and the main valley floodplain. The subcatchments were further discretized such that canopy interception, infiltration, soil moisture storage, actual evapotranspiration (AET), vertical percolation, and surface runoff routing were calculated at the level of topographically defined response units: plateaus, hillslopes, cliffs, and canyon floors. Surface runoff was routed across units in a catena to the subcatchment outlet with opportunity for infiltration

along the flow path. Hillslope interflow and mountain bedrock groundwater flows were modeled as lumped linear reservoirs at the sub-catchment scale, receiving percolated water from all topographic units and discharging to the floodplain alluvial aquifer. Groundwater flow through this alluvial aquifer was modeled using a 50 m finite element grid governed by Darcy's Law, allowing a dynamic connection to the floodplain channel. Floodplain canopy interception of precipitation, infiltration or runoff of through-fall, soil moisture storage and percolation to the water table, and AET were also calculated by grid cell. The floodplain channel received subcatchment surface flow when a direct channel connection was present and channel flow was modeled using a diffusive wave approximation. Two-way exchange of water between the aquifer and channel was governed by relative elevation and bed conductivity. For a more detailed description of the model construction refer to Chapter 1 and 2.

The model was calibrated using a multi-criteria procedure against multiple datasets of surface flows and groundwater levels: gauged catchment outlet streamflow for 2012-2013, estimated monthly catchment outflow for 1991-2013, observed presence/absence of flow in tributary catchment channels and the central floodplain channel for 2012-2013, and observed floodplain groundwater depths for 2012-2013 (Chapter 2). Given the high dimensionality of the model structure (42 calibration parameters), the relatively short gaged streamflow record, uncertainties in observational datasets, simplifications in process representation, and incomplete commensurability of observational data and model parameters and outputs, the calibration procedure did not attempt to produce a single optimized parameter set. Instead, thresholds of acceptability were applied to various model

output goodness-of-fit measures to patterns in the datasets in order to constrain the range of model parameter values considered likely and used in further model application. The resulting model and accepted parameter space reproduced 2012-2013 daily streamflow with a Nash-Sutcliffe efficiency (NSE) of 0.87-0.92 and 1991-2013 monthly flows with an NSE of 0.79-0.85, predicted annual mean flow within 0.5 m^3/s and maximum monthly averaged flows within 1 m^3/s of the observed, and modeled floodplain groundwater fluctuations with an R^2 of 0.79-0.81 and an accuracy in the range of depth fluctuation within 0.5 m against the observations (Chapter 2). Accepted models had errors in average annual yield of 3-20%, with a mean of 12%.

To assess potential impacts of changes in thicket canopy cover on streamflow and groundwater in the alluvial aquifer, the parameterization of the hillslope and cliff topographic units were changed to reflect intact versus degraded thicket scenarios. Three scenarios were considered: current conditions, complete thicket degradation, and fully intact thicket cover. In previous research described above, the loss of thicket canopy cover has been associated with reduced LAI, interception, soil infiltration and water holding capacity, surface roughness, and ET rates (Mills and Fey, 2004b; Lechmere-Oertel et al., 2005b; Mills and Cowling, 2010; Cowling and Mills, 2011; van Luijk et al., 2013; Meijninger and Jarmain, 2014). Based on these studies the parameter value ranges shown in Table 3-1 were applied for each scenario. In the model a daily canopy interception threshold for throughfall was calculated as a function of LAI. Data from (van Luijk et al., 2013) indicated an event average interception of 3 mm under a full canopy and this value was scaled based on the LAI differences between the cover scenarios. Soil properties sampled under spekboom

canopy and in open areas were spatially averaged using the estimated percent canopy cover to estimate hillslope averaged properties for each scenario. The ratios between soil properties for canopy and bare sites in other studies were applied, however the values were adjust based on the model calibration values for the current cover scenario. Given the daily time-step, spatial scale of modeled units, and other simplifications of model process representation, model soil parameters do not have a one to one relationship with physical properties measured at point locations, however the order of magnitude of change between scenarios was assumed to be consistent.

Model AET was calculated using a evapotranspiration coefficient (ET_k) for each vegetation type. This coefficient was applied to the remaining PET demand after canopy storage evaporation, with the resulting AET being limited by available soil moisture and the decline in ET rate when soil moisture is below field capacity, approaching zero at the wilting point. ET coefficients for spekboom thicket were assumed to be in a similar ranges observed for mountain fynbos and greater than renosterveld based on the comparative regional AET values estimated from satellite data and energy balance modeling by Meijninger and Jarmain (2014). Scintillometry based measurements in mountain fynbos suggested ET coefficients ranging from 0.3 to 0.5 (Dzikiti et al., 2014). A ET_k value of 0.2 was estimated for a South African rangeland vegetation consisting of grasses and karroid shrubs on shallow rocky soils (Palmer and Yunusa, 2011), comparable to the cover in severely degraded former thicket.

To account for the uncertainty in the parameterization, the model was run 100 times for each scenario to represent the calibrated parameter space. Parameter sets were selected from the 720 sets in the calibration exercise with acceptable model performance in recreating observed surface runoff, streamflow, and groundwater patterns as described in Chapter 2. Sets of thicket area parameters for degradation and restoration scenarios were selected using Latin Hypercube sampling within ranges in Table 3-1. This resulted in an output distribution for each scenario, allowing for conservative change detection. The model for each scenario was run over 43 years of climate data, from 1970-2012, to assess the response to a range of climate conditions and storm events. The first 5 years (1970-1974) were considered a spin-up period for groundwater levels and change analyses were done for model output for the 1975-2012 water years. The water year was defined as April to March and water years were divided into two seasons, summer (April-September) and winter (October-March), for analyses. To estimate catchment and subcatchment-wide precipitation and PET demand, daily gage data from 6 stations, two within the catchment and four within 20 km (South African Weather Services, South African Agricultural Research Council), was scaled using the monthly precipitation and temperature surfaces (2 km resolution) of Lynch (2003) and Schulze and Maharaj (2004). The estimated catchment mean annual precipitation (MAP) for this period was 270 mm while the PET was 1335 mm, giving an average aridity index (MAP/PET) of 0.2. Over this period annual total rainfall was highly variable, ranging from 139 to 415 mm (Figure 3-4). Patterns and seasonal distribution also ranged widely with the number of days with over 5mm of rain in a year ranging from 9 to 32. Maximum day rainfall in a year ranged from 12 mm to 57 mm and the maximum month rainfall in a year ranged from 28 mm to 113 mm.

Table 3-1 Model parameter value ranges for thicket cover scenarios

Parameter	Intact thicket cover	Current cover	Complete thicket loss
Vegetation properties			
Canopy cover (%)	65 (55-75)	20 (15-25)	8 (5-12)
LAI	2 (1.6-2.4)	0.6 (0.4-0.8)	0.2 (0.1-0.3)
Maximum canopy interception (mm)	3 (2.4-3.6)	0.9 (0.6-1.2)	0.3 (0.1-0.5)
Evapotranspiration coefficient (ET_k)	0.45 (0.4-0.5)	0.35 (0.3-0.4)	0.2 (0.1-0.3)
Surface roughness (Manning's n)	0.2 (0.1-0.3)	0.1 (0.06-0.14)	0.05 (0.02-0.07)
Soil properties			
Infiltration rate (mm/day)	80 (75-95)	35 (30-40)	15 (10-20)
Saturated water content	0.50 (0.55-0.45)	0.40 (0.42-0.38)	0.35 (0.37-0.33)
Field capacity water content	0.18 (0.20-0.16)	0.15 (0.16-0.14)	0.13 (0.14-0.12)
Wilting point water content	0.12 (0.13-0.11)	0.09 (0.10-0.08)	0.06 (0.07-0.05)

Figure 3-4 (top) Daily rainfall and PET for the Baviaanskloof catchment area 1970-2013 (below) annual total precipitation showing distribution between summer and winter months and the annual aridity index

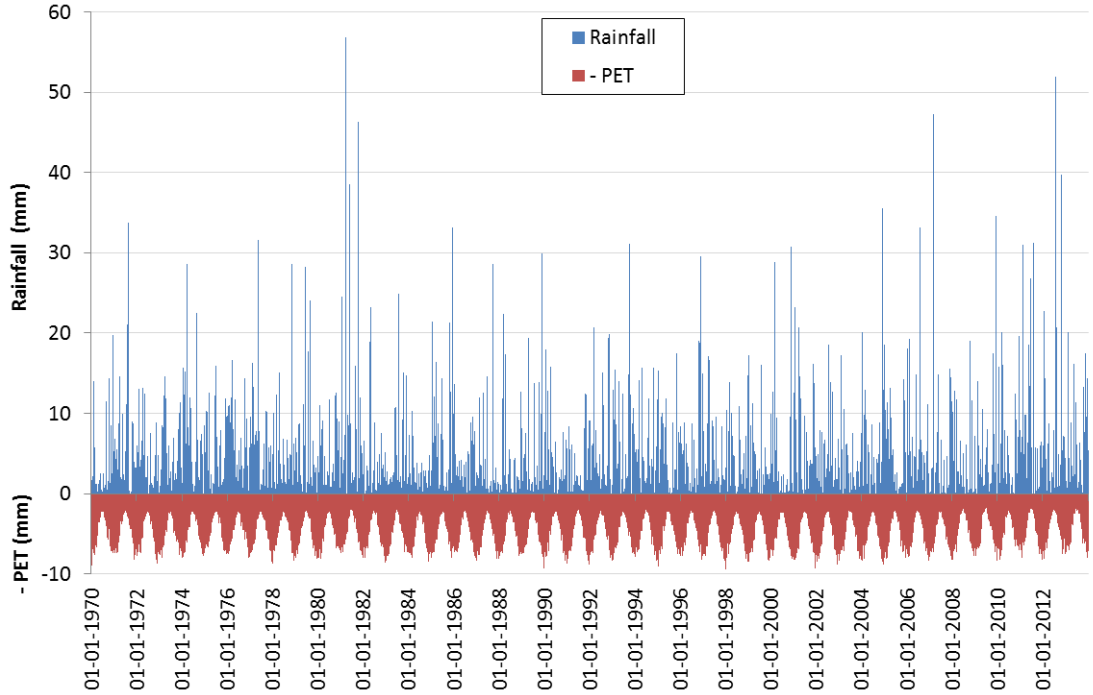

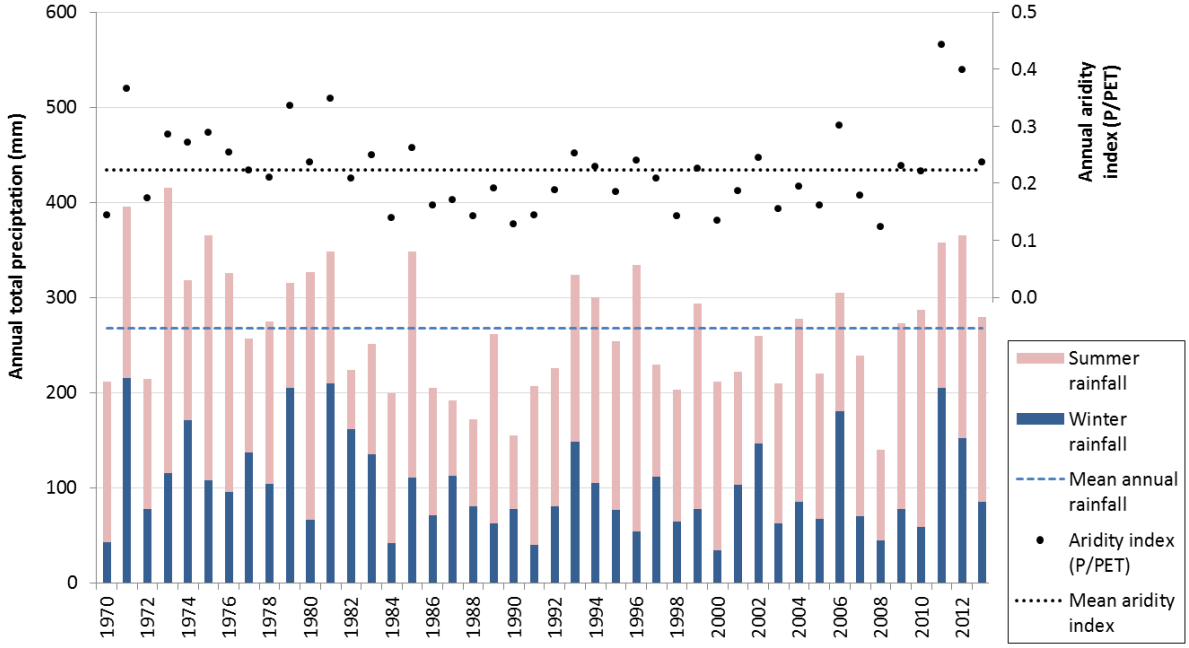

3.2.3 Output analyses

For the set of model runs for each vegetation cover scenario the mean and 95 percent confidence intervals of the following statistics were calculated: average annual water yield, average annual minimum monthly flow, average of the daily flows for the fourteen largest flow peaks in the period (annual excedence probability of 10%), average depth to groundwater in the alluvial aquifer (spatially averaged), average annual maximum depth to groundwater in the alluvial aquifer (spatially averaged). These statistics were chosen to assess impacts relevant to water supply and flood management. To assess changes in the flow path of water through the catchment the following were also calculated: average annual AET in the catchment and in the thicket area and the proportion of which was due to canopy interception, average annual overland flow from the thicket area and leaving the tributary subcatchments, average annual interflow leaving the tributary subcatchments, and average annual mountain bedrock baseflow leaving the tributary subcatchments. Changes were considered significant when p-values of paired t-tests between the scenario sets had p-values of less than 0.05 and likely differences between scenarios are given as the minimum and maximum differences between the 95% confidence interval ranges of the means.

Within the modeled time period, multi-year dry and wet periods were identified to compare the effects of vegetation cover change under different climatic conditions. It was observed previously that winter rainfall events typically resulted in higher runoff ratios compared to the response to similar events in summer, however antecedent wetness played a large role (Chapter 1). The periods of 1986-1988, 1990-1992, and 2007-2008 (using water years as defined above) were classified as dry due to having below average annual rainfall

values, annual aridity indices (P/PET), and relatively low proportions of winter rainfall (Figure 3-4). The periods of 1979-1981, 1993-1994, and 2011-2012 were classified as wet due to above average annual rainfall values, annual aridity indices, and winter rainfall fraction for the period.

3.3 Results

3.3.1 Effects on catchment scale water yield and streamflow

When compared to modeled yields for the current condition, simulations of complete degradation of hillslope spekboom thicket cover predicted a 12-17 Mm^3 (41-62%) increase in the catchment's long-term annual average water yield (Table 3-2, Figure 3-8). This was the result of large increases in modeled surface runoff from the hillslopes and a reduction in AET. Catchment-wide restoration of full thicket canopy cover was predicted to result in a 5-8 Mm^3 (22-27%) decrease in annual average streamflow yield compared to the current condition due to increased AET and small quantities of recharge to slow release groundwater stores. Restoration of thicket canopy cover was predicted to increase average annual catchment AET by 5-8 Mm^3 (2-3%) compared to the current state. Complete conversion of hillslope thicket vegetation to the degraded state, ephemeral grass with low densities of small trees, was predicted to decrease average annual catchment AET by 7-12 Mm^3 (2-4%). Differences in mean values were all significant at an alpha of 0.05.

Table 3-2 Long term (1975-2012) average annual water balances for the Baviaanskloof catchment and internally modeled land units under different scenarios of hillslope thicket cover

Location / spatial scale	Flux	Annual volume (Mm^3/ year)					
		Degraded thicket		Current cover		Intact thicket	
		Mean	95% CI	Mean	95% CI	Mean	95% CI
Catchment	Precipitation	323		323		323	
	AET	278	1.4	288	1.3	295	0.8
	Streamflow	44	1.5	29	1.0	23	0.6
Mountain tributary sub-catchments	Precipitation	307		307		307	
	AET	249	1.5	260	1.2	267	0.6
	Overland flow to fan head	22	1.0	4.8	0.1	1.9	0.3
	Interflow to floodplain	23	0.8	29	0.9	26	0.5
	Mountain bedrock outflow	9.0	0.5	9.0	0.6	8.9	0.5
Hillslope	Precipitation	185		185		185	
	AET	130	1.1	141	0.9	150	0.4
	Canopy interception	20	0.8	42	1.1	66	0.9
	Overland flow	24	1.1	4	0.1	0.2	0.1
	Infiltration	142	0.3	139	1.2	118	0.9
	Percolation	32	0.1	39	0.8	35	0.4
Central valley alluvial fill (fans and floodplain)	Precipitation	16		16		16	
	AET	29	0.3	28	0.2	28	0.2
	Alluvial aquifer input to channel (net)	19	1.6	25	1.5	21	1.0
	Overland flow inputs to channel	25	1.1	3.6	0.7	1.0	0.2

Figure 3-5 Long-term average water balance diagram for the Baviaanskloof catchment as modeled with degraded hillslope thicket.

Quantities are in million cubic meters (Mm^3) of water per year. Hillslope surface water fluxes are a subset of the tributary subcatchment fluxes.

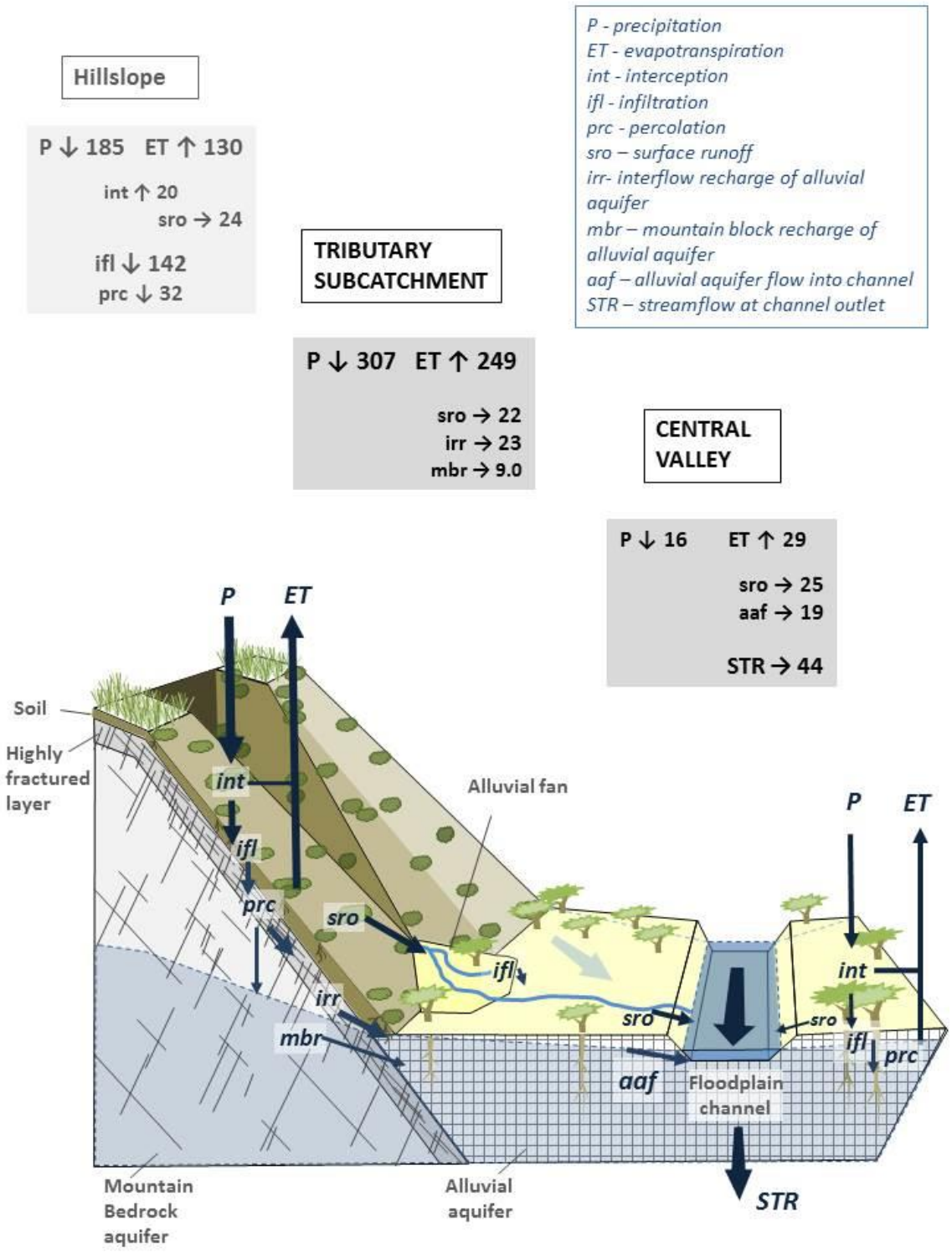

Figure 3-6 Long-term average water balance diagram for the Baviaanskloof catchment as modeled with restored intact hillslope thicket.

Quantities are in million cubic meters (Mm^3) of water per year. Hillslope surface water fluxes are a subset of the tributary subcatchment fluxes.

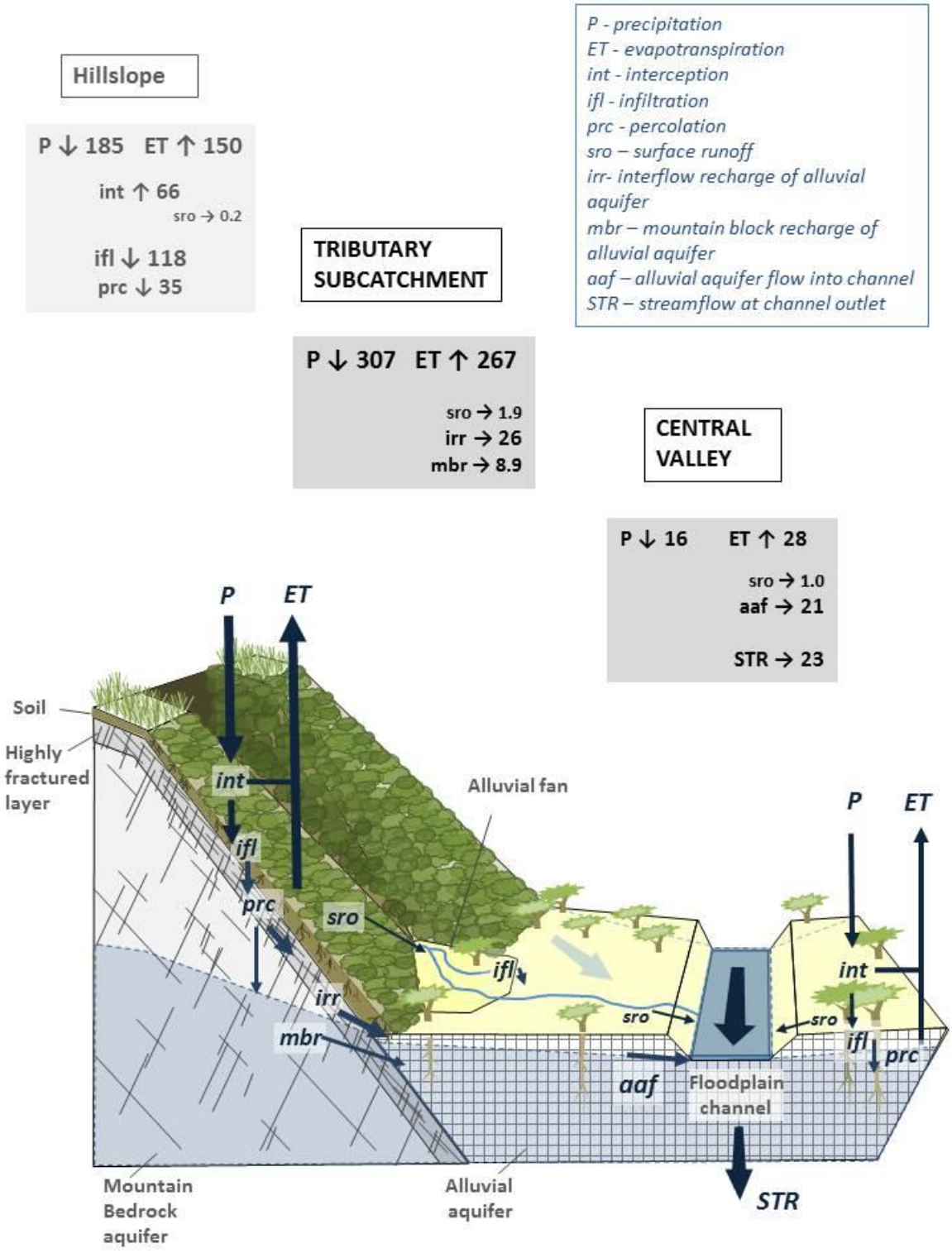

An increase in annual water yield with a loss of hillslope canopy cover was predicted for all the years simulated (Figure 3-7), while magnitudes and proportional differences varied between wet and dry years (Figure 3-8). When comparing scenario outputs over the set of dry years described above (mean annual precipitation 237 mm), the predicted increase in dry year annual average water yield between current and degraded thicket scenarios was 9-11 Mm^3 (77-100%), a larger proportional change than seen when comparing means of all years (41-62%). The increase in predicted mean annual yield for wet years with the loss of thicket cover was 17-26 Mm^3 (28-42%), a smaller proportional change. The inter-annual fluctuation in water yield was greater in the degraded scenario than in the current and restored thicket scenarios. The lower interception, infiltration, and AET in the degraded case made the catchment much more responsive to rainfall events. As such, the predicted differences between the current and restored thicket scenarios changed less between dry and wet years: the predicted decrease in mean dry year water yield was 1.9-3.1 Mm^3 (17-28%) and in mean wet year yield was 11-17 Mm^3 (17-27%). Due to decreased AET and increased runoff sensitivity to small rainfall events in the degraded case, the model predicted a greater increase in summer flows than in winter flows with the loss of thicket cover (Figure 3-8). In this scenario, modeled yields were similar for summer and winter, whereas winter yields were predicted to be greater than summer yields given increased vegetation cover with high summer ET demand.

With minor exceptions, daily modeled streamflow values were consistently higher in the low canopy cover scenario than the current and intact thicket scenarios in both wet and dry periods (Figure 3-7). In the driest periods, the differences between daily flow estimates for

the scenarios were negligible relative to model accuracy and not statistically significant (e.g. differences of 0.02-0.03 m^3/s in flows between degraded and completely restored scenarios during the summer of 1990). However, the hypothesized potential increase in baseflow with increased canopy cover was not evident in the model results. Modeled mean annual minimum monthly flows decreased from 0.10-0.13 m^3/s in the current scenario to 0.07-0.09 m^3/s with intact thicket, while it increased to 0.16-0.18 m^3/s in the degraded case. The only times when modeled streamflow was higher for the current and restored scenarios than in the degraded case were during one to three day periods following a flow peak when flood flows from the degraded catchment were predicted to peak and recede more quickly than in the scenarios with more vegetation and soil retention (Figure 3-9). Modeled peak flows (those with annual exceedance probabilities under 10%) were predicted to increase by 22-26 m^3/s (34-43%) with the loss of thicket canopy cover and decrease by 34-38 m^3/s (56-60%) with thicket canopy restoration compared to the current scenario.

Figure 3-7 Modeled catchment water yield (total streamflow output) by water year for 1975-2012 for scenarios of current, fully intact, and fully degraded thicket cover on hillslopes.

Scenarios were represented by parameter ranges. Means and confidence intervals of the simulations sets run within these ranges are shown

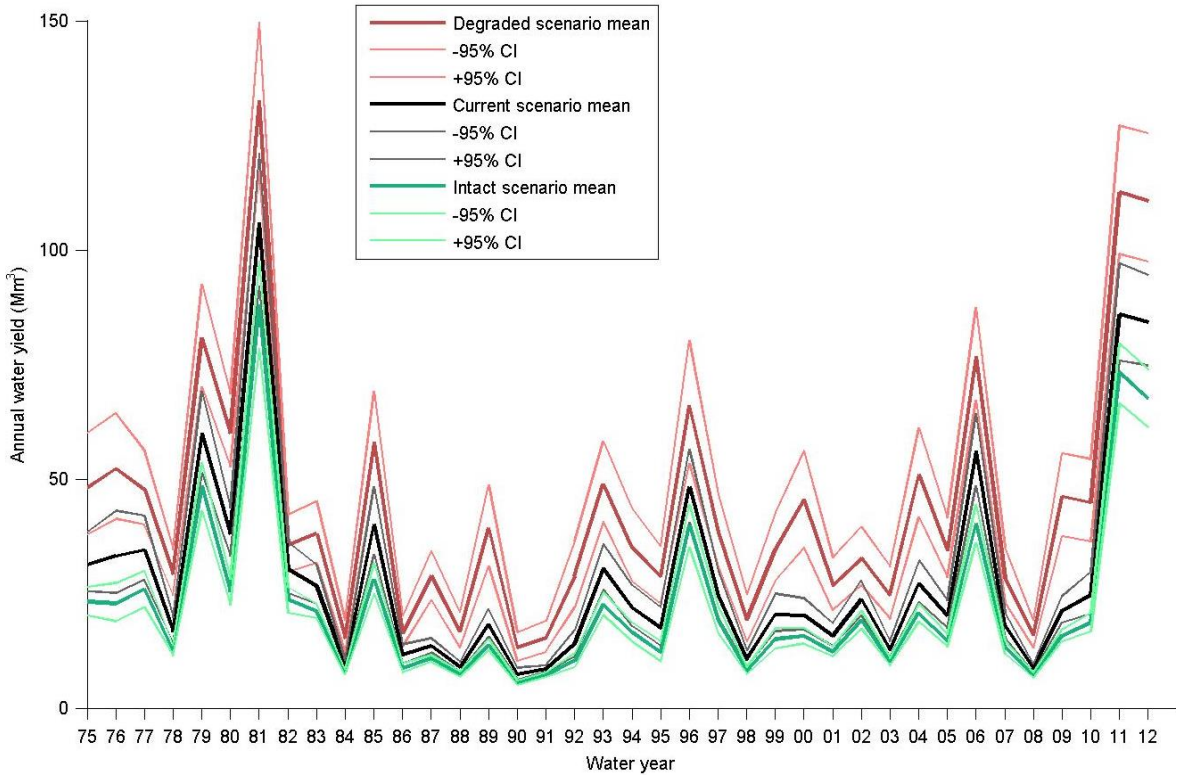

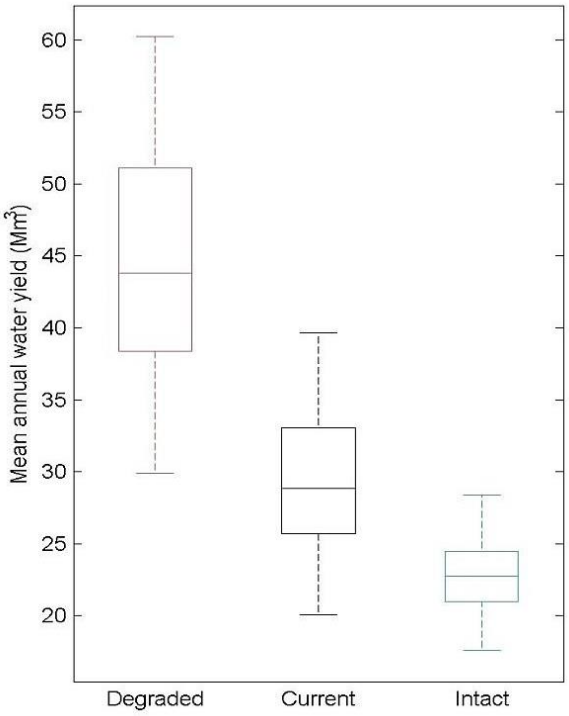

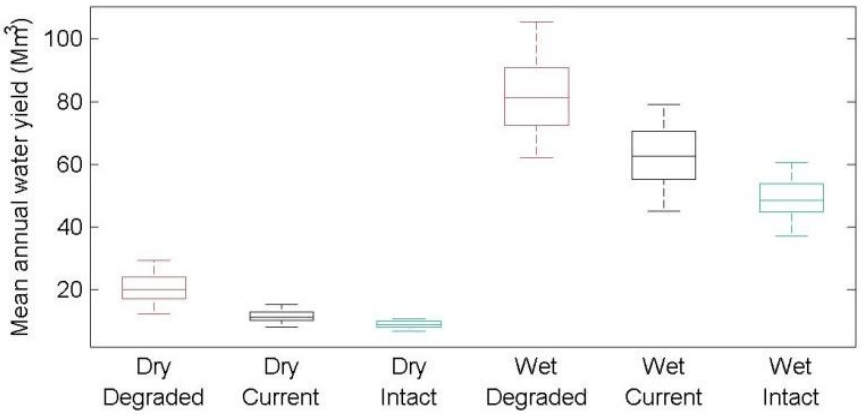

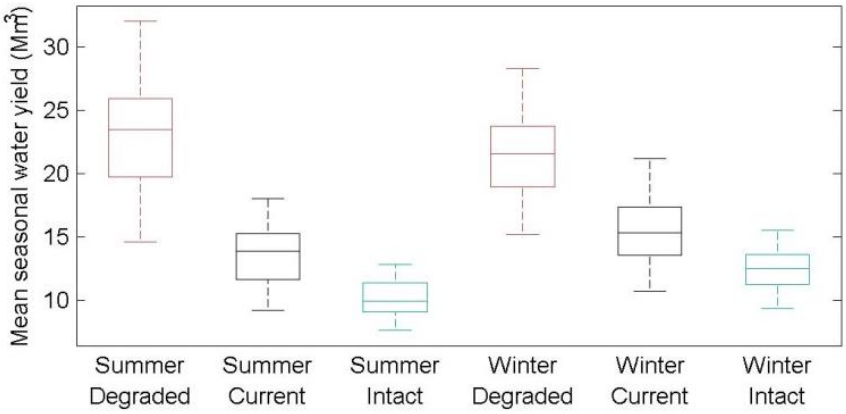

Figure 3-8 Boxplots showing distributions of modeled mean annual and seasonal water yields for different thicket cover scenarios for: all simulated years (left), selected dry and wet years (center), and summer and winter months for all years (bottom)

Figure 3-9 Modeled daily flow hydrographs for demonstration dry (1990, top) and wet (2011, bottom) years showing differences in flow peaks and recessions between hillslope thicket cover scenarios

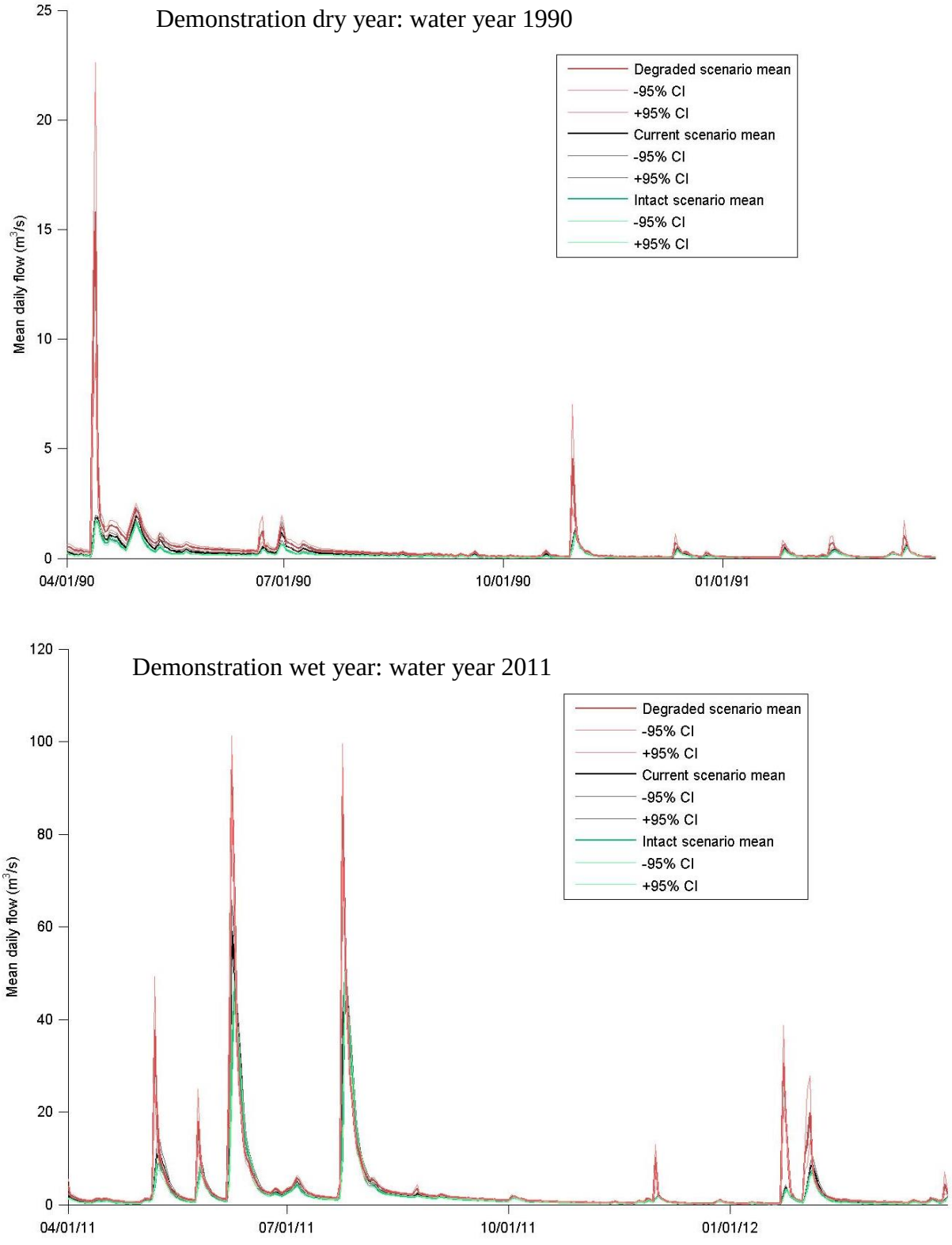

Figure 3-10 Modeled floodplain average groundwater depth in the central floodplain by water year for 1975-2012 for scenarios of current, fully intact, and fully degraded thicket cover on hillslopes.

Scenarios were represented by parameter ranges. Means and confidence intervals of the simulations sets run within these ranges are shown

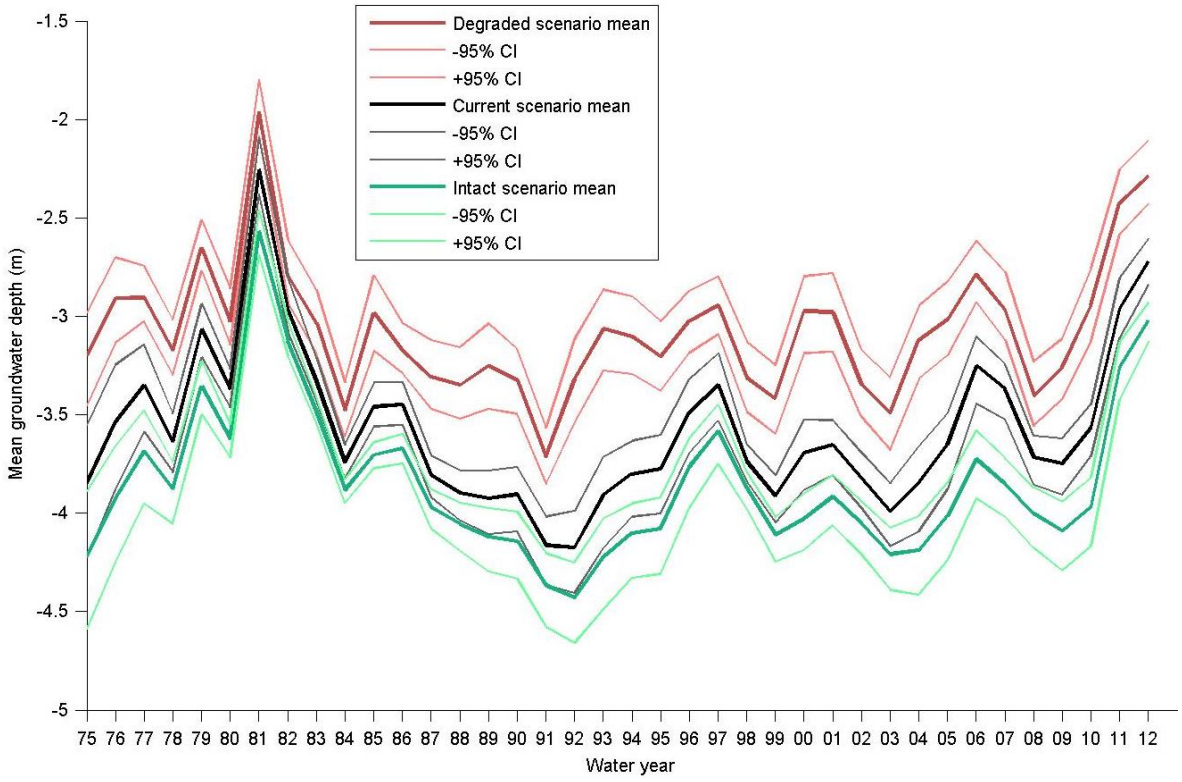

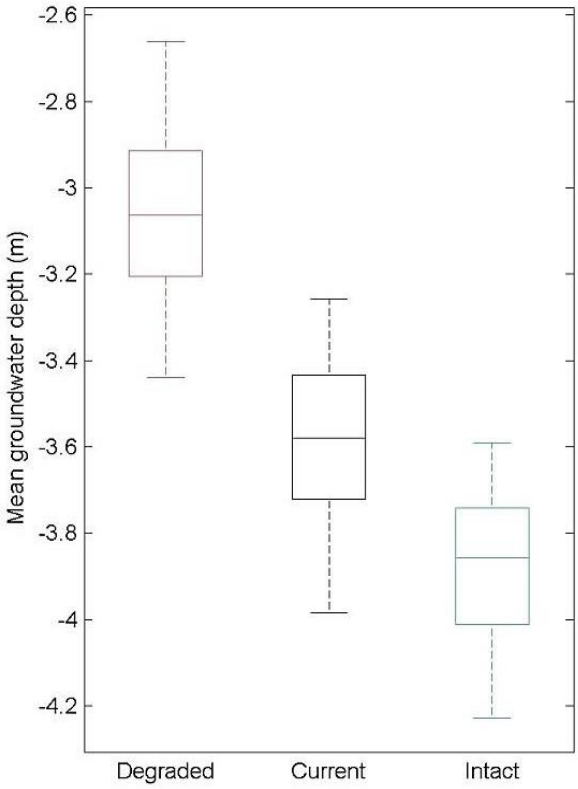

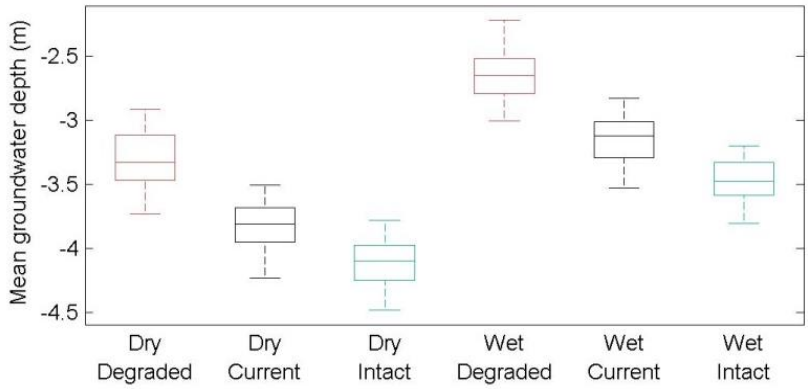

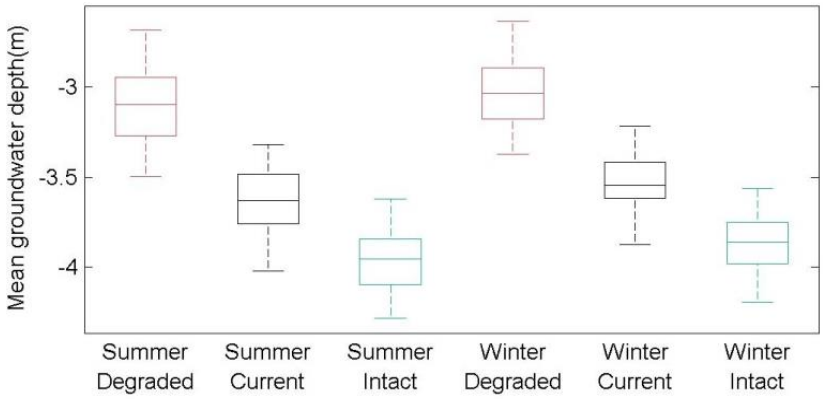

Figure 3-11 Boxplots showing the distributions of modeled mean annual and seasonal floodplain groundwater depth for different thicket cover scenarios for: all simulated years (left), selected dry and wet years (center), and summer and winter months for all years (bottom)

3.3.2 Effects on floodplain groundwater depth

The modeled spatially and temporally averaged depth to groundwater in the central floodplain was 3.0-3.1 m in the degraded thicket scenario, shallower than results for the current cover (3.55-3.65 m) or intact thicket (3.87-3.94 m) scenarios (Figure 3-10, Figure 3-11). The predicted water table depth differences between scenarios for average annual mean, minimum, maximum, seasonal, and wet and dry period depths were always less than a meter (Figure 3-11), relatively small compared to the observed seasonal fluctuations of 3-8 m at various sites. This trend of higher average floodplain groundwater levels in the degraded case was consistent for modeled average water depths for dry and wet years, although there was a greater difference between scenarios in wet years. As with catchment streamflow, there was greater inter-annual fluctuation in the modeled groundwater levels in the degraded thicket case than in the current or restored thicket cases (Figure 3-10). Because of the predicted increased proportion of subsurface flow through the subcatchments with intact thicket, and fewer surface flow and interflow floodplain recharge events, as described further below, there was more delay in aquifer recharge in wet periods and a more slow and steady decline in prolonged dry periods due to ET.

3.3.3 Effects on surface and subsurface flow paths

The model structure allowed for analyses of water fluxes for different landscape units along the flow path to the catchment outlet (illustrated in Figure 3-5 and Figure 3-6). The predicted changes in catchment streamflow and floodplain groundwater levels were the result of various modelled changes in the surface and subsurface flows originating on the

hillslopes and passing through canyon floors, alluvial fans, the floodplain, and channel network. The scenario models, as parameterized, succeeded in recreating some of the patterns observed in field studies of spekboom thicket. Modeled canopy interception in intact thicket made up 35-37% of precipitation on the hillslopes in the simulation period, similar to the 31-46% seen by Cowling and Mills (2011) and van Luijk et al. (2013). Modeled surface runoff on the hillslopes increased five times on average when the thicket cover was degraded. This was more than the doubling in runoff observed by van Luijk et al. (2013) between areas of 45% and 5% cover, but was in keeping with the 6 fold increase in sediment transport detected in that study. Those field observations were made on a hillslope with a deeper soil profile and lower slope (28%) than much of the Baviaanskloof thicket area (40% average slope) and did not include storms of the magnitudes seen in the multi-decadal modeled period, and so may reasonably be expected to be lower than the long-term, catchment-scale average.

Loss of thicket canopy cover has been seen to reduce soil infiltration rates, conductivity, and water holding capacity (Mills and Fey, 2004b, 2004a; Mills and Cowling, 2010; van Luijk et al., 2013), and the degraded thicket model scenario was parameterized as such. This resulted in a significant increase in overland flow from the hillslopes; however, despite the lower infiltration rates, over the 38-year modeled period, greater volumes of water were predicted to infiltrate into hillslope soils in the degraded thicket scenario compared with intact thicket (141-142 Mm^3/yr vs. 117-119 Mm^3/yr , Table 3-2). Part of this can be explained by the 22-25 Mm^3/yr greater average canopy interception evaporation losses predicted in the intact case. As expected given the soil parameterization, of the water

predicted to reach the soil surface as through-fall, there was greater proportional infiltration predicted in the intact thicket than in the degraded scenario: 97-99% of throughfall over the simulation period infiltrated under intact thicket and 85-87% in the degraded case. During rainfall events that significantly exceeded the thicket canopy's interception capacity, predicted daily infiltration volumes were greater in the intact thicket than in the degraded scenario, while the reverse was true for smaller events producing little or no through-fall in the intact thicket (Figure 3-12).

The proportion of rainfall in large events played a large role in determining the differences in total infiltration and percolation between scenarios at different time scales. In the wettest years, such as 1981 and 2012, predicted total hillslope infiltration was greater in intact thicket than degraded (Figure 3-13). During medium magnitude rainfall events the current, partially degraded, thicket cover scenario actually had the greatest infiltration of the three scenarios due to the balance of the canopy interception losses and soil infiltration rates. Due to the greater hydrologic conductivity of the soils under the intact thicket and greater infiltration in large events, model results suggested a greater volume of water can percolate into the fractured bedrock in wetter years given intact thicket cover compared to degraded (Figure 3-12). This occurred in years when there was more total infiltration in the degraded case (Figure 3-13 c vs. d). Some of the predicted additional infiltrated volumes in the degraded thicket came from infiltration during smaller rainfall events, which did not exceed the estimated canopy interception thresholds in intact thicket and also did not result in soil moisture exceeding field capacity in the degraded thicket. As a result much of this infiltrated volume was predicted to be stored in the soil and to leave later as ET. The result was a

slightly higher predicted long term average percolation in the intact compared to degraded case (34-35 Mm^3/yr vs. 31-32 Mm^3/yr, Table 3-2). Of the three scenarios, the current cover scenario was actually predicted to have the greatest average volume of percolation (38-40 Mm^3/yr), due to the medium interception losses, infiltration rates and conductivities, ET losses, and the event distribution of the rainfall.

The changes in hillslope scale processes between scenarios influenced the quantity and pathway of water reaching the alluvial fans and floodplain from the tributary subcatchments. As hypothesized, there was a greater annual average surface flow predicted from the tributary subcatchments with the loss of hillslope thicket cover and this difference was proportionally greater than the change in streamflow at the catchment scale. While simulations predicted a 41-62% increase in average catchment outlet streamflow moving from the current to degraded scenario and a 83-98% from intact to degraded, modeled tributary sub-catchment surface outflows increased by five-fold from current to degraded and twenty-fold from intact to degraded (Table 3-2). The higher percolation predicted for the current and intact thicket scenarios meant that there was greater average interflow predicted for these scenarios (28-30 Mm^3/yr and 26-27 Mm^3/yr) than in the degraded scenario (24-25 Mm^3/yr), and made up larger proportions of the total subcatchment outflow to the floodplain (67-70% vs 42-44%). Due to the slow outflow estimated for the mountain bedrock aquifer, there was no significant difference in model average annual outflow from this source between the scenarios. The predicted 1-6 Mm^3 increase in annual average interflow with increased thicket cover was smaller than the 16-20 Mm^3 increase in overland flow and 8-20 Mm^3 decrease in AET from the tributary subcatchments predicted for the

degraded thicket case. As such, the average mountain tributary subcatchment total surface and subsurface input to the central valley's alluvial fill was predicted to increase with the loss of thicket cover by 8-15 Mm^3 (19-37%) compared to the current scenario and 15-21 Mm^3 (39-59%) compared to the intact thicket scenario. Because the increase in interflow volume with increased thicket cover was only predicted to occur in wetter years, the same periods when the largest predicted increases in overland flow for the degraded case occurred, the trend of increased total subcatchment outflow with loss of thicket cover was consistent in the model for the entire simulation period.

Figure 3-12 Modeled fluxes in mountain subcatchments : (a) precipitation, (b) total overland flow (OLF) output, (c) total infiltration, (d) total percolation, (e) total interflow output

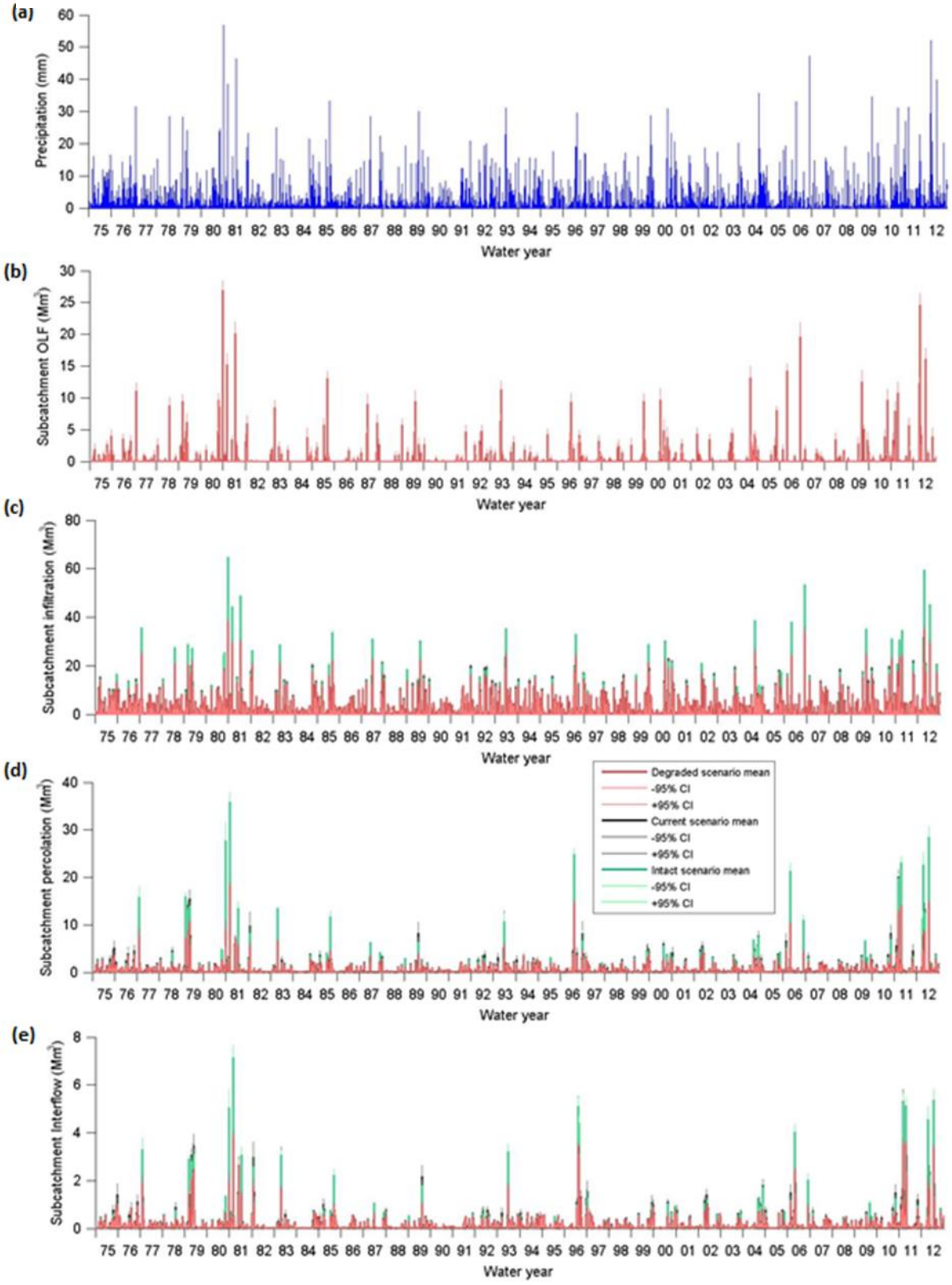

Figure 3-13 Modeled annual fluxes in mountain subcatchments : (a) precipitation, (b) total overland flow (OLF) output, (c) total infiltration, (d) total percolation, (e) total interflow output

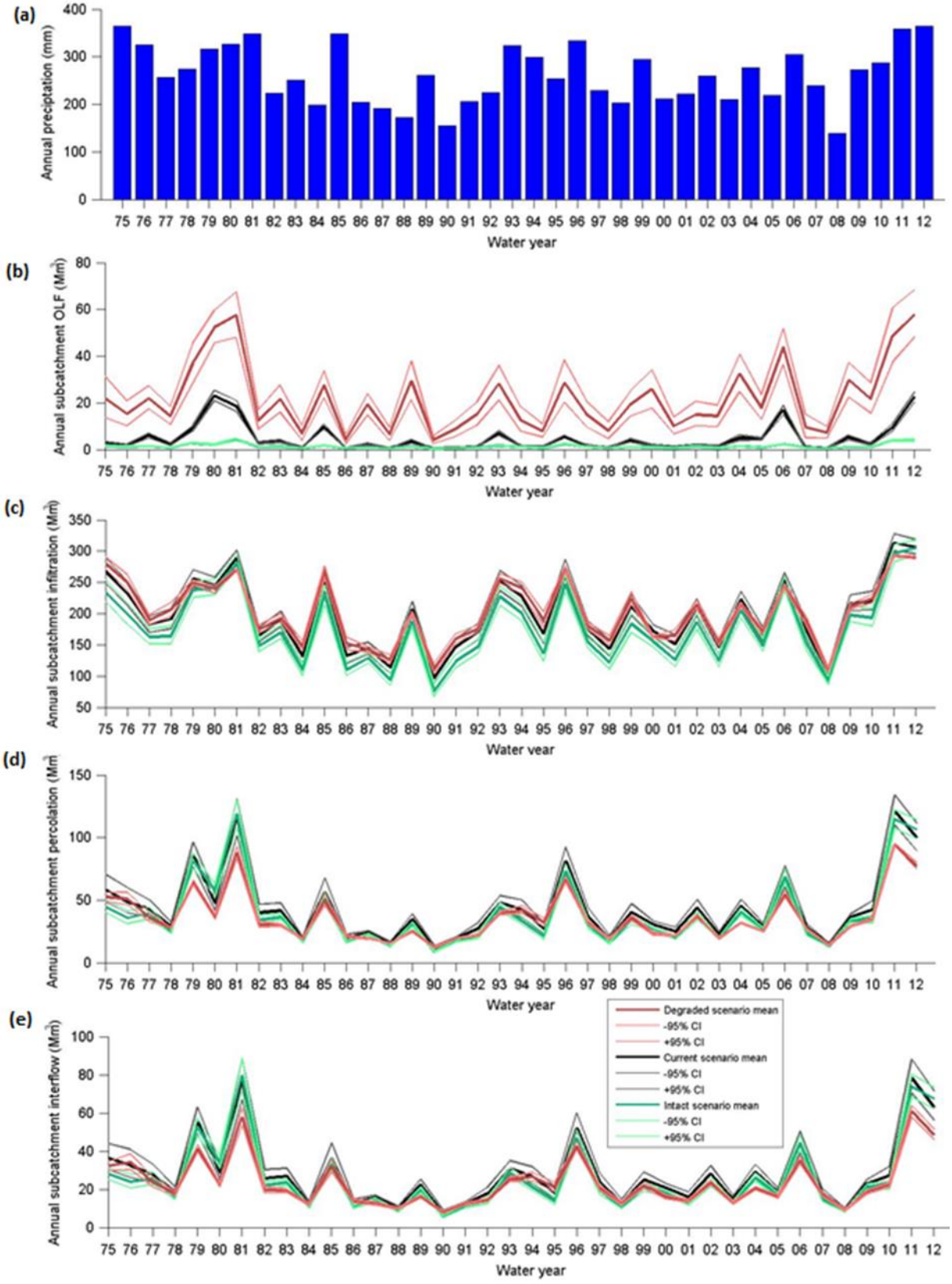

The central valley alluvial fill did dampen the changes that occurred on the hillslopes. Even in the degraded thicket scenario during major flood events, infiltration on the fan and floodplain channels and surfaces, as well as decreased slope and roughness, reduced modeled flood flow peaks to the catchment outlet compared to the peaks in surface outflow from the mountain tributaries (Figure 3-14). In all cases a portion of the overland flow received from the subcatchments infiltrated into the alluvium. However, due to the greater total inputs in the degraded case creating shallower groundwater tables, there was more saturation overland flow on the floodplain in wet periods in this scenario, leading to a small predicted net increase in average annual overland flow inputs to the main channel beyond those received by the subcatchments (23-25 Mm^3 vs. 20-22 Mm^3). In the current and intact thicket scenario a net loss in overland flow crossing the floodplain was predicted (Table 3-2).

On average, a slightly larger volume, and a much larger proportion, of water entering the floodplain channel in the intact and current thicket scenarios was predicted to come from subsurface flows: 25-28 Mm^3/yr (88-92%) in the current and 28-30 Mm^3/yr (95-99%) in the intact, versus 18-21 Mm^3/yr (43-47%) in the degraded scenario. The reason for the slightly lower net volume entering the channel from the aquifer in the degraded case on average was the generally higher streamflow modeled for this scenario. This reduced the groundwater gradient toward the channel in the alluvial aquifer in the model and led to more infiltration into the aquifer both from the channel and from overbank flows during high flow events than in the current and intact thicket scenarios. In all cases, annual AET modeled for the central valley was greater than the precipitation received by this land unit. The deep roots of the floodplain vegetation were able to access the alluvial aquifer which was recharged by the

mountain areas. There was little difference in central valley AET between the scenarios (Table 3-2) because the root depth used in the model was such that predicted differences in water tables between the scenarios were not large enough to significantly change the vegetation's average access to water between the different cases.

Figure 3-14 Modeled daily average flow rates for (a) total overland flow (OLF) output (b) streamflow at Baviaanskloof catchment outlet

Shown on same axis scale to demonstrate reduction in peak flows

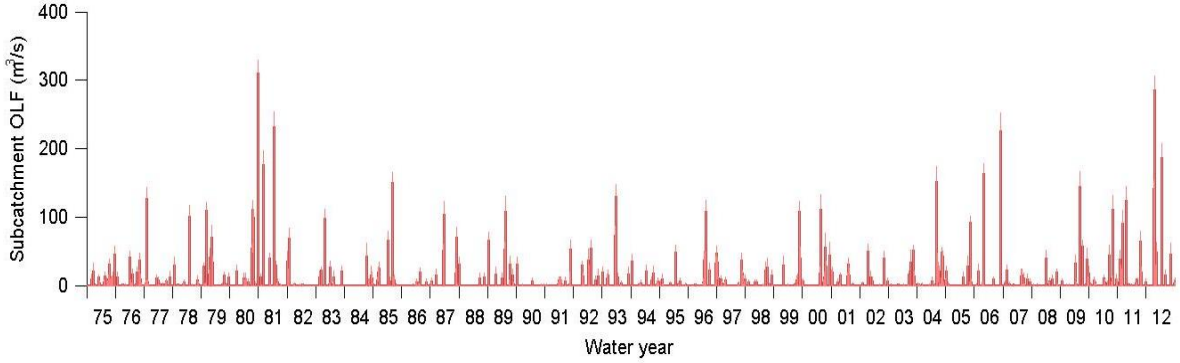

(b)

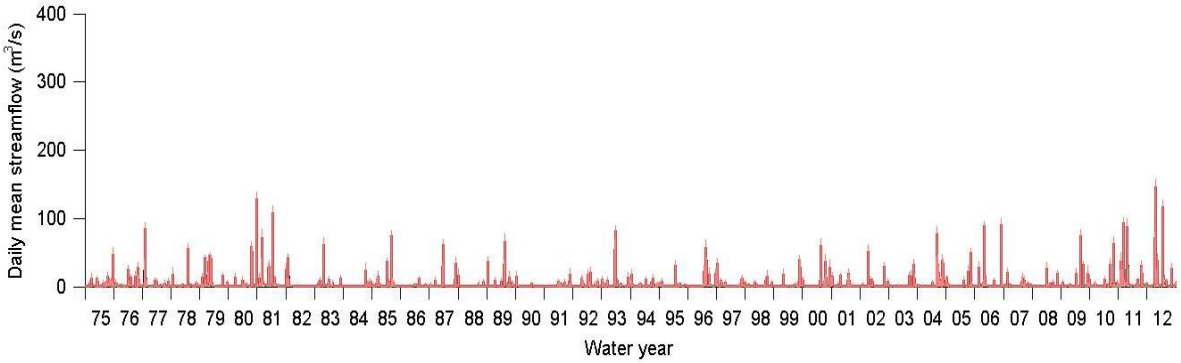

3.4 Discussion

The model results in this study indicated that further degradation of spekboom thicket cover in the Baviaanskloof catchment would likely increase catchment annual water yields, increase flood intensities, and raise floodplain groundwater levels, while restoration of thicket would do the opposite. These trends were consistent with the expected increased AET with increased vegetation and the increased runoff with vegetation losses seem in other observational and modeling studies in semi-arid areas (Bhark and Small, 2003; Dunjó et al., 2004; Bautista et al., 2007; Turnbull et al., 2010; Peña-Arancibia et al., 2012). The overall magnitude of the predicted change was consistent with past paired catchment experiments summarized in meta-study by Brown et al. (2005) suggesting a 5-10 mm increase in annual yield for each 10% of catchment area cleared of bush/shrub cover and a 17-20 mm increase for deciduous forest clearance. Converting the estimated change in average outflow to depth over the Baviaanskloof catchment area, an average 15-19 mm decrease was predicted with thicket restoration which effectively amounted to an 18% increase in cover (45% increase in cover density over 40% of the catchment). However, there were changes in modeled processes and patterns between the hillslope vegetation scenarios that were a particular function of the climate and landscape geomorphology of the Baviaanskloof catchment as a semi-arid, mountainous, meso-scale catchment, with steep slopes and relatively thin, high conductivity soils on hillslopes, and a high conductivity central valley alluvial fill. This setting accounts for the modeled degree of changes in flow and catchment scale dampening of hillslope scale changes, the lack of a predicted increase in baseflow with increased thicket cover, seasonal responses, and changes in proportions of surface and subsurface flows. This

study highlights the importance of including as much understanding about the landscape flow paths as is available into the model structure for a meso-scale catchment.

The change in assumed vegetation cover was greater between the current and fully intact thicket scenarios, going from 20% to 65% estimated average canopy cover, compared to that between the current and degraded thicket scenarios, going from 20% to 8%. As such it could be expected that the decrease in water yield with restoration of thicket would be greater than the increase from full degradation if driven solely by a difference in canopy interception and transpiration demand. However, this was not the case in the model outputs. Complete degradation was predicted to increase average annual yield by greater quantities than the decrease predicted with complete restoration compared to the current scenario: the low-end, model estimate of the increase in the average annual yield for 1975-2012 with complete thicket degradation was 12 Mm^3 or 41%, which was greater than the high-end estimate of the decrease in annual average yield with full thicket restoration (8 Mm^3 or 27%). This was partially a function of the parameterization of the hillslope soils and vegetation for the different scenarios, as informed by field observations. A large decrease in infiltration capacity has been observed with the complete loss of thicket cover on hillslopes due to high erosion losses of topsoil without further litter replenishment leaving a rock covered surface and/or capped soils, and a loss of high infiltration pockets of thicket in the partially degraded case (Mills and Fey, 2004b, 2004a; Mills and Cowling, 2010; van Luijk et al., 2013; Lechmere-Oertel and Kerley, 2008; Lechmere-Oertel et al., 2005b; Mills et al., 2005). While soil water holding capacity and ET rates were assumed to increase with increased vegetation cover, high conductivity through the relatively thin soil profile led to

greater percolation to the interflow zone in the model, which in turn had a high flow rate out of the hillslopes. This likely reduced the modeled increase in AET with the increase in thicket cover compared to what would be predicted with lower conductivity soils and a deeper soil profile.

As predicted, routing of flows across and through the central valley alluvial fill and channel network did dampen the changes in peak surface flows observed at the catchment outlet between scenarios as compared to changes predicted in the mountain subcatchments. For example, during the largest peak flow event modeled in the simulation period (25/03/1981), the combined surface flow output from all mountain tributary subcatchments onto the central valley had a day average flow of 272-352 m^3/s under the degraded thicket scenario, while the daily streamflow peak predicted for the catchment outlet was 130-170 m^3/s for this event. For this event, the predicted decrease in peak flow between the degraded and restored thicket scenarios was 241-327 m^3/s (88-93%) for the summed surface outflow of the subcatchments and 60-120 m^3/s (46-71%) for streamflow at the catchment outlet. This reduction of surface flow impact with catchment scale was both due to slowing and infiltration in parts of the floodplain reducing surface flow extremes, and due to flow contributions from the floodplain to the channel predicted to occur in both scenarios. Modeled interflow from the mountain subcatchments into the floodplain aquifer was greater in the current and intact thicket scenarios than in the degraded case, particularly during large rainfall events. If there had less alluvial aquifer recharge from this subsurface pathway, there would have been less floodplain contribution to the channel outflows in these

scenarios, and the catchment scale differences between the degraded and intact thicket scenarios would have been larger.

However, due in part to the geomorphology of the Baviaanskloof catchment and assumed nature of the floodplain vegetation, the central valley floodplain ended up having an insignificant impact in dampening long-term average flow changes between scenarios when comparing mountain subcatchment outflows to those at the catchment outlet. The difference in modeled average annual catchment water yield between the intact and degraded scenarios was similar to that of the annual average surface outflows summed across the subcatchments: an increase of 19-24 Mm^3 versus one of 19-21 Mm^3. Because of the high conductivity of the alluvial fill material, some of the increased overland flow in the degraded scenario was predicted to recharge the floodplain aquifer and result in a shallower floodplain groundwater table. However, the floodplain and fans in the Baviaanskloof are relatively small compared to the mountain subcatchments feeding them, taking up only 5% of the catchment surface area, and are highly conductive, dominated by sand and cobble fill. This limits their capacity to buffer flows over longer time-scales. The Baviaanskloof's central floodplain is long and relatively narrow. Water tables are consistently close to the surface in narrow valley reaches and also in more downstream sections of the floodplain, perennially feeding channel flows in these areas. The shallower groundwater table in the degraded scenario increased the production of overland flow in the wettest parts of the floodplain in extreme or prolonged wet events, compensating for subcatchment overland flow inputs that had been infiltrated elsewhere. Had the floodplain been much larger in proportion to the mountainous area with a deeper water table, this may not have occurred.

In addition, the deep rooting floodplain vegetation in the model meant that there was little difference in predicted average floodplain AET between scenarios despite the predicted change in the groundwater table. If the vegetation had very short roots that did not reach the saturated zone in either case there would have been little difference between scenarios. However, if the roots lie close to the water table, increases in recharge could result in increases in AET and decreases could decrease AET. This would dampen the resulting effects on the groundwater table.

The results of these simulations did not provide support for a hypothesized increase in baseflow or dry period flow with an increase in thicket cover. At the hillslope and tributary subcatchment scale, some of the processes that could produce a net increase in delayed flows were evident in the model, however were not predicted to be of a sufficient magnitude, or result in a sufficient flow delay, to see an increase in low flows at the catchment outlet. Both modeled annual average and large storm event percolation and interflow were greater for the current and intact thicket scenarios compared to the degraded scenario; however, the added volume was relatively small compared to the modeled surface flow increase in the degraded scenario. It was small compared to the additional AET predicted with increased vegetation cover, which made percolation less frequent in drier periods. The significant increases in percolation and interflow with increased thicket cover occurred in the wettest events with relatively low frequency. In an area with a more regular climate pattern with an annual wet season during which the canopy interception capacity is more regularly overwhelmed, a stronger signal of seasonally lagged flows due to the additional percolation would be more likely to immerge. In the more erratic and arid

environment of the Baviaanskloof, succulent plants, capable of storing water for long periods between significant soil wetting rainfall events, dominate the hillslope thicket.

In addition, the drainage of the interflow zone in the Baviaanskloof hillslopes was estimated to be relatively fast, modeled with a calibrated linear reservoir drainage constant of 35-56 days (Chapter 2). This meant that even in the largest storm events on record, when the interflow differences between the intact and degraded scenarios were predicted to be at their greatest, there was only a detectably greater streamflow predicted in the intact thicket case compared to the degraded case for a period 3 to 5 days occurring within a week of the flow peak. In a case where the passage from the interflow zone to the floodplain and from the floodplain to the main river channel were slower, such as may be expected in a catchment with lower slopes and/or less conductive soil and sediment or less highly fractured rock and/or a larger floodplain with low ET losses, the predicted increase in infiltration and percolation to the interflow zone predicted at the hillslope scale here could have resulted in an increase in flows reaching the main channel months or seasons after the recharge event. In addition, in the model of the Baviaanskloof, drainage in the mountain bedrock aquifer was assumed to be extremely slow based on calibration results, on the order of thousands of years, meaning that any additional recharge to this aquifer was predicted to have a negligible impact on average annual outflows from this source, even when a 38 year period was considered. If this aquifer were faster draining, increased hillslope wet event recharge with greater vegetation cover could also result in an increase in baseflow.

While attempts were made to incorporate modeling uncertainties into the change analyses by using outputs of ensembles of model runs in the parameter space for each scenario, there are unaccounted for uncertainties that should be noted. The predicted differences in flow patterns between the hillslope scenarios hinged on various thresholds in the catchment model, such as canopy infiltration and soil field capacity, and the frequency and extent to which they were exceeded in the climate record. Results of key interest, such as the occurrence of increased baseflow with increased thicket vegetation, were also determined by the drainage rates of the model's linear reservoirs representing interflow zone and mountain bedrock aquifer storage and outflow and the floodplain aquifer conductivity. The parameter values determining these groundwater flows were not predicted to change between scenarios and parameter ranges were estimated in a multi-criteria calibration procedure using multiple available data sources. However, the time-series of daily streamflow data for calibration was relatively short (2 years). Fortunately a 22-year estimated monthly flow time-series was available. As such model outputs for daily flows and peaks are likely to be less accurate than longer term averaged values. Parameter values for soil and vegetation were similarly calibrated for the current situation, however the ranges of these parameters for the degraded and intact thicket in the scenarios were scaled up and down based on literature values from field sampling to which model parameters may or may not be directly proportionally commensurate. Spatial patterns of vegetation cover densities across the hillslopes were also not considered in the model, assumed to be a secondary effect to a large scale change in average canopy cover.

The calibrated model for the current scenario over-estimated daily streamflow peak responses to small rainfall events (less than 15 mm). Flow responses to larger events and longer term flows were more accurate, likely due to some commensurate under-estimation of low flows, and model NSEs of 0.87-0.92 against the short-term monitored daily flow record and 0.79-0.85 against the longer term estimated monthly record were achieved The further increase in responsiveness to smaller rainfall events in the degraded scenario accounted for some of the differences in yield between the scenarios, so it is possible that this flow increase is over-estimated. The long time-scale of the simulated period, including many larger rainfall and streamflow events which are likely to be more accurately simulated, does increase confidence in the results for changes in long-term average flows and patterns between the model scenarios. Flow differences between scenarios in the driest periods simulated were not significant. However, while model inaccuracies in low flow prediction may have resulted in inaccurate predictions of changes in low flows between the scenarios, it can be said that given the existing understanding of catchment flow patterns based on available local data and literature which was incorporated into the model development (Chapters 1 and 2) that there is bit evidence to support a significant increase in baseflow given restoration of thicket on the hillslopes of the Baviaanskloof. Further improvement of model low flow prediction could be achieved in the future, given longer-term daily flow data.

The results of the simulations in this study do represent the current understanding of catchment processes and hydrologic responses to hillslope thicket cover change in the Baviaanskloof that is available for decision making, however further analyses are needed to

understand the full implications on realized water supply and other land and catchment management concerns to assess trade-offs. In considering large scale restoration of spekboom thicket cover on the hillslopes, simulations indicate that average annual catchment water yields would decrease and there was no evidence of an increase in low flows. Results of this study indicated that peak flood flows would substantially decrease with thicket restoration, which would have positive impacts for local communities in terms of reducing flood damages to farms, roads, and homes that are already experienced during high flow events. While further degradation of the thicket cover, which could occur if livestock grazing is maintained and/or increased, would increase catchment outflows across seasons, increased flows occurring in wet periods when the Kouga reservoir is already overflowing would need to be discounted to estimate the realized increase in supply and may cause increased flood damages both in the catchment and in areas downstream of the reservoir. In order understand actual increases in available supply for downstream users, the results of this study need to be further coupled with a reservoir model. Such an assessment would also need to account for sediment transport, as the significant increases in surface runoff on the hillslopes and flood peaks in the channel predicted in the degraded thicket scenario would increase sediment transport to the reservoir, reducing its storage capacity and life-span. Restoration of thicket cover, on the other hand, was predicted to increase the proportion of the catchment outflow passing through subsurface rather than surface flow paths, likely to have a positive impact on water quality.

Model results also indicated a decline in the floodplain water table with complete thicket restoration. The decrease from the current scenario was never more than 1m which is not

substantial compared to inter-annual and seasonal variabilities already dealt with by local irrigators. Nevertheless, it could result in an increase pumping costs over long periods. It is also possible that the increased peak flows resulting from the degraded scenario could result in increased floodplain channel incision, potentially having a draining effect on the floodplain aquifer in periods of flow recession, a possibility explored further in Chapters 4, 5, and 6.

3.5 Conclusion

South African subtropical thicket is highly sensitive to canopy cover loss with livestock grazing and has been extensively degraded by human land use over much of its range (Lechmere-Oertel et al., 2005a; Lloyd et al., 2002; Mills et al., 2005). This area includes large portions of region water supply catchment for the Eastern Cape Province. While plot-scale observational studies have shown the impacts of thicket canopy loss on interception, soil infiltration and water holding capacity, storm runoff, and erosion (Mills and Fey, 2004b, 2004a; Mills and Cowling, 2010; Cowling and Mills, 2011; van Luijk et al., 2013), these trends had not yet been incorporated into a catchment scale model to explore long-term hydrological effects at larger scales. This study modelled the potential impacts of changes in thicket cover in a case study catchment, the Baviaanskloof River catchment, on streamflow, floodplain groundwater levels, and water fluxes at different landscape positions and spatial scales over a 38 year climate record. Model simulations predicted a 41-62% increase average annual catchment water yield for the simulation period given a decrease in

average thicket canopy cover on the catchments hillslopes from the 20% canopy cover, the estimated current state, to 8% canopy cover, predicted with full degradation. The predicted increased yield, due to increased storm runoff and decreased AET on hillslopes, was accompanied by a predicted 34-43% increase flood peak magnitude for the largest flow events on record, likely to have implications for flood damages, erosion, and sedimentation of the water supply reservoir. Full restoration of hillslope thicket cover to estimated average 65% canopy cover was predicted to decrease average annual water yields by 22-27% and decrease flood flow peaks by 56-60%. The modeled increase in yield with a decrease in canopy cover was consistent over wet and dry years and seasons. Despite a modeled increase in hillslope percolation to the interflow zone with restored thicket cover, there was no evidence that this would result in an increase in baseflow detectable at the catchment outlet.

The Baviaanskloof is a semi-arid mountainous catchment in which steep mountain tributaries feed onto a central valley with a coarse alluvial fill. It was observed that routing surface and subsurface flows from the mountain areas across and through the central valley alluvial fill significantly reduced flood peaks compared to those predicted at the tributary catchment outlets. This also resulted in a reduction in the change in flow peaks between the different modelled scenarios. However, because of the relatively small size and high conductivity of the floodplain, it did not result in a significant reduction in the changes in long-term average catchment water yields between scenarios compared to those predicted for the mountain tributaries. The floodplain groundwater table was predicted to be shallower on average in the degraded thicket scenario due to increased recharge from overland flows in

storm events; however, the difference between scenarios was small relative to seasonal fluctuation. The results of this study demonstrated the importance of considering landscape flow paths routing when modelling large and topographically diverse catchments, particularly when examining flood intensities.

3.6 References

Bautista, S., Mayor, A.G., Bourakhouadar, J., and Bellot, J. (2007). Plant spatial pattern predicts hillslope semiarid runoff and erosion in a Mediterranean landscape. Ecosystems *10*, 987–998.

Bhark, E.W., and Small, E.E. (2003). Association between plant canopies and the spatial patterns of infiltration in shrubland and grassland of the Chihuahuan Desert, New Mexico. Ecosystems *6*, 185–196.

Biederman, J.A., Harpold, A.A., Gochis, D.J., Ewers, B.E., Reed, D.E., Papuga, S.A., and Brooks, P.D. (2014). Increased evaporation following widespread tree mortality limits streamflow response. Water Resour. Res. *50*, 5395–5409.

Bosch, J.M., and Hewlett, J.D. (1982). A review of catchment experiments to determine the effect of vegetation changes on water yield and evapotranspiration. J. Hydrol. *55*, 3–23.

Brown, A.E., Zhang, L., McMahon, T.A., Western, A.W., and Vertessy, R.A. (2005). A review of paired catchment studies for determining changes in water yield resulting from alterations in vegetation. J. Hydrol. *310*, 28–61.

Bruijnzeel, L.A. (2004). Hydrological functions of tropical forests: not seeing the soil for the trees? Agric. Ecosyst. Environ. *104*, 185–228.

Calder, I.R., and Dye, P. (2001). Hydrological impacts of invasive alien plants. Land Use Water Resour. Res. *1*, 1–8.

Cowling, R.M., and Mills, A.J. (2011). A preliminary assessment of rain throughfall beneath Portulacaria afra canopy in subtropical thicket and its implications for soil carbon stocks. South Afr. J. Bot. *77*, 236–240.

Dunjó, G., Pardini, G., and Gispert, M. (2004). The role of land use–land cover on runoff generation and sediment yield at a microplot scale, in a small Mediterranean catchment. J. Arid Environ. *57*, 239–256.

Dzikiti, S., Schachtschneider, K., Naiken, V., Gush, M., and Le Maitre, D. (2013). Comparison of water-use by alien invasive pine trees growing in riparian and non-riparian zones in the Western Cape Province, South Africa. For. Ecol. Manag. *293*, 92–102.

Dzikiti, S., Jovanovic, N.Z., Bugan, R., Israel, S., and Maitre, D.L. (2014). Measurement and modelling of evapotranspiration in three fynbos vegetation types. Water SA *40*, 189–198.

Euston-Brown, D.I.W. (2006). Baviaanskloof Mega-Reserve Project: Vegetation mapping contract report on methodology, vegetation classification and short descriptions of habitat units (South Africa: Eastern Cape Parks & Tourism Agency).

Gwate, O., Finca, A., Mantel, S., Gibson, L., Munch, Z., and Palmer, A. (2015). Rethinking the clearing of Acacia mearnsii in rangelands: biophysical characteristics of black wattle infestation in the north Eastern Cape, South Africa. Manuscr. Prep.

Hargreaves, G., and Samani, Z. (1982). Estimating potential evapotranspiration. J. Irrig. Drain. Div.-Asce *108*, 225–230.

Hoffman, M., and Cowling, R. (1990). Desertification in the Lower Sundays River Valley, South-Africa. J. Arid Environ. *19*, 105–117.

Kerley, G.I.H., Knight, M.H., and Kock, M. de (1995). Desertification of subtropical thicket in the Eastern Cape, South Africa: Are there alternatives? Environ. Monit. Assess. *37*, 211–230.

Lechmere-Oertel, R.G., and Kerley, G.I.H. (2008). Litter dynamics across browsing-induced fenceline contrasts in succulent thicket, South Africa. South Afr. J. Bot. *74*, 651–659.

Lechmere-Oertel, R.G., Kerley, G.I.H., and Cowling, R.M. (2005a). Patterns and implications of transformation in semi-arid succulent thicket, South Africa. J. Arid Environ. *62*, 459–474.

Lechmere-Oertel, R.G., Cowling, R.M., and Kerley, G.I.H. (2005b). Landscape dysfunction and reduced spatial heterogeneity in soil resources and fertility in semi-arid succulent thicket, South Africa. Austral Ecol. *30*, 615–624.

Le Maitre, D.C., van Wilgen, B.W., Gelderblom, C.M., Bailey, C., Chapman, R.A., and Nel, J.A. (2002). Invasive alien trees and water resources in South Africa: case studies of the costs and benefits of management. For. Ecol. Manag. *160*, 143–159.

Line, D.E., and White, N.M. (2007). Effects of Development on Runoff and Pollutant Export. Water Environ. Res. *79*, 185–190.

Lloyd, J.W., van den Berg, E., van Wyk, E., and Palmer, A.R. (2002). Patterns of Degradation and Transformation in the Thicket Biome (South Africa: Terrestrial Ecology Research Unit, Dept of Zoology, Nelson Mandela Metropolitan University).

van Luijk, G., Cowling, R.M., Riksen, M.J.P.M., and Glenday, J. (2013). Hydrological implications of desertification: Degradation of South African semi-arid subtropical thicket. J. Arid Environ. *91*, 14–21.

Lynch, S.D. (2003). Development of a Raster Database of Annual, Monthly and Daily Rainfall for Southern Africa (Pretoria, South Africa: Water Research Commission (WRC)).

Ma, X., Xu, J., Luo, Y., Prasad Aggarwal, S., and Li, J. (2009). Response of hydrological processes to land-cover and climate changes in Kejie watershed, south-west China. Hydrol. Process. *23*, 1179–1191.

Meijninger, W.M.L., and Jarmain, C. (2014). Satellite-based annual evaporation estimates of invasive alien plant species and native vegetation in South Africa. Water SA *40*, 95–108.

Midgley, J.J., and Scott, D.F. (1994). Use of stable isotopes of water (d and o-18) in hydrological studies in the Jonkershoek valley.

Mills, A., and Fey, M. (2004a). Transformation of thicket to savanna reduces soil quality in the Eastern Cape, South Africa. Plant Soil *265*, 153–163.

Mills, A.J., and Cowling, R.M. (2006). Rate of Carbon Sequestration at Two Thicket Restoration Sites in the Eastern Cape, South Africa. Restor. Ecol. *14*, 38–49.

Mills, A.J., and Cowling, R.M. (2010). Below-ground carbon stocks in intact and transformed subtropical thicket landscapes in semi-arid South Africa. J. Arid Environ. *74*, 93–100.

Mills, A. j., and Fey, M. v. (2004b). Effects of vegetation cover on the tendency of soil to crust in South Africa. Soil Use Manag. *20*, 308–317.

Mills, A.J., Cowling, R.M., Fey, M.V., Kerley, G.I.H., Donaldson, J.S., Lechmere-Oertel, R.G., Sigwela, A.M., Skowno, A.L., and Rundel, P. (2005). Effects of goat pastoralism on ecosystem carbon storage in semiarid thicket, Eastern Cape, South Africa. Austral Ecol. *30*, 797–804.

Mills, A.J., Turpie, J., Cowling, R.M., Marais, C., Kerley, G.I.H., Lechmere-Oertel, R.G., Sigwela, A.M., and Powell, M. (2007). Assessing costs, benefits and feasibility of subtropical thicket restoration in the Eastern Cape, South Africa. In Restoring Natural Capital: Science, Business and Practice, J. Aronson, S.J. Milton, and J. Blignaut, eds. (Washington DC: Island Press), pp. 179–187.

Moolman, H.J., and Cowling, R.M. (1994). The impact of elephant and goat grazing on the endemic flora of South African succulent thicket. Biol. Conserv. *68*, 53–61.

Palmer, A.R., and Yunusa, I.A.M. (2011). Biomass production, evapotranspiration and water use efficiency of arid rangelands in the Northern Cape, South Africa. J. Arid Environ. *75*, 1223–1227.

Peña-Arancibia, J.L., van Dijk, A.I.J.M., Guerschman, J.P., Mulligan, M., (Sampurno) Bruijnzeel, L.A., and McVicar, T.R. (2012). Detecting changes in streamflow after partial woodland clearing in two large catchments in the seasonal tropics. J. Hydrol. *416–417*, 60–71.

Price, K. (2011). Effects of watershed topography, soils, land use, and climate on baseflow hydrology in humid regions: A review. Prog. Phys. Geogr. *35*, 465–492.

Refsgaard, J.C., and Storm, B. (1995). MIKE SHE. In Computer Models of Watershed Hydrology, V.P. Singh, ed. (Water Resources Publications), pp. 809–846.

Roets, W., Xu, Y., Raitt, L., and Brendonck, L. (2008). Groundwater discharges to aquatic ecosystems associated with the Table Mountain Group (TMG) aquifer: A conceptual model. Water SA *34*, 77–88.

Schulze, R.E., and Maharaj, M. (2004). Development of Database of Gridded Daily Temperature for Southern Africa (Pretoria, South Africa: Water Research Commission (WRC)).

Sigwela, A.M., Kerley, G.I.H., Mills, A.J., and Cowling, R.M. (2009). The impact of browsing-induced degradation on the reproduction of subtropical thicket canopy shrubs and trees. South Afr. J. Bot. *75*, 262–267.

Smit, S. (2013). Observation of changes in vegetation cover density in the Baviaanskloof catchment using field sampling and remotely sensed NDVI (Normalized Difference Vegetation Index). BSc Thesis. University of Applied Science Van Hall Larenstein.

Soltau, L., Smith-Adao, L., and Bugan, R. (2011). Baviaanskloof resistivity survey to define water level and depth to bedrock (Stellenbosch, South Africa: Center for Scientific and Industrial Research (CSIR)).

Stednick, J.D. (1996). Monitoring the effects of timber harvest on annual water yield. J. Hydrol. *176*, 79–95.

Steinwand, A.L., Harrington, R.F., and Groeneveld, D.P. (2001). Transpiration coefficients for three Great Basin shrubs. J. Arid Environ. *49*, 555–567.

Stuart-Hill, G.C. (1992). Effects of Elephants and Goats on the Kaffrarian Succulent Thicket of the Eastern Cape, South Africa. J. Appl. Ecol. *29*, 699–710.

Turnbull, L., Wainwright, J., and Brazier, R.E. (2010). Changes in hydrology and erosion over a transition from grassland to shrubland. Hydrol. Process. *24*, 393–414.

Vlok, J.H.J., Euston-Brown, D.I.W., and Cowling, R.M. (2003). Acocks' Valley Bushveld 50 years on: new perspectives on the delimitation, characterisation and origin of subtropical thicket vegetation. South Afr. J. Bot. *69*, 27–51.

van der Vyver, M.L., Cowling, R.M., Mills, A.J., and Difford, M. (2013). Spontaneous Return of Biodiversity in Restored Subtropical Thicket: Portulacaria afra as an Ecosystem Engineer. Restor. Ecol. *21*, 736–744.

Xu, Y., Titus, R., Holness, S.D., Zhang, J., and Tonder, G.V. (2002). A hydrogeomorphological approach to quantification of groundwater discharge to streams in South Africa. Water SA *28*, 375–380.

Xu, Y., Wu, Y., and Beekman, E.H. (2003). The role of interflow in estimating recharge in mountainous catchments. In Groundwater Recharge Estimation in Southern Africa, Y. Xu, and E.H. Beekman, eds. (Paris, France: UNESCO).

Chapter 4 Streamflow and groundwater impacts of channelization on alluvial fans in a meso-scale, semi-arid, mountainous catchment

4.1 Introduction

Alluvial fans are common topographic features in arid mountainous environments where they are sites of significant groundwater recharge (Blissenbach, 1954; Hooke, 1967; Bull, 1977; Hendrickx et al., 1991; Munevar and Marino, 1999; Houston, 2002; Blainey and Pelletier, 2008). However, alterations due to human activities may change their form and function in the landscape. Fans develop at mountain fronts where steep mountain streams abruptly lose velocity upon reaching a relatively flat floodplain and so deposit much of their sediment load. Fans' convex shape, ephemeral surface flows, and episodic sediment deposition generally result in shifting, disparate surface flow paths across the fan. This can be a flood risk when dwellings or infrastructure are located on or close to alluvial fans. In areas where settlements or agriculture have been established on or near fans, development is often accompanied by flood protection measures such as channelization and levee or berm construction (Phillips, 1998). Confining alluvial fan flood flows into single channels, which may otherwise have dispersed across the fan surface, reduces the opportunity for infiltration and recharge on the fan. It is therefore possible that local flood control on alluvial fans could increase streamflow peaks and decrease baseflows in downstream areas, a trade-off that may be important to consider in catchment management. This study uses coupled hydraulic and hydrologic modelling to explore the potential impacts of alluvial fan channelization on

catchment-scale water yield, flood peaks, low flows, and floodplain groundwater levels in a case-study catchment: the Baviaanskloof River catchment in the Eastern Cape of South Africa. It was hypothesized that widespread alluvial fan channelization in this catchment is likely to increase downstream flood peaks and decrease baseflow.

Previous research on hydrologic processes on alluvial fans has primarily focused on detailed study or modelling of groundwater recharge and/or flood risks on individual large fans, looking at processes and water balances for the fan and the catchment area that feeds it (Munevar and Marino, 1999; Herron and Wilson, 2001; Houston, 2002; Mukhopadhyay et al., 2003; Niswonger et al., 2005; Blainey and Pelletier, 2008). The impacts of infiltration on alluvial fans on the overall water balance and flow patterns of the larger catchments in which they occur have less often been quantitatively assessed. Potential larger catchment scale impacts of fan flow path alteration have not yet been explored in published literature. Such assessments would allow possible trade-offs between local flood protection and downstream flood and water supply impacts to be more quantitatively understood. The purpose of this study is therefore to incorporate alluvial fan processes into a meso-scale catchment hydrologic model and use this model to estimate potential impacts of fan channelization on the magnitude and timing of flows through the catchment. The 1,234 km^2 Baviaanskloof catchment has 62 alluvial fans flanking its central valley floodplain, over half of which have been cultivated and at least 25 of which have been altered for flood protection. This catchment supplies water to both local agricultural users within the catchment and to a regional reservoir serving downstream urban and agricultural areas.

Upstream activities affecting low flow period water supplies to downstream users have become a focus of catchment management in the area (Jansen, 2008).

Having different sizes and forms, the effects of channelization on different individual fans will vary. It was hypothesized that widespread channelization across many fans in the Baviaanskloof would decrease average infiltration on the fans, increase streamflow peaks in the downstream floodplain channel, increase average depth to groundwater in the floodplain alluvial aquifer, and decrease baseflow in the floodplain channel. Infiltration and recharge on fans is controlled by many factors: surface and channel morphology, fan material permeability, vegetation, and the magnitude and timing of incoming flows. On large fans comprised primarily of coarse material, it is common for high flows to completely infiltrate before reaching the fan toe (Hooke, 1967). Smaller fans, even those composed of finer material, can also have significant impacts on surface-subsurface flow partitioning: (Herron and Wilson, 2001) found that, on a 0.4 ha fan at the base of a 26 ha mountain catchment, 20-100% of event surface runoff received was infiltrated depending on storm intensity and antecedent moisture conditions. Channel dimensions relative to the flow received have been found to be a significant factor determining total infiltration (Blainey and Pelletier, 2008).

In the Baviaanskloof, surface flows across some of the catchments' fans following large rainfall events have been observed to reach the main river channel, contributing to the downstream flood peak (Chapter 1). The magnitude of storm required for surface flows from the mountains to reach the fans varies with antecedent conditions, but generally 30 mm in a day is needed for surface flows to reach the fan from the contributing catchment and 50 mm

for significant flows to cross the fans and reach the floodplain channel. However, when heavy storms occur in dry periods, significant infiltration is also observed along the main floodplain channel, additionally attenuating floods before they reach the catchment outlet. As such, the catchment-scale flood peak impact of alluvial fan channelization in the Baviaanskloof was predicted to be greater when antecedent conditions are sufficiently wet for the floodplain groundwater table to be close to the channel elevation over much of the floodplain. In this case there would be less loss of channel flow on the floodplain and so the infiltration on the fans would be more critical to determining the peak flow. Baseflow in the main floodplain channel is fed by the floodplain alluvial aquifer, which is continuous with the alluvial fan deposits (Chapter 1). Additional infiltration on fans could lead to additional recharge of the alluvial aquifer and hence increased baseflow. The magnitude of the impact of fan alteration on the floodplain baseflow will be mitigated by plant water use both on the fan, controlling net recharge, and on the floodplain, where deep rooted vegetation can access the alluvial aquifer, potentially using much of the additional recharge water.

Modeling studies of fan hydrology have generally built purpose-specific models of the fan area alone, obtaining the incoming flows at the apex from field observations or separate models and not explicitly looking at processes beyond the fan toe. In these studies the consideration of fan surface flows has ranged in complexity and scale, from detailed grid cell level surface flow routing routines using a digital elevation map (DEM) of the fan surface topography and cell level calculations of infiltration (Blainey and Pelletier, 2008) to coarser consideration of the entire fan as a single divergent plane subject to kinematic flow routing based on estimated average slope and roughness (Mukhopadhyay et al., 2003). Generally the quantity of groundwater recharge on the fan during events has been calculated

without further explicit consideration of groundwater flow leaving the fan and its fate within a larger catchment. Exceptions have been Herron and Wilson (2001) who estimated a subsurface drainage rate from the fan based on piezometer data, and Munevar and Marino (1999) who added alluvial fan recharge to a finite element groundwater model the regional aquifer of the Salinas Valley.

Widely used distributed and semi-distributed catchment model structures made available in software, such as HEC-HMS (USACE-HEC, 2010), SWAT (Arnold et al., 1998), WARMF (Herr and Chen, 2012), and MIKE-SHE (Refsgaard and Storm, 1995), among others, range in their capability to explicitly consider processes typical of alluvial fans. Until more recently many readily available model structures were based on observations of processes and linkages in small to medium scale temperate or wet catchments, with dominantly convergent topographies (Beven, 2001; Giertz and Diekkrüger, 2003; Herron and Wilson, 2001). In such environments it is reasonable to route surface runoff produced on different land units directly to channels, without landscape flow path infiltration, and to route channel flows directly to the catchment outlet, without overbank spillage. However, catchment-scale models which can include landscape surface flow infiltration, channel seepage losses, and allocation of overbank spillage water onto the surface of an alluvial fan land unit, such as the MIKE-SHE/MIKE 11 coupled hydrologic-hydraulic modeling system (Graham and Butts, 2005; Refsgaard and Storm, 1995), could be used to approximate fan surface processes within the catchment, similar to the methods used in fan-scale modeling by Niswonger et al. (2005) and Blainey and Pelletier (2008). At the catchment scale, model representation of groundwater flow may also be important as groundwater recharge on alluvial fans can feed aquifers of concern (Munevar and Marino, 1999) and downstream

surface water bodies (Woods et al., 2006). This could be included in catchment models in a variety of ways such as: coupling surface processes to a finite element groundwater model, using linear or non-linear reservoir drainage functions for a theoretical alluvial fan groundwater reservoirs connected in series to a floodplain aquifer model reservoir, or by adding fan recharge to a single combined fan-floodplain aquifer model reservoir.

In this study, the scale of the Baviaanskloof catchment, and the available information on surface and subsurface properties and processes with which to parameterize a model, made a fully distributed gridded model of surface and subsurface flow for the entire catchment area inappropriate (Chapter 1). As such, a semi-distributed, hydrologic response unit (HRU) model based on topographic units for the mountain tributary subcatchments which feed the fans was coupled to a finer scale, gridded, surface and groundwater model of the central valley's alluvial fans, floodplain, and channel network. This was done using the MIKE-SHE/MIKE 11 modeling system. In addition to overbank flooding, the fan and floodplain model also included dynamic two-way exchange of water between the alluvial aquifer and the channel network based on relative water heights and material conductivity. While the groundwater table in the alluvial fans is known to remain below the fan channel, this was not the case in the floodplain (Chapter 1). Consideration of the fluctuating surface-subsurface connection between the floodplain aquifer and main river channel was therefore considered necessary to directly model how baseflow may be affected by the amount of aquifer recharge in the valley alluvium, including recharge on the fans.

Infrequent surface flows and deep groundwater tables make monitoring arid alluvial fan processes challenging, while high spatial variability of fan surface material permeability can

provide further challenges to characterization for modelling (Blainey and Pelletier, 2008). However, modelling the alluvial fans as an integrated part of a larger catchment model allowed information available from other spatial scales, such as catchment outlet streamflow and floodplain groundwater levels, to be brought to bear in the parameterization of the fan through model calibration. Due to the lack of information on each fan in the catchment, average soil and vegetation properties were estimated and applied uniformly to all the fans in the model. Values were guided by available data (Bobbins, 2011), aerial photography, and sampling on selected fans, but were then further constrained through catchment scale model calibration based on time-series of floodplain groundwater levels and streamflow at perennially flowing locations (Chapter 2). As impacts are predicted to vary with climate conditions, fan channel scenarios were modelled over 38 years of observed weather to look at long-term average impacts across a range of conditions and specific event impacts.

4.2 Methods

4.2.1 Alluvial fan characteristics

A detailed description of the Baviaanskloof catchment is provided in Chapter 1, Section 1.2.1. A study of the form of the alluvial fans in the catchment was done by Bobbins (2011) and supplementary analyses of georeferenced aerial photography for 2009 (South African National Geospatial Information) and limited field sampling were done for this study. Bobbins (2011) used stereograph analyses to delineate 58 alluvial fans. An additional four were identified from the 2009 photography. In the very narrow main valley reaches there is

insufficient space on the valley floor away from the main river channel for the fan deposits to accumulate outward from the mountain front. During periodic high flood flows the main river has capacity to carry tributary sediment deposits away down-valley. However, almost all tributary subcatchments feeding onto wide valley reaches terminate in alluvial fans, and subcatchments terminating in fans make up 43% of the total catchment area. Fan surface areas ranged from 0.03 to 1.4 km^2 with an average of 0.2 km^2. Fan area was linked to the size of the contributing catchment area and in some cases limited by toe trimming by the main river channel in the floodplain (Bobbins, 2011). Fan surface slopes ranged from 0.4% to 20% with an average of 5% (Bobbins, 2011), in contrast to the average 30% slope of the topography in the subcatchments and the lower floodplain longitudinal slope of 0.7%.

The Baviaanskloof area has been used for livestock grazing and cultivated agriculture for over a century, and this has come with significant modification of many of the alluvial fans. Evidence of cultivation on the fan surface in the form of cleared fields was observed on 42 of the 62 alluvial fans. In response to widespread flood damages in the 1970s and 1980s, the South African government actively promoted and subsidized flood protection measures (Jansen, 2008). In the Baviaanskloof this took the form of earthworks to reorient channels and build berms, both on the fans and the main floodplain. In addition, significant loss of vegetation cover due high grazing pressure on the hillslopes of the tributary subcatchments is likely to have impacted channels on the alluvial fans by increasing storm runoff and hence increasing peak tributary surface flows reaching the fans. Modeling of tributary subcatchment outflows under scenarios of fully intact hillslope thicket cover compared to

those predicted for the current open canopy condition suggested that the quantity of surface flow reaching the fans could have increased by 80-86% (Chapter 3).

Continuous channels from the apex of a fan all the way to the main river channel in the floodplain were identified from aerial photography for over half of the fans, 39 out of 62, while the remainder showed evidence of more dispersive flows either on the fan surface or upon reaching the floodplain (Figure 4-1 to 4-3). The development of an entrenched channel on a fan is not always due to direct anthropogenic modification. It can occur with intensification of runoff events, declining sediment delivery to the fan, and/or a lowering of the local base level, as driven by larger landscape, climate, and/or tectonic factors (Blair and Mcpherson, 1994; Harvey, 2002; Clarke et al., 2010). Channel connectivity to the main river is more easily developed when the main floodplain channel is located at the fan the toe, effectively lowering the fan's local base level to the river channel thalweg, rather than the floodplain surface. (Bobbins, 2011) observed 'toe trimming' by current or historical courses of the floodplain channel for 33 fans, 23 of which are among those with currently visible channel connectivity to the main river. However, for 25 of the 39 fans with observed channel connectivity, alteration of the fan surface flow path due to human activity was also clearly evident in the form of cultivated fields across the majority of the fan surface confining the active flow area, obvious channel straightening or diversions away from infrastructure, and/or visible berms (examples shown in Figures 4-2 and 4-3). Additionally, for 14 of these fans, man-made, or man-entrenched and bermed, channels from the fan toe across the floodplain to the main river channel were observable, following paths that avoid agricultural fields (example shown in Figure 4-3).

Channel dimensions were measured in the field for 9 sample fans (Bobbins, 2011) and channel widths were estimated from georeferenced aerial photographs for the remaining fans. Fan channel widths near the fan apex ranged from 5-23 m with a mean of 11 m. On fans without a completely entrenched channel, the channel often split into multiple flow paths growing progressively shallower and narrower moving toward the fan toe. Channel depths on the field surveyed, entrenched, channel fans ranged from 0.4-3 m with depths fluctuating along the fan length. Channels were generally gravel and cobble bedded with loamy-sand and sandy-loam banks, but those that were less entrenched graded to sand and gravel bed deposits moving down the fan.

Fan sediment deposits were found to be primarily sands, loamy sands, and sandy loams with high gravel and cobble content (20-80% by volume). Exposed sediment profiles in incised fan channels, toe trimmed fans, and excavated soil pits showed distinct layers with varying rock contents indicating channel shifting across the fan and/or wetter periods of higher coarse material transport capacity. In addition to surface samples taken on transects of two sample fans by Bobbins (2011), four 2 m deep soil profile pits were excavated on two sample fans (on the north and south side of the valley) with texture samples taken and double ring infiltrometer measurements made at each distinct layer encountered. Saturated conductivities measured on the fan surface with a double ring infiltrometer ranged from 20-500 mm/hr with a mean of 124 mm/hr, while those taken in cobble dominated layers during soil profile excavation were 80-1100 mm/hr with a mean of 333 mm/hr.

Figure 4-1 Baviaanskloof catchment landform delineation showing tributary subcatchments, alluvial fans, and the central valley floodplain. Channel connectivity of tributary subcatchments is highlighted.

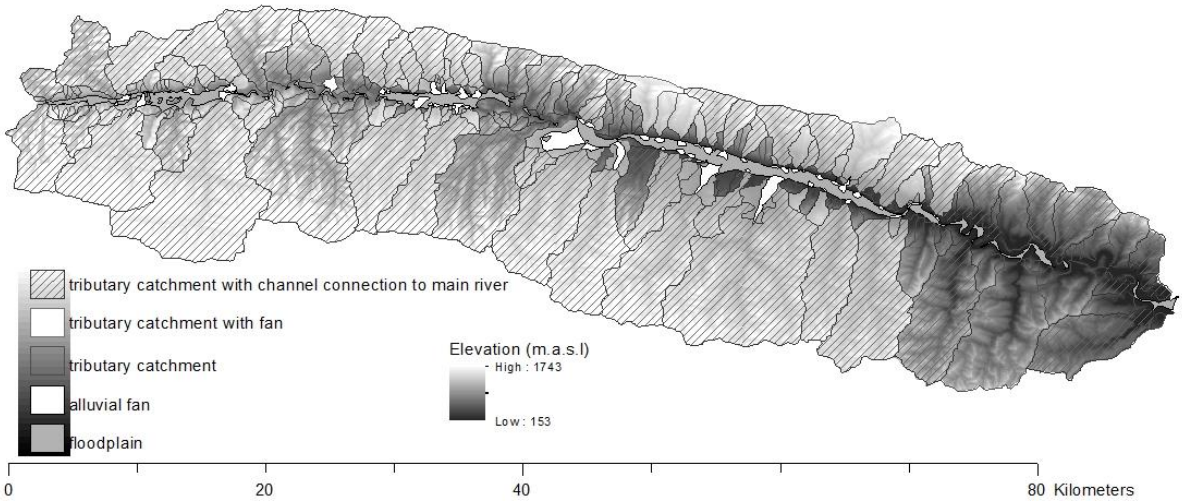

Figure 4-2 Aerial photo time-series showing manual channel re-routing and berm construction on an alluvial fan in the Baviaanskloof (Gannalandkloof fan) to protect a downstream field and dam from flooding and sediment deposition.

The channel was shifted to the western side of the fan and a 2m high berm was constructed to keep it there. This new channel became entrenched and older flow paths became inactive and vegetated.

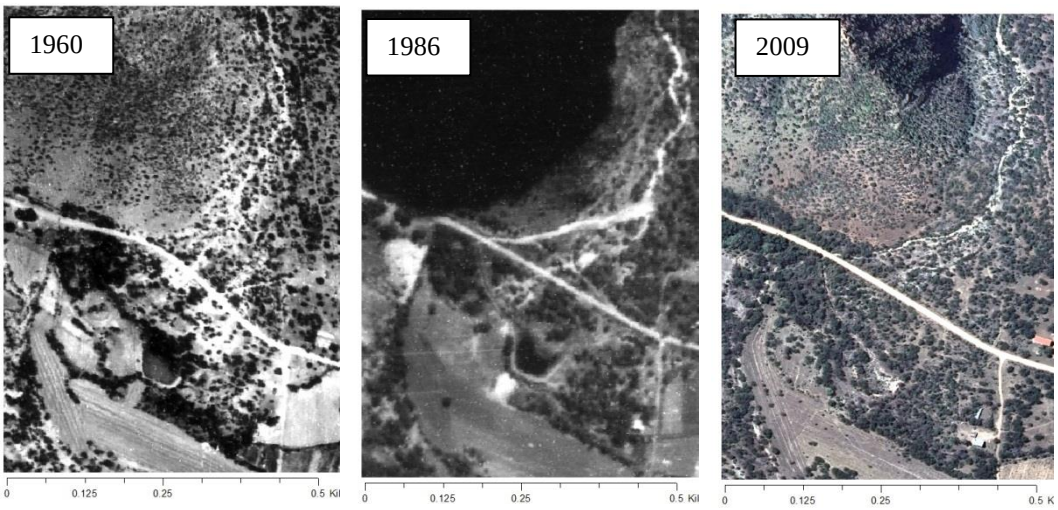

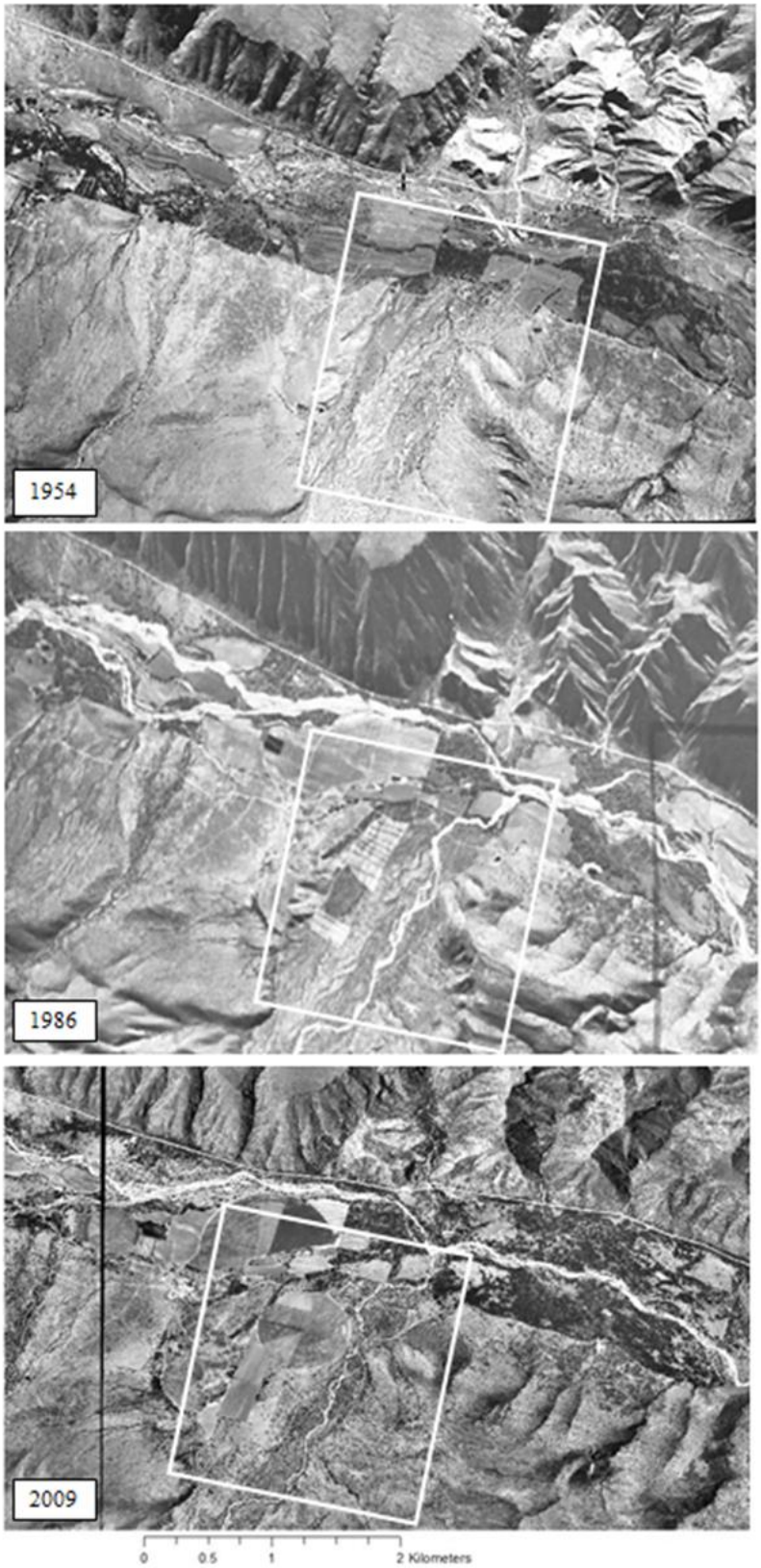

Figure 4-3 Aerial photo time-series showing channelization on an alluvial fan in the Baviaanskloof catchment (Tchandokloof fan running South to North) to make way for agricultural fields and construction of an entrenched channel connection with the main river (running West to East)

4.2.2 Scenario modelling

The scale of likely streamflow and groundwater impacts from increased alluvial fan channelization in the Baviaanskloof was explored using a calibrated model of the catchment in its current condition and manipulating the model's channel network to represent different fan condition scenarios. Three scenarios of alluvial fan condition were considered: the current state with 39 of the 62 fans channelized; channelization on all 62 fans, hereafter referred to as the 'channelized scenario'; and assumed restoration of dispersive flow paths on 25 apparently altered fans, leaving 14 channelized fans, hereafter referred to as the 'restored scenario.' The 14 fans assumed to remain channelized in the restored scenario were those for which the aerial photography record did not show clear indication of human alteration and generally had the fan toe up against the main river channel, a natural driver of channel development on alluvial fans. A daily time-step, semi-distributed model was constructed for the current state and calibrated against available groundwater, surface runoff, and streamflow data (Chapter 2). This model was built using the MIKE-SHE/MIKE-11 modeling system (Refsgaard and Storm, 1995), based on a conceptual model informed by field observations of surface and groundwater flows, soil and vegetation properties, and topography (Chapter 1). A basic description of the model structure is given below, focusing on conceptualization of alluvial fan flows. For a more detailed description of the model construction and calibration refer to Chapter 2.

The model was structured to explicitly consider alluvial fan processes within the catchment, with finer scale process representation on fans and the floodplain than for the

mountain tributaries. Using topographic data (30 m resolution NASA Shuttle Radar Topography Mission, SRTM, data), the catchment area was discretized into mountain tributary subcatchments and the central valley alluvial fill (the fans and main floodplain) as described in Chapter 1. Within the subcatchments, canopy interception, infiltration, soil moisture storage, actual evapotranspiration (AET), vertical percolation, and surface runoff routing were calculated at the level of topographically defined hydrologic response units (HRUs): plateaus, hillslopes, cliffs, and canyon floors. Surface runoff was routed across HRUs in a catena, with opportunity for infiltration along the flow path. Surface flow reaching the outlet of each subcatchment was added to the channel network at the head of the alluvial fan. Hillslope interflow and mountain bedrock groundwater flows were modeled as lumped linear reservoirs at the sub-catchment scale, receiving percolated water from all topographic units and discharging to the alluvial aquifer boundary. Groundwater flow through the alluvial aquifer was modeled using a finite element grid governed by Darcy's Law, with a dynamic connection to the channel network. On the fans and floodplain, canopy interception, infiltration, surface runoff overland flow routing, soil moisture storage, AET, and percolation to the water table were also calculated by grid cell.

The gridded surface and subsurface model of the fans and floodplain had a 50 m resolution using sink filled, smoothed SRTM data for the model surface topography. This ensured that basic alluvial fan forms were included in the surface flow routing. In the finite element groundwater model a smooth bottom depth profile was assumed with an average depth of 20 m under the central floodplain grading to 5 m at the mountain front, based on resistivity data by (Soltau et al., 2011). The topography of the bedrock below the alluvium

may not be regular and may be deeper than 20 m, however it was assumed that the floodplain groundwater table is relatively smooth, permanently above the bedrock interface, and remained above a 20 m depth throughout the simulated period. This last assumption is supported by 15 m deep farm water supply boreholes in the alluvium that have never run dry in living memory (Chapter 1).

Channel flow was modeled using a diffusive wave approximation. Two-way exchange of water between the aquifer and channel was governed by relative water surface elevation and bed material conductivity. Overbank flows, as calculated in the channel hydraulic model, were added into the gridded surface flow routing routine of the fan and floodplain surface. This water could infiltrate into the alluvium, evaporate, or flow downslope, potentially re-entering the channel further down-valley. The channel network was mapped from georeferenced aerial photography and field survey. Channel cross sections for the floodplain were obtained from topographic survey (Powell, 2015). In the model, the surface flow from every tributary subcatchment was routed to a channel that connects to the main river channel in the floodplain. For subcatchments feeding onto alluvial fans assumed to be channelized and connected to the main river, this connecting channel was given the average observed fan channel dimensions on modified fans in the catchment: 11 m width, 1 m depth, trapezoidal. For those with fans that were not channelized, the model fan channel dimensions decreased to a negligible size (2 m width, 0.2 m depth) by the toe of the fan such that the majority of the flood flow would exceed channel dimensions and be added to the model surface flow routing on the fan. Infiltration through the fan channel beds was also calculated based on the alluvial fill conductivity.

This model was calibrated using a multi-criteria procedure against multiple datasets of surface flows and groundwater levels: gauged catchment outlet streamflow for 2012-2013, estimated monthly catchment outflow for 1991-2013, observed presence/absence of flow in tributary catchment channels and the central floodplain channel for 2012-2013, and observed floodplain groundwater depths for 2012-2013 (Chapter 2). Given the high dimensionality of the model structure (42 calibration parameters), the relatively short gaged streamflow record, uncertainties in observational datasets, simplifications in process representation, and incomplete commensurability of observational data and model parameters and outputs, the calibration procedure did not attempt to produce a single optimized parameter set. Instead, thresholds of acceptability were applied to various model output goodness-of-fit measures to patterns in the datasets in order to constrain the range of model parameter values considered likely. The resulting model and accepted parameter space reproduced 2012-2013 daily streamflow with a Nash-Sutcliffe efficiency (NSE) of 0.87-0.92 and 1991-2013 monthly flows with an NSE of 0.79-0.85, predicted mean flow within 0.5 m^3/s and maximum monthly flows within 1 m^3/s of the observed, and modeled floodplain groundwater fluctuations with an R^2 of 0.79-0.81 and an accuracy in the range of depth fluctuation within 0.5 m against the observations (Chapter 2). Accepted models had errors in average annual yield of 3-20%, with a mean of 12%.

To account for the uncertainty in the parameterization, the model was run 100 times for each scenario to represent the calibrated parameter space. Parameter sets were selected from the 720 sets in the calibration exercise with acceptable model performance in recreating observed surface runoff, streamflow, and groundwater patterns as described in Chapter 2.

The same 100 parameter sets were applied in each of the three alluvial fan channel scenarios, such that the channel network was the only factor differing between them. These sets of runs resulted in likely output distributions for each scenario, allowing for conservative change detection.

In order to capture the response to a variety of storm sizes and antecedent conditions, the model of each scenario was run using 43 years of climate data from 1970-2012. The first 5 years (1970-1974) were considered a spin-up period for groundwater levels and change analyses were done for model output for the 1975-2012 water years. The water year was defined as April to March. To estimate catchment and subcatchment-wide precipitation and PET demand, daily gage data from 6 stations, two within the catchment and four within 20 km (South African Weather Services, South African Agricultural Research Council), was scaled using the monthly precipitation and temperature surfaces (2 km resolution) of (Lynch, 2003) and (Schulze and Maharaj, 2004).

4.2.3 Output analyses

For the set of model runs for each alluvial fan channelization scenario the mean and 95 percent confidence intervals of the following statistics were calculated: average annual water yield, average annual minimum monthly flow, average of the daily flows for the fourteen largest flow peaks in the period (annual exceedance probability of 10% or less), average depth to groundwater in the floodplain aquifer (spatially averaged), average annual maximum depth to groundwater in the floodplain aquifer (spatially averaged). These

statistics were chosen to assess the scale of impacts relevant to water supply and flood management. To assess changes in the flow path of water through the catchment due to alluvial fan channelization, modeled patterns of infiltration on alluvial fans, recharge to the alluvial aquifer, AET on the fan and floodplain area, flow from the alluvial aquifer into the main floodplain channel, and surface flow reaching the main floodplain channel from the tributary subcatchments were compared between the alluvial fan scenarios.

Within the modeled time period, multi-year dry and wet periods were identified, as described in Chapter 3, Section 3.2.3, to compare the effects of fan channelization under different conditions. The statistics described above were also calculated separately for these periods and for winter and summer seasons. To test the hypothesis that the difference in flood flow response between channelized and restored scenarios would be larger when antecedent conditions were wetter, and the floodplain could absorb less of the additional flood peak from the channelized fans, flow responses to particular storm events were compared across a range of antecedent conditions. Storm events considered were those with over 30 mm of rainfall in a day and the antecedent conditions were explored by looking at modeled total effective rainfall (precipitation – AET) in antecedent periods of different lengths before the event (5 days, 1 month, 6 months, 1 year, and 2 years) and also by looking at the floodplain groundwater depth. Effective rainfall was looked at in addition to groundwater depth because soil moisture on the fans and floodplain in the unsaturated zone above the alluvial aquifer water table would also play a role in the storm response.

4.3 Results

4.3.1 Effects on catchment scale water yield and streamflow

The modeling results in this study indicated that the alternative alluvial fan form scenarios considered, channelization on all fans or restoration of dispersive flow paths on altered fans, were not likely to have a large impact on the long-term average annual water yield of the Baviaanskloof catchment compared to predicted yield for the current state and compared to model uncertainties. However, restoration of fans' dispersive flow paths was predicted to decrease peak flows and increase low flows in certain conditions. The fully channelized scenario had a modeled annual average water yield of 30-32 Mm^3 for the period from 1975-2012, compared to 28-31 Mm^3 predicted for the current state, and 26-28 Mm^3 for the restored fan scenario (Table 4-1). While the differences between the mean predicted yields of the alternative scenarios and that of the current state were not significant ($p>0.05$), the 2-6 Mm^3 (7-21%) increase in average annual yield between the fully channelized and fully restored scenarios was statistically significant ($p=0.02$). Differences in mean predicted yields for individual years were not statistically significant between scenarios, but means for the channelized scenario runs were consistently higher than those of the restored scenario for all modeled years (Figures 4-4 and 4-5). This change in average yield can be attributed to the predicted increased infiltration of surface flow on the alluvial fans in the restored scenario resulting in a small increase in predicted annual average AET in the central valley. In the channelized scenario a greater, though not statistically significantly so, quantity of water (3.1-5.3 Mm^3) was predicted to reach the main river channel via surface flow paths compared to the restored scenario (2.5-3.5 Mm^3) on average. Much of this water would

leave the catchment more quickly and not be available for AET. As expected, given that surface flows on fans only occur in large rainfall events, the differences in water yields for individual years were more pronounced in wet years and insignificant in dry years (Figures 4-4 and 4-5).

The magnitudes of the largest modeled peak flows, considered as daily flow events with an annual exceedance probability of 10% or less, increased with widespread channelization on the alluvial fans. Average flow rates for such events were predicted to be similar for the current and channelized scenarios (60-62 m^3/s vs 62-64 m^3/s), but significantly lower for the restored scenario (52-53 m^3/s), decreasing by 11-17% from the current state and 15-24% from the channelized scenario. Effects of event magnitude and antecedent conditions on the influence of channelization were evident in daily hydrographs (Figure 4-6). When multiple small events occurred in succession, such as in 04/1990, soils became progressively more saturated and proportionally more flow was produced in the restored scenario, reducing the difference between this and the channelized scenario, compared to the first event in a sequence. However, as hypothesized, differences in large rainfall event ($\geq$30 mm) flows between the channelized and restored fan scenarios were generally greater when antecedent conditions were wetter and floodplain groundwater tables were higher, with linear regression analyses suggesting this could explain 30-40% of the variation in peak differences between events (Figures 4-7 and 4-8). As would be expected given the relatively fast draining soils, antecedent conditions considered over progressively longer time periods prior to the event became less and less important explanatory factors (r^2 values decreasing to 0.12 when looking at the entire year preceding the event). Interestingly, the effective

rainfall in the preceding two years had a greater correlation coefficient ($r^2 = 0.3$) than that for 6 months or one year, perhaps an indication that longer term wet or dry conditions dictate larger changes in floodplain groundwater tables that influence the storm response. The flood response difference had a similar degree of correlation with the modeled average floodplain groundwater level ($r^2 = 0.3$).

Table 4-1 Long term (1975-2012) average annual water balances for the Baviaanskloof catchment and internally modeled land units under different scenarios of alluvial fan channelization

Location / spatial scale	*Flux*	Annual volume (Mm^3/ year)					
		Channelized		Current		Restored	
		Mean	*95% CI*	Mean	*95% CI*	Mean	*95% CI*
Catchment	***Precipitation***	323		323		323	
	AET	288	*1.1*	288	*1.3*	291	*1.5*
	Streamflow	31	*1.0*	29	*1.0*	27	*1.0*
Mountain tributary sub-catchments	***Precipitation***	307		307		307	
	AET	260	*1.2*	260	*1.2*	260	*1.2*
	Overland flow to fan head	4.8	*0.1*	4.8	*0.1*	4.8	*0.1*
	Interflow to floodplain	29	*0.9*	29	*0.9*	29	*0.9*
	Mountain bedrock outflow	9.0	*0.6*	9.0	*0.6*	9.0	*0.6*
Central valley alluvial fill (fans and floodplain)	***Precipitation***	16		16		16	
	AET	28	*0.3*	28	*0.2*	31	*0.3*
	Alluvial aquifer input to channel (net)	27	*1.3*	26	*1.5*	24	*1.0*
	Overland flow inputs to channel	4.2	*1.1*	3.6	*0.7*	3.0	*0.5*

Figure 4-4 Modeled catchment water yield (total streamflow output) by water year for 1975-2012 for scenarios of the current state, restored, and channelized alluvial fans.

Means and confidence intervals of the simulations sets run within the parameter ranges considered are shown

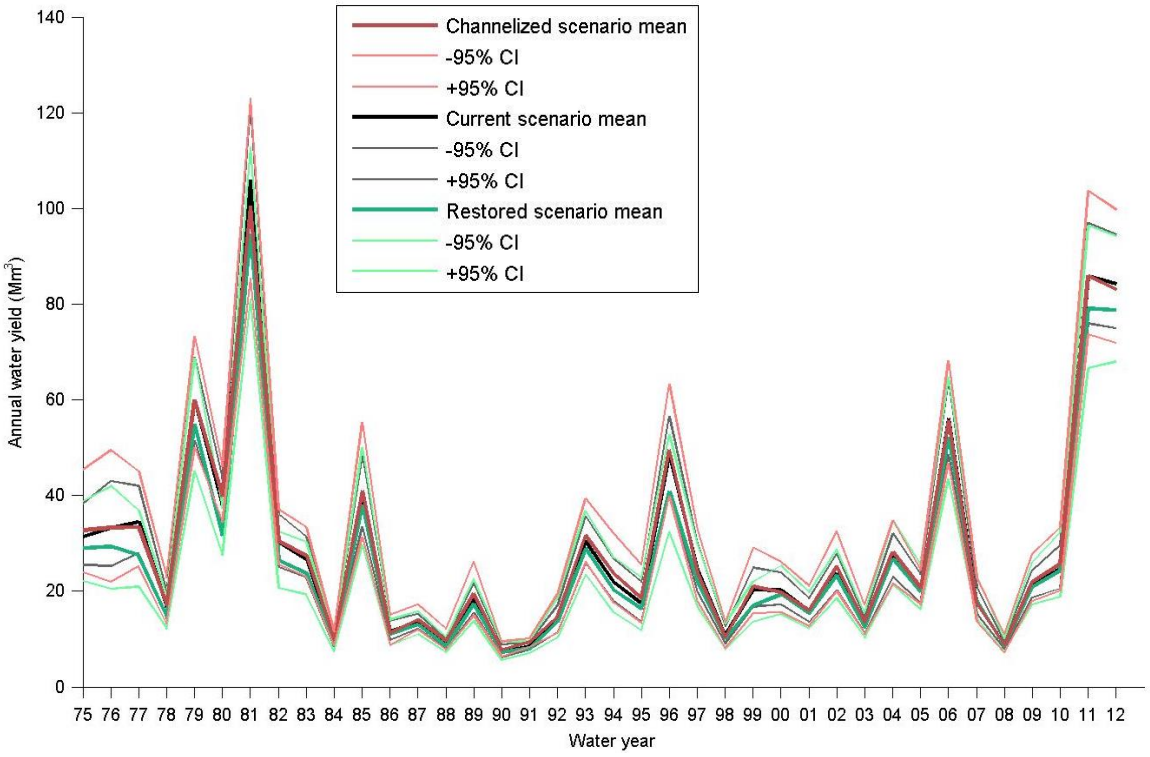

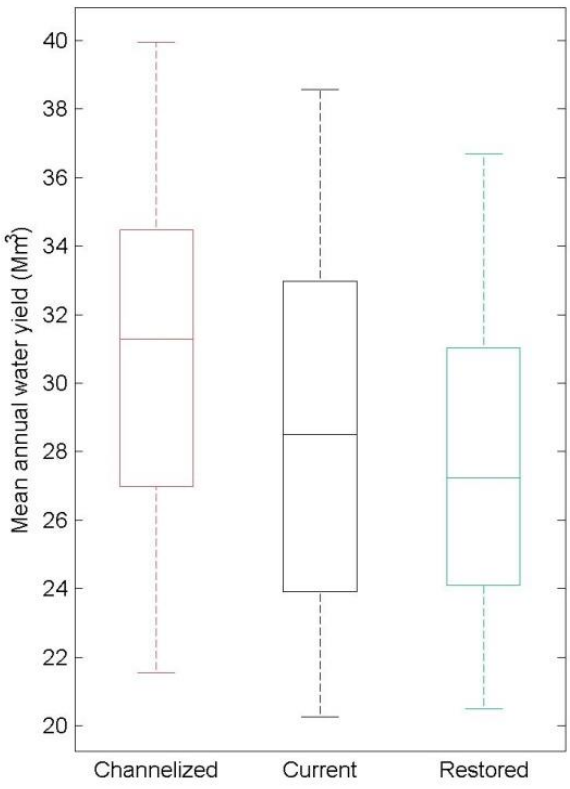

Figure 4-5 Boxplots showing the distributions of modeled mean annual and seasonal water yields for different alluvial fan scenarios for: all simulated years (left), selected dry and wet years (center), and summer and winter months for all years (bottom)

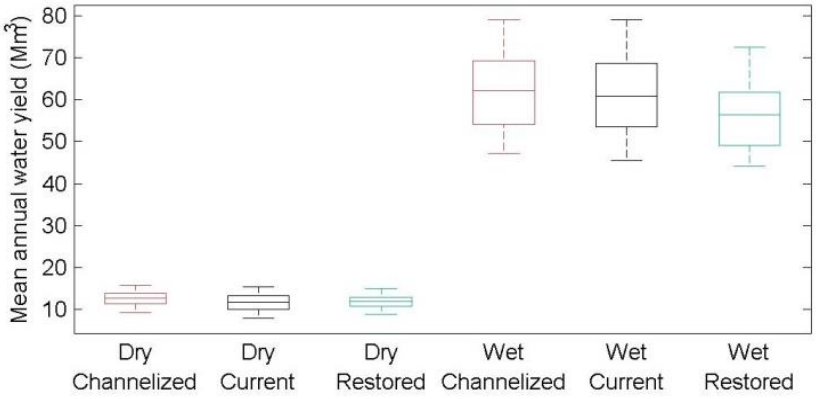

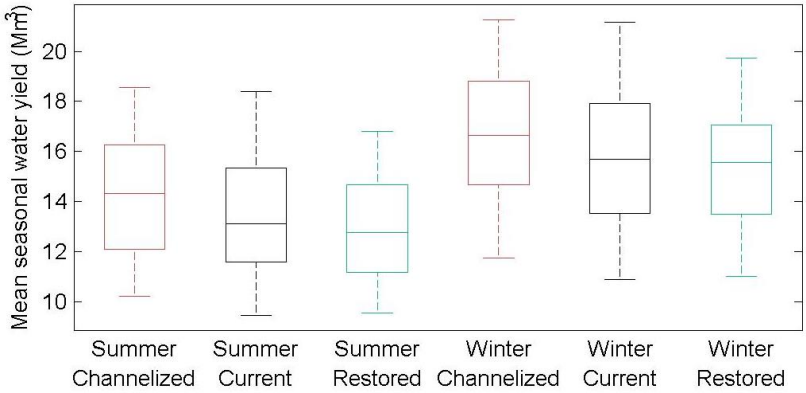

Figure 4-6 Modeled daily flow hydrographs for demonstration dry (1990, top) and wet (2011, bottom) years showing differences in flow peaks and recessions between alluvial fan scenarios

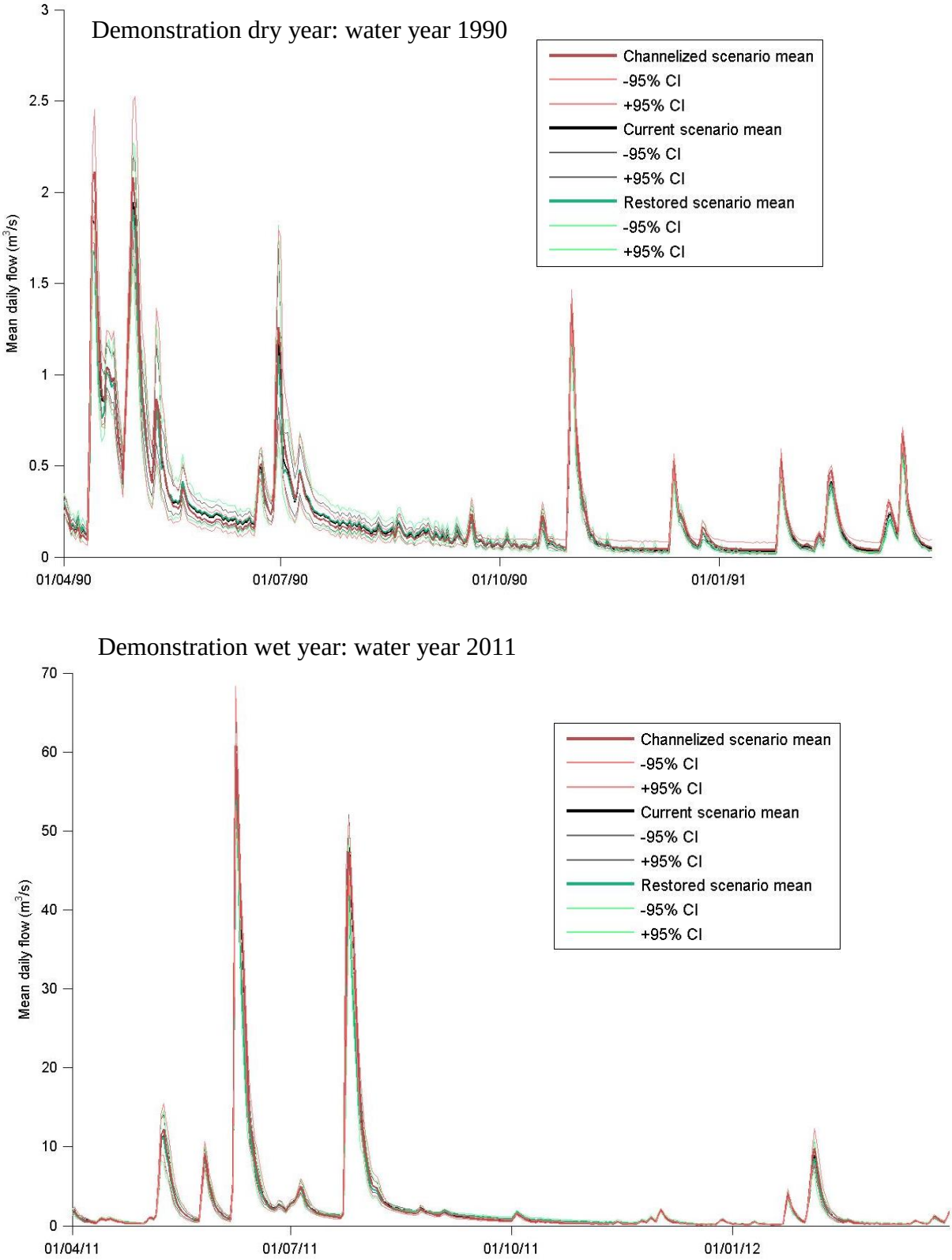

Figure 4-7 Variation in the differences in large storm event streamflow between the channelized and restored alluvial fan scenarios given different antecedent wetness conditions manifest as the mean floodplain groundwater depth.

Large storm events were defined as ≥30mm/day. Event response flow was total

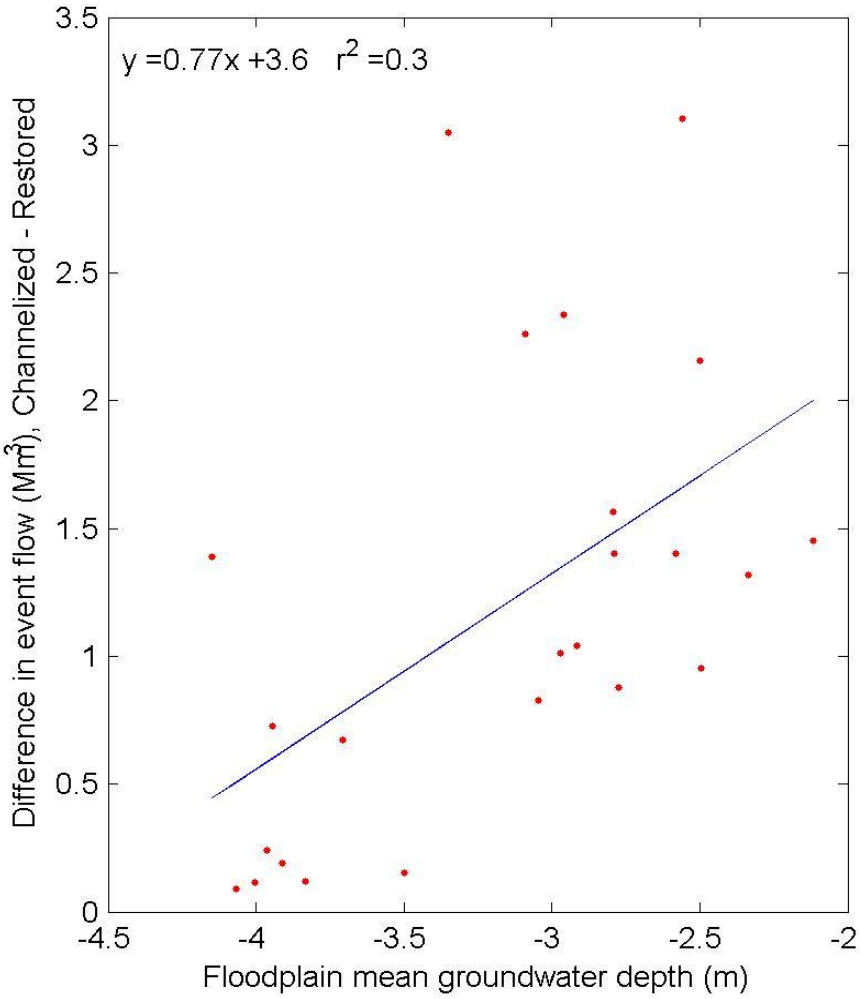

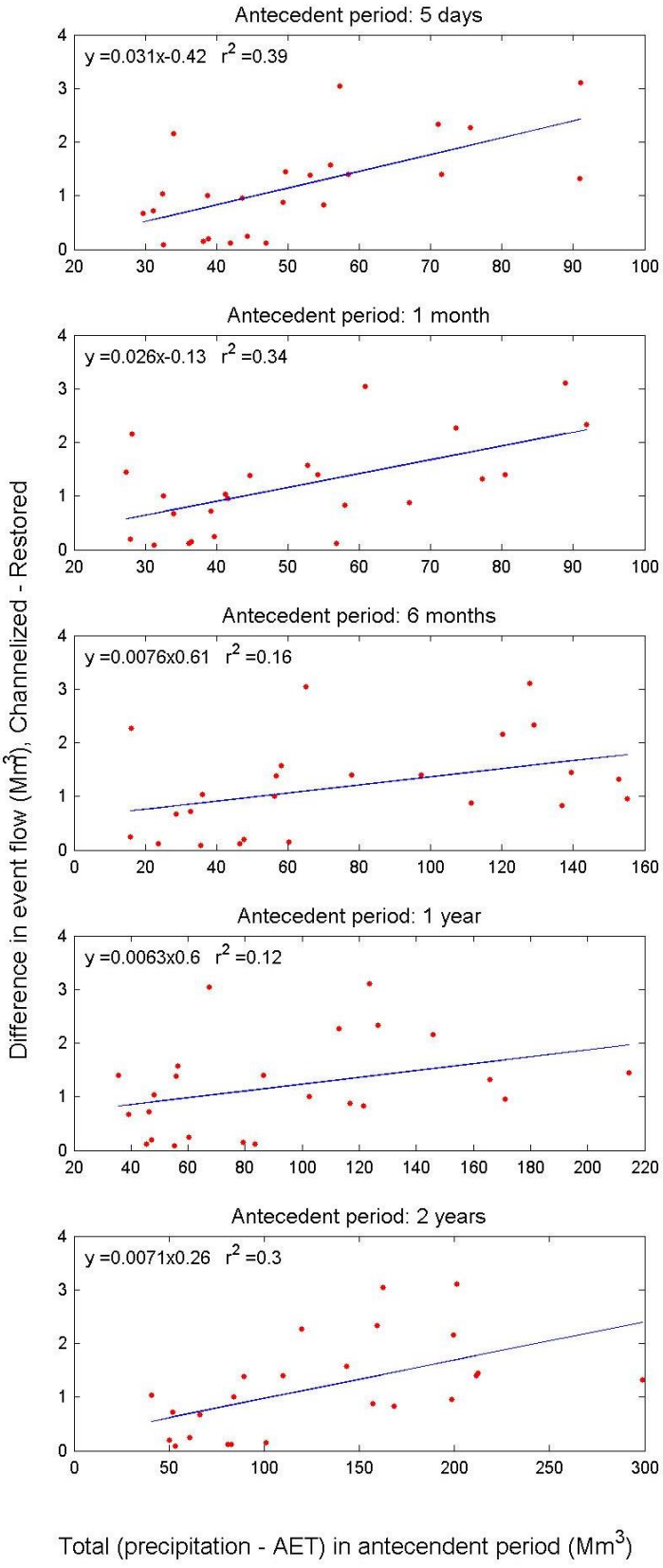

Figure 4-8 Variation in the differences in large storm event streamflow between the channelized and restored alluvial fan scenarios given different antecedent wetness conditions.

Large storm events were defined as ≥30mm/day. Event response flow was total streamflow during the event and following day. Antecedent wetness was indicated by the total effective precipitation

Figure 4-9 Daily flow duration curve for different alluvial fan scenarios showing the distribution of daily flow values modeled for the period 1975-2012

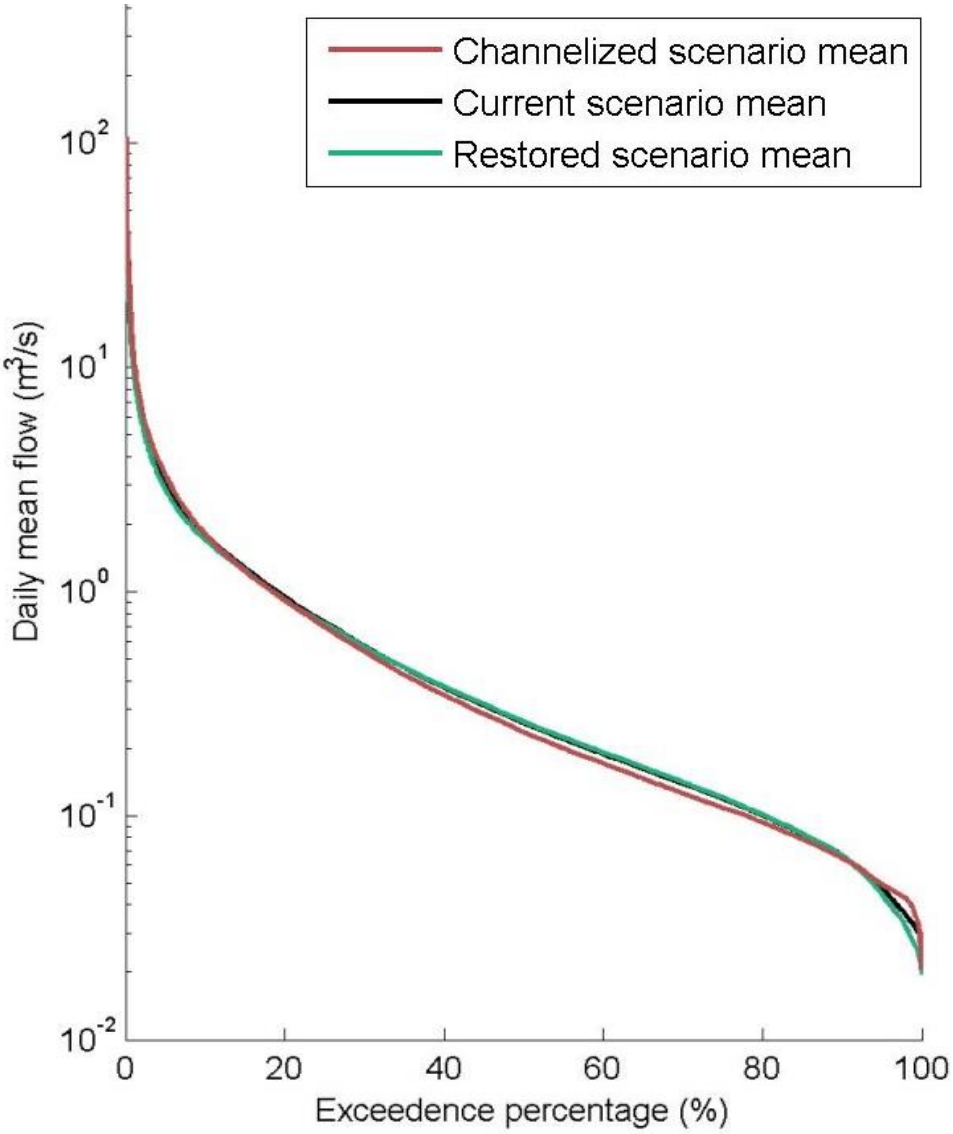

The model results in this study did indicate that restoring dispersive flow paths on alluvial fans in the Baviaanskloof could increase average baseflows between storm peaks, however not in the driest and warmest months on record. This is evident in the flow duration curve (Figure 4-9) and in wet and dry year hydrographs (Figure 4-6). Daily differences between scenarios were not statistically significant, but differences were consistent enough that long term indices were discernably different. The mean annual minimum monthly flow rate modeled for 1975-2012 was 10% (0.01 m^3/s) higher in the restored than the channelized fan scenario ($p=0.04$). This difference was driven by the wetter years, as the mean annual minimum monthly flows for the selected dry years were not significantly different between scenarios. Simulations predicted that additional infiltration on the restored alluvial fans would result in greater volumes of delayed, subsurface flows through the alluvial aquifer reaching the main river channel in weeks to months after a significant rainfall event, such that streamflows were highest in the restored scenario in these periods. This was seen in wet years and following small flow peaks in dry years. For example, the largest flow peaks in 1990, a dry year, and in 2011, a wet year, occurred between May and August and while modeled peak flows were consistently larger in the channelized scenario, modeled streamflow in the baseflow periods following these peaks was greatest for the restored scenario until October in 1990 and December in 2011 (Figure 4-6).

In summer months baseflows were similar amongst the scenarios and marginally greater in the channelized scenario in some years (Figure 4-6). In these warmer periods ET demands were greater and the soils drier so that less of the extra infiltrated volume modeled on alluvial fans in the restored scenario was predicted to reach the groundwater table. The

occasionally greater summer baseflows predicted for the channelized fan scenario, such as in 01/1991 (Figure 4-6), were the result of modeled flows from smaller storms crossing the absorbent alluvial fans more quickly, with less opportunity infiltration, such that greater volumes reached the floodplain. Being summer with drier soils, infiltration along the channel flow path was also predicted to occur in the channelized scenario. Having more of the infiltration occur lower down in the landscape where the groundwater table is closer to the surface, as opposed to further up on the fans as in the restored scenario, meant that more of this infiltrated volume could percolate to the water table and later contribute to baseflow. Being a dry year, average depths to the water table on the alluvial fans were predicted to be relatively large (5-7 m) compared to those on the central floodplain (3-4 m). When compared to observed hydrographs, it was found that small flow peak responses to minor rainfall events are generally overestimated in this model (Chapter 2) and so it is likely that this effect of channelization on the dry period flow response is also overestimated.

4.3.2 Effects on floodplain groundwater depth

Model outputs indicated that channelization of alluvial fans in the Baviaanskloof could result in a slightly deeper floodplain groundwater table on average and conversely that restoration of dispersive flow paths on fans could raise the water table (Figures 4-10 and 4-11). While the difference in mean central floodplain groundwater depth for the modeled period between the restored and channelized scenario was statistically significant ($p=0.02$), the magnitude of the difference (0.1-0.2 m) was small compared to seasonal and interannual fluctuations. This difference in groundwater table did result in more alluvial aquifer flow

into the main river channel creating the small, but detectable, increase in average modeled baseflow in the restored case over the channelized fan scenario. Modeled differences between groundwater depths were larger for dry years that wet years (Figures 4-10 and 4-11). However, in the dry periods the greater depth of the groundwater table meant that there was less interaction between the groundwater table and the main floodplain channel and so the higher mean elevation of the groundwater table in the restored scenario had little impact on baseflow in the driest periods on record.

Figure 4-10 Modeled floodplain average groundwater depth in the central floodplain by water year for 1975-2012 for scenarios of the current state, restored, and channelized alluvial fans.

Means and confidence intervals of the simulations sets run within the parameter ranges considered are shown

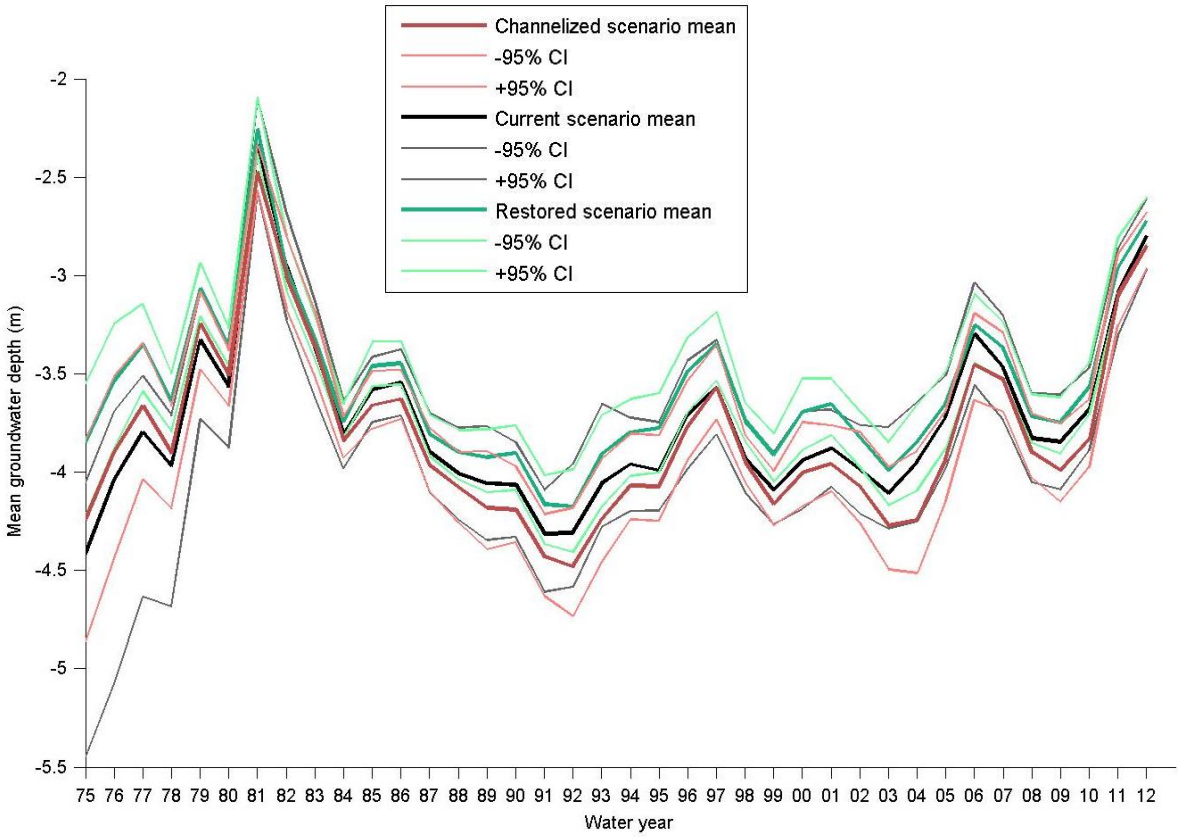

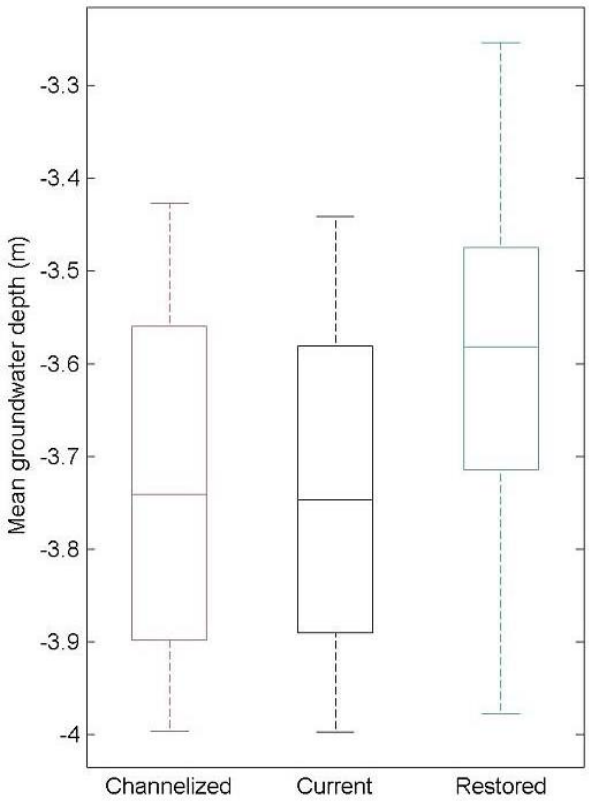

Figure 4-11 Boxplots showing the distributions of modeled mean annual and seasonal floodplain groundwater depth for different alluvial fan scenarios: all simulated years (left), selected dry and wet years (center), and summer and winter months for all years (bottom)

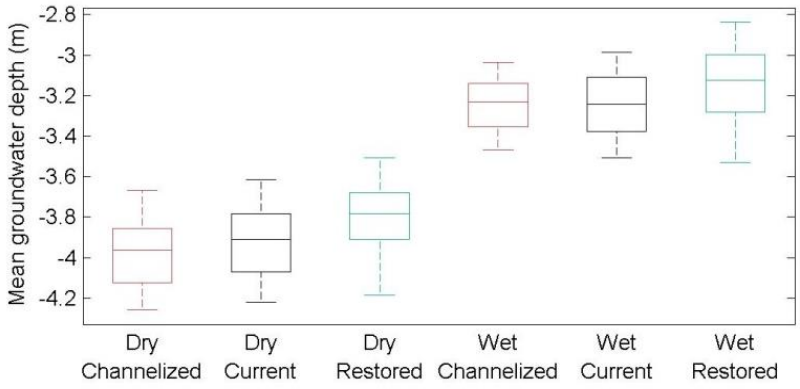

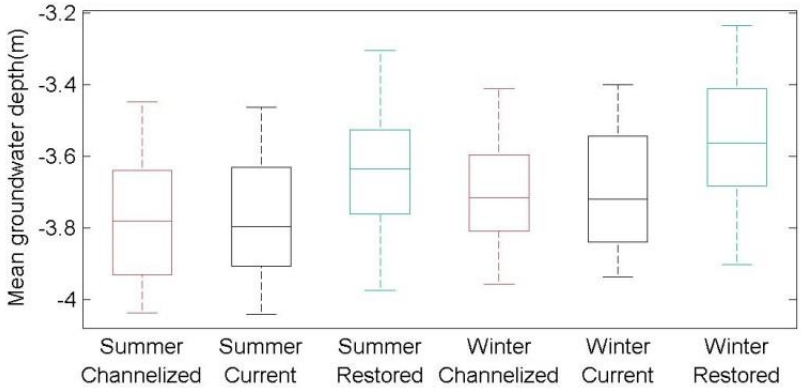

Various modeled patterns of infiltration and percolation in the central valley alluvial fill gave rise to the observed differences in the groundwater tables and baseflows between scenarios. These patterns illustrate the role of climate in determining the magnitude of flow and groundwater differences between scenarios.In large rainfall events infiltration and percolation to the alluvial aquifer were consistently predicted to be greater in the restored alluvial fan scenario (Figure 4-12 b& d), with most of this being attributable to differences in processes on the alluvial fans (Figure 4-12 c&e). In large flow events, due to the higher surface flow peaks predicted in the channelized scenario, more overbank flows and larger inundated areas were modeled in the floodplain in this case. This added to total infiltration and alluvial aquifer recharge predicted in these events in the channelized alluvial fan scenario, reducing the difference in net alluvial aquifer recharge and catchment scale flow between the channelized and restored fan scenarios compared to the differences in volumes seen on the fan areas alone.

In smaller events the differences between scenarios were smaller and the trends more variable. Smaller rainfall events, under 30 mm, were not predicted to produce surface flows from many of the mountain tributary subcatchments feeding onto the fan heads. In such cases infiltration of rainfall falling directly on the fan and floodplain surface was generally predicted to be similar between the scenarios. In instances of wetter antecedent conditions on the restored alluvial fan soils from a recent surface flow event, infiltration of rainfall on the alluvial fan soils on the wetted restored fans was predicted to be lower than on the drier fan surfaces in the channelized case. Nevertheless percolation was more often predicted to be greater in the restored scenario in these smaller events, even if infiltration was not (Figure

4-12 b&c vs. d&e), as soils were closer to field capacity soil moisture and groundwater tables were shallower in the restored case compared to the channelized scenario. In the case of relatively small surface flow events occurring in drier periods, bed infiltration on the alluvial fan channels and floodplain channels themselves was also significant. Because the water was concentrated in the channels in the channelized scenarios, localized saturation developed and percolation was predicted, while in the restored scenario, in which water dispersed across the fan surface, saturated conditions were not reached and there was less percolation, despite greater infiltration. This indicated that if rainfall fell primarily in small events in the warmer summer months, it is possible for the channelized scenario to result in greater alluvial aquifer recharge than the restored case.

Figure 4-12 Precipitation and modeled scenario daily infiltration and recharge of the alluvial aquifer for the entire central valley (floodplain and fans) and fan area only: (a) precipitation, (b) total infiltration, (c) infiltration on fans, (d) total recharge, (e) recharge on fans

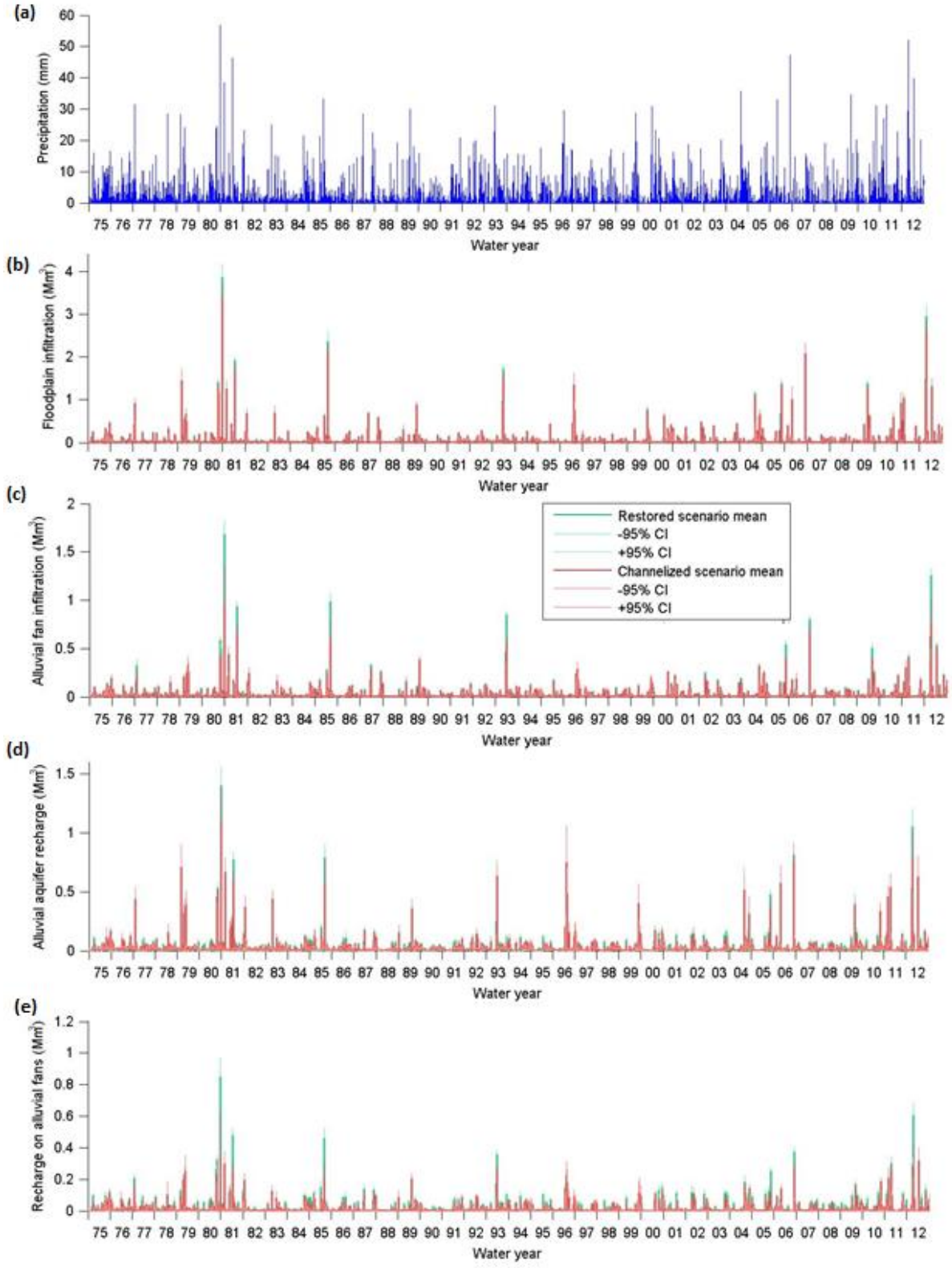

4.4 Discussion

This modeling exercise supported the hypotheses that alterations to flow paths across alluvial fans in a catchment like the Baviaanskloof, a meso-scale semi-arid mountainous catchment, can discernably alter catchment-scale streamflow and groundwater patterns, despite fans only making up 1% of the catchment's surface area. Comparing a scenario in which all 62 fans had a channel connection with the central valley floodplain's trunk channel to one in which only 14 fans were channelized and the remaining 48 had dispersive surface flow paths, indicated that widespread channelization could result in higher flood peaks, lower average baseflows, greater average water yield to the catchment outlet, and a lower average water table in the floodplain. However, the differences in average yields and groundwater tables between the channelized and restored fan scenarios were small compared to the seasonal and interannual fluctuations experienced in this region, and also compared to the uncertainty in the model. Long-term trends were statistically significant, but differences in daily flows were only discernable in extreme high flow events. The most notable effect was the change in catchment outlet peak flows, with fan channelization increasing the largest peaks by 15-24% (9-12 m^3/s) compared to those predicted in the restored scenario. Modeled roughness and overbank flooding in the floodplain reduced peak flow intensities at the catchment outlet, so more extreme peak flow differences between channelized and restored scenarios would be experienced by catchment residents in floodplain areas further upstream. Increased flood impacts downstream of the alluvial fans should therefore be weighed up against the more local benefits of the flood protection engineering on the fans.

In general the processes modeled on the alluvial fans in the different scenarios followed expected patterns, with greater surface flows on channelized fans and greater infiltration on restored fans, the downstream impacts of which were influenced by antecedent conditions. However, the role of weather patterns and floodplain conditions in the net catchment response to fan channelization led to some unexpected results. For example it could be seen as somewhat counter-intuitive to find that modeled baseflows could be larger in some dry periods in the channelized case compared to the restored case. This was predicted by the model following rainfall events in certain dry summer periods which still had relatively high floodplain groundwater tables from previous wet periods. In such cases, infiltration of surface runoff was predicted to occur further down the flow path on the floodplain in the channelized case compared to occurring up on the drier alluvial fan surfaces in the restored fan scenario. More of the water infiltrating on the wetter floodplain was able to percolate and influence baseflow than water infiltrating on the dry fan. In addition, having infiltration more spatially concentrated in the channels in these dry periods also led to greater predicted percolation. Given the model's overprediction of the flow peak response to small rainfall events at the catchment outlet (Chapter 2), it is likely that the minor surface flows predicted for these events, and hence this effect on summer baseflows, were overestimated for the Baviaanskloof. Nevertheless this result does illustrate that this outcome is possible in certain conditions.

The depth of the floodplain groundwater table was seen to have a noticeable role in determining the catchment scale response to alluvial fan channelization. The effects of alluvial fan channelization were most salient in the largest flood events, those occurring with

wet antecedent conditions. Flood peaks were more enhanced in the channelized case, and baseflows following large rainfall events were more notably increased in the restored case, when the floodplain groundwater table was shallower. In dry periods, when the water table was deeper, the floodplain acted as a buffer to surface flows in a similar fashion to the fans and so changes to fan form had less notable impacts. These results highlight the need to look at and model changes on alluvial fans in their dynamic landscape contexts in order to predict downstream impacts. They also highlight the importance of assessing change over time periods that capture the interannual variation in floodplain groundwater levels in catchments like this.

The magnitude and direction of the effects of alluvial fan channelization modeled were a function of geomorphology and climate of the Baviaanskloof. Being an arid environment with coarse, high conductivity, alluvial fills and having a relatively narrow floodplain, both the surface and subsurface flow paths between the mountain fronts and the catchment outlet are relatively short compared to what may be seen in catchments of similar size in wetter environments with finer sediments and wider floodplains. In the case of the Baviaanskloof, the rate of drainage from the sites of infiltration on alluvial fans to the floodplain channel played a role in how much and how long the additional alluvial aquifer recharge on the fans in the restored scenario would continue to elevate baseflows compared to the more channelized cases. Longer and slower flow paths could mean more prolonged effects on low flows, but could also result in less of an increase in baseflow, or even a decrease, if infiltrated water on restored fans does not percolate and/or is completely used by ET. Well-draining soils and sporadic rainfall in the Baviaanskloof case also meant that antecedent soil

moisture conditions on alluvial fan surfaces were not often close to saturation at the beginning of a rainfall event. If conditions were such that saturation or infiltration excess overland flow commonly occurred on fan surfaces, the impact of alluvial fan channelization on peak flows could be expected to be smaller in wet periods as significant surface flows may also be produced on the restored fan. Overbank flooding in the downstream floodplain channel had a dampening effect on the increase in flow peaks predicted at the Baviaanskloof catchment outlet in the channelized case. Flood peak increases due to fan channelization would likely be greater in catchments with less effective floodplains. The effects of alluvial fan channelization on both peak flows and baseflows in the Baviaanskloof were most notable during and following large rainfall events, particularly those in occurring in winter and/or in generally wet years. If such events were less frequent, the impact of the alluvial fans on catchment flows would be reduced. This would also be the case if warmer temperatures resulted in increased AET in the floodplain lowering the groundwater table.

This study was intended as an explorative case study into the potential impacts of the changes in alluvial fan geomorphology on catchment-scale hydrologic patterns of management interest in this kind of setting. Change detection was limited by modeling uncertainties, which could be reduced with additional hydrometric data and field sampling. Nevertheless the model structure used was assumed to be adequately representative of the patterns of flow through a catchment with the general characteristics of the Baviaanskloof, based on its ability to recreate observed patterns of streamflow and floodplain groundwater levels (Chapter 2).

Due to the catchment scale and necessary modeling simplifications, the scenarios of change on the alluvial fans considered here were commensurably simple. Average channel dimensions and surface and subsurface properties were applied to all fans. Some of the heterogeneity among the fans was captured in terms of the different fans' sizes, shapes, distances from the main floodplain channel and catchment outlet, and the sizes, shapes, land unit distributions, and different rainfall quantities received by their contributing mountain subcatchments. It is possible that consideration of heterogeneous channel, vegetation, and soil properties amongst the fans could produce different results than those predicted, however it was assumed that these would be second order differences compared to that between widespread fan channelization and widespread dispersive flow paths on fans. Applying currently observed fan channel dimensions to all fans was assumed to represent extension of current agricultural practices onto, and upcatchment of, the currently unchannelized fans, without additional large scale engineering or intensification. Further manual widening of alluvial channels is possible but the sustained depth of the channel on the alluvial fan will be limited by the local base level at its connection with the floodplain channel. It can be assumed that increasing the channel capacity used in the channelized scenario would have further increased the change in flow peaks and baseflows up to the point at which the maximum outflow from the subcatchments on record is accommodated.

The effects of channelization or of restoration of alluvial fans on streamflow and groundwater levels in the Baviaanskloof catchment predicted in this study were small relative those predicted to accompany large scale changes in hillslope vegetation cover (Chapter 3). The same model structure used here was applied previously to examine the

potential impacts of restoration or further degradation of the subtropical thicket vegetation that is endemic to the regions' hillslopes and highly vulnerable to livestock grazing. Covering 40% of the Baviaanskloof catchment surface area, restoration of thicket canopy cover from a current estimated average density of 20% to 65% was predicted to decrease peak flows by 56-60% and decrease average annual yields by 22-27% for the modeled 1975-2012 period. Similar to alluvial fan restoration, more rainfall was predicted to infiltrate and recharge active groundwater pools in large rainfall events in the restored thicket scenario. However, the restoration of thicket was also assumed to come with large increases in canopy interception losses and ET demand, which was not the case for the restored alluvial fan scenario. As such, unlike with the alluvial fan restoration scenario, over the long-term the AET losses and improved hillslope soil moisture retention in the restored thicket scenario were predicted to outweigh the additional subsurface flows and no increase in baseflow was predicted.

The results from the vegetation change study highlight a potentially important simplification applied in this study to be addressed in further research. While changes in forms of alluvial fans were explored in their broader landscape context, contexts that may have given rise to specific alluvial fan forms were not explicitly considered. For example, the increased flow peaks predicted with the loss of hillslope thicket cover may have helped to create and maintain the observed channel dimensions on some of the currently channelized fans. These increased flows could have led to channel erosion and incision of the main floodplain channel, lowering the base level to which fan flow paths adjust over time. Similarly, if all the alluvial fans in the catchment were channelized, as modeled here,

the increased flow peaks this was predicted to cause could also lead further floodplain channel incision. In this study the floodplain channel dimensions were held constant between fan scenarios. It was assumed that most fans could have dispersive flow paths restored while maintaining the current vegetation cover in their contributing catchments and the current downstream floodplain channel morphology. This may be a short-term engineering reality, but it is possible some restored fan states could not be realistically maintained against larger-scale geomorphic processes in the long-term without substantial ongoing effort. Streamflow and groundwater impacts of combined vegetation and channel restoration and degradation scenarios, which may better represent sustainable landscape forms, will be explored in a subsequent study (Chapter 6). The results here highlight the impact of alluvial fan form alone on the flows through catchments with similar characteristics to the Baviaanskloof.

4.5 Conclusions

Alluvial fans are a common landform in relatively dry mountainous environments (Blissenbach, 1954; Hooke, 1967; Bull, 1977; Hendrickx et al., 1991; Munevar and Marino, 1999; Houston, 2002; Blainey and Pelletier, 2008) and yet they have received little to no consideration in modelling of meso-scale catchments to date. This study demonstrated how basic alluvial fan processes could be incorporated into a medium complexity catchment model. This model was then used to explore the impacts of altered alluvial fan morphologies on catchment-scale streamflow and floodplain groundwater levels for a case study catchment in which many fans have been channelized for local flood protection. Although

alluvial fans only account for 1% of the surface area of the Baviaanskloof catchment, 43% of the mountainous tributary subcatchment area drains onto alluvial fans at the margins of the central valley floodplain. As such it was hypothesized that widespread channelization of the flow paths across these fans would detectably increase streamflow peaks and decrease alluvial aquifer groundwater recharge and hence baseflow. Scenario modeling results using a calibrated, coupled hydraulic-hydrologic model of the catchment supported these hypotheses. Changes in alluvial fan form were predicted to have the most notable, and statistically detectable, catchment scale impacts during wetter periods and the largest flow events. Results indicated that restoration of more dispersive flow paths across alluvial fans could reduce flood peaks by as much as 11-17% from the current condition and 15-24% compared to a scenario in which all fans were channelized.

A small net decrease in the long term average yield was predicted for the restored fan scenario, due to additional AET from water infiltrating on fan surfaces; however, due to model uncertainties and variable climate, modeled changes in long term water yields compared to the current scenario were not statistically significant. A small increase in average groundwater levels in the floodplain and a 10% increase in long-term annual minimum monthly flow were predicted in the restored scenario compared to the channelized scenario. Due to the fast draining nature of the coarse alluvial fill in the Baviaanskloof, increased baseflow was predicted for several months following large storm events in wet or winter periods, but not predicted in the driest summer months on record when AET was higher, fan soils drier, and the groundwater table lower. The impacts of these small, but temporally consistent, changes in low flows on realized water supply availability requires

further assessment in the context of the local water supply systems. The occurrence of large rainfall events in winter months played a large role in the additional recharge on restored fans. The role of alluvial fan form in determining streamflow and groundwater levels was sensitive to weather patterns and geomorphic context. This highlights the need for local modelling to understand the impacts of alluvial fan changes in other catchment contexts.

Despite modeling uncertainties, the results of this study do make clear that the most notable change to be expected with restoration of alluvial fans is a decrease in flood intensity in downstream areas. Potential increases in water supply in dry periods appear likely to be relatively small, but results do not suggest a large loss in annual average water yield with restoration. Relative benefits of channelizing alluvial fan surfaces for local flood control compared to the impacts of predicted flood intensities downstream appears to be a more salient tradeoff to consider in the Baviaanskloof case, rather than a major tradeoff between flood control on fans and major impacts on downstream water supply. This may play out differently in other areas with different geomorphologies and climates. This study demonstrates a method for considering alluvial fan processes in a meso-scale catchment model which could be replicated in other areas, to compare the roles of alluvial fans in catchment scale hydrologic responses in different climate and geologic regions and to inform catchment management.

4.6 References

Arnold, J.G., and Fohrer, N. (2005). SWAT2000: current capabilities and research opportunities in applied watershed modelling. Hydrol. Process. *19*, 563–572.

Arnold, J.G., Srinivasan, R., Muttiah, R.S., and Williams, J.R. (1998). Large area hydrologic modeling and assessment - Part 1: Model development. J. Am. Water Resour. Assoc. *34*, 73–89.

Beven, K. (2001). How far can we go in distributed hydrological modelling? Hydrol Earth Syst Sci *5*, 1–12.

Blainey, J.B., and Pelletier, J.D. (2008). Infiltration on alluvial fans in arid environments: Influence of fan morphology. J. Geophys. Res. Earth Surf. *113*, n/a – n/a.

Blair, T., and Mcpherson, J. (1994). Alluvial Fans and Their Natural Distinction from Rivers Based on Morphology, Hydraulic Processes, Sedimentary Processes, and Facies Assemblages. J. Sediment. Res. Sect. -Sediment. Petrol. Process. *64*, 450–489.

Blissenbach, E. (1954). Geology of Alluvial Fans in Semiarid Regions. Geol. Soc. Am. Bull. *65*, 175–190.

Bobbins, K.L. (2011). Developing a form-process framework to describe the functioning of semi-arid alluvial fans in the Baviaanskloof Valley, South Africa (S.l.: s.n.]).

Bull, W.B. (1977). The alluvial-fan environment. Prog. Phys. Geogr. *1*, 222–270.

Clarke, L., Quine, T.A., and Nicholas, A. (2010). An experimental investigation of autogenic behaviour during alluvial fan evolution. Geomorphology *115*, 278–285.

Euston-Brown, D.I.W. (2006). Baviaanskloof Mega-Reserve Project: Vegetation mapping contract report on methodology, vegetation classification and short descriptions of habitat units (South Africa: Eastern Cape Parks & Tourism Agency).

Giertz, S., and Diekkrüger, B. (2003). Analysis of the hydrological processes in a small headwater catchment in Benin (West Africa). Phys. Chem. Earth Parts ABC *28*, 1333–1341.

Graham, D.N., and Butts, M.B. (2005). Flexible, integrated watershed modelling with MIKE SHE. In Watershed Models, V.P. Singh, and D.K. Frevert, eds. (Boca Raton, FL, USA: Taylor and Francis Group), pp. 245–272.

Hargreaves, G., and Samani, Z. (1982). Estimating potential evapotranspiration. J. Irrig. Drain. Div.-Asce *108*, 225–230.

Harvey, A.M. (2002). The role of base-level change in the dissection of alluvial fans: case studies from southeast Spain and Nevada. Geomorphology *45*, 67–87.

Hendrickx, J.M.H., Khan, A.S., Bannink, M.H., Birch, D., and Kidd, C. (1991). Numerical analysis of groundwater recharge through stony soils using limited data. J. Hydrol. *127*, 173–192.

Herr, J.W., and Chen, C.W. (2012). Warmf: Model Use, Calibration, and Validation. Trans. Asabe *55*, 1385–1394.

Herron, N., and Wilson, C. (2001). A water balance approach to assessing the hydrologic buffering potential of an alluvial fan. Water Resour. Res. *37*, PP. 341–351.

Hooke, R.L. (1967). Processes on Arid-Region Alluvial Fans. J. Geol. *75*, 438–460.

Houston, J. (2002). Groundwater recharge through an alluvial fan in the Atacama Desert, northern Chile: mechanisms, magnitudes and causes. Hydrol. Process. *16*, 3019–3035.

Jansen, H.C. (2008). Water for Food and Ecosystems in the Baviaanskloof Mega Reserve: Land and water resources assessment in the Baviaanskloof (Wageningen, The Netherlands: Alterra).

Lynch, S.D. (2003). Development of a Raster Database of Annual, Monthly and Daily Rainfall for Southern Africa (Pretoria, South Africa: Water Research Commission (WRC)).

Midgley, J.J., and Scott, D.F. (1994). Use of stable isotopes of water (d and o-18) in hydrological studies in the Jonkershoek valley.

Mukhopadhyay, B., Cornelius, J., and Zehner, W. (2003). Application of kinematic wave theory for predicting flash flood hazards on coupled alluvial fan–piedmont plain landforms. Hydrol. Process. *17*, 839–868.

Munevar, A., and Marino, M.A. (1999). Modeling analysis of ground water recharge potential on alluvial fans using limited data. Ground Water *37*, 649–659.

Niswonger, R.G., Prudic, D.E., Pohll, G., and Constantz, J. (2005). Incorporating seepage losses into the unsteady streamflow equations for simulating intermittent flow along mountain front streams. Water Resour. Res. *41*, W06006.

Phillips, B.M. (1998). Levee design for flood protection on alluvial fans (New York: Amer Soc Civil Engineers).

Powell, R. (2015). Recent degradation along the upper-middle reaches of the Baviaanskloof River-floodplain: An examination of drivers of change and best rehabilitation practices. PhD dissertation. Rhodes University.

Refsgaard, J.C., and Storm, B. (1995). MIKE SHE. In Computer Models of Watershed Hydrology, V.P. Singh, ed. (Water Resources Publications), pp. 809–846.

Roets, W., Xu, Y., Raitt, L., and Brendonck, L. (2008). Groundwater discharges to aquatic ecosystems associated with the Table Mountain Group (TMG) aquifer: A conceptual model. Water SA *34*, 77–88.

Schulze, R.E., and Maharaj, M. (2004). Development of Database of Gridded Daily Temperature for Southern Africa (Pretoria, South Africa: Water Research Commission (WRC)).

Soltau, L., Smith-Adao, L., and Bugan, R. (2011). Baviaanskloof resistivity survey to define water level and depth to bedrock (Stellenbosch, South Africa: Center for Scientific and Industrial Research (CSIR)).

USACE-HEC (2010). Hydrologic Modeling System, HEC-HMS v3.5. User's Manual.

Woods, S.W., MacDonald, L.H., and Westbrook, C.J. (2006). Hydrologic interactions between an alluvial fan and a slope wetland in the central rocky mountains, USA. Wetlands *26*, 230–243.

Xu, Y., Titus, R., Holness, S.D., Zhang, J., and Tonder, G.V. (2002). A hydrogeomorphological approach to quantification of groundwater discharge to streams in South Africa. Water SA *28*, 375–380.

Xu, Y., Wu, Y., and Beekman, E.H. (2003). The role of interflow in estimating recharge in mountainous catchments. In Groundwater Recharge Estimation in Southern Africa, Y. Xu, and E.H. Beekman, eds. (Paris, France: UNESCO),.

Chapter 5 Streamflow and groundwater impacts of floodplain channel incision in a meso-scale, semi-arid catchment

5.1 Introduction

Geomorphological research has progressively improved understanding of how forms of river channels change in response to various human activities and land cover alterations (Gregory, 2006; James and Marcus, 2006). Recent developments in hydrologic and hydraulic modeling allow assessment of the potential repercussions of these changes on catchment-scale hydrology. This study applies such methods to look at potential streamflow and groundwater impacts of floodplain channel incision in a semi-arid, mountainous, water-supply catchment in South Africa: the Baviaanskloof. Anthropogenically enhanced river channel incision is common globally (Beechie et al., 2008; Bravard et al., 1997) and semi-arid regions are particularly prone due to their more flashy hydrology and less cohesive river beds and banks (Finlayson and Brizga, 1993; Pollock et al., 2007; Simon and Collison, 2002). In some contexts channel incision can significantly lower local groundwater levels and impact both local and downstream streamflow patterns, influencing riparian and riverine ecology, flood risk, and water supply (Loheide and Gorelick, 2007; Hammersmark et al., 2008; Loheide and Booth, 2011; Ohara et al., 2014; Essaid and Hill, 2014; Hammersmark et al., 2010; Loheide and Gorelick, 2005; Booth and Loheide, 2010; Tomlinson et al., 2011).

Recognition of potential incision impacts has driven efforts to quantify local effects of incision, to actively restore channel forms to less incised states, and to quantify the effectiveness of restoration interventions. While local riparian zone habitat impacts have received significant attention (Booth and Loheide, 2010; Loheide and Booth, 2011; Loheide and Gorelick, 2005, 2007; Schilling et al., 2006; Steiger et al., 2005), more wide-ranging and downstream effects have been less often quantified and are of increasing interest for catchment management. This study therefore uses modeling to explore potential meso-catchment scale impacts of floodplain channel incision and pre-incision, or restoration, scenarios in the Baviaanskloof case-study catchment. Streamflow from the Baviaanskloof supplies water to a regional reservoir that feeds downstream commercial agriculture and urban areas, while local irrigated agriculture primarily relies on the alluvial aquifer. The region is already water stressed and demand is growing, so factors that may impact streamflow and local groundwater are of interest for water supply management (Jansen, 2008).

Recently developed hydraulic and hydrologic modeling methods that include dynamic surface-subsurface flow coupling allow for simulation of the catchment-scale impacts of changing channel forms in their landscape and climatic contexts. To date such modeling methods have been applied to study channel incision impacts in montane meadow sites in snow-melt fed catchments of the western United States, illustrating that the magnitude and, in the case of baseflow, even the direction of change are sensitive to the local aquifer material conductivity, regional groundwater sources, riparian vegetation, and climate

patterns (Hammersmark et al., 2008; Ohara et al., 2014; Essaid and Hill, 2014). Comparable incision impact assessments have not yet been published in other settings. This study aims to further contribute to understanding of potential catchment-scale hydrologic impacts of floodplain incision in different contexts by using coupled surface-subsurface modeling to predict incision effects on a warmer, drier system, with more sporadic rain events, a floodplain dominated by high conductivity coarse material, and deep rooting floodplain vegetation.

Observed channel incision in the Baviaanskloof floodplain, over a meter in the past two decades, is likely driven by direct channel modification for local flood protection, catchment-scale vegetation cover change, and extreme weather events (Powell, 2015, Chapter 3, Chapter 4). River channels deepen when flow velocities through a reach frequently have sufficient energy to transport the bed material and bedload supplies from upstream are not sufficient to compensate (Harvey and Watson, 1986). While this can occur as part of landscape evolution due climate and tectonic shifts, human activities can also drive or hasten the process (Beechie et al., 2008; Comiti et al., 2011; Finlayson and Brizga, 1993; Mark, 2001; Schumm and Hadley, 1957; Surian et al., 2009; Tucker et al., 2006). Changing land cover in ways that result in increased storm runoff intensity, such as increasing catchment impervious area, increasing flows through point sources and upland channelization, and direct channel modifications, such as berm building for flood protection, can all result in incising channels. The resulting channel incision depth will depend on the particle size distribution of the floodplain material compared to the shear stresses of the flow

regime, and deepening can be followed by widening and potentially aggradation, depending on bank cohesion and vegetation, climate patterns, and upstream or up-catchment sediment supplies (Beechie et al., 2008; Langendoen et al., 2009; Simon et al., 2000).

Previous studies have demonstrated that channel incision can alter groundwater and streamflow patterns in various ways at different temporal and spatial scales. Increasing channel capacity in a floodplain can reduce the frequency and extent of overbank flooding, potentially reducing local alluvial aquifer recharge and increasing flood peaks reaching downstream areas (Lach and Wyzga, 2002; Sholtes and Doyle, 2011; Wyzga, 1996). Deepening a channel that receives seepage flow from a floodplain aquifer can result in drawdown of the surrounding water table, the depth and spatial extent of which is determined by the aquifer material and sources of aquifer recharge (Essaid and Hill, 2014; Loheide and Booth, 2011; Lowry et al., 2010; Schilling et al., 2004, 2006). Channel incision can result in increased baseflow (Essaid and Hill, 2014) or decreased baseflow (Ohara et al., 2014) depending on the context. If it does not draw down the surrounding aquifer significantly relative to its recharge sources, channel incision can increase baseflow because of increased connectivity with the aquifer (Essaid and Hill, 2014). However, if the aquifer is not adequately replenished relative to the increased drainage rates, the increased groundwater flow into the deepened channel could draw down the aquifer to a point at which it contributes less or no flow into the channel, eventually decreasing baseflow during prolonged dry periods (Essaid and Hill, 2014; Loheide and Booth, 2011). These results indicate that in some settings there could be potential trade-offs between local flood

protection measures and land management and water supply availability which are worthwhile exploring.

Several observational and modeling studies have explored the magnitudes of these effects in specific locations. Schilling et al. (2004) installed piezometer transects across a silty floodplain with a 3 m incised channel in Walnut Creek, Iowa, finding 1-2 m fluctuations in the groundwater depth within 30 m of the channel related to changes in river water surface levels. Using a model of an archetypal loam alluvial floodplain, Loheide & Booth (2011) similarly predicted a 1 m decline in the average water table over a 100 m riparian area due to 2.4 m channel incision. Tague et al. (2008) observed streamflow and groundwater levels upstream and downstream before and after a restoration project on the Trout Creek, California. They detected an 11-24% increase in summer month baseflow and approximately 0.4 m higher groundwater levels once the channel bed had been raised and sinuousity restored. Hammersmark et al. (2008) calibrated a coupled hydraulic-hydrologic model of the Bear Creek Meadow, California, a montane meadow with a silt loam and sand and gravel aquifer, against observed streamflow and groundwater levels. Using this model to assess the impacts of pond and plug restoration along a channel previously incised by roughly 2 m, they estimated restoration raised the spring average meadow groundwater table by 1.2 m, decreased peak flows by 12-25%, and increased downstream baseflow. Ohara et al. (2014) modeled a similar case of pond and plug restoration for the Last Chance Creek of the Feather River basin, California. Modeling the meadow and inflows from the surrounding

catchment area over 10 year period, they estimated channel restoration can result in a 10-20% increase in dry season baseflow and a 10-20% of decrease in flood peaks.

Essaid and Hill, (2014) modeled impacts of channel incision scenarios on a snow-melt fed montane meadow within the Sagehen watershed, California, using a nine year period of observed climate data. The results for this area differed from the previous meadow studies, demonstrating the context specific nature of channel incision impacts. In the Sagehen model, channel incision was predicted to decrease wet season flow and increase baseflow (Essaid and Hill, 2014), the opposite direction of change to the predictions for Bear Creek (Hammersmark et al., 2008) and Last Chance Creek meadows (Ohara et al., 2014). Consistent with the other studies, Essaid and Hill (2014)'s model predicted that deepening channels by 4 m would draw down the meadow groundwater table by roughly 2 m. However, the extent of the lower groundwater table in the incised scenario for Sagehen allowed for much greater infiltration of incoming hillslope runoff and interflow reaching the meadow margins in the snowmelt season. Overbank flooding from the main channel, which would decrease flood peaks, was not predicted to occur even in the un-incised case. As a result, instead of reducing overbank flooding, the dominant predicted impact of channel incision on wet season patterns in Sagehen was the added infiltration of inputs from surrounding hillslopes on the drier meadow, decreasing both total and peak wet season flow (Essaid and Hill, 2014). In the dry season, in contrast to intermittently flowing channels in Bear Creek meadow (Hammersmark et al., 2008), the modeled Sagehen meadow water table remained above the channel bed, contributing to channel flow, throughout the study period

in all scenarios (Essaid and Hill, 2014). This was due to relatively high and consistent predicted recharge from surrounding mountain bedrock and seasonal hillslope runoff. Modeled dry season baseflow increased with channel depth due to increased aquifer contact and increased water table slope from mountain front to channel. Overall, although predicted incision impacts on local meadow conditions and seasonal streamflow were notable, modeled changes in annual streamflow leaving the Sagehen catchment were relatively small because decreased wet season flow was roughly balanced by increased dry season flow. The maximum modeled change in total annual streamflow was a 3% increase during a dry year (Essaid and Hill, 2014).

The Baviaanskloof floodplain and catchment differs in climate, aquifer properties, vegetation, and resulting flow regime to these meadow systems, and as such the impacts of channel incision on streamflow and groundwater patterns were expected to differ. The Baviaanskloof is a drier system (mean annual precipitation of 270 mm) with a variable rainfall pattern and little defined seasonality. The floodplain alluvium is dominated by sand and cobble layers with high conductivity. As with the montane meadows, observations indicate that the alluvial aquifer is fed by mountain bedrock groundwater and by hillslope surface and interflow (Chapter 1). Unlike the snowmelt fed meadows, there is not a regular seasonal pulse of significant recharge. While streamflow at the catchment outlet is perennial, the upstream floodplain varies in width and in parts of the wide valley reaches the water table falls below the channel during prolonged dry periods. Due to high conductivity alluvium and the variability in recharge events, the floodplain water table fluctuates on the

order of meters over months in response to weather events (Chapter 1), greater variability than seen in the siltier, more regularly and slowly recharged snow-melt meadow systems.

It was hypothesized that a deepened channel would increase baseflow at the Baviaanskloof outlet early in groundwater recession periods following recharge events, due to increased connectivity to the aquifer, but decrease baseflow when a dry period persisted for months to years, due to insufficient recharge to compensate for the incision aquifer drawdown. Such a pattern was suggested for drier systems by Essaid and Hill (2014), based on running their Sagehen model with half of the observed precipitation. In this setting they noted that incision resulted in a gradual year upon year drawdown of the alluvial aquifer as extra channel drainage exceeded the recharge, and hypothesized it would eventually result in declining baseflow, although the nine-year simulation period was too short for this to manifest in the Sagehen catchment. It was hypothesized, given the drier conditions and highly responsive groundwater table, that this condition could develop during multi-year, below-average rainfall periods experienced in the Baviaanskloof.

Channel incision was expected to increase flood peaks at the catchment outlet of the Baviaanskloof, as seen in several of the previous incision studies (Hammersmark et al., 2008; Ohara et al., 2014; Tague et al., 2008). In this catchment, flows from hillslopes and tributaries generally infiltrate into the highly conductive alluvial fans and floodplain, only reaching the main floodplain channel as surface flow during major flood events. In such events, overbank flooding is observed even at current levels of incision. Unlike what can

occur in wet meadows in snowmelt season, periods in which the groundwater table is at the ground surface over large areas of the floodplain, preventing further infiltration of incoming hillslope flow, are rarely observed in the current condition of Baviaanskloof (Chapter 1). Therefore added infiltration of incoming surface flows on a floodplain made drier due to channel incision, predicted to dampen incised scenario peak flow in the Sagehen meadow (Essaid and Hill, 2014), was not predicted to be a significant differentiating factor in the Baviaanskloof given further incision. Instead it was hypothesized that decreased overbank flows due to increased channel capacity would result in an increase in peak flow reaching the catchment outlet.

Channel incision can reduce floodplain evapotranspiration (ET) when the water table falls below the vegetation root depth (Essaid and Hill, 2014). However, it has been observed that over time deeper-rooted, more dryland adapted vegetation can come to dominate riparian areas around incised channels (Hammersmark et al., 2010; Loheide and Booth, 2011; Loheide and Gorelick, 2005, 2007). In the Baviaanskloof, deep rooted *Acacia karroo* trees are currently the dominant canopy species in the savanna type vegetation of the floodplain. These trees can have root depths of up to 40 m (Selaolo, 1998) and it was assumed can consistently withdraw water from the alluvial aquifer in the Baviaanskloof. Incision would likely decrease ET from by ephemeral grasses and herbs, but it is expected the overall impact will be minor. There are small areas of reed dominated wetlands associated with groundwater springs at mountain fronts in the Baviaanskloof and soil profiles provide evidence these once had much greater coverage across the floodplain than at

present (Powell, 2015). It is possible that channel incision water table drawdown is partially responsible for reducing wetland extent and that channel restoration would increase their coverage. It is not clear that ET withdrawals from groundwater-tapping *A. karroo* would be significantly different from herbaceous wetland ET, but would likely be somewhat less due to the greater depth from which water must be drawn in the dryland case. Nevertheless, because it was predicted that incision would reduce overbank flooding and increase peak flows, meaning that more water would leave the catchment more quickly during large events, it is hypothesized that there would be less total AET in the incised case.

These hypotheses were tested by constructing and calibrating a model of the Baviaanskloof catchment area with explicit consideration of the interaction between the floodplain channel and alluvial aquifer (Chapter 1 & 2), and applying different floodplain channel scenarios. Unlike Hammersmark et al., 2008, sufficient observational data on incoming surface and subsurface flows into the floodplain was not available over a wide range of locally experienced climate conditions. As such, the entire contributing catchment was modeled, similar to the approach of Ohara et al., 2014 and Essaid and Hill, 2014. Because of the large scale of the Baviaanskloof catchment (1,234 km^2) and more highly episodic aquifer recharge events, different spatial and temporal scales were employed than in these previous studies. To address the relative paucity of data with which to parameterize meso-scale catchment processes, a coarser spatial resolution model using topographically defined hydrologic response units (HRUs) was used for the mountain and hillslope areas feeding into a finer-resolution finite element gridded model of the floodplain. A similar

strategy was employed by Hipsey et al. (2011) to look at potential impacts of catchment-scale changes on fine-scale processes in floodplain wetlands. Changes due to incision were then assessed using models run with 38 years of observed climate data to capture multiple wet and dry periods during which different response patterns were predicted.

5.2 Methods

5.2.1 Floodplain channel change description

A detailed description of the Baviaanskloof catchment is provided in Chapter 1, Section 1.2.1. The Baviaanskloof area has been used for livestock grazing and cultivated agriculture for over a century, resulting in changes to the both the vegetation cover and the channel network that are likely to have intensified peak flows through the floodplain. Livestock grazing on hillslope areas, which would otherwise support closed canopy subtropical thicket, has resulted in degraded, open canopy vegetation over more than a third of the catchment area (Euston-Brown, 2006; Lechmere-Oertel et al., 2005; Sigwela et al., 2009, Chapter 3). This vegetation cover change was found to decrease soil infiltration and double observed plot-scale storm runoff (van Luijk et al., 2013), and modeling suggests it may have increased floodplain channel peak flows by 56-60% compared to a scenario of intact thicket cover (Chapter 3).

In response to widespread flood damages in the 1970s and 1980s, the South African government actively promoted and subsidized flood protection measures (Jansen, 2008). In the Baviaanskloof this took the form of earthworks to reorient channels and build berms, both on the alluvial fans and the floodplain. The extent of channel alteration was assessed using aerial photography from 1954, 1972, 1986, and 2009 (Figure 5-1). Evidence of agricultural land use was observed on 42 of the 62 alluvial fans and on 25 fans channel modification and a channel connection to the main floodplain channel were evident (Chapter 4). Previous modeling suggested that this increased channel connectivity between mountain tributaries and the trunk stream could have increased peak flows in the range of 11-17% beyond flow expected given more dispersive flow paths on alluvial fans (Chapter 4). In addition, in several locations the main channel was straightened and berm building and infilling were used to confine flows from a braided multi-channel path into a single channel (Figure 5-1). Across the catchments' largest wide floodplain reach (19.8 km long, 1 km wide), a multiple channel form was observed in 1954 imagery with 34 km of channel and what appeared to be multiple flood-outs. In 2009 a single 23.6 km channel was mapped crossing this reach.

Channel incision of up to 2 m was observed in several floodplain reaches, likely as a result of extreme weather events and multiple human activities enhancing peak flows (Powell, 2015). Incision in the past 40 years was observable in abandonment of formerly river-fed furrows, active in the 1970s, which in 2012 had intakes a meter above the bankfull channel. Channel cross-sections surveyed in 2011-2012 along 25 km of a wide floodplain

reach generally showed an inset bankfull channel within a wider channel creating stepped terraces (Figure 5-2, (Powell, 2015)) typical of deepening and widening cycles during incision (Beechie et al., 2008; Schumm and Parker, 1973; Shepherd and Schumm, 1974; Simon and Rinaldi, 2006). Average dimensions of the inset channel were 21 m across and 1.1 m deep, while the wider channel had an average top-width of 48 m and 0.5 m banks, giving a total average depth of 1.6 m below the floodplain surface. Soil pit transects and cut-bank profiles showed a 0.5-1.5 m thick layer of loamy sand/sandy loam overlying a cobble dominated layer spanning the floodplain (Chapter 1). The current channel has incised into this cobble layer and, given the cross section shape and more erodible bank material, has likely also widened compared to a pre-settlement condition. Active headcuts observed in the cobble bed (Figure 5-3) indicate further incision may be possible through this more resistant material in the current flow regime.

Figure 5-1 Aerial photograph time series of a wide floodplain reach in the Baviaanskloof demonstrating change in the floodplain and river channel from 1954 to 2009 in response to floods events, agricultural field establishment, and berm building and direct channel modification.

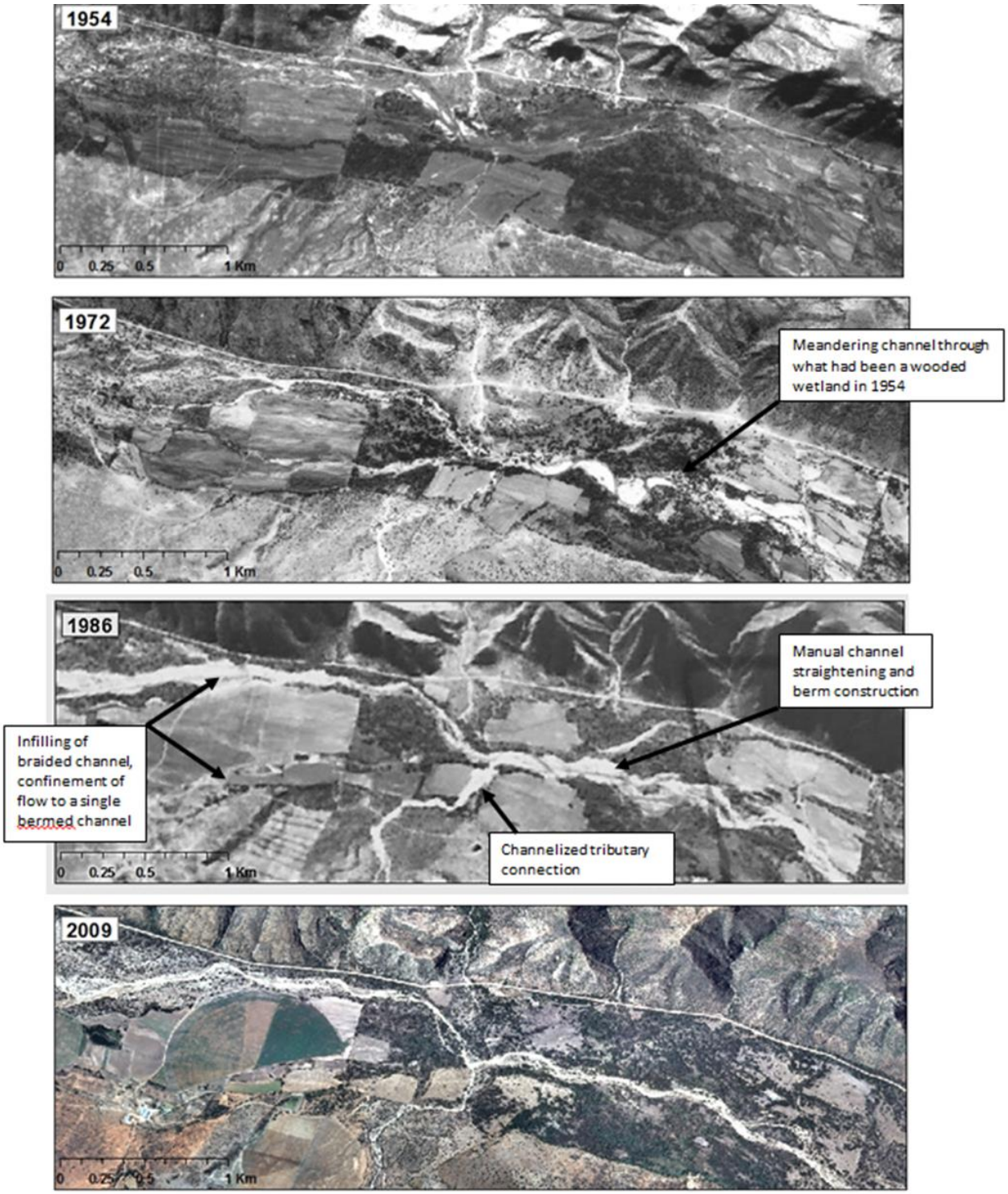

Figure 5-2 Map of a wide floodplain reach in the Baviaanskloof catchment showing channel survey points were thalweg elevation and channel dimensions were measured and points where more detailed cross sections were surveyed (Powell 2015).

Examples of surveyed floodplain topography cross sections (plotted north to south) are shown for marked locations A and B in figures below. These illustrate the incised inset channel within the active channel and abandoned former channels, irrigation furrows (often dug following former channels), and man-made berms on the floodplain.

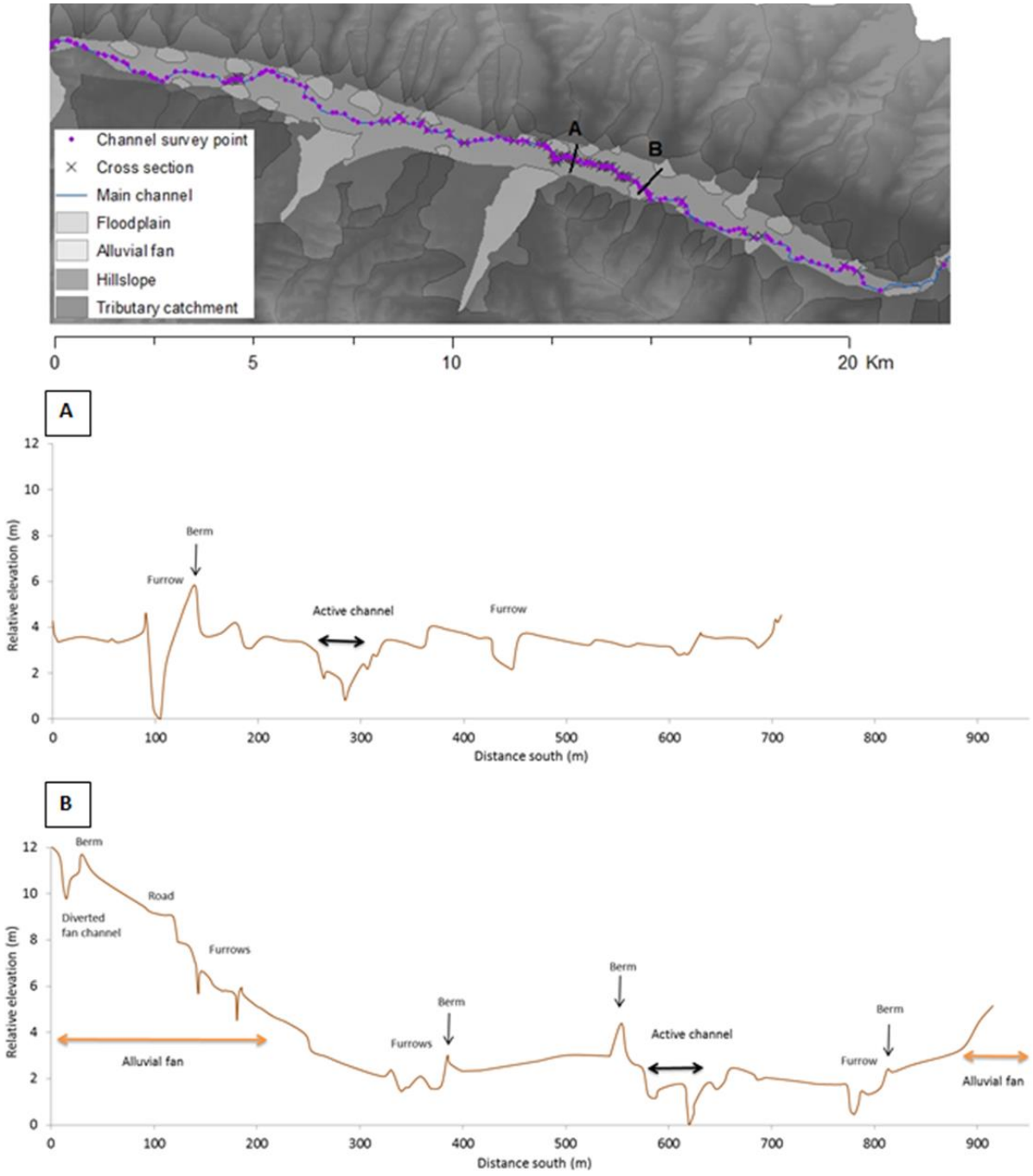

Figure 5-3 Photographs taken during channel topographic surveys in a wide floodplain reach of the Baviaanskloof catchment during a dry period in 2011.

The image on the left shows a cut bank with layers of loamy sand and sandy loam overlying a layer dominated by cobble into which the current channel has incised. The image on the right shows an active head-cut inset within the larger channel reaching the floodplain water table.

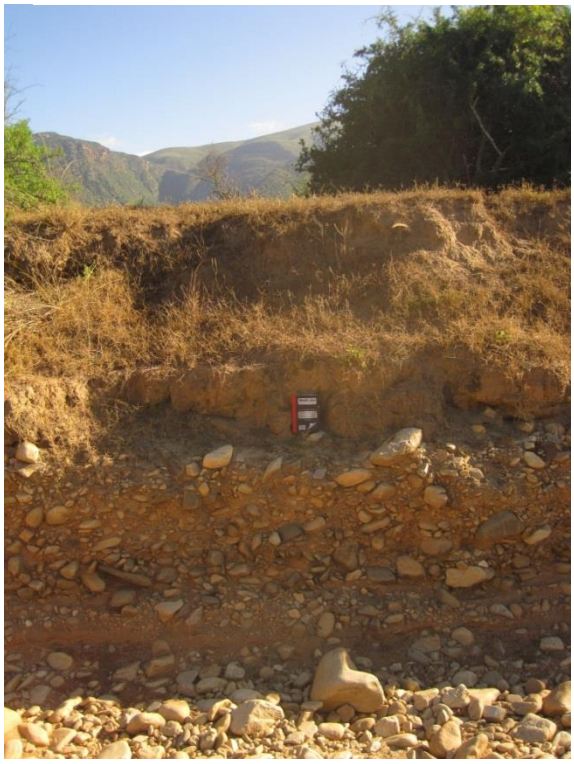

5.2.2 Scenario modeling

Potential impacts of floodplain channel incision on streamflow and floodplain aquifer levels in the Baviaanskloof were estimated using several generalized channel form scenarios applied within a calibrated model of the floodplain and contributing catchment. In addition to the observed current channel state, three alternative channel scenarios were considered: a hypothetical restoration scenario with a smaller, shallower channel; a 1 m further incision scenario; and an extreme 3 m further incision scenario. A basic description of the model structure and performance is given below while detailed descriptions of the model construction and calibration are given in Chapter 2.

Defining an achievable and desirable restored channel form will require further geomorphic, hydraulic, and ecological analyses and stakeholder engagement beyond the scope of this exploratory modeling study. The restoration scenario applied here was used to look at the impacts of a shallower channel thalweg and smaller channel capacity, as is it appears such a condition once existed. The current average channel thalweg depth below the floodplain surface was 1.6 m. In the restored scenario, the dimensions of the current inset bankfull channel were applied such that thalweg depth was 1 m, which is similar to the average depth of the cobble-dominated layer in the floodplain. In the first further incision scenario it was assumed the channel could incise an additional meter from its current state, such that the average depth was 2.5 m. The second, more extreme incision scenario, an additional 3 m of incision was assumed producing a 4.5 m deep channel. Given the coarse bed material and infrequent high flows, this depth of incision was considered unlikely in the

Baviaanskloof floodplain without major further changes to land cover, channel engineering, and/or climate; however it was applied to explore any potential change in patterns of the response to incision given more extreme drainage of the floodplain similar to the 4 m incision scenario of applied in the Sagehen meadow model of Essaid and Hill (2014). These four scenarios will be further referred to by the depth of the channel thalweg below the floodplain surface: 1 m for the restored scenario, 1.5 m for the current state scenario, 2.5 m for the 1 m further incision scenario, and 4.5 m for the 3 m further incision scenario.

A multi-scale, daily time-step model of the Baviaanskloof catchment was constructed and calibrated using the MIKE-SHE/MIKE-11 modeling system (Refsgaard and Storm, 1995), based on a conceptual model informed by field observations of surface and groundwater flows, soil and vegetation properties, and topography (Chapter 1). In order to consider both the finer-scale floodplain processes governing the impacts channel incision would have on the aquifer-channel interaction as well as the processes occurring over the large catchment area that contribute variable surface and subsurface inflows to the floodplain, the floodplain and its contributing catchment were modeled at different scales. A coarser spatial scale and process conceptualization were applied in modeling the mountain areas to estimate time-series of incoming flows which were input into a higher resolution model of the floodplain. Within the subcatchments, canopy interception, infiltration, soil moisture storage, actual evapotranspiration (AET), vertical percolation, and surface runoff routing were calculated at the level of topographically defined hydrologic response units (HRUs). Surface flow reaching the subcatchment outlet was input to the floodplain model at

the head of the alluvial fan. Hillslope interflow and mountain bedrock groundwater flows were modeled as lumped linear reservoirs at the sub-catchment scale, receiving percolated water from all topographic units and discharging to the floodplain aquifer boundary. Groundwater flow through the alluvial aquifer was modeled using a finite element grid governed by Darcy's Law, with a dynamic connection to the channel network. On the fans and floodplain, canopy interception, infiltration, surface runoff routing, soil moisture storage, AET, and percolation to the water table were calculated by grid cell.

The gridded surface and subsurface model of the fan and floodplain area had a 50 m resolution using sink filled, smoothed SRTM data for the model surface topography. In the finite element groundwater model a smooth bottom depth profile was assumed with an average depth of 20m under the central floodplain grading to 5m at the mountain front, based on resistivity data by (Soltau et al., 2011). The topography of the bedrock below the alluvium may not be regular and may be deeper than 20 m, however it was assumed that the floodplain groundwater table is relatively smooth, permanently above the bedrock interface, and remained above 20 m depth throughout the simulated period. This last assumption is supported by 15 m deep farm water supply boreholes in the alluvium that have never run dry in living memory (Chapter 1).

Channel flow was modeled in a coupled hydraulic model using a diffusive wave approximation. Two-way exchange of water between the aquifer and channel was governed by relative water surface elevation and bed material conductivity. Overbank flows were

added into the gridded surface flow routing routine such that this water could infiltrate into the alluvium, evaporate, or flow downslope, potentially re-entering the channel further downvalley. The channel network was mapped using aerial photography, while the channel cross sections for the different scenarios were based on field topographic survey (Powell, 2015). Alluvial fan channel cross sections were generalized based on surveys of sample fans (Chapter 4, Bobbins, 2011). Surface flow from every tributary subcatchment was routed to a channel that connects to the main river channel in the floodplain. For subcatchments feeding onto alluvial fans currently channelized and connected to the main river, this connecting channel was given the average observed fan channel dimensions on modified fans in the catchment: 11m width, 1m depth, trapezoidal. For those with fans that were not obviously channelized, the model fan channel dimensions decreased to a negligible size (2m width, 0.2m depth) by the toe of the fan such that the majority of the flood flow would exceed channel dimensions and be added to the surface flow routing in the model.

This model was calibrated using a multi-criteria procedure against multiple datasets of surface flows and groundwater levels (Chapter 2). The resulting model and accepted parameter space reproduced 2012-2013 daily streamflow with a Nash-Sutcliffe efficiency (NSE) of 0.87-0.92 and 1991-2013 monthly flows with an NSE of 0.79-0.85, predicted mean flow within 0.5 m^3/s and maximum monthly flows within 1 m^3/s of the observed, and modeled floodplain groundwater fluctuations with an R^2 of 0.79-0.81 and an accuracy in the range of depth fluctuation within 0.5 m against the observations (Chapter 2). Accepted models had errors in average annual yield of 3-20%, with a mean of 12%.

To account for the uncertainty in the parameterization, the model was run 100 times for each scenario to represent the calibrated parameter space. Parameter sets were selected from the 720 sets in the calibration exercise with acceptable model performance in recreating observed surface runoff, streamflow, and groundwater patterns as described in Chapter 2. The same 100 parameter sets were applied in each channel scenario, such that the channel network was the only factor differing between them. These sets of runs resulted in likely output distributions for each scenario, allowing for conservative change detection. In order to capture the response to a variety of storm sizes and antecedent conditions, the model of each scenario was run using 43 years of climate data from 1970-2012, using gauge data applied as described in Chapter 2, Section 2.2. The first 5 years (1970-1974) were considered a spin-up period for groundwater levels and change analyses were done for model output for the 1975-2012 water years. The water year was defined as April to March.

5.2.3 Output analyses

For the set of model runs for each channel scenario, the mean and 95 percent confidence intervals of the following statistics were calculated: average annual water yield, average annual minimum monthly flow, average daily flow for the fourteen largest flow peaks in the period (annual exceedance probability of 10%), and average depth to groundwater in the floodplain aquifer (spatially averaged). These statistics were chosen to assess the scale of impacts relevant to water supply and flood management. To assess changes in the flow path

of water through the floodplain due to channel incision, modeled patterns of infiltration on the floodplain, recharge to the alluvial aquifer, floodplain AET, flow from the alluvial aquifer into the main floodplain channel, and overbank flooding from the main channel were compared between the channel scenarios. Within the modeled time period, multi-year dry and wet periods were identified, as described in Chapter 3, Section 3.2.3, to compare the effects of fan channelization under different conditions. The statistics described above were also calculated separately for these periods.

5.3 Results

5.3.1 Effects on catchment scale water yield and streamflow

Channel incision in the Baviaanskloof floodplain was predicted to increase the average annual catchment water yield for the modeled period. The 2.5 m channel scenario was estimated to increase the average annual yield by 3-7 Mm^3 (8-24%, p=0.009), associated with a decrease in AET from the floodplain and an increase in net alluvial aquifer input to the river compared to with the current (1.5 m) channel (Table 5-1). There was a trend of increasing predicted average annual yield with increasing incision over the scenarios considered, however differences in modeled average yields between the restored (1 m) channel (27-29 Mm^3) and current (1.5 m) channel scenarios (28-31 Mm^3) and between the two further incision scenarios, 2.5 m channel (33-35 Mm^3) and 4.5 m channel (35-37 Mm^3),

were not statistically significant. The predicted decrease in average central valley AET with increased channel incision, linked to the changes in average yield, was attributable to both the reduction in floodplain inundation, and hence surface water evaporation, and to the lowered water table, both described further in Sections 3.2 and 3.3 below. It had been assumed that the 20 m rooting depth of the floodplain and fan vegetation applied in the model would mean that rarely was vegetation highly water limited in any scenario. However, there were higher elevation areas on the alluvial fans and floodplain margins where the water table depth was close to the 20 m root depth and fell below this more frequently in the incised scenarios.

Although the average annual streamflow for the 38-years modeled was predicted to increase with incision, there were periods during which the restored (1 m) channel scenario was predicted to have the highest streamflow of the four scenarios (Figures 5-4 to 5-7). Modeled streamflow peaks were consistently higher in the more incised scenarios, but results suggested recession period flows following large events could be higher in the restored scenario. The 2.5 m channel was predicted to increase flow for the largest peaks by 22-32% (14-19 m^3/s) compared to the current 1.5 m scenario, while restoration of a shallower channel with lower capacity was predicted to decrease peaks by 14-20% (9-13 m^3/s). During recession periods following major storm peaks, generally after events large enough to produce a daily mean flow of 20 m^3/s or more, the model predicted higher streamflow values for the restored (1 m) channel scenario compared to those with more incised channels over periods of 10 days up to 3 weeks. After this period, baseflow in the

restored channel scenario was predicted to fall below that predicted for the more incised scenarios. This pattern is evident in daily hydrographs of a typical dry and wet year (Figure 5-4), and is reflected in the distribution of modeled daily flow values over the modeled period (Figure 5-5). Because these larger flow events were relatively infrequent the restored scenario had higher modeled flows than the more incised scenarios for daily flows with exceedance probabilities of 1-3% (Figure 5-5) and annual yields were generally lower in the restored scenario.

Differences in mean modeled yields for individual water years were not statistically significant; however, there were years for which the mean of the modeled annual yield for the restored scenario runs was slightly larger than means for the more incised scenarios (Figure 5-6). This occurred for the 1979, 1981, and 2012 water years. These were wet years for which the previous year also had above average rainfall (Figure 5-3). Higher restored scenario means were not predicted for high rainfall years with low rainfall in the preceding year, such as 1985, 1996, and 2006. The 1980 water year, which had above average rainfall and was preceded by wet years, also did not have a higher mean modeled yield for the restored scenario. Unlike 1979, 1981, and 2012, the 1980 water year had the majority of its rainfall occurring in summer months (Chapter 3, Figure 3-4), when event runoff ratios were typically low due to drier soils (Chapter 1). As described further in Section 5.3.3 below, in prolonged wet periods, the model predicted near surface saturation over more floodplain area in the restored scenario than with more incised channels, which increased the catchment's runoff ratio during storm events.

In dry periods models predicted greater flows in the more incised scenarios (Figures 5-4 to 5-6). The average annual minimum monthly flow for the 38 year period was 0.05-0.07 m^3/s (47-71%) greater for the 2.5 m channel scenario compared to the 1.5 m scenario ($p=0.001$). The predicted average annual minimum monthly flow for the restored (1 m) channel scenario was also slightly larger than the current (1.5 m) channel scenario, greater by 0.01 m^3/s (10%), although the difference was not statistically significant ($p=0.06$). As shown in the daily flow distribution curve for the model output time series (Figure 5-5), the scenarios of further channel incision (2.5 m and 4.5 m channels) were predicted to have higher flows than the 1.5 m channel current scenario over most of the period, while the restored scenario showed less notable differences from the current scenario for daily flow ranges with a 30% or greater probability of exceedance.

Table 5-1 Long term (1975-2012) average annual water balances for the Baviaanskloof catchment and internally modeled land units under different floodplain channel scenarios

Location / spatial scale	*Flux*	Annual volume (Mm^3/ year)							
		Incised 3m *(average depth: 4.5m)*		**Incised 1m** *(average depth: 2.5m)*		**Current** *(average depth: 1.5m)*		**Restored** *(average depth: 1m)*	
		Mean	***95% CI***	**Mean**	***95% CI***	**Mean**	***95% CI***	**Mean**	***95% CI***
Catchment	***Precipitation***	323		323		323		323	
	AET	283	*1.2*	286	*1.1*	289	*1.4*	292	*1.3*
	Streamflow	36	*1.0*	34	*1.0*	29	*1.1*	28	*0.9*
Mountain tributary sub-catchments	***Precipitation***	307		307		307		307	
	AET	260	*1.2*	260	*1.2*	260	*1.2*	260	*1.2*
	Overland flow to fan head	5	*0.1*	5	*0.1*	5	*0.1*	5	*0.1*
	Interflow to floodplain	29	*0.9*	29	*0.9*	29	*0.9*	29	*0.9*
	Mountain bedrock outflow	9	*0.6*	9	*0.6*	9	*0.6*	9	*0.6*
Central valley alluvial fill (fans and floodplain)	***Precipitation***	16		16		16		16	
	AET	23	*0.1*	26	*0.2*	29	*0.2*	32	*0.2*
	Alluvial aquifer input to channel (net)	33	*2.4*	31	*1.1*	26	*1.5*	18	*3.0*
	Overland flow inputs to channel	2.7	*0.2*	3.0	*0.2*	3.6	*0.7*	10	*0.5*

Figure 5-4 Modeled daily flow hydrographs for demonstration dry (1990, top) and wet (2011, bottom) years showing differences in flow peaks and recessions between floodplain channel scenarios

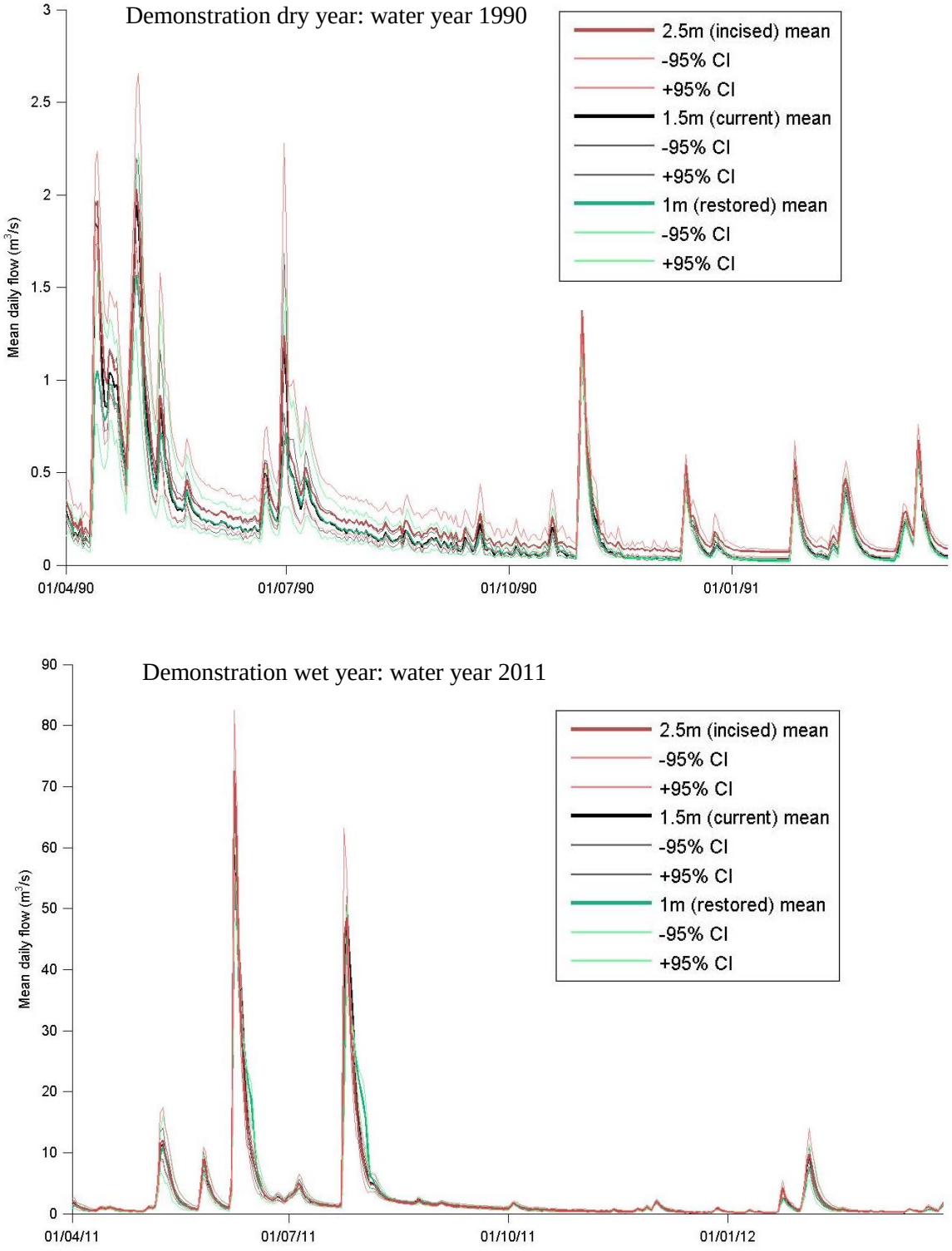

Figure 5-5 Daily flow duration curve for different floodplain channel scenarios showing the distribution of daily flow values modeled for the period 1975-2012

Inset graph has expanded the x-axis for greater visibility of the low frequency, high flow value portion of the curve, values with an exceedance probability of 5% or less.

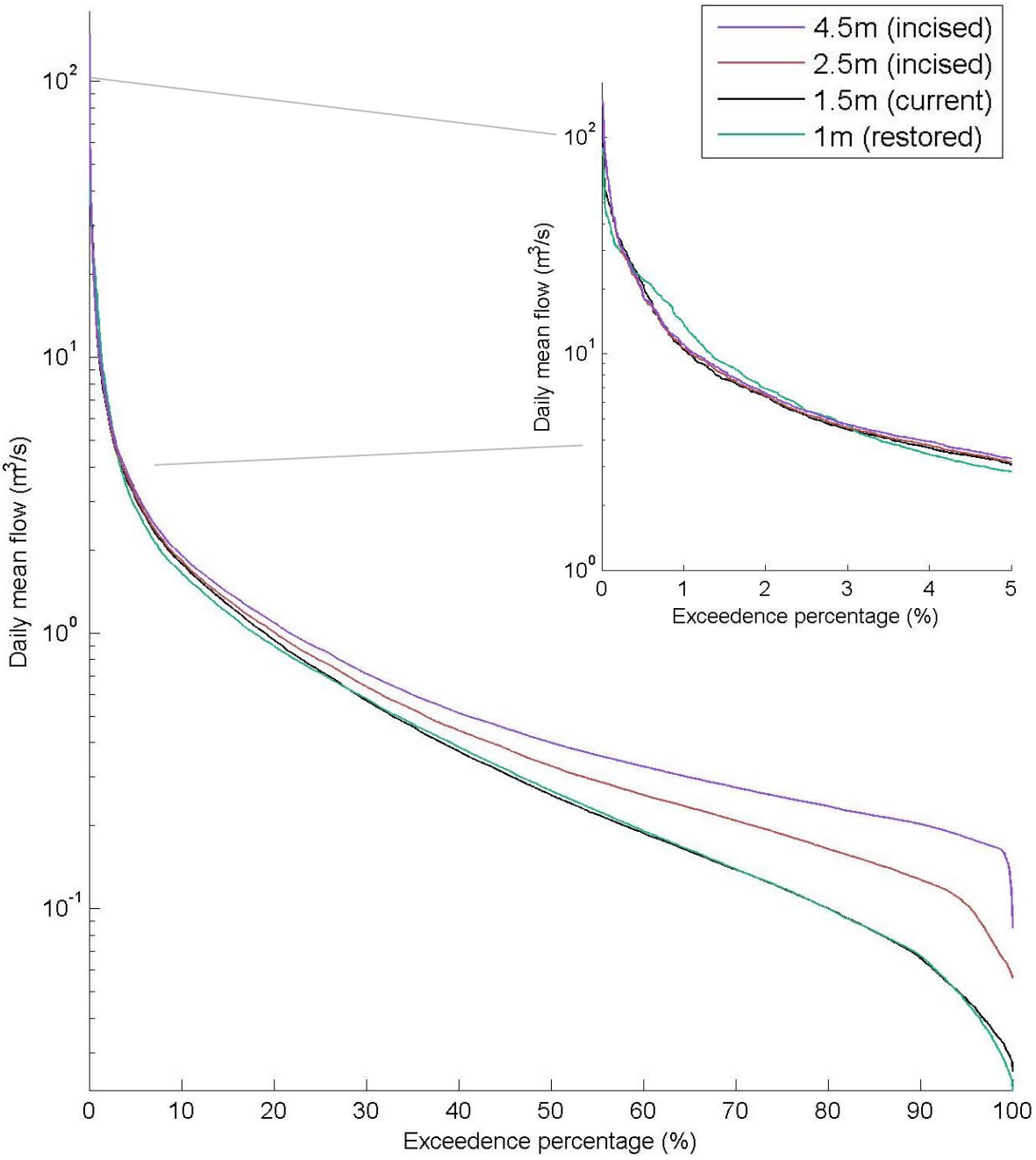

Figure 5-6 Modeled catchment water yield (total streamflow output) by water year for 1975-2012 for floodplain channel scenarios of the current state, a restored shallow channel, and further incision by 1m (top) and by 3m (bottom).

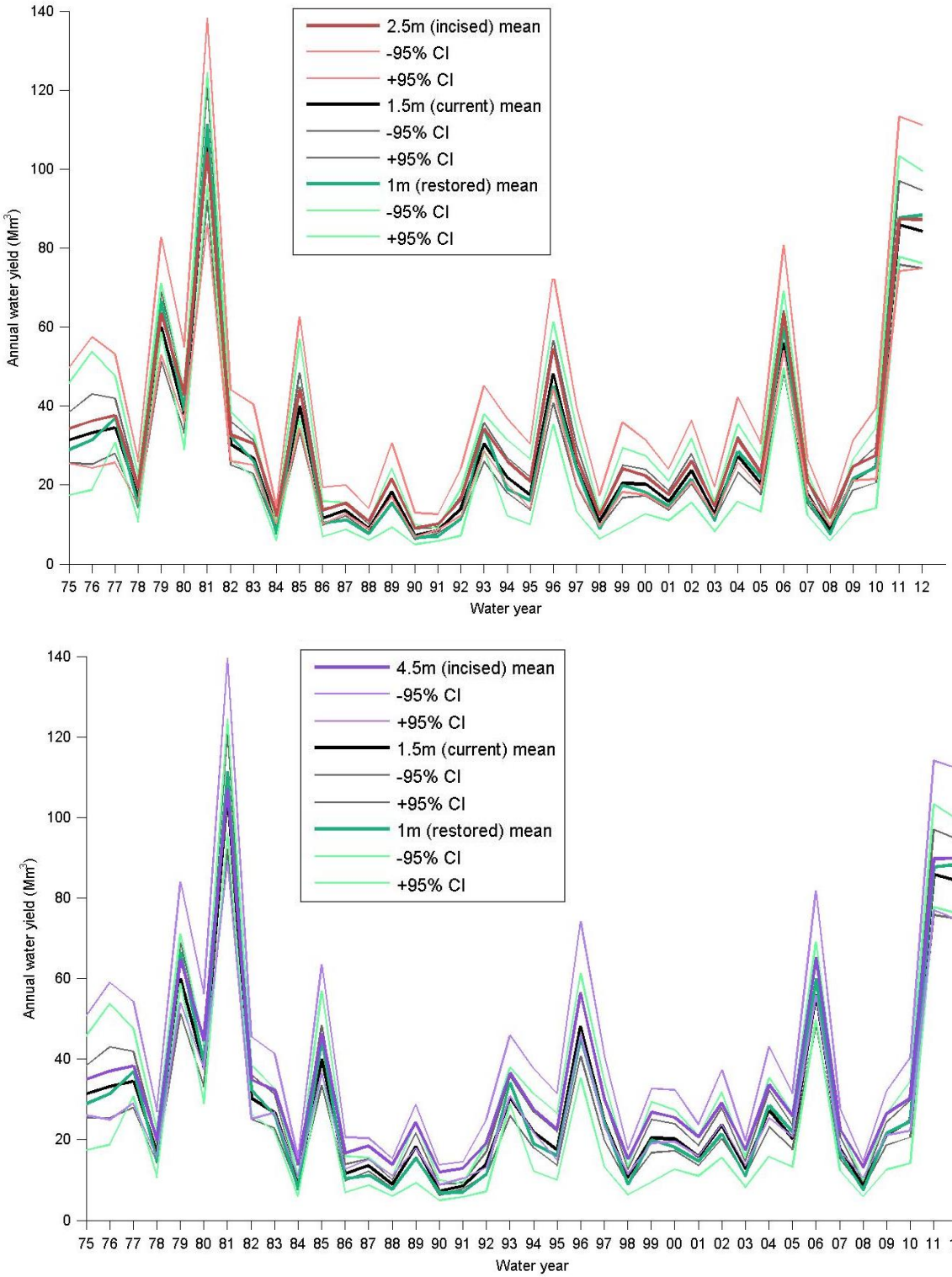

Comparing the predicted streamflow patterns for the more extreme incision scenario, the 4.5 m channel, to those predicted with a 2.5 m channel, higher baseflows were predicted with no significant increase in modeled peak flow given the greater incision (Figure 5-5). The mean annual minimum monthly flow at the catchment outlet was predicted to double with the 4.5 m channel compared to that of the current channel scenario, increasing by 0.11-0.14 m^3/s (99-134%). In the 2.5 m channel scenario there was no indication of a declining difference in baseflow between incised and less incised cases with drier conditions (Figure 5-5). Such a decline would have been indicative of periods when additional aquifer drainage due to incision came close to, or exceeded, floodplain recharge, causing progressively increasing aquifer drawdown and decreasing connectivity between the aquifer and channel. This pattern was apparent with the 4.5 m deep channel, seen as a sharpened decline in low flow values at the tail end of the daily flow distribution (Figure 5-5). This was only predicted to occur in extreme dry periods that were relatively rare in the 38 years modeled, when daily flows were so low that there was a 97% probability of exceedance. Despite the increase in baseflow with the 4.5 m channel, there were still high rainfall years and recession periods following large flow peaks during which the restored (1 m) channel scenario had the highest mean modeled yields, although differences were smaller than with the 2.5 m channel (Figures 5-5 and 5-6). Mean yields for individual years were not statistically different between scenarios.

5.3.2 Effects on floodplain groundwater depth

Increasing the depth of the main river channel compared to the current scenario was predicted to have a net draining effect on the floodplain alluvial aquifer: 1 m of further incision (2.5 m channel) resulted in a modeled 0.9-1.0 m increase in depth of the spatially and temporally averaged water table, and 3 m of further incision (4.5 m channel) resulted in a modeled 2.3-2.5 m increase (Figures 5-7 and 5-8). Modeled ongoing alluvial aquifer recharge at the mountain front meant that the average water table was lowered by less than the incision depth despite the high conductivity of the aquifer material. In the restoration scenario, the shallower, lower capacity, 1 m deep channel was predicted to result in a 0.6-0.7 m rise in the water table over the current scenario, slightly more than the 0.5 m rise in the thalweg.

Differences in modeled average groundwater depths between scenarios were statistically significant for individual water years, and the ranking of depths between the scenarios remained consistent throughout the modeled period. However, greater incision resulted in less fluctuation in groundwater levels between wet and dry years (Figure 5-7), such that the differences between scenarios were greater in the selected wet years than in the selected dry years (Figure 5-8). This is indicative of more modeled aquifer recharge during large rainfall events in the restored scenario when compared to the incised scenarios. This was accounted for by large increases in overbank flooding in the restored channel scenario, described further in Section 3.3 below. The estimated rates of subsurface recharge of the alluvial aquifer from the surrounding mountain areas in the model meant that a relatively constant,

albeit deeper, water table was maintained in the incision scenarios, despite the almost complete loss of overbank flooding as a periodic recharge source. Due to the interannual variability in rainfall and recharge, and the high conductivity of the alluvium, modeled floodplain average water table depths for different water years fluctuated by as much as 2 m over 1975-2012 in the current and restored channel scenarios.

Modeled water table depths varied spatially over the floodplain. In all the channel scenarios the modeled water table remained high enough for the aquifer to consistently feed channel flow in certain locations throughout the 38 years. Constantly gaining river reaches in the models occurred particularly in more downstream areas and where the valley floor between mountain fronts narrowed, consistent with field observations of perennial streamflow at such locations (Chapter 1). Because of the geomorphology and topography of the catchment, and estimated rates of aquifer recharge at mountain fronts, the additional drainage due to incision was not predicted to result in eventual dry period disconnection between the aquifer and channel in the considered scenarios and weather patterns. As evident in the baseflow results described above, net aquifer to channel flow contribution was predicted to change both with channel depth and between wet and dry periods. The overall shallower groundwater table in the restored scenario also resulted in slightly higher floodplain AET and notable changes in surface flows on the floodplain as described further below.

Figure 5-7 Modeled floodplain average groundwater depth in the central floodplain by water year for 1975-2012 for scenarios of the current state, restored, and further incision of the floodplain channel.

Means and confidence intervals of the simulations sets run within the parameter ranges considered are shown

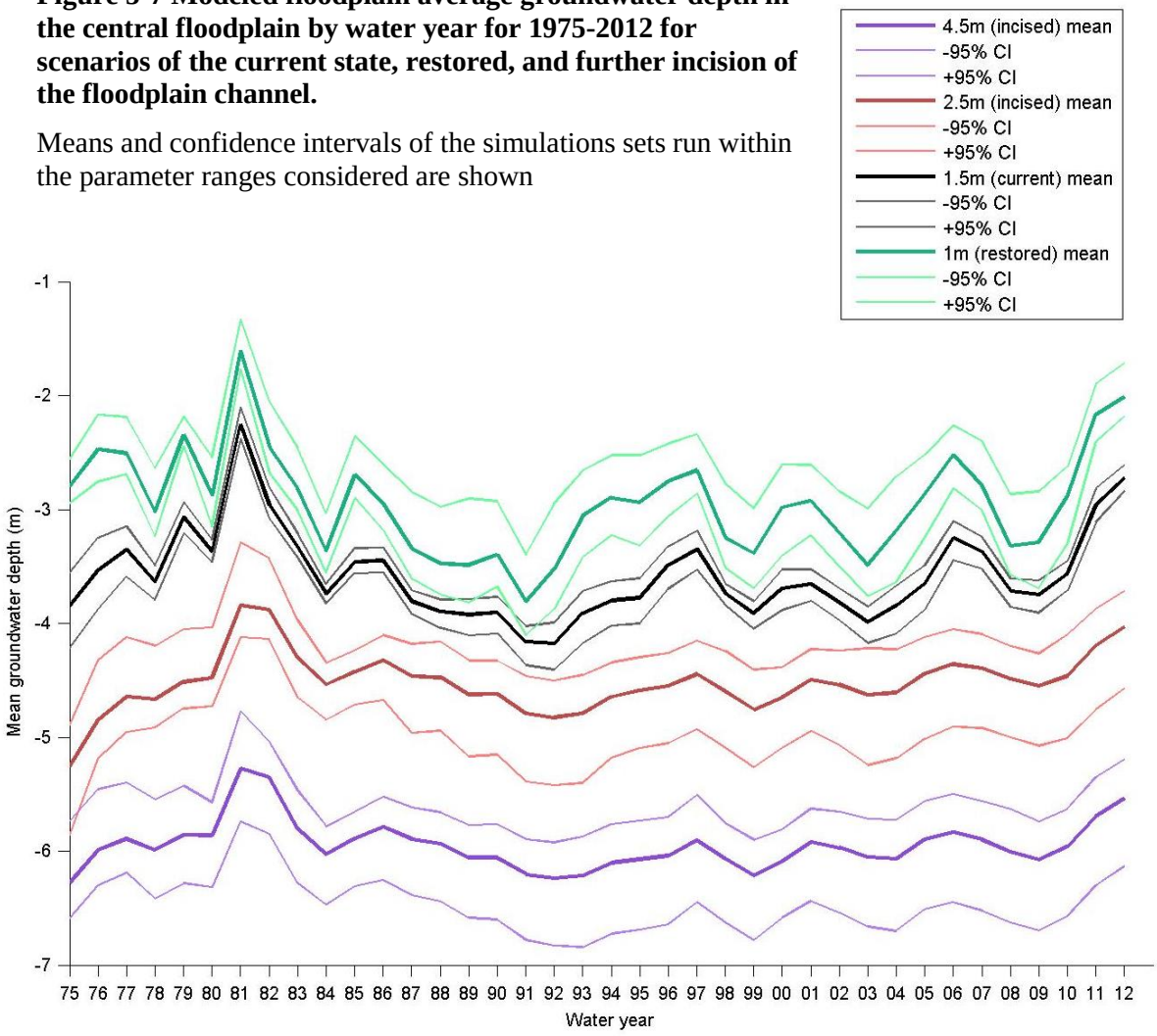

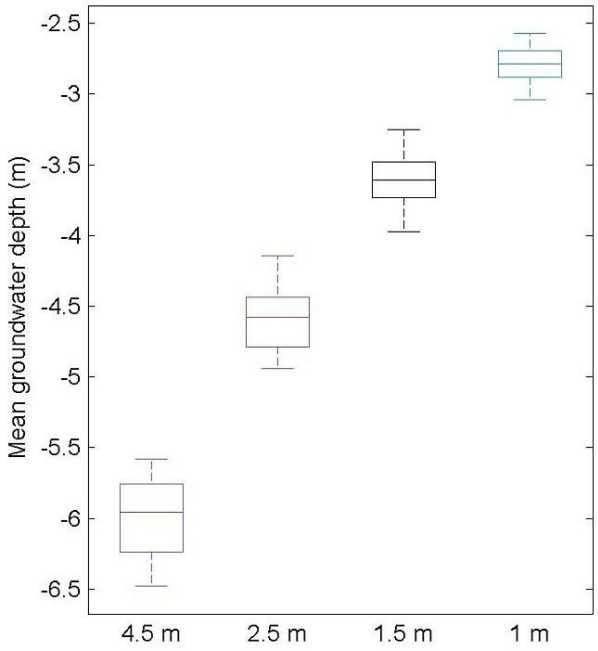

Figure 5-8 Boxplots showing the distributions of modeled mean annual and seasonal floodplain groundwater depth for different floodplain channel scenarios, labelled by depth: all simulated years (left), selected dry and wet years (right)

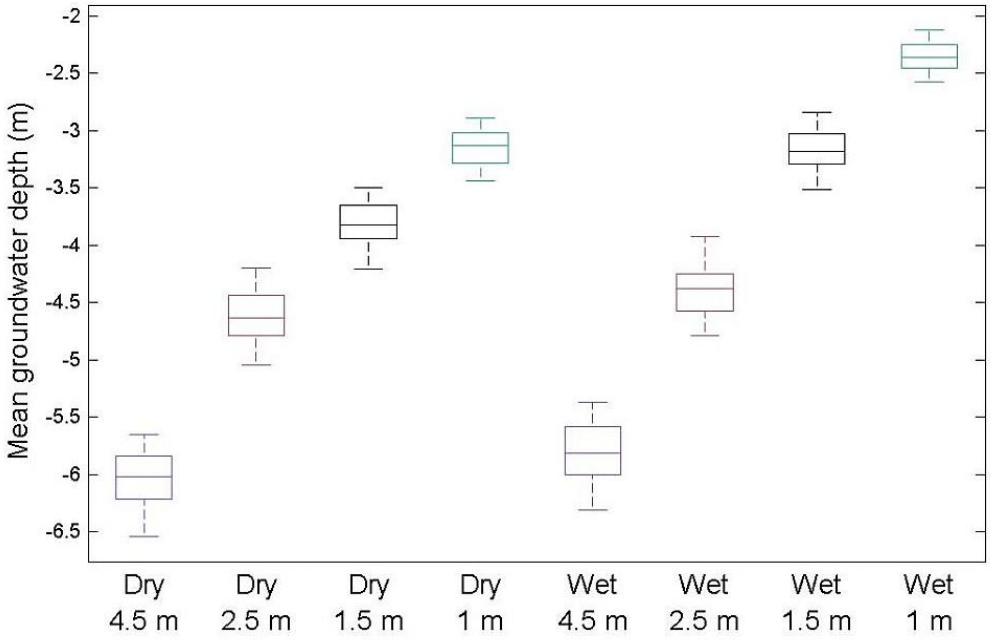

5.3.3 Effects on surface and subsurface flow through the floodplain

Modeling results indicated how floodplain channel incision in the Baviaanskloof is likely impacting various surface and subsurface flow paths in the floodplain, producing streamflow and groundwater changes described above. The channel scenarios applied in this study resulted in large differences in the extent and frequency of modeled overbank flooding (Figure 5-9 b&c). Given the current channel form scenario, overbank flooding was predicted to occur in 20 of the 38 years modeled. In these wetter years generally 20-40 ha of the floodplain would be inundated in two or three events per year, after which surface water would recede completely within 1-2 weeks. Following the largest flow event on record, 25/03/1981, simulation results predicted 100-130 ha would have been inundated at the peak with 3 weeks needed for the surface water to recede completely. The modeled average flooded area for 1975-2012 with the current channel scenario was 0.50-0.55 ha. In contrast, for the restoration scenario, with a smaller channel that was 0.5 m shallower, floodplain inundation was predicted to occur to some degree in every year modeled. Events inundating 20-60 ha were predicted to occur 5-10 times in most years and recession periods were longer, such that in wet years areas of 5-20 ha could remain inundated for months. As such, the average inundated area predicted in the restored channel scenario was 8.8-9.7 ha. The modeled inundation peak in March 1981 was 130-160 ha in this scenario and, due to multiple smaller events following, the floodplain surface was not predicted to dry out completely for 9 months. By comparison, the 2.5 m channel scenario was predicted to only have overbank flooding in 7 of the 38 years considered, in events typically inundating 1-2 ha for 2-3 days. The range of predicted inundated area for the 1981 maximum was 2-29 ha in

this scenario. With the 4.5 m channel model the maximum event inundated area was predicted to be 1-3 ha in 1981, while other major events were predicted to result in less than 1 ha of inundation only lasting for a day.

Both the differences in channel capacity and the differences in modeled floodplain groundwater levels between scenarios were responsible for the predicted differences in inundation with incision. The shallower groundwater table predicted in the current and restored scenarios resulted in larger areas of the floodplain where the water table was near the surface compared to the more incised scenarios. This resulted in larger areas of surface saturation developing at low points in the floodplain topography more frequently during high rainfall events. Even during events that did not result in overbank flooding, saturation excess surface flows were produced in riparian areas and low points in the floodplain in the restored scenario, some of which fed channel flows. This also meant that inundation in the restored scenario, both from saturation excess and from overbank flooding, was predicted to persist for longer as there was less capacity for infiltration compared to the drier floodplain soils modeled in the incised scenarios. Evaporation from surface water was partially responsible for the higher floodplain ET predicted in the restored scenario (Table 5-1).

The decreases in peak flows and the short-term increases in recession period flows following large events that were predicted for the restored (1 m) channel scenario were attributable to this increased overbank flooding. Overbank flooding meant that flow down the valley length was slowed due to greater roughness and more of the surface water was

lost to infiltration and ET compared to channelized flows. Overbank flows were negligible in both the 2.5 m and 4.5 m channel scenarios. These scenarios had similar peak flows to one another despite a large difference in channel size. The predicted increase in delayed flow in the restored channel scenario during the weeks following a major flow event occurred as infiltrated overbank flood water recharged the floodplain aquifer, increasing subsequent inputs from the aquifer to the river channel. This was not predicted to occur following smaller events and in drier periods when there was less substantial overbank flooding, less input from direct rainfall and from the mountain areas, a lower antecedent water table relative to the channel, and drier soils meaning less net recharge.

Differences in predicted central valley infiltration and recharge between the scenarios varied over the range of wet and dry conditions modeled. The restored scenario had the highest annual recharge only in some of the wet years (Figure 5-9). This reflected different annual balances between the increased opportunity for infiltration and recharge in the restored scenario, due to increased overbank flooding, and the decreased capacity for infiltration in the restored scenario, due to the shallower water table and hence wetter floodplain. Large rainfall events were predicted to result in alluvial aquifer recharge from multiple sources: direct subsurface inputs along the mountain fronts as well as infiltration and percolation of effective rainfall, channel flows, overbank flows, and incoming surface flows from the mountain areas. Channel incision did not affect the subsurface inputs from the mountain areas in the model. Incision did greatly reduce predicted overbank flooding (Figure 5-9 b&c). This resulted in less modeled total valley infiltration and recharge during

very large events (Figure 5-9d), accounting for lower predicted wet year totals with the 2.5 m channel than with the 1 m channel (Figure 5-9e). In the restored (1 m) scenario, the higher average groundwater table resulted in more floodplain area more frequently developing saturated soils near the surface in the model. This limited infiltration of rainfall, of incoming surface flows, and of overbank flood water on lower lying areas when rainfall events occurred with wet antecedent conditions. In contrast, the drier floodplain predicted for the incised scenarios promoted infiltration and, in large enough events, percolation. As such, more total valley infiltration was predicted for the incised scenarios in periods when rainfall events were smaller and did not cause significant overbank flooding differences between scenarios. When multiple events or relatively wet years occurred in succession without very large overbank flood differences, the developing wet antecedent conditions could result in decreased overall alluvial aquifer recharge in the restored case compared to the incised case (e.g. 1993 vs. 1994 in Figure 5-9c). The overall pattern of rainfall events in 1975-2012 meant that the long-term average recharge from surface sources in the restored (1 m) channel scenario and the further incision (2.5 m) scenario were predicted to be almost the same.

Despite the shallower groundwater table in the restored scenario, baseflows, fed by the alluvial aquifer inputs to the channel, were predicted to be lower in the restored (1 m) channel scenario than in the further incision (2.5 m and 4.5 m) channel scenarios. The levels of incision considered did not result in sufficient aquifer drawdown to significantly decrease the catchment-scale connection between the alluvial aquifer and the channel in the model.

Estimated recharge of the alluvial aquifer in the incised scenarios was such that the increased average depth of the water table was predicted to be less than the increase in depth of the thalweg. Incision was predicted to lead to a greater total flow from the aquifer into the channel, even in dry periods, despite some up-valley reaches along the floodplain becoming disconnected from the aquifer. The deeper channels maintained aquifer connectivity in more areas down-valley, and inflow rates were greater due to increased groundwater gradients from the mountain fronts to the lowered channel. The shallower 1 m channel in the restored case had lower groundwater gradients and was disconnected from the aquifer over more of its length more often in dry periods. This lead to both more channel infiltration losses and less net incoming water from the alluvial aquifer to feed channel baseflow on average (Table 5-1). While the long-term average modeled increase in the water table elevation in this 1 m channel scenario was slightly greater than the rise in the thalweg level compared the current (1.5 m) channel, the water table elevation was much more variable in this scenario, showing a greater increase over the current scenario during wet periods than in dry times. Additional recharge from overbank flooding during wet periods in the restored scenario did lead to greater predicted inflows from the alluvial aquifer into the channel and higher streamflows in post peak recessions, but this did not persist into the dry periods due to the fast draining alluvium.

Figure 5-9 Precipitation and modeled daily and annual flooded area and floodplain aquifer recharge for alternative scenarios: (a) precipitation, (b) daily inundated floodplain area, (c) annual average inundated floodplain area, (d) daily recharge of alluvial aquifer from surface sources, (e) annual recharge of alluvial aquifer from surface sources

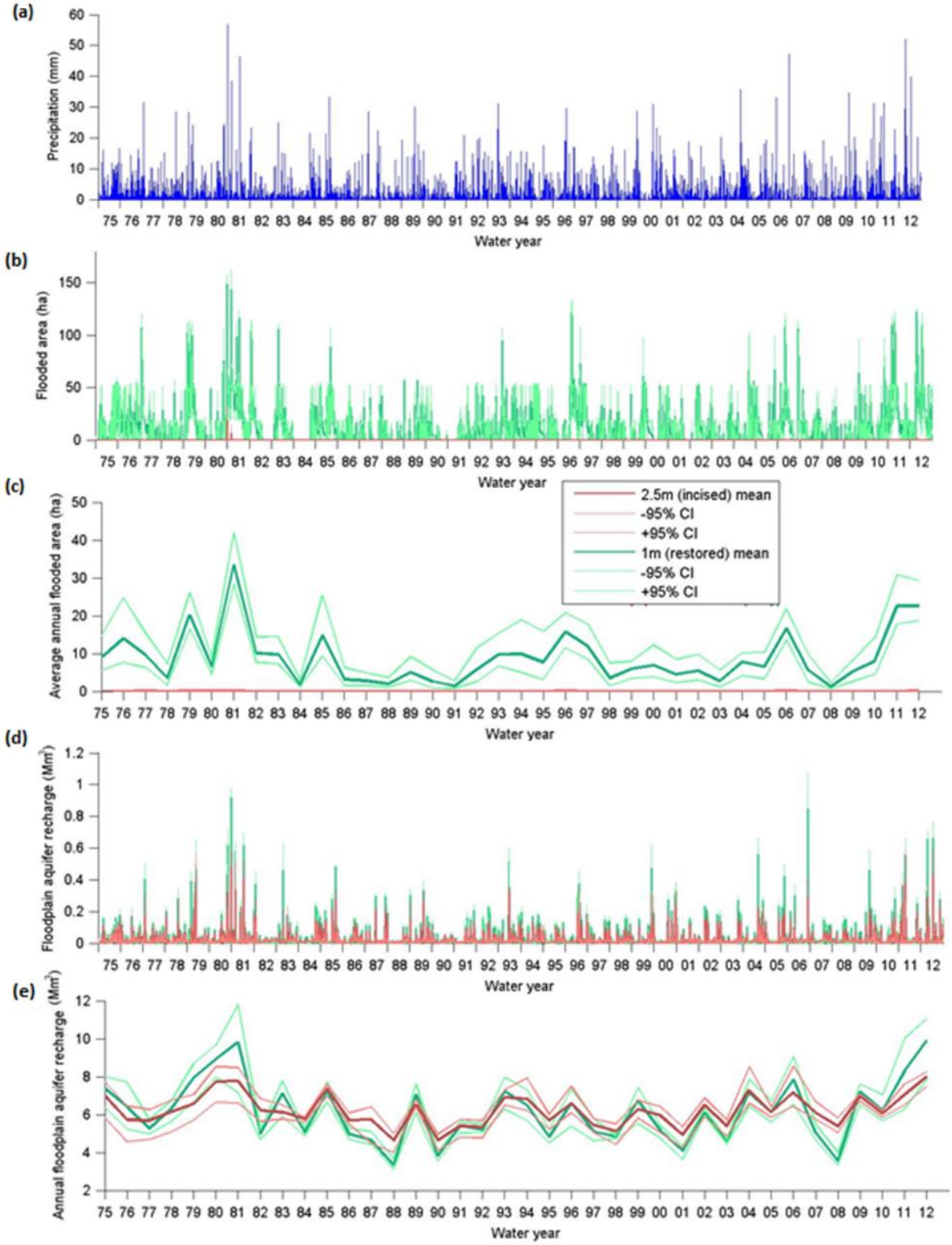

5.4 Discussion

The simulations in this study supported some but not all of the hypotheses regarding the impacts of floodplain channel incision in Baviaanskloof catchment, and the results highlighted tradeoffs to consider in restoration planning as well as needs for further research in this and similar environments. Model outputs were consistent with the hypotheses that channel incision in this setting would decrease overbank flooding, increase peak flows at the catchment outlet, lower the average floodplain aquifer groundwater level, and decrease annual average AET from the floodplain. However model results did not indicate that the degree of incision currently observed (1.5 m deep channel), or the further incision depths considered (2.5 m and 4.5 m channels), would be likely to result in decreased baseflow at the catchment outlet in dry periods or dry years given the weather patterns of the past 38 years. In fact, further channel incision was predicted to increase baseflow across the simulation period, while modeled impacts of assumed channel restoration (establishing a lower capacity, 1 m deep channel) on baseflow were too small to be statistically significant. The most notable predicted downstream impact of channel restoration was the reduction in peak flows at the catchment outlet: a 14-20% modeled reduction in flows with a 10% or lower annual exceedance probability. Within the floodplain, channel restoration was predicted to result in a significant rise in the groundwater, as well as a large increase in overbank flooding and floodplain inundation, likely to have ecological and land use implications.

Compared to the case of a shallower floodplain channel, it was originally anticipated that increased floodplain aquifer drainage into a more deeply incised channel would initially increase streamflow following a large, aquifer-recharging, rainfall event, but that this faster initial outflow of the event recharge water could subsequently result in decreased baseflow later on in an extended dry period. For channel incision to result in a decrease in aquifer inputs into the channel, the slope of the water table in the direction of the channel would need to decrease, and/or the water table would need to drop below the channel, more so than with a less incised channel. This could occur if presumed initial faster drainage in the incised case exceeded the net aquifer recharge over time. Development of such conditions had been thought possible in the semi-arid Baviaanskloof due to the area's sporadic distribution of large rainfall events and prolonged dry periods, deep rooting floodplain vegetation that can access the aquifer to meet ET demands, and the likely reduction in floodplain aquifer event recharge in the incised channel case due to decreased overbank flooding.

However, contrary to these hypotheses, when floodplain channel incision and restoration scenarios were applied in a calibrated model of the entire Baviaanskloof catchment with locally observed weather patterns over multiple decades, decreasing baseflow with increased incision was not predicted to occur, even during dry periods with multiple consecutive years of below-average annual rainfall. Instead, with the exception of the predicted change in peak flows, the differences in modeled streamflow between the scenarios were almost the opposite of what had been expected: modeled initial post-peak recession flows following

large rainfall events were highest with the shallowest channel and modeled baseflows later on in dry periods were highest in the most incised scenario. As described in Sections 3.1-3.3 above, these predictions were the result of the combination of the estimated rates of alluvial aquifer recharge from the surrounding mountain areas, the rates of groundwater flow through the aquifer material into the channel, the distribution of rainfall events, and the shape of the central valley. Predicted floodplain aquifer recharge from the surrounding mountains was sufficient to maintain groundwater levels above the channel in downvalley and narrow floodplain reaches in all channel scenarios, even in dry periods. The 2.5 and 4.5 m channels were predicted to result in more aquifer to channel flow in these areas than the 1.5 m deep current scenario channel, leading to consistently higher baseflows. Models predicted significantly more overbank flooding in the 1 m restored case, leading to greater net aquifer recharge during large flow events; however, the high conductivity aquifer material meant that this added recharge was predicted to drain into the channel in a period of weeks and so did not affect much of the baseflow period. Because of the mountain front recharge rates, the recharge during overbank flooding was not critical in maintaining the water table above the channel later on in the dry periods. It should be noted however that restoration was not predicted to decrease baseflow from the current scenario in most conditions.

There was some indication in the model outputs that if channel incision were more extreme and dry periods lasted for longer, a situation of incision drainage exceeding alluvial aquifer recharge rates could develop and curtail dry period baseflows in this type of

catchment. This was seen in the steep decline in the low-flow end of the flow distribution curve in the deepest channel scenario considered. However, this was only predicted for the lowest 2% of daily flow values in a 38 year period with a scenario of 3 m of further channel incision beyond the current level, an extreme scenario considered for exploratory purposes rather than being probable in this geomorphic setting. As such this decline in baseflow seems unlikely to occur in the Baviaanskloof without substantial changes in conditions.

This study used the model of the Baviaanksloof catchment as a demonstration case to assess likely responses of a semi-arid, mountainous, meso-scale catchment to floodplain channel incision and restoration. Some of the characteristics of the catchment found to drive the response patterns were the rate and temporal constancy of floodplain aquifer recharge from the surrounding mountains, the high conductivity of the floodplain alluvium, and the frequencies of high flow events resulting in overbank flooding in different channel conditions. Had recharge rates from the mountains been lower or more highly curtailed in dry periods, had the alluvium had a much lower conductivity, and had overbank flooding been more critical to maintaining a water table above the channel in subsequent dry periods, the pattern of streamflow change with incision could have been quite different. This was evident when comparing the results for the Baviaanskloof catchment to those predicted for snowmelt-fed montane meadows in the western United States in comparable channel scenario modeling studies (Essaid and Hill, 2014; Hammersmark et al., 2008; Ohara et al., 2014). Some of the responses in Baviaanskloof model were similar, such as the lowered water table and reduced peak flows, but there were notable differences due to the different

catchment context, such as opposite direction of change in baseflow to some of the meadow responses.

As expected, the higher conductivity of the sand and cobble alluvium of the Baviaanskloof floodplain led to greater predicted lowering of the water table relative to incision depth when compared to predictions for more loam dominated floodplains. (Hammersmark et al., 2008) predicted 1.2 m lower floodplain average water table with 2m of incision in Bear Creek meadow, the average drawdown being 60% of the incision depth, while average drawdowns predicted for the Baviaanskloof floodplain were 80-90% of the incision depths. Having similar floodplains widths, roughly 1 km, the spatially averaged water table depths were considered comparable between the two cases.

Increases in predicted peak flows with incision in the Baviaanskloof was linked to the degree of predicted change in overbank flooding between scenarios, in keeping with the different patterns reported across the different meadow studies. In the Bear Creek and Last Chance Creek meadow models, restoration scenarios were specifically designed to recreate active floodplains and were predicted to decrease flow peaks on the order of 10-20% compared to pre-restoration, incised channel forms (Hammersmark et al., 2008; Ohara et al., 2014). A similar result was predicted for the Baviaanskloof, with a 14-20% decrease in downstream peak flows predicted with the assumed restored scenario. In Essaid and Hill (2014)'s model of the Sagehen meadow, overbank flooding was not predicted to occur in any scenario and incision was actually predicted to decrease wet season peak and average flows.

Similarly, when there was minimal change in predicted overbank flooding between scenarios in the Baviaanskloof, as when comparing the 2.5 m and 4.5 m channels, an increase in flow peaks with incision was not detected. However, unlike in the Sagehen model, there was no overall decrease in wet period flow predicted moving from the 2.5 m to the 4.5 m channel (Figures 5-5 and 5-6). This indicates that the drier, lower water table floodplain in the 4.5 m scenario did not buffer the streamflow from flows coming from the surrrounding catchment any more than the floodplain in the 2.5 m scenario. This was likely due to a combination of factors: several channelized connections between mountain tributary subcatchments and the main channel, limiting flow onto the fan and floodplain surfaces and potential for infiltration; more extreme runoff events, with less opportunity for infiltration before incoming surface flows reach the channel, dominating the overall wet period response compared to the balance of events in Sagehen; and wet event recharge from interflow and any infiltration that did occur in either case reaching the channel relatively quickly due to the high conductivity alluvium.

Unlike the predictions for the Baviaanskloof catchment, some of the meadow studies predicted or observed an increase in summer baseflow with channel restoration to a less incised state (Hammersmark et al., 2008; Ohara et al., 2014; Tague et al., 2008). In these meadow systems, significant floodplain recharge events generally occurred seasonally, during the annual spring snowmelt. Large wet events were more episodic in the Baviaanskloof, occurring every few years without strong seasonality. In the meadows, in the restored channel scenarios, additional recharge due to more overbank flooding and/or

slower drainage of mountain front recharge from snowmelt, a result of the lower water table slope between the mountain front and shallower channel, would lead to higher water tables developing of the course of the wet seasons compared to what would occur with a more incised channel. This was also seen in high rainfall events in the Baviaanskloof; however, lower conductivity soils in the meadows delayed subsequent flow from the aquifer into the channel by more than the few weeks predicted for the Baviaanskloof, extending the increased delayed flow into the dry summer period. In addition, aquifer recharge periods due to snow-melt would be more prolonged, months compared to the day to week long events in the Baviaanskloof, and the dry periods in the meadows are of shorter duration, often being just the summer months. As such a delay in meadow outflow with channel restoration on the order of a month or two would result an increase in summer baseflow. In the Baviaanskloof, additional wet period recharge with the restored channel was also not critical to maintaining the water table above the channel in dry periods, due to the balance of other recharge sources.

The quantification of channel incision and potential channel restoration impacts in the Baviaanskloof were limited by model uncertainties and simplifications in modeling and in channel scenarios. Some of the model uncertainty was considered here by using ensembles of behavioral parameter sets, those which produced acceptable streamflow and groundwater predictions against observed data (Chapter 2). Parameter uncertainty limited change detection in streamflow between scenarios, resulting in overlapping ranges of predicted values, particularly for daily values. In some cases, as in comparing the restored and current

channel scenario, even long term average yields were not statistically detectably different. This indicates that real yield differences between these scenarios are likely to be relatively small. Comparing model outputs to observational datasets it was seen that the model overestimates the runoff response to small rainfall events. This could mean that small event overbank flooding was likely over-estimated in the current and restored channel scenarios. However floodplain recharge due to overbank flooding turned out not to be a significant determinant of dry period baseflow and relatively quick return flows into the channel meant that the effects of this on predictions of overall yields are likely to be small. The model structure and parameter values represent current understanding of catchment processes, but could be further evaluated and improved given more observational data.

The scenarios of channel change considered here could also be further refined both by geomorphological predictions of likely further incision levels and of pre-incision conditions. The restoration scenario used here did not explicitly include the braided channel forms observed in historical aerial photographs. It was assumed that the additional predicted overbank flooding, resulting in downvalley floodplain surface flow, during large flow events in the restoration scenario would approximate the pattern of flow that would have been estimated had additional, shallow, rough, channel area been instead added to the hydraulic model. This could be evaluated in further study, but the given simplifications of broader catchment processes and floodplain characteristics in the model (Chapters 1 and 2), highly refined channel form scenarios would have been a mis-match in complexity. It is also possible that restoration of a shallower floodplain channel form is not practically feasible

without restoring the vegetation and tributary channelization conditions throughout the catchment that are likely to have increased flow peaks reaching the floodplain (Chapters 3 and 4) and so such a state would not exist within the catchment conditions in which it was modeled here.

Despite these uncertainties, the results of this study do indicate that the restoration of the floodplain channel in the Baviaanskloof to a shallower, lower capacity state, would likely have larger impacts on peak flows and local floodplain habitat conditions than on long-term water supply availability. There was a small predicted decrease in overall water yield in the restoration scenario which was not statistically robust, but could be assessed against downstream water supply systems. The reduced flood peaks in the restored scenario could improve water quality and reduce reservoir sedimentation downstream. The larger rainfall events that would result in more overbank flooding in the restored case are those which would cause the most overland flow and erosion in the hillslopes and erosion of channel bed and bank material. Some of this eroded material could be carried to the catchment outlet and downstream reservoir if these flows remain in a deep channel and are not slowed by flowing across the rougher floodplain surface. A coupled sediment transport model could be used to assess this in future.

In considering active river channel restoration, positive and negative impacts on water supply would need to be weighed up with local impacts within the catchment. The predicted increase in groundwater levels with channel restoration was significant and could improve

supply availability for users within the catchment and restore wetlands, however attendant flooding implications would need to be assessed and tradeoffs made. Channel restoration was predicted to decrease flood peaks and potentially damages experienced downstream; however, the notable increase in predicted inundated area in the floodplain warrants further assessment of local impacts on inhabited and agricultural areas. The more regular and widespread predicted inundation with channel restoration is in keeping with the soil profile evidence of previously existing permanent and semi-permanent wetlands (mottled and gleyed layers in first 50 cm; Powell, 2015) over larger areas of the floodplain compared to the current state. This suggests restoration of the channel would likely be effective in restoring wetland habitat in the Baviaanskloof. The channel scenarios applied in this model assumed a change in average depth and channel capacity throughout the length of the channel. It may be possible to achieve changed channel forms in certain reaches in order to balance some of the potential benefits in terms of habitat and groundwater supply and potential flooding impacts over different areas of the catchment. The impacts of different spatial patterns of channel form change and the geomorphic stability of this would require further research and modeling.

5.5 Conclusions

This study used coupled surface-subsurface hydraulic and hydrologic modeling to assess the potential impacts of floodplain channel incision on a semi-arid meso-scale catchment: the Baviaanskloof, South Africa. While it is understood that river channel form can impact

flooding, riparian habitat, groundwater levels, streamflow patterns, and water quality, the impacts of channel incision will vary with the catchment context, and relatively little research has been done on responses in semi-arid systems. Model simulations of different river channel form scenarios in the Baviaanskloof catchment indicated that further incision from the current state is likely to result in a lowered average water table in the floodplain as well as increased peak flows, increased baseflows, and a greater average annual water yield at the catchment outlet. Restoration of a shallower, lower capacity channel was predicted to notably increase overbank flooding and cause a rise in the water table in the floodplain while decreasing peak flows at the catchment outlet.

Predicted changes in average annual yield and baseflow were small and not statisically significant at the level of certainty afforded by the model, but the means of ensemble runs for each scenario suggested a slight decrease in average annual yield and increase in average annual minimum monthly flow. While the predicted changes in the floodplain water table, overbank flooding, and downstream peak flows were consistent with responses predicted and observed in wetter environments (Essaid and Hill, 2014; Hammersmark et al., 2008; Loheide and Booth, 2011; Ohara et al., 2014; Schilling et al., 2004, 2006; Tague et al., 2008), the predicted changes in baseflow were notably different. In the Baviaanskloof model, the combination of ongoing floodplain aquifer recharge from mountain area subsurface inputs, the highly irregular and episodic pattern of large, rainfall-driven recharge events, prolonged dry periods, the high conductivity of the floodplain alluvium, and the downstream narrowing of the floodplain all resulted in maintained greater flows from the

alluvial aquifer into the channel over the majority of the modeled period when channels were deepened by 1-3 m. This illustrates the need to model potential impacts of channel incision and restoration within the larger catchment context.

Floodplain channel incision enhanced by human activities is common globally and is often a focus river restoration programmes and catchment management more generally. Modeling results for the Baviaanskloof catchment indicated that channel restoration in this context would likely come with both local and downstream benefits and drawbacks that would need to be considered. The channel restoration scenario considered here was not predicted to have a large impact on downstream average annual yields or baseflows compared to the current scenario. It was predicted to reduce flood peaks which could have downstream benefits in terms of reduced sedimentation of the downstream water supply reservoir and reduced flood damages in downstream areas. Within the Baviaanskloof catchment, the predicted rise in the floodplain aquifer water table could result in increased water availability to catchment residents and an increase floodplain habitat, however the increased floodplain inundation may also have negative implications for agriculture, infrastructure, and inhabited areas on the floodplain. The predictions of this study, and predictions for additional alternative channel forms, could be further coupled with sediment transport models, water supply system models, flood impact assessments, and habitat restoration goals to better evaluate potential tradeoffs and inform future interventions.

5.6 References

Beechie, T.J., Pollock, M.M., and Baker, S. (2008). Channel incision, evolution and potential recovery in the Walla Walla and Tucannon River basins, northwestern USA. Earth Surf. Process. Landf. *33*, 784–800.

Bobbins, K.L. (2011). Developing a form-process framework to describe the functioning of semi-arid alluvial fans in the Baviaanskloof Valley, South Africa.

Booth, E., and Loheide, S. (2010). Effects of evapotranspiration partitioning, plant water stress response and topsoil removal on the soil moisture regime of a floodplain wetland: implications for restoration. Hydrol. Process. *24*, 2934–2946.

Bravard, J., Amoros, C., Pautou, G., Bornette, G., Bournaud, M., Creuzé des Châtelliers, M., Gibert, J., Peiry, J., Perrin, J., and Tachet, H. (1997). River incision in south-east France: morphological phenomena and ecological effects. Regul. Rivers Res. Manag. *13*, 75–90.

Comiti, F., Da Canal, M., Surian, N., Mao, L., Picco, L., and Lenzi, M.A. (2011). Channel adjustments and vegetation cover dynamics in a large gravel bed river over the last 200 years. Geomorphology *125*, 147–159.

Essaid, H.I., and Hill, B.R. (2014). Watershed-scale modeling of streamflow change in incised montane meadows. Water Resour. Res. *50*, 2657–2678.

Euston-Brown, D.I.W. (2006). Baviaanskloof Mega-Reserve Project: Vegetation mapping contract report on methodology, vegetation classification and short descriptions of habitat units (South Africa: Eastern Cape Parks & Tourism Agency).

Finlayson, B.L., and Brizga, S.O. (1993). Anastomosing channels and arroyo development on the Nogoa River, Central Queensland, Australia. Sediment. Geol. *85*, 179–190.

Gregory, K.J. (2006). The human role in changing river channels. Geomorphology *79*, 172–191.

Hammersmark, C., Rains, M., and Mount, J. (2008). Quantifying the hydrological effects of stream restoration in a montane meadow, northern California, USA. RIVER Res. Appl. *24*, 735–753.

Hammersmark, C.T., Dobrowski, S.Z., Rains, M.C., and Mount, J.F. (2010). Simulated Effects of Stream Restoration on the Distribution of Wet-Meadow Vegetation. Restor. Ecol. *18*, 882–893.

Hargreaves, G., and Samani, Z. (1982). Estimating potential evapotranspiration. J. Irrig. Drain. Div.-Asce *108*, 225–230.

Harvey, M.D., and Watson, C.C. (1986). Fluvial Processes and Morphological Thresholds in Incised Channel Restoration1. JAWRA J. Am. Water Resour. Assoc. *22*, 359–368.

Hewitson, B., and Crane, R. (2010). Gridded Area-Averaged Daily Precipitation via Conditional Interpolation.

Hipsey, M.R., Vogwill, R., Farmer, D., and Busch, B.D. (2011). A multi-scale ecohydrological model for assessing floodplain wetland response to altered flow regimes (Christchurch: Modelling & Simulation Soc Australia & New Zealand Inc).

James, L.A., and Marcus, W.A. (2006). The human role in changing fluvial systems: Retrospect, inventory and prospect. Geomorphology *79*, 152–171.

Jansen, H.C. (2008). Water for Food and Ecosystems in the Baviaanskloof Mega Reserve: Land and water resources assessment in the Baviaanskloof (Wageningen, The Netherlands: Alterra).

Lach, J., and Wyzga, B. (2002). Channel incision and flow increase of the upper Wisloka River, southern Poland, subsequent to the reafforestation of its catchment. Earth Surf. Process. Landf. *27*, 445–462.

Langendoen, E.J., Lowrance, R., and Simon, A. (2009). Assessing the impact of riparian processes on streambank stability. ECOHYDROLOGY *2*, 360–369.

Lechmere-Oertel, R.G., Kerley, G.I.H., and Cowling, R.M. (2005). Patterns and implications of transformation in semi-arid succulent thicket, South Africa. J. Arid Environ. *62*, 459–474.

Loheide, S.P., and Booth, E.G. (2011). Effects of changing channel morphology on vegetation, groundwater, and soil moisture regimes in groundwater-dependent ecosystems. Geomorphology *126*, 364–376.

Loheide, S.P., and Gorelick, S.M. (2005). A local-scale, high-resolution evapotranspiration mapping algorithm (ETMA) with hydroecological applications at riparian meadow restoration sites. Remote Sens. Environ. *98*, 182–200.

Loheide, S.P.I., and Gorelick, S.M. (2007). Riparian hydroecology: A coupled model of the observed interactions between groundwater flow and meadow vegetation patterning. Water Resour. Res. *43*, 16 PP.

Lowry, C.S., Deems, J.S., Loheide II, S.P., and Lundquist, J.D. (2010). Linking snowmelt-derived fluxes and groundwater flow in a high elevation meadow system, Sierra Nevada Mountains, California. Hydrol. Process. *24*, 2821–2833.

van Luijk, G., Cowling, R.M., Riksen, M.J.P.M., and Glenday, J. (2013). Hydrological implications of desertification: Degradation of South African semi-arid subtropical thicket. J. Arid Environ. *91*, 14–21.

Lynch, S.D. (2003). Development of a Raster Database of Annual, Monthly and Daily Rainfall for Southern Africa (Pretoria, South Africa: Water Research Commission (WRC)).

Mark, G. (2001). Recent formation of arroyos in the Little Missouri Badlands of southwestern North Dakota. Geomorphology *38*, 63–84.

Midgley, J.J., and Scott, D.F. (1994). Use of stable isotopes of water (d and o-18) in hydrological studies in the Jonkershoek valley.

Ohara, N., Kavvas, M.L., Chen, Z.Q., Liang, L., Anderson, M., Wilcox, J., and Mink, L. (2014). Modelling atmospheric and hydrologic processes for assessment of meadow restoration impact on flow and sediment in a sparsely gauged California watershed. Hydrol. Process. *28*, 3053–3066.

Pollock, M.M., Beechie, T.J., and Jordan, C.E. (2007). Geomorphic changes upstream of beaver dams in Bridge Creek, an incised stream channel in the interior Columbia River basin, eastern Oregon. Earth Surf. Process. Landf. *32*, 1174–1185.

Powell, R. (2015). Recent degradation along the upper-middle reaches of the Baviaanskloof River-floodplain: An examination of drivers of change and best rehabilitation practices. PhD dissertation. Rhodes University.

Refsgaard, J.C., and Storm, B. (1995). MIKE SHE. In Computer Models of Watershed Hydrology, V.P. Singh, ed. (Water Resources Publications), pp. 809–846.

Roets, W., Xu, Y., Raitt, L., and Brendonck, L. (2008). Groundwater discharges to aquatic ecosystems associated with the Table Mountain Group (TMG) aquifer: A conceptual model. Water SA *34*, 77–88.

Schilling, K., Zhang, Y.K., and Drobney, P. (2004). Water table fluctuations near an incised stream, Walnut Creek, Iowa. J. Hydrol. *286*, 236–248.

Schilling, K., Li, Z., and Zhang, Y. (2006). Groundwater - surface water interaction in the riparian zone-of an incised channel, Walnut Creek, Iowa. J. Hydrol. *327*, 140–150.

Schulze, R.E., and Maharaj, M. (2004). Development of Database of Gridded Daily Temperature for Southern Africa (Pretoria, South Africa: Water Research Commission (WRC)).

Schumm, S.A., and Hadley, R.F. (1957). Arroyos and the semiarid cycle of erosion [Wyoming and New Mexico]. Am. J. Sci. *255*, 161–174.

Schumm, S., and Parker, R. (1973). Implications of Complex Response of Drainage Systems for Quaternary Alluvial Stratigraphy. Nat.-Phys. Sci. *243*, 99–100.

Selaolo, E.T. (1998). Tracer studies and groundwater recharge assessment in the eastern fringe of the Botswana Kalahari, The Letlhakeng-Botlhapatlou Area. PhD dissertation. Vrije Universiteit.

Shepherd, R., and Schumm, S. (1974). Experimental Study of River Incision. Geol. Soc. Am. Bull. *85*, 257–268.

Sholtes, J.S., and Doyle, M.W. (2011). Effect of Channel Restoration on Flood Wave Attenuation. J. Hydraul. Eng. *137*, 196–208.

Sigwela, A.M., Kerley, G.I.H., Mills, A.J., and Cowling, R.M. (2009). The impact of browsing-induced degradation on the reproduction of subtropical thicket canopy shrubs and trees. South Afr. J. Bot. *75*, 262–267.

Simon, A., and Collison, A.J.C. (2002). Quantifying the mechanical and hydrologic effects of riparian vegetation on streambank stability. Earth Surf. Process. Landf. *27*, 527–546.

Simon, A., and Rinaldi, M. (2006). Disturbance, stream incision, and channel evolution: The roles of excess transport capacity and boundary materials in controlling channel response. Geomorphology *79*, 361–383.

Simon, A., Curini, A., Darby, S., and Langendoen, E.J. (2000). Bank and near-bank processes in an incised channel. Geomorphology *35*, 193–217.

Soltau, L., Smith-Adao, L., and Bugan, R. (2011). Baviaanskloof resistivity survey to define water level and depth to bedrock (Stellenbosch, South Africa: Center for Scientific and Industrial Research (CSIR)).

Steiger, J., Tabacchi, E., Dufour, S., Corenblit, D., and Peiry, J. -L (2005). Hydrogeomorphic processes affecting riparian habitat within alluvial channel–floodplain river systems: a review for the temperate zone. River Res. Appl. *21*, 719–737.

Surian, N., Ziliani, L., Comiti, F., Lenzi, M.A., and Mao, L. (2009). Channel adjustments and alteration of sediment fluxes in gravel-bed rivers of North-Eastern Italy: potentials and limitations for channel recovery. River Res. Appl. *25*, 551–567.

Tague, C., Valentine, S., and Kotchen, M. (2008). Effect of geomorphic channel restoration on streamflow and groundwater in a snowmelt-dominated watershed. Water Resour. Res. *44*, 10 PP.

Tomlinson, M.J., Gergel, S.E., Beechie, T.J., and McClure, M.M. (2011). Long-term changes in river–floodplain dynamics: implications for salmonid habitat in the Interior Columbia Basin, USA. Ecol. Appl. *21*, 1643–1658.

Tucker, G.E., Arnold, L., Bras, R.L., Flores, H., Istanbulluoglu, E., and Sólyom, P. (2006). Headwater channel dynamics in semiarid rangelands, Colorado high plains, USA. Geol. Soc. Am. Bull. *118*, 959–974.

Wyzga, B. (1996). Changes in the magnitude and transformation of flood waves subsequent to the channelization of the Raba River, Polish Carpathians. Earth Surf. Process. Landf. *21*, 749–763.

Xu, Y., Titus, R., Holness, S.D., Zhang, J., and Tonder, G.V. (2002). A hydrogeomorphological approach to quantification of groundwater discharge to streams in South Africa. Water SA *28*, 375–380.

Xu, Y., Wu, Y., and Beekman, E.H. (2003). The role of interflow in estimating recharge in mountainous catchments. In Groundwater Recharge Estimation in Southern Africa, Y. Xu, and E.H. Beekman, eds. (Paris, France: UNESCO).

Chapter 6 Modeling cumulative hydrologic impacts of both vegetation and channel restoration in a semi-arid, meso-scale catchment

6.1 Introduction

Large-scale changes in both land cover and river channels impact catchment-scale hydrologic processes, potentially altering water supply availability, flood intensities, and aquatic and riparian habitats (Bosch and Hewlett, 1982; Brown et al., 2005; Hammersmark et al., 2008, 2010; Loheide and Gorelick, 2007; Ohara et al., 2014; Price, 2011; Tague et al., 2008). Land and water management can better achieve desired results if the hydrologic impacts of these changes are considered, and hydrologic modeling can assist (Mirchi et al., 2010). However, while it is understood that diverse human activities in a catchment often directly alter multiple catchment properties simultaneously, and that land cover and channel changes can influence one another (Gregory, 2006; James and Marcus, 2006; Osterkamp and Hupp, 2010; Wheaton et al., 2011), the impacts of changes in vegetation and channel networks on catchment-scale hydrologic responses are not often modeled in concert. Loss of vegetation cover can result in increased flood peaks and increased sediment transport, the balance of which will result in either incising (Balling and Wells, 1990; Beechie et al., 2008; Booth, 1990) or aggrading river channels (Bravard et al., 1997; Gomez et al., 1998; Keesstra et al., 2005). Despite this, the effects of differing scenarios of vegetation cover on catchment hydrology are routinely modeled without explicit consideration of attendant changes in

channel network properties. Additionally in large-scale landscapes with multiple land managers and stakeholders, decisions about different kinds of activities in different locations can be made independently by different parties based on conceptions about individual impacts rather than cumulative ones.

A few examples of scenarios of combined land cover and channel changes in hydrologic modeling have come from urbanization studies, assuming direct human channel modification (e.g. He and Hogue, 2012), and from reach-scale modeling of riparian vegetation-channel interactions (e.g. Loheide and Gorelick, 2007). This study explores the potential importance of considering both vegetation and channel changes in concert in a mountainous, semi-arid, rural agricultural meso-scale catchment, using proposed restoration scenarios for the Baviaanskloof catchment, South Africa as a case study. It was hypothesized that the effects predicted for an individual type of change would be sensitive to the assumed catchment setting in terms of the upslope vegetation and/or channel network properties, and, due to multiple interacting thresholds of flow path connectivity in this catchment, that the impacts of multiple simultaneous changes would not be simply additive.

Connected flow paths of water and sediment within a catchment mean that activities in one location can change form and function in another and the downstream, or 'down-catchment', impacts of a change can be contingent on conditions along the surface and subsurface flow paths. For example, a change in hillslope vegetation can be expected to have a different level of impact on catchment outlet streamflow depending on how directly

flows from the hillslopes reach a defined channel network, the continuity and capacity of this network, the channel-floodplain interactions, and the channel-aquifer interactions between the hillslope and streamflow in the downstream channel. This poses a challenge to impact assessment in mountainous, semi-arid, meso-scale catchments. In such settings significant lowland alluvial fill deposits, in the form of fans and floodplains, are often composed of coarse, conductive material and are seldom saturated. These forms frequently act as buffers to surface flow through the landscape and create settings where surface-subsurface flow interactions have a dominant impacts on streamflow timing and magnitude (Ajami et al., 2011; Karen, 2009; Maneta et al., 2008). In this kind of catchment, thresholds of surface flow connectivity throughout the catchment are only episodically met and large portions of the overall flow through the catchment may pass through more complex surface-subsurface flow paths. As such, changes in channels that would alter channel-floodplain and channel-aquifer interactions can be expected to influence how much hillslope vegetation alterations can impact meso-catchment scale streamflow in such an environment.

Many commonly used medium complexity hydrologic model structures do not explicitly consider aspects of landscape connectivity that are important in arid and semi-arid settings in their representations of catchment processes (Maneta et al., 2008). Recent modelling tools that allow for land-unit flow path catenas, dynamic hydrologic/hydraulic model coupling, surface and groundwater model coupling can be used to better represent observed landscape connectivity at a catchment scale and allow for assessment of its importance (Arnold et al., 2010; Essaid and Hill, 2014; Hammersmark et al., 2008; Hipsey et al., 2011;

Loheide and Booth, 2011; Maneta et al., 2008; Ohara et al., 2014). In this study the coupled MIKE-SHE/MIKE 11 hydrologic/hydraulic modelling system (Refsgaard and Storm, 1995) was be used to build a model of the Baviaanskloof catchment that explicitly considers surface and subsurface connectivity between hillslopes, tributary channels, alluvial fans, the main valley floodplain and the main floodplain river channel as informed by field observations (Chapters 1 and 2).

The Baviaanskloof catchment area was used as a case-study of a semi-arid, meso-scale catchment for which a conceptual model of landscape flow connectivity has been established (Chapters 1 and 2), and in which several changes in vegetation and channel network properties in different locations have been described ((Bobbins, 2011; Jansen, 2008; van Luijk et al., 2013a; Powell, 2015; Smit, 2013; Chapters 3-5). Settled agriculture has been ongoing in the catchment for over a century. Intensive livestock grazing on hillslopes that support sensitive, endemic subtropical thicket vegetation resulted in a reduction in canopy cover in many areas, to 5% from what would likely have been close to 70%, resulting in 30% average cover on the hillslopes overall (Euston-Brown, 2006; Lechmere-Oertel et al., 2005a; Sigwela et al., 2009; Smit, 2013). Direct channel modification though construction of earthen berms and dredging, filling, and reorientation of channels occurred on the alluvial fans and central valley floodplain to establish agricultural fields and provide flood protection (Jansen, 2008). This increased the channel network connectivity between mountain areas and the trunk river channel in the floodplain. The trunk channel shows evidence of incision and widening in recent decades (Chapter 5, Powell, 2015).

There is concern about the loss of both thicket and floodplain wetland habitats due to these changes, as well as loss of ecosystem services, such as sustained agricultural productivity, carbon storage, flood protection, prevention of siltation in the downstream water supply reservoir, local groundwater availability, and potentially flow regulation and water supply in dry periods (Jansen, 2008). Outflow from the Baviaanskloof catchment feeds a regionally important reservoir that supplies downstream commercial agriculture as well as growing domestic and industrial demands in the Nelson Mandela Bay Metropolitan area. These concerns have motivated catchment-scale restoration proposals for the area promoting active restoration of hillslope thicket cover, recreating dispersive flow paths on channelized alluvial fan surfaces, and restoring a less incised channel form on the floodplain. Understanding the potential streamflow and groundwater impacts of achieving these states, and how different changes would likely interact, would be helpful for catchment management and restoration planning.

Prior modeling of single intervention restoration scenarios for the Baviaanskloof, in which one aspect of anthropogenic alteration in the catchment was presumed to be reversed while the rest of the landscape remained in its current condition, demonstrated individual impacts of hillslope vegetation cover change (Chapter 3), alluvial fan channelization (Chapter 4), and floodplain channel incision (Chapter 5) on streamflow output and floodplain groundwater. Catchment-wide thicket restoration had the largest predicted impact on streamflow, driven by large differences in large storm event runoff, while floodplain channel restoration had the largest predicted impact on groundwater levels,

driven by decreased aquifer drainage into the shallower channel and recharge in overbank flooding events. Model results indicated that restoring hillslope thicket vegetation cover could reduce floodpeaks by 56-60% (34-43 m^3/s) and the annual average water yield by 22-27% (5-8 Mm^3), if the channel network across the central valley alluvial fans and floodplain remained unchanged. As a result of predicted greater water retention and ET on restored hillslopes reducing runoff to the floodplain, model results indicated a potentially deepened floodplain water table by 0.2-0.4 m on average. Baseflow was predicted to decrease, with a 20-30% (0.03-0.04 m^3/s) modeled reduction in mean annual minimum monthly flow. Recreating less channelized alluvial fan surfaces was predicted to reduce flood peaks by a much smaller amount, 11-17% (7-10 m^3/s). Modeled fan restoration impacts on annual average yield, baseflow, and average floodplain groundwater levels were not statistically detectable. It is notable that the predicted mean water table was 0.14 m shallower with restored fans, the opposite direction of change to that predicted with thicket restoration. Reducing floodplain channel incision was similarly predicted to reduce peak flows, with a 14-20% (9-13 m^3/s) decrease modeled. The impact on average yield was not detectable in the model. Average floodplain groundwater levels were predicted to rise by 0.6-0.7 m; however a significant change in baseflow was not predicted. Because the decreased depth of the channel resulted in less connectivity with the aquifer in dry periods, baseflows in the driest periods on record were predicted to decrease slightly.

6.1.1 Modeling both vegetation and channel change

Single intervention studies quantify likely effects of individual types of changes which could be achieved in the Baviaanskloof catchment through active restoration and landscape engineering. Scenarios in which both vegetation cover and channel network properties change may be more realistic long-term states. Stakeholders may choose to engage in multiple active restoration interventions, but even if only a single type of active restoration is successfully implemented, connectivity between hillslopes, alluvial fans, and the floodplain river channel mean that a large upslope change could alter forms downstream. The increase in peak flows due to the loss of hillslope thicket cover in the Baviaanskloof was likely substantial (Chapter 3), and could have been partly responsible for the current levels of channel incision. Restoration of thicket cover could contribute to reversing these channel changes. Similarly, alluvial fan restoration would also affect flow peaks (Chapter 4), and hence erosion and deposition patterns in the floodplain. More 'down-catchment' restoration interventions on fans and floodplains could be implemented without altering the upslope vegetation, but this may prove impractical without intervening to reduce flood flow intensities coming from upslope. Vegetation cover change has not been the only factor driving channel incision: berm construction, dredging, and manual reorientation contributed. Removing berms and employing various active channel engineering techniques could re-create more dispersive fan and floodplain flow paths. Such interventions would need to be more substantial to withstand the more extreme flood events and prevent re-incision if the hillslope thicket vegetation remains in its current state.

Scenarios of simultaneous vegetation and channel changes were modeled in this study to explore the potential importance of considering combined impacts and landscape connectivity and evolution, without claiming that the particular combinations of specific properties applied here are more realistic future states for the Baviaanskloof. This would require quantitative estimates of sediment transport beyond the scope of this study. The likelihood and timeline of channel infilling occurring as a result of up-catchment restoration interventions would depend upon the incoming sediment supply. If hillslope thicket and/or fans are restored, peak flow event magnitudes would decrease. This could mean that flow events of sizes which would mobilize sediment in higher slope areas, but deposit it on the flatter surfaces in the central valley, may occur more frequently and represent a greater proportion of events than events large enough to mobilize bed material throughout the channel. This new flow regime could result in net aggradation over time. However, restoration would simultaneously reduce sediment quantities leaving hillslopes and fans during storm events. In the Baviaanskloof, large, relatively mobile, sediment supplies on fans and floodplain surfaces, the catchments' steep slopes, and periodic large flow events make it unlikely that the system would be sediment starved by upland restoration. Decreased sediment supply due to reforestation has been seen to result in channel incision in other semi-arid areas (Keesstra et al., 2005). Even so, manual channel interventions could create a less incised floodplain channel form, subsequently maintained by reduced event flows from simultaneous up-catchment restoration. A state in which all three proposed types of restoration changes are maintained appears theoretically achievable, but quantitative estimation of likely resulting channel properties would entail further geomorphic study.

It was hypothesized that when both the hillslope vegetation and the valley channel network (fan and floodplain) properties were changed to their assumed restored states in the Baviaanskloof catchment model, predicted patterns of streamflow and groundwater responses would differ from those predicted for single intervention scenarios. Some predicted process changes for different interventions would reinforce one another, while others would counteract each other. Overall decreases in both predicted average water yield and peak flow were expected, due to the dominant decrease in runoff from the hillslopes predicted when thicket cover is restored. In addition, reduced large event flows from restored thicket hillslopes then reaching restored, less channelized, alluvial fans would lead to a greater proportion of the incoming event flow being infiltrated on the fan. Previous modeling indicated that, in smaller events and dry antecedent conditions, directing water to infiltrate on the fan surfaces less frequently resulted in a rise in the alluvial aquifer, compared to infiltration occurring on the comparatively wetter floodplain, because of thicker, drier, unsaturated zones on the fans (Chapter 4). This pattern may occur more frequently when both thicket and fans are restored, further decreasing average yield.

However, in wet periods, higher alluvial aquifer recharge was predicted both with alluvial fan restoration and with floodplain channel restoration (Chapter 4 and 5), and floodplain groundwater levels were also predicted to rise with channel restoration due to less drainage (Chapter 5). Combining these effects could result in more floodplain saturation during extreme events in wet periods, reducing the floodplain's capacity to buffer flow peaks and potentially adding to peak flow through saturation surface runoff created on the

floodplain. However, this was not predicted to be a frequent or significant occurrence when the hillslope thicket was also restored, due to the overall reduction in runoff and floodplain recharge. It was hypothesized that the average floodplain water table would be shallower than in the current state if all three restoration interventions were successfully implemented, but the increase would be less than if the river channel alone was restored, due to the decreased inflow from the surrounding hillslopes.

6.1.2 Predicted sensitivity of restoration impacts to catchment setting

Comparing model outputs using different combinations of vegetation and channel network properties allows for analyses of the sensitivity of predicted restoration effects to assumed baseline catchment condition or the conceptualization and/or parameterization of the broader catchment. Differences in the predicted impacts of vegetation change given different channel network settings and differences in the predicted impacts on channels changes given different up-catchment vegetation cover highlight how sensitive these kinds of impact predictions may be to potential assumptions made about their settings in this type of catchment and model. Large differences in effects with changes in setting may be of import for other cases in which vegetation changes are modeled in meso-scale catchments with little consideration or available information on channel network properties and processes.

It was hypothesized that the impact of vegetation cover change on flood peaks would be greater in a setting in which the channel network more efficiently drained the landscape. In the Baviaanskloof case this implies that hillslope thicket restoration would have larger impacts when the alluvial fans are more channelized and the floodplain channel is more incised. If more dispersive flow paths were restored on alluvial fans and the floodplain channel was shallower with lower capacity, more of the incoming surface flows from hillslopes would be expected to infiltrate on the fan and floodplain surfaces, reducing flow peaks at the catchment outlet. Thicket restoration would reduce surface runoff to the central valley by the same amount in any channel network setting, but, in the less incised channel setting, a greater proportion of this reduction would be runoff that would have otherwise infiltrated on the valley alluvium and not contributed to the streamflow peak in any case. It was similarly hypothesized that the predicted impact of restoring thicket on average annual yield would be smaller given less channelization. However it was predicted that thicket restoration could result in a greater increase in the depth of the groundwater table when the channel network is in a restored state. A greater proportion of the hillslope runoff would be contributing to floodplain recharge in this setting. Therefore a reduction in incoming runoff could have a proportionally larger impact on groundwater levels, and potentially also on baseflow.

In the case of restoring less incised and less connected channel network conditions in the central valley, it was hypothesized that these changes would result in greater reductions of peak flow in a setting with more incoming surface runoff from the contributing tributary

subcatchment areas than in a setting with less incoming runoff. In the Baviaanskloof case study, the reduction in estimated flow peaks when using restored floodplain channel conditions in the model was predicted to be smaller if the hillslope thicket vegetation was assumed to be in an intact state than in its current state. During large rainfall events, overbank flooding was the mechanism by which the less incised floodplain channel was predicted to result in lower peak flows. In the case of intact thicket, peak flow values would be smaller and the threshold for overbank flooding would be less often met and the extent of the flooding would be smaller, resulting in less proportional flood attenuation. This would also reduce alluvial aquifer recharge during flood events such that the difference in the groundwater table due to channel restoration may also be less when the hillslope thicket is intact.

6.2 Methods

6.2.1 Scenario modeling

A detailed description of the Baviaanskloof catchment is given in Chapter 1, Section 1.2.1. The potential streamflow and groundwater impacts of simultaneously restoring hillslope thicket cover, recreating dispersive flow paths on alluvial fan surfaces, and re-establishing a shallower, lower capacity floodplain channel were estimated by changing vegetation and channel properties in a calibrated model of the Baviaanskloof catchment. A multi-scale, daily time-step model of the Baviaanskloof catchment was constructed and

calibrated using the MIKE-SHE/MIKE-11 modeling system (Refsgaard and Storm, 1995), based on a conceptual model informed by field observations of surface and groundwater flows, soil and vegetation properties, and topography (Chapter 1). A detailed description of the model structure and performance is given in Chapters 1 and 2.

In the 'full restoration' scenario, thicket area vegetation and soil parameters in the model were changed from their calibrated value ranges for the current catchment state to those predicted for thicket areas unimpacted by grazing, based on available published field studies (Mills and Fey, 2004; Lechmere-Oertel et al., 2005b; Mills and Cowling, 2010; Cowling and Mills, 2011; van Luijk et al., 2013b; Meijninger and Jarmain, 2014). These parameter values are given in Chapter 3. Channels crossing alluvial fans were assigned average dimensions from field and aerial photograph analyses (11 m wide, 1 m deep) in the current scenario. In the restoration scenario, channel dimensions on altered fans were decreased to 2 m width and 0.2 m depth at the fan toe such that most surface flow would disperse onto the fan surface. In the model of the current scenario the floodplain river channel had the dimensions of field surveyed cross sections: an inset bankfull channel with an average width of 21 m and depth of 1.1 m within a wider incised channel with an average width of 48 m and 0.5 m banks such that the channel thalweg was a total of 1.6 m below the floodplain surface (Chapter 5). In the restored scenario the dimensions of the inset bankfull channel were applied such that the average total channel width was 21 m and the thalweg 1.1 m below the floodplain surface.

As a comparative case, a 'full degradation scenario' was also modeled. In this scenario all three aspects of anthropogenic catchment alteration being assessed - hillslope thicket loss, alluvial fan channelization, and floodplain channel incision – were assumed to be more enhanced than in the current scenario. In this model set-up, vegetation and soil parameters assumed for completely degraded thicket, a state with ephemeral grasses, sparse small trees (5% canopy cover), and low infiltration capacity soils, based on available published field studies (Mills and Fey, 2004; Lechmere-Oertel et al., 2005b; Mills and Cowling, 2010; Cowling and Mills, 2011; van Luijk et al., 2013b; Meijninger and Jarmain, 2014) as described in Chapter 3, were applied to all hillslopes. All alluvial fans, even those currently observed to be unchannelized, were assumed to have a direct channel connection to the trunk channel in the floodplain and the floodplain channel was assumed to be 2.5 m deep, 1 m deeper than currently observed. Prior modeling did not indicate significant decreases in dry period baseflow when individual aspects of the catchment were assumed degraded beyond their current states (Chapters 3-5). This combined degradation scenario was modeled to test whether or not this would be likely if the landscape became even more fast-draining, through further losses of interception and infiltration capacity on the hillslopes and greater channel network efficiency in the central valley.

To test the sensitivity of the predicted effects of individual changes, vegetation or channel restoration, to up-catchment or down-catchment conditions, various scenarios with different combinations of restored and current model parameterizations were run. To examinme the sensitivity of the effects predicted for thicket restoration to channel network

conditions, scenarios with current and restored thicket parameterization were simulated with the alluvial fans and floodplain channels with their current state scenario dimensions and with their restored scenario dimensions. Similarly, to assess sensitivity of predicted channel restoration outcomes to the conditions of the up-slope areas, current and restored floodplain channel scenario dimensions were applied with current and restored hillslope thicket and alluvial fan parameterizations. Schematic diagrams of the scenarios modeled are given in Figures 6-1 and 6-2.

Figure 6-1 Schematic of models used to estimate the impacts of combined vegetation and channel changes showing the combinations of landscape unit property sets applied for hillslopes, alluvial fans, and the floodplain channel

Floodplain channel		Less incised			Current			Further incision		
Alluvial fans		Most fans dispersive	Current	All channelized	Most fans dispersive	Current	All channelized	Most fans dispersive	Current	All channelized
Hillslope vegetation	Intact	FULL RESTORATION								
	Current					CURRENT				
	Degraded									FULL DEGRADATION

Figure 6-2 Schematics of models used to assess the sensitivity of predicted restoration intervention impacts to their catchment settings showing the combinations of landscape unit property sets applied to assess: A) vegetation restoration impact sensitivity to the channel network properties, B) floodplain channel restoration impact sensitivity to upslope conditions

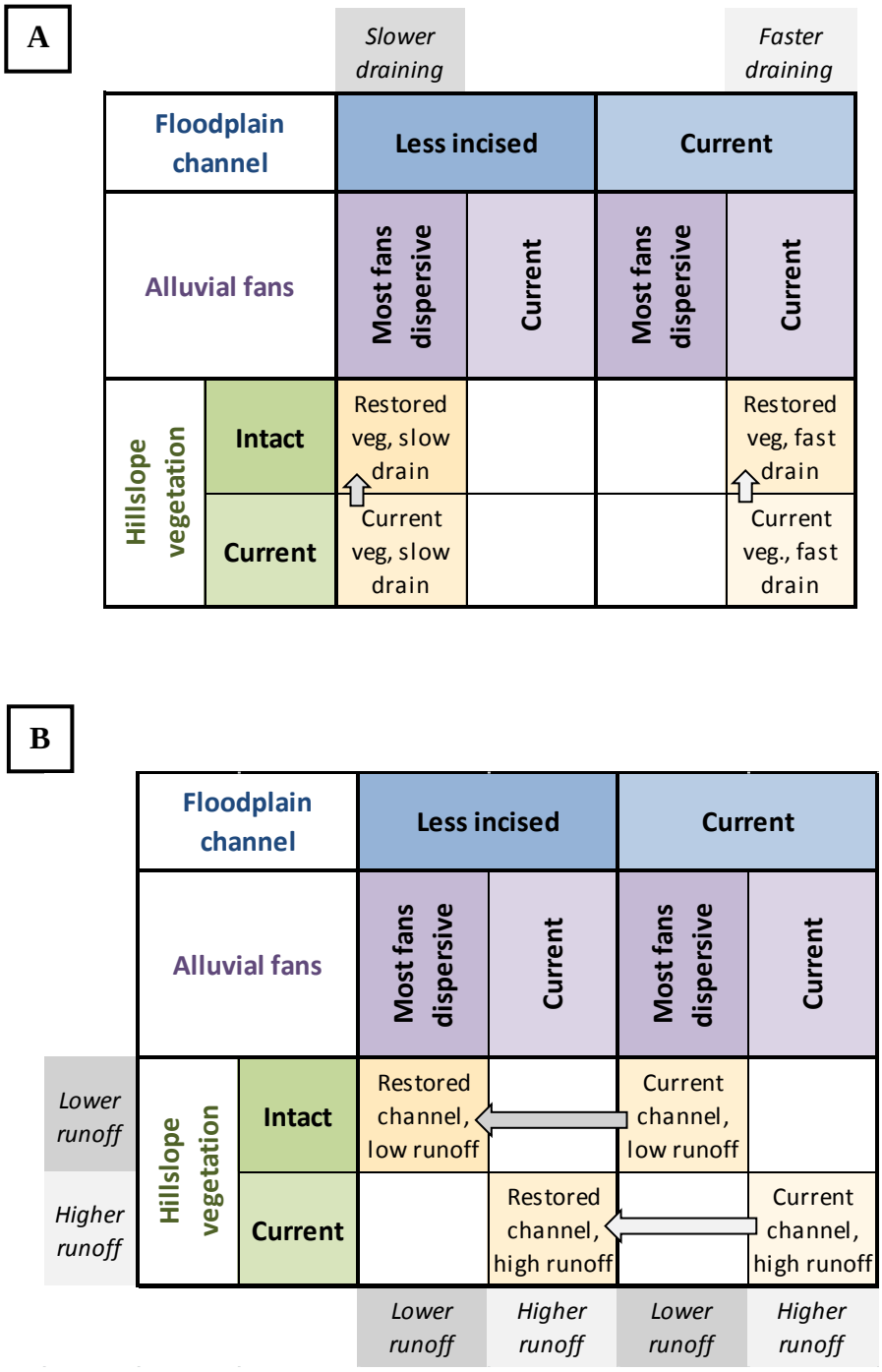

To account for the uncertainty in the parameterization, the model was run 100 times for each scenario to represent the calibrated parameter space. Parameter sets were selected from the 720 sets in the calibration exercise with acceptable model performance in recreating observed surface runoff, streamflow, and groundwater patterns as described in Chapter 2. The same 100 base parameter sets were applied in each scenario, such that the channel network properties or vegetation parameters were the only factors differing between them. For alternate hillslope thicket cover scenarios different to the current calibrated values, new sets of hillslope vegetation and soil parameters were selected in the same way over the assumed changed value distributions and randomly combined with the sets of parameters for the remainder of the catchment to make 100 total sets per scenario. These sets of runs resulted in likely output distributions for each scenario, allowing for conservative change detection.

In order to capture the response to a variety of storm sizes and antecedent conditions, the models for each scenario were run using 43 years of climate data from 1970-2012. The first 5 years (1970-1974) were considered a spin-up period for groundwater levels and change analyses were done for model output for the 1975-2012 water years. The water year was defined as April to March.

6.2.2 Output analyses

For the set of model runs for each scenario, the mean and the 95 percent confidence interval of the following statistics were calculated: average annual water yield, average annual minimum monthly flow, average daily flow for the fourteen largest flow peaks in the period (annual flow exceedance probability of 10%), and average depth to groundwater in the floodplain aquifer (spatially averaged). These statistics were chosen to assess the scale of impacts relevant to water supply and flood management. To assess changes in the flow path of water onto the alluvial fans and through the floodplain, modeled patterns of incoming surface and subsurface flows reaching the central valley, infiltration on the fans and floodplain, recharge to the alluvial aquifer, floodplain AET, flow from the alluvial aquifer into the main floodplain channel, and overbank flooding from the main channel were compared between the scenarios. Within the modeled time period, multi-year dry and wet periods were identified, as described in Chapter 3, Section 3.2.3, to compare the effects of fan channelization under different conditions. The statistics described above were also calculated separately for these periods.

To assess the sensitivities of predicted restoration effects to the catchment setting, time-series of differences in the above-listed outputs were calculated for models with and without restoration in each catchment setting. These time-series of changes were used to estimate the same statistics as listed above for the predicted effects in a catchment setting, for example: the mean and 95 percent confidence interval of the average annual change in water yield due to thicket restoration given a fast draining valley channel network. These metrics were then

compared between the different catchment settings to determine if differences in restoration effects between two different settings were statistically significant, for example: detecting a significant difference between the mean change in annual water yield due to thicket restoration with a faster draining valley channel network and the mean change in annual yield due to thicket restoration with a slower draining valley.

6.3 Results

6.3.1 Combined impact of multiple restoration activities

Model simulations predicted that simultaneously restoring hillslope thicket cover, alluvial fan surfaces, and the floodplain channel form would result in a decrease in the average annual water yield and in peak flows. The full restoration scenario was predicted to result in a rise in the average groundwater level in the floodplain compared to the current catchment state, however model outputs did not provide evidence for an associated increase in baseflow. The modeled average annual water balance for the full restoration scenario, current state scenario, and full degradation scenario for the 1975-2012 simulation period are shown in Table 6-1, Figure 6-3, and Figure 6-4. Predicted changes in key outputs given the assumed restoration changes are presented in Table 6-2. The modeled distribution of daily flow values for different scenarios are shown as flow duration curves in Figure 6-5 and compared to individual restoration scenarios in Figure 6-9.

The modeled average annual yield for the full restoration scenario was 19-20 Mm^3, 32-37% less than the 28-30 Mm^3 predicted for the current state. An increase in AET was predicted both for the subcatchments and the central valley fans and floodplain. Restoring hillslope thicket was predicted to increase average annual AET on the hillslopes by 6-8 Mm^3. This meant that the annual volume of water predicted to reach the central valley alluvial fill decreased by approximately the same amount, which, although it was a small proportional increase in AET (2-3%), was a relatively substantial proportional decrease, 14-18%, of the subcatchment outflow predicted in the current scenario. Decreased predicted hillslope surface runoff due to the greater modeled canopy interception and soil infiltration resulted in a 2.7-3.3 Mm^3 (55-68%) decrease in annual average surface flow predicted from the subcatchments. Increased soil moisture retention and plant transpiration resulted in a further predicted 2.4-4.2 Mm^3 (9-14%) decrease in average annual interflow reaching the central valley, while predicted mountain block aquifer outflows were not significantly changed. Central valley AET was predicted to increase by 4-5% (15-18%) in the restored case. Although a decrease in water received from the subcatchments was predicted, water was generally more available to vegetation in the central valley in the restoration scenario model as a result of: greater diffuse infiltration and soil moisture replenishment on restored alluvial fan surfaces during large events, a shallower average alluvial aquifer water table, and an increase in overbank flooding during large events due to the lower capacity floodplain channel (Table 6-2).

The predicted annual yields were consistently lower in the full restoration scenario compared to those modeled for the current catchment state over the 38 years modeled (Figure 6-6). Differences were smaller in dry years than wet years (Figure 6-7). Despite having less surface and interflow from the subcatchment areas, the full restoration scenario was predicted to have greater streamflow than in the current scenario for short periods, a few days to a week, during the recession following a large flow event (demonstrated in the hydrograph for 2011 in Figure 6-9). This was predicted because of additional overbank flooding and alluvial aquifer recharge modeled during the event resulting in more delayed flow into the channel in the restoration scenario. A similar pattern was predicted when only the floodplain channel was assumed to be restored to a less incised state (Chapter 5). However, when only the channel was restored, the floodplain received more inflows off the more degraded hillslopes, the modeled catchment outlet flow increase due to delayed flow into the channel was larger, occurred in more events, and lasted multiple weeks, resulting in an increase in flows with an exceedance probability of 1-3% in the restored channel case compared to the current state model (Chapter 5, Figure 6-9).

Table 6-1 Long term (1975-2012) average annual water balances for the Baviaanskloof catchment, and internally modeled land units, under different scenarios of catchment restoration and degradation in terms of hillslope thicket cover, alluvial fan surface channelization, and floodplain channel incision.

Location / spatial scale	*Flux*	Annual volume (Mm^3/ year)					
		Full degradation		**Current**		**Full restoration**	
		Mean	***95% CI***	**Mean**	***95% CI***	**Mean**	***95% CI***
Catchment	***Precipitation***	323		323		323	
	AET	273	*1.5*	288	*1.3*	300	*1.8*
	Streamflow	48	*1.4*	29	*1.0*	19	*0.6*
Mountain tributary sub-catchments	***Precipitation***	307		307		307	
	AET	249	*1.5*	260	*1.2*	267	*0.6*
	Overland flow to fan head	22	*1*	4.8	*0.1*	1.9	*0.3*
	Interflow to floodplain	23	*0.3*	29	*0.9*	26	*0.5*
	Mountain bedrock outflow	9.0	*0.5*	9.0	*0.6*	8.9	*0.5*
Central valley alluvial fill (fans and floodplain)	***Precipitation***	16		16		16	
	AET	24	*0.3*	28	*0.2*	33	*0.4*
	Alluvial aquifer input to channel (net)	38	*1.5*	26	*1.5*	16	*1.0*
	Overland flow inputs to channel	9.9	*0.5*	3.6	*0.7*	3.0	*0.5*

Figure 6-3 Long-term average water balance diagram for the Baviaanskloof catchment modeled with degraded hillslope thicket, channelized alluvial fans, and an incised river channel.

Quantities are in million cubic meters (Mm^3) of water per year.

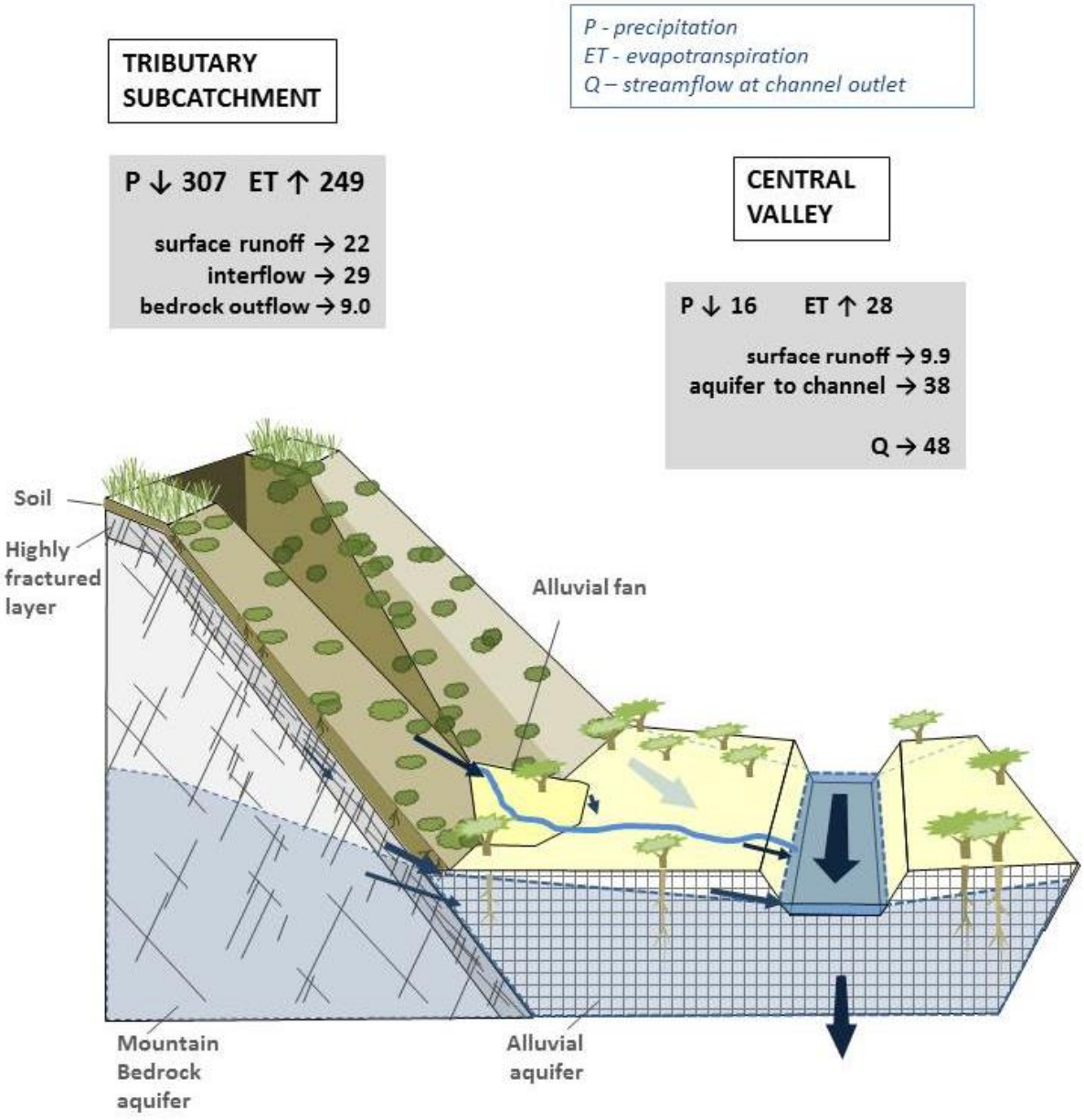

Figure 6-4 Long-term average water balance diagram for the Baviaanskloof catchment modeled with restored hillslope thicket, dispersive alluvial fans, and a less incised river channel.

Quantities are in million cubic meters (Mm^3) of water per year.

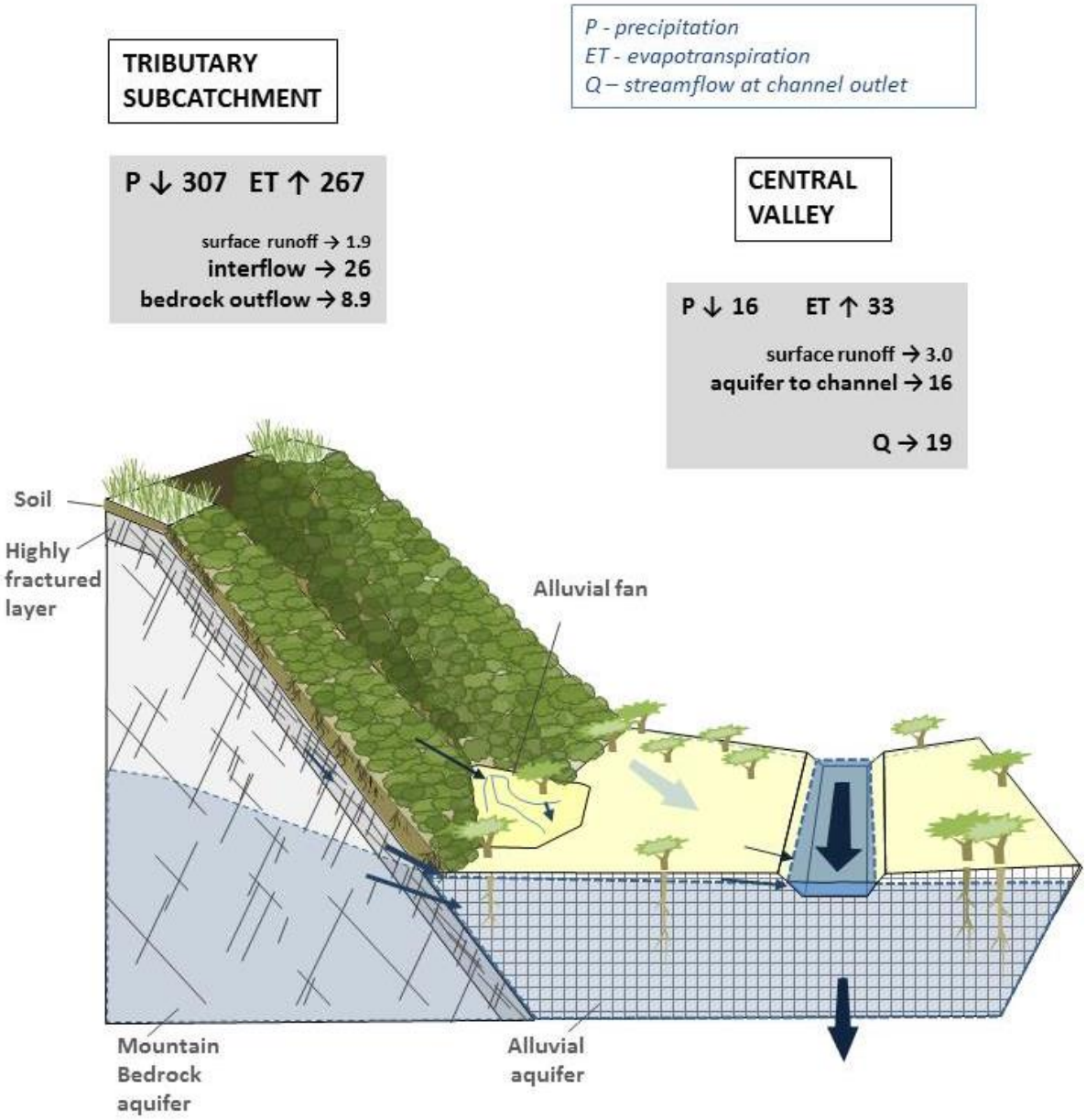

Figure 6-5 Daily flow duration curves for the full restoration, full degradation, and current condition scenarios showing the distribution of daily flow values modeled for the Baviaanskloof catchment outlet for the period 1975-2012.

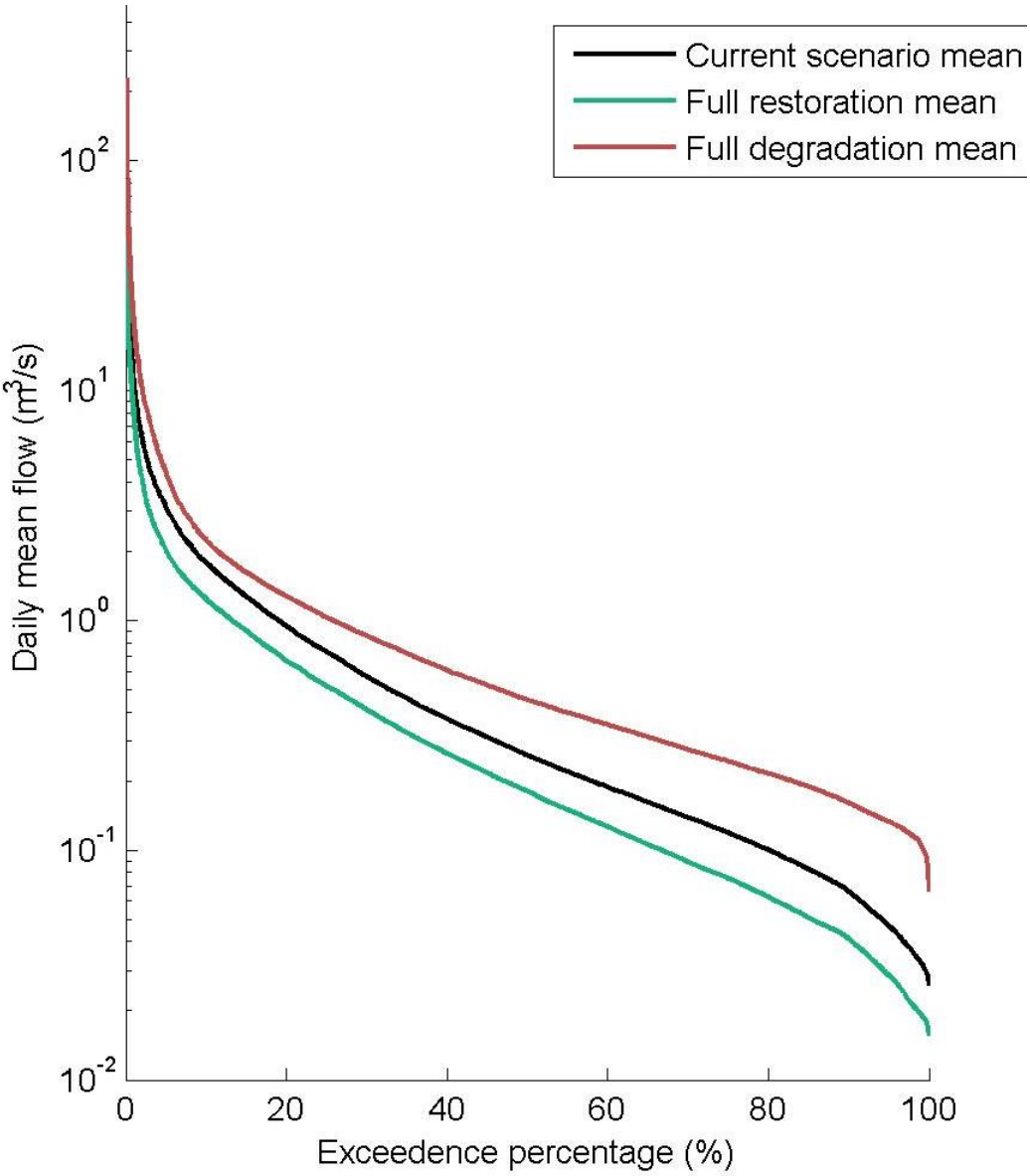

Figure 6-6 Modeled catchment water yield (total streamflow output) by water year for 1975-2012 for scenarios of current conditions, full restoration, and full degradation of hillslope thicket, alluvial fan surfaces, and floodplain channels.

Scenarios were represented by parameter ranges. Means and confidence intervals of the simulations sets run within these ranges are shown

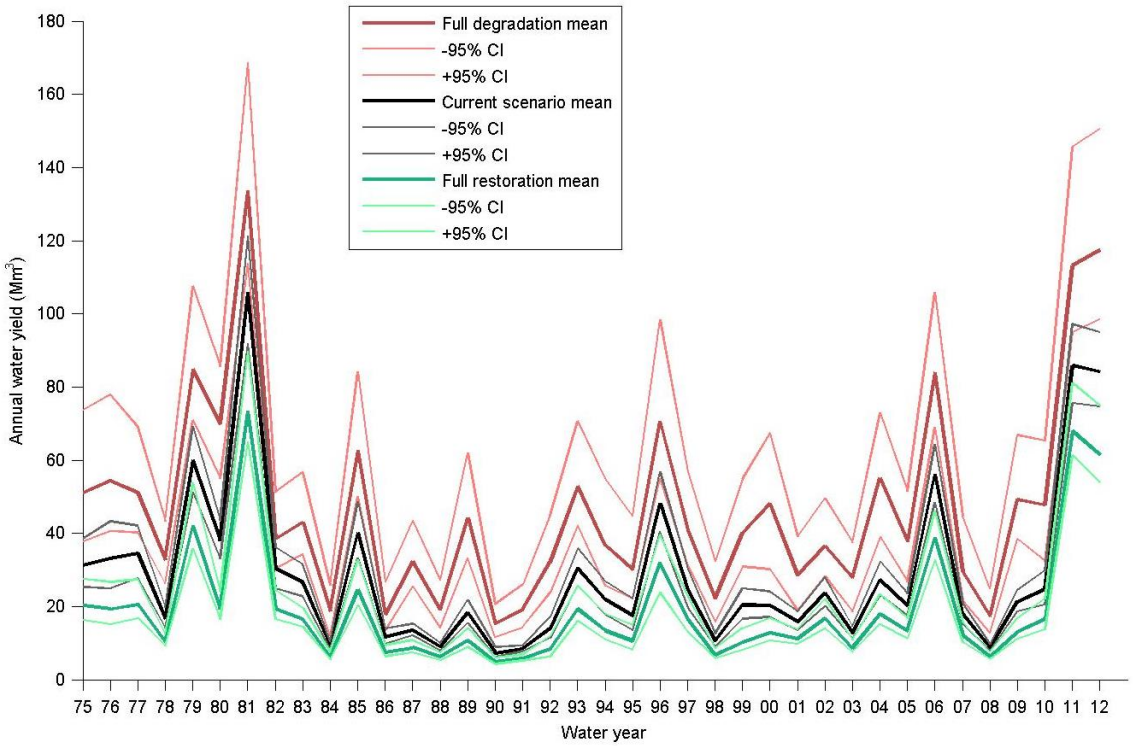

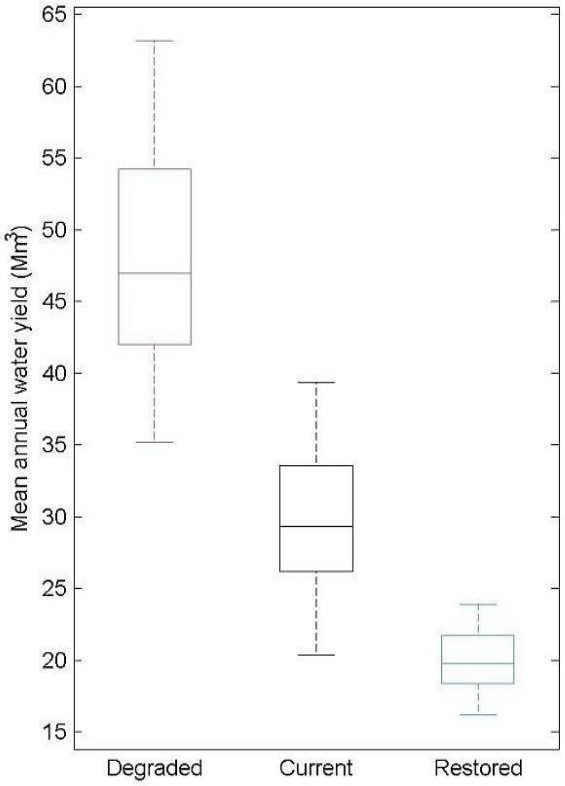

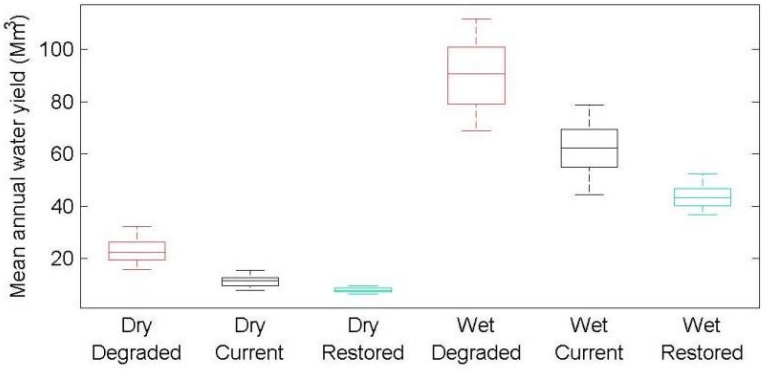

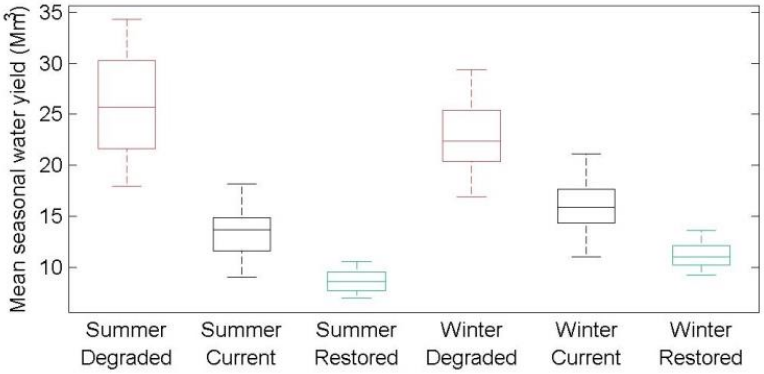

Figure 6-7 Boxplots showing the distributions of modeled mean annual and seasonal water for current, full restoration, and full degradation scenarios for: all simulated years (left), selected dry and wet years (center), and summer and winter months for all years (bottom)

Figure 6-8 Modeled daily flow hydrographs for demonstration dry (1990, top) and wet (2011, bottom) years showing differences in flow peaks and recessions between full restoration, full degradation, and current state scenarios

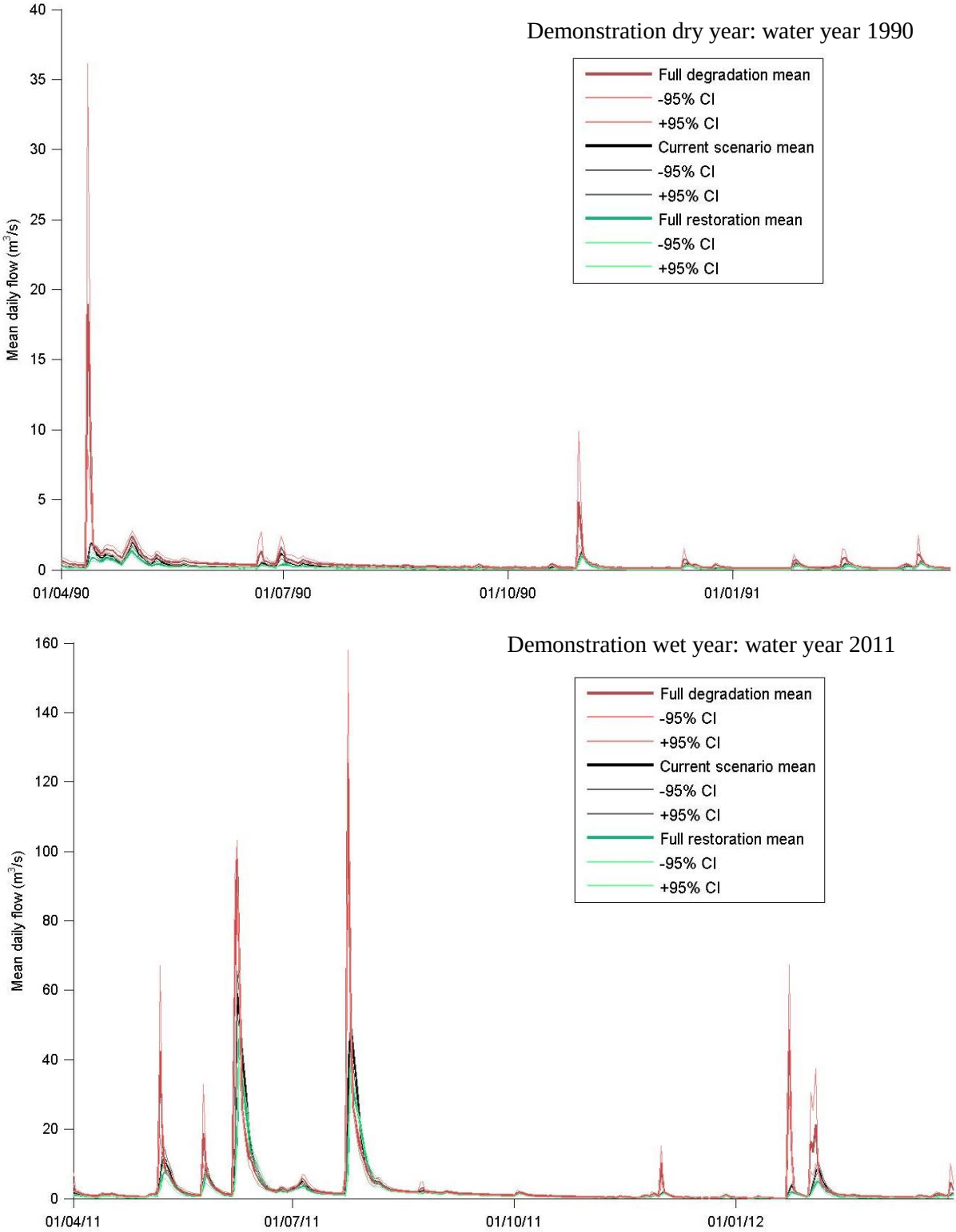

Figure 6-9 Daily flow duration curves for different individual restoration type scenarios and the full restoration scenario showing the distribution of daily flow values modeled for the Baviaanskloof catchment outlet for the period 1975-2012.

Inset graph has expanded the x-axis for greater visibility of the low frequency, high flow value portion of the curve, values with an exceedence probability of 5% or less.

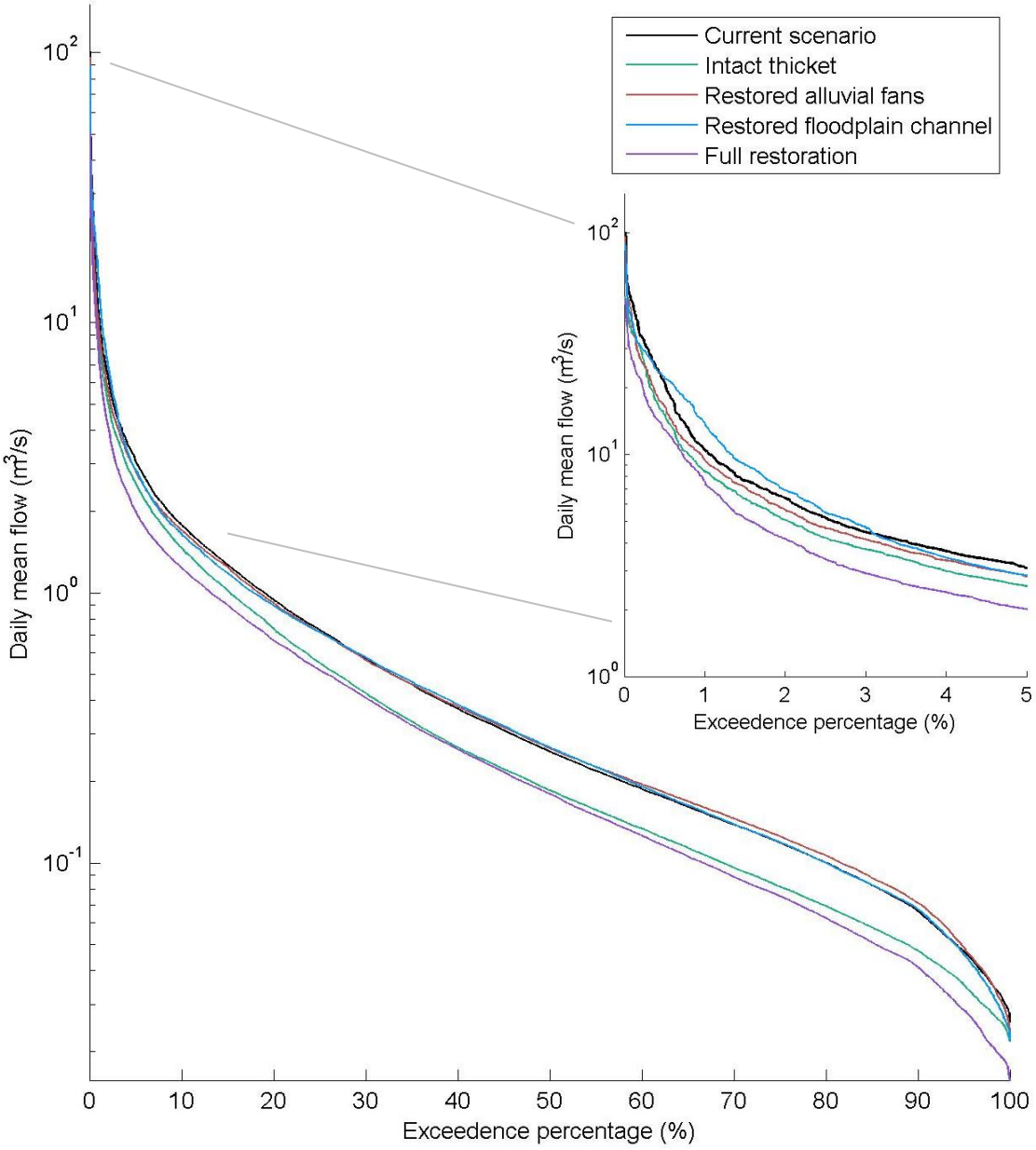

Peak flows for events with an annual exceedance probability of 10% or less were predicted to decrease by 41-44 m^3/s (69-71%) from current state predictions when given all three restoration changes in concert. Baseflow was also predicted to decrease, with the mean minimum monthly streamflow in a year decreasing by 0.03-0.05 m^3/s (20-40%). The average depth to groundwater in the floodplain was predicted to decrease by 0.3-0.4 m. Because the channel thalweg was 0.5 m higher in the full restoration scenario than the current, this rise in the groundwater level did not result in a modeled increase in overall flow from the aquifer into the channel, which would have resulted in an increase in baseflow.

The modeled groundwater table was consistently higher in the fully restored scenario over the modeled period. This was primarily due to the balance between constant subsurface recharge of the alluvial aquifer from the mountain bedrock, roughly the same across the scenarios, and less drainage of the floodplain in the full restoration scenario with a shallower, lower capacity channel. The full restoration scenario actually had *lower* predicted average alluvial aquifer recharge from surface flow sources for 1975-2012 than the current and full degradation cases. This was due to the rainfall distribution and different responses predicted for different sized rainfall events in wet and dry periods. Even though there was less inflow from the subcatchments in the full restoration scenario, large rainfall events resulted in significantly more recharge of the alluvial aquifer in this scenario than the current state. This was in keeping with the patterns described for individually restoring the alluvial fans or the floodplain channel, due to greater opportunity for infiltration on the fan and the floodplain surfaces from overbank flooding (Chapters 4 and 5). However, in drier periods,

there was more alluvial aquifer recharge modeled in the current state than the fully restored. This was both due to more small-event runoff from more degraded hillslopes flowing on to the central valley and because these incoming surface flows were able to more directly reach the floodplain channel and infiltrate there, rather than being dispersed across drier fan surfaces where infiltrating water was more subject to retention in unsaturated soils rather than percolation.

The change in modeled daily streamflow distribution with all three proposed restoration interventions together compared to changes predicted when only one intervention was considered is demonstrated in the flow duration curves in Figure 6-9. Effect sizes for different impacts of interest are given in Table 6-2. The decrease in average yield (8-11 Mm^3) was significantly greater than that predicted for individual interventions (Table 6-2). The predicted decrease in peak flow (41-44 m^3/s) was also larger than for the individual restoration interventions, though not statistically significantly larger than for thicket restoration alone (34-43 m^3/s). The predicted decrease in average annual minimum monthly flow with full restoration was similar and not significantly different from thicket restoration (0.03-0.05 m^3/s vs 0.03-0.04 m^3/s). Unlike with thicket restoration alone, the average groundwater table was predicted to rise with simultaneous restoration at all three landscape positions, but by less than the rise predicted when the floodplain channel alone was restored (0.3-0.4 m vs 0.6 -0 .8 m).

It was initially hypothesized that changes predicted when all three restoration activities were modeled together would not simply be the sum of the predicted impacts of the different restoration activities modeled individually. The modeled 8-11 Mm^3 decrease in annual average yield with full restoration was roughly the sum of the decreases in yields predicted for each intervention, but the flow duration curve and other statistics indicated more complex interactions. For example, the highest flows decreased less and lowest flows decreased more than would be expected if individual intervention impacts were additive. The predicted decrease in peak flows with full restoration smaller than the sum of predicted individual intervention responses. During large rainfall events occurring in already wet periods, the combined impact of both restored alluvial fans and floodplain led more surface saturation runoff in the central valley. This counter-acted some of the reduction in large event runoff from the restored hillslopes and the slowing of central valley surface flows on fan and floodplain surfaces instead of channels. The decrease in catchment outlet baseflow with full restoration during some of the driest periods, flows with 70-95% daily exceedance probabilities in the flow duration curve (Figure 6-9), was greater than the decrease predicted due to the thicket restoration alone. Models had predicted increases in streamflow with alluvial fan restoration and insignificant change with floodplain channel restoration over flows of this frequency (Figure 6-9), so if changes were additive, streamflow should be slightly greater than in the thicket restoration scenario. The increased drop in low flows seen instead was due to combined effects of dispersed infiltration on dry fan surfaces and lowered aquifer to channel connectivity due to the raised channel thalweg relative to the water table which had been lowered by decreased mountain subcatchment area runoff.

Figure 6-10 Modeled floodplain average groundwater depth in the central floodplain by water year for 1975-2012 scenarios of current conditions, full restoration, and full degradation of hillslope thicket, alluvial fan surfaces, and floodplain channels.

Scenarios were represented by parameter ranges. Means and confidence intervals of the simulations sets run within these ranges are shown

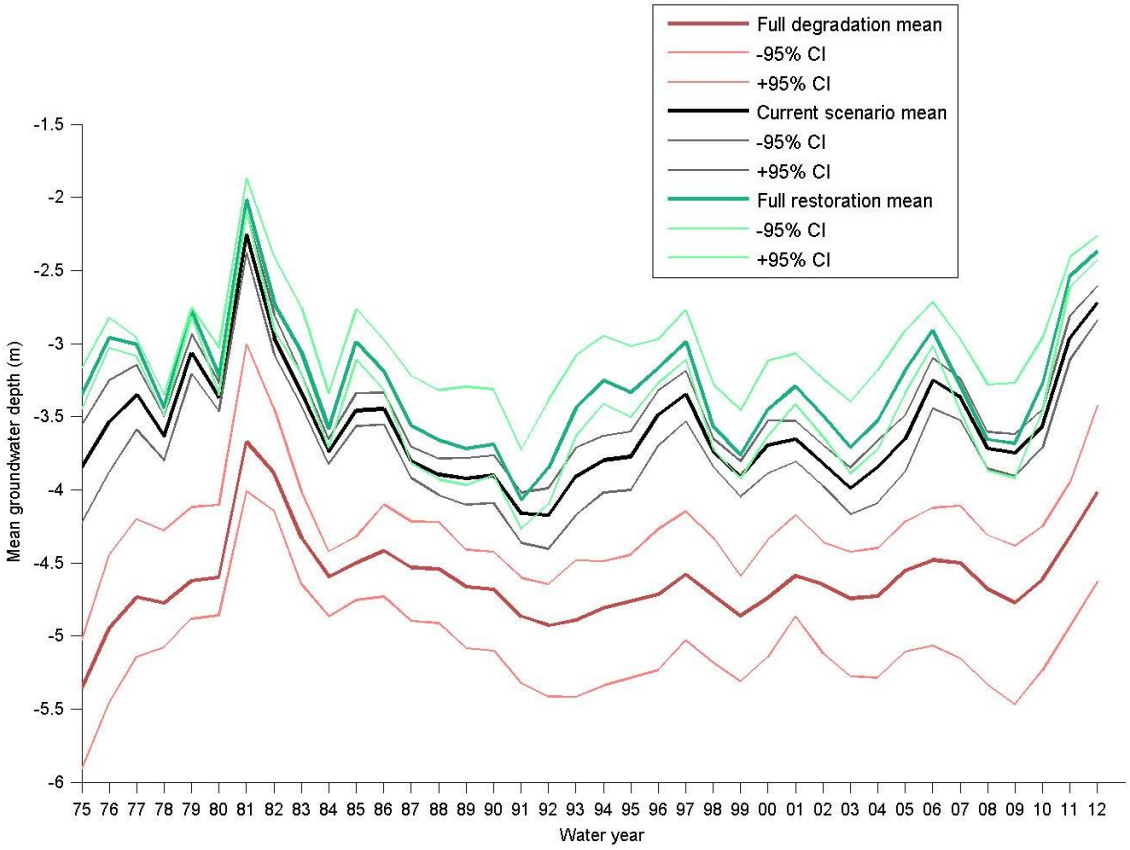

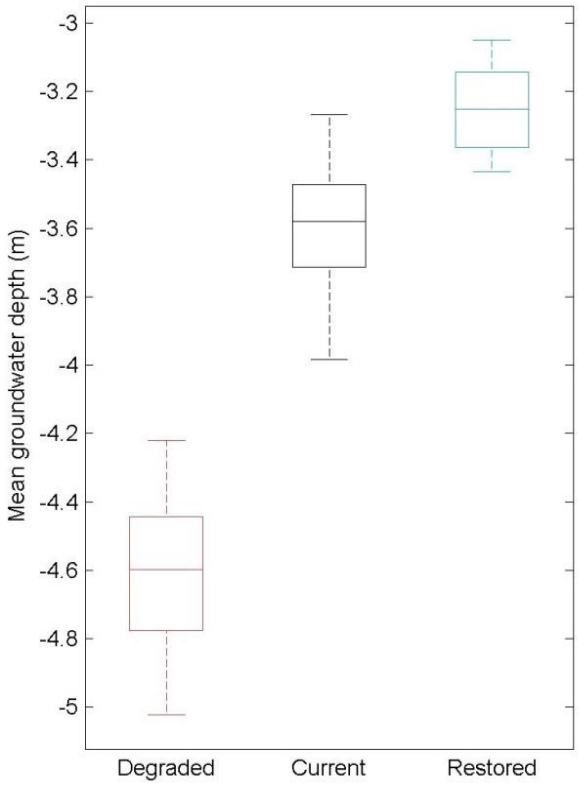

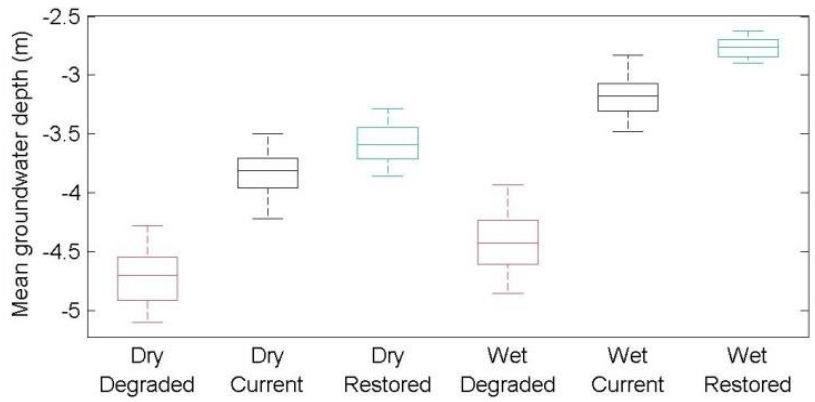

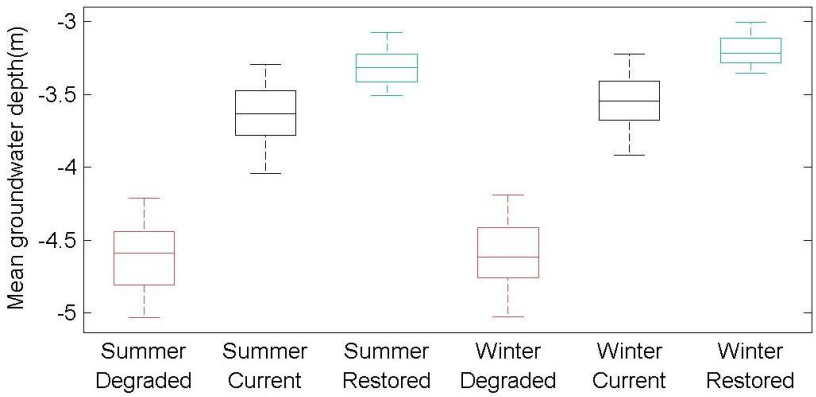

Figure 6-11 Boxplots showing the distributions of modeled mean annual and seasonal floodplain groundwater depth for current, full restoration, and full degradation scenarios for: all simulated years (left), selected dry and wet years center), and summer and winter months for all years (bottom)

The full degradation scenario was considered to test whether or not this could result in lower baseflow in dry periods than predicted in the current scenario. Model results did not give evidence that this would be the case. Even though the predicted groundwater table in the floodplain was significantly lowered (1-1.1 m on average, Figures 6-10 & 6-11), channel connectivity with the aquifer remained, particularly in narrow downstream parts floodplain, feeding flows into the deepened channel. There was a steep decrease in baseflow predicted for the driest periods on record, shown in the sharp decline in the tail end of the flow duration curve (Figure 6-5). This indicates an increasing rate of decline in the alluvial aquifer supply to the channel, likely when drawdown exceeds aquifer recharge (Essaid and Hill, 2014). A similar steep decline in baseflow was also predicted in a modeled scenario with a 4.5 m deep floodplain channel with the catchment otherwise in its current condition (Chapter 5). This decline was not predicted with 2.5 m deep channel applied in the current catchment (Chapter 5); however, in the full degradation scenario applied here, in which a 2.5 m deep channel was coupled with the decrease in recharge predicted with more alluvial fan channelization and the decrease in interflow predicted with increased thicket degradation (Table 6-1). However, model results suggest that more extreme and/or prolonged dry periods than those experienced in 1975-2012 would be needed for baseflow in the fully degraded case to reach or decline below those predicted for current or restored scenarios. Predicted annual flows and baseflows remained highest in the fully degraded scenario throughout the modeled period.

In the full degradation scenario landscape, modeled summer water yields were greater than winter water yields (Figure 6-7). In the current state of the catchment this was not observed (Chapter 1), nor modeled for the current state scenario, because although rainfall seasonality is low and some of the largest rainfall events do occur in the summer, runoff ratios in this season are generally low due to dry antecedent conditions, infiltration, and higher ET along the flow paths (Chapter 1). In the high runoff, fast draining, full degradation scenario little water was accessible for AET and summer and winter rainfall responses were predicted to be more similar.

6.3.2 Restoration impact sensitivity to catchment setting

Thicket restoration impact sensitivity to channel network properties

It had been hypothesized that hillslope thicket cover restoration would have a bigger impact on peak flows when the channel network through the central valley was more efficient in carrying flows to the catchment outlet compared to when the alluvial fans and floodplain channel were restored and hence more effective at buffering the catchment outlet from storm flows through dispersive flow paths and overbank flooding. This was supported by the model output: hillslope thicket restoration was predicted to result in a significantly greater magnitude decrease in catchment peak flows when the channel network was faster draining than when it was restored: 34-43 m^3/s in the fast draining case vs. 23-26 m^3/s in the slower draining case (Table 6-2). Because of decreased predicted outflows when the central

valley is slower draining, the proportional decrease in peaks due to thicket restoration was the same (56-60%) for the two settings. The buffering effect of the restored floodplain was evident in the much larger change in average overbank flooded area due to thicket restoration in the restored channel setting (2-3 ha decrease) compared to the faster draining setting (0.1-0.2 ha). This shows that, in the restored channel network setting, much of the reduced hillslope runoff volumes when thicket is restored were from flows that would have otherwise caused overbank flooding. This water would have been more subject to infiltration and ET in this setting and less likely to have influenced catchment outlet flow compared to the faster draining channel network setting. Hillslope thicket restoration was also predicted to have a larger impact on the average annual water yield of the catchment when the channel network was assumed to be faster draining, but the difference was not statistically significant.

It had been anticipated that the floodplain groundwater levels could be more sensitive to hillslope thicket restoration in the restored channel setting. This was presumed due to a likely larger change in alluvial aquifer recharge from overbank flooding water with the change in incoming mountain area runoff in the restored channel setting than in the faster draining one. A larger change in overbank flooding due to thicket restoration was modeled in the restored channel setting. However, the model results did not indicate that this was a dominant process in determining the longer-term average groundwater table elevation. The relatively fast predicted return flow of event recharge water into the channel in wet periods (on the order of weeks, Chapter 5), reduced duration of the influence of large overbank

flooding events on the alluvial aquifer. The predicted change in the average groundwater table due to thicket restoration was actually smaller when channels were less incised: water table declines of 0.1-0.2 m vs. 0.2-0.4 m. The greater aquifer drainage into the deeper channel made groundwater levels in the more incised channel setting more vulnerable to the reduction in runoff from the hillslopes. Even though the water table was lowered more by thicket restoration in the faster draining setting, the predicted decrease in average minimum monthly flows due to thicket restoration was not discernably different between the channel settings. The differences in water tables were less than the 0.5 m difference in the channel depth between the scenarios.

Floodplain channel restoration impact sensitivity to hillslope vegetation and alluvial fan properties

As hypothesized, the magnitude of change in peak flows resulting from floodplain channel restoration was predicted to be smaller in a setting with less incoming surface runoff: a 3-5 m^3/s predicted decrease in a lower runoff setting compared to 9-13 m^3/s given higher runoff from degraded hillslopes and channelized fans (Table 6-2). The proportional predicted decrease was similar for the two settings (15-22% and 14-20%). The magnitude increase in the modeled average overbank flooding area due to channel restoration was smaller in the lower runoff setting (7 ha vs. 9-10 ha), but represented a larger proportional increase than the change in higher runoff setting, increasing the proportional impact on reducing flood peaks. The predicted decrease in average floodplain groundwater depth with channel restoration was similar in the two runoff settings and the changes in average

minimum monthly flow due to channel restoration were not statistically significant in either upslope runoff setting.

Channel restoration appeared to have a larger impact on average annual yield when the floodplain received less runoff: in the low runoff setting a 1-3 Mm^3 decrease in average annual yield was predicted as a result of channel restoration, while in the high runoff setting the predicted change was not statistically significant. Restoring the channel increased overbank flows in both runoff settings, but in the high runoff setting much of the overbank flow in larger events later entered the channel as return flow, reducing the impact of overbank flooding on annual yields. In the lower runoff case there was less proportionate return flow due to less saturation. This pattern is evident in the average flow duration curves of the model output (Figure 6-12), which show higher 1-3% exceedance probability flows with channel restoration than without it in the high runoff setting due to the delayed flow out of the restored floodplain after a large flood event, but consistently lower flow with channel restoration in the lower runoff setting.

Table 6-2 Modeled restoration impact summary for different intervention scenarios in different assumed catchment settings, simulated for 1975-2013

* indicates that the change due to the restoration intervention in the given setting was statistically significant,
# indicates that the difference in restoration effect size between the two settings was statistically significant,
+ indicates that the difference in restoration effect size between full restoration and the vegetation restoration in the current catchment was statistically significant,
significance threshold of $p \leq 0.05$

Intervention		**Full restoration**	**Restore hillslope thicket cover**			**Restore floodplain channel form**		
Setting		***(vs. current state)***	**Fast draining valley** ***(Current fan & floodplain channels)***	**Slow draining valley** ***(Restored fan & floodplain channels)***		**High incoming runoff** ***(Current hillslope cover & fan surfaces)***	**Low incoming runoff** ***(Restored hillslope cover & fan surfaces)***	
Impact measure								
Change in annual average yield	Mm^3	- 8-11 *+	- 5-8 *	- 4-7 *		-3 +1	- 1-3 *	
	%	- 32-37%	- 22-27%	- 16-25%		-8 +5%	- 4-13%	
Change in average peak flow magnitude	m^3/s	- 41-44 *	- 34-43 *	- 23-26 *	#	- 9-13 *	- 3-5 *	#
	%	- 69-71%	- 56-60%	- 56-60%		- 14-20%	- 15-22%	
Change in average annual minimum monthly flow	m^3/s	- 0.03-0.05 *	- 0.03-0.04 *	- 0.03-0.04 *		+ 0.008-0.01	-0.002 +0.003	
	%	- 20-40%	- 20-30%	- 27-35%		+10%	-2 +5%	
Change in average depth to floodplain groundwater	m	- 0.3-0.4 *+	+ 0.2-0.4*	+ 0.1-0.2 *	#	- 0.6-0.8 *	- 0.7-0.8 *	
	%	- 8-11%	+ 6-10%	+ 3-7%		- 17-21%	- 19-21%	
Change in average annual area of overbank flooding	ha	+ 6-7 *+	- 0.1-0.2*	- 2-3 *	#	+ 9-10 *	+ 6.8-7.3 *	#
	%	+ 1120-1330%	- 30-40%	- 23-33%		+ 1660-2020%	- 2020-2340%	

Figure 6-12 Daily flow duration curves for modeled scenarios showing predicted flow distributions for 1975-2012, demonstrating predicted impacts of floodplain channel restoration given different upslope settings.

High runoff: hillslope thicket is in its current degraded state and fans have current levels of channelization,
Low runoff: thicket and fan surfaces are assumed to be in intact, unchannelized states.
Inset graph has expanded the x-axis for greater visibility of the low frequency, high flow value portion of the curve, values with an exceedence probability of 5% or less.

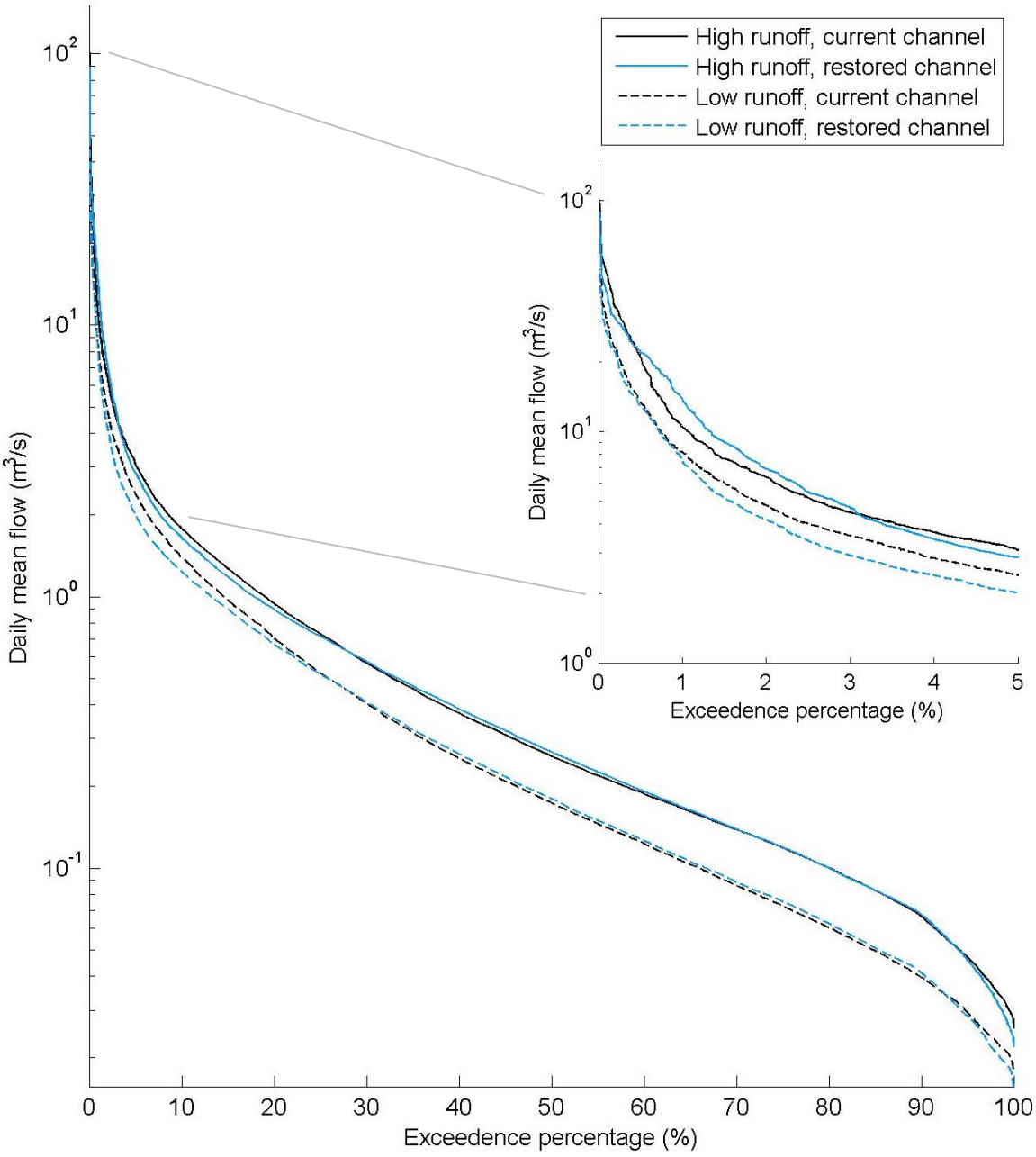

6.4 Discussion

The results of this study illustrate the potential importance of considering linked changes in vegetation and channel properties in hydrologic modeling of semi-arid, meso-scale catchments. Model outputs for the Baviaanskloof case study indicate that a failure to do so could result in significant over and under estimation of changes to peak flows, average water yields, floodplain inundation, and floodplain groundwater water levels, all of which are of concern for catchment management. Land cover change scenarios are often modeled by altering model land cover properties without considering changes in channel properties that may arise due to altered geomorphic processes. In smaller and/or wetter catchments in which channel-floodplain and/or channel-aquifer interactions are likely less significant, this may be less of a concern. Channel properties become more important with increasing catchment scales (Uhlenbrook et al., 2004) and fluctuating channel-aquifer interactions can be significant drivers of streamflow patterns in semi-arid areas (Essaid and Hill, 2014; Karen, 2009; Maneta et al., 2008). In the model of the Baviaanskloof catchment, which was structured to explicitly include observed patterns of surface and subsurface landscape and channel connectivity, the predicted impacts of hillslope vegetation restoration on floodplain groundwater levels and catchment outlet streamflow patterns were found to be significantly sensitive to the connectivity and capacity of the channel network.

When it was assumed that hillslope thicket vegetation could be restored in the Baviaanskloof without any change to the current alluvial fan and floodplain channel network

properties, the predicted impacts on total water yield and the average floodplain groundwater table were significantly different than when it was assumed that restoration of thicket cover could eventually result in less channelized alluvial fans and a less incised floodplain channel. When concurrent changes in the central valley channel network were applied in the model (full restoration scenario), the predicted decrease in average annual water yield was 38-60% greater due to additional water retention and ET in the central valley. The predicted reduction in flood peaks was also greater for the full restoration scenario than for thicket restoration alone, although the difference was not statistically significant. The floodplain water table was predicted to rise by 8-11% when all three factors changed, the opposite direction of change to the 6-10% deepening predicted when thicket restoration alone was considered.

Some of the differences in modeled outputs between scenarios did not show the patterns initially expected. This was the result of multiple interacting thresholds of connectivity along surface and subsurface flow paths and the flashy local rainfall pattern, demonstrating the usefulness of quantitative models in integrating many complex and dynamic processes. For example, it was originally hypothesized that restoring both the hillslope vegetation and the valley channel network in the Baviaanskloof catchment would result in a larger decrease in flood peaks than the sum of the impacts predicted for individually implemented changes. Model outputs instead suggested that the reduction in peak flows with full restoration would be less than the sum of the individual intervention responses.

The reasoning behind the initial assumption of a greater decrease in flood peaks had been that reduced event surface runoff from mountain subcatchments due to thicket restoration would then have a higher proportional loss to infiltration on the restored alluvial fans and floodplain. Antecedent conditions on the central valley were initially expected to also be somewhat drier in this scenario, further promoting infiltration, because of less surface flow and interflow from the restored subcatchments in prior events. However, it was found that, due to the estimated rate of relatively consistent subsurface flow from the mountain bedrock aquifer into the floodplain alluvial aquifer in the calibrated Baviaanskloof model, the restoration of a shallower, lower capacity channel in the floodplain, less capable of draining the aquifer, could still result in a rise in the groundwater table level, despite receiving less surface flow and interflow from restored hillslopes. The large peak flow events considered, those with annual exceedance probabilities of 10% or less, occurred during generally wet periods and were sufficiently extreme that they still resulted in development of surface and near surface saturation on the restored floodplain even with lowered inputs from restored hillslopes. Infiltration and alluvial aquifer recharge on restored alluvial fans predicted during wet periods further contributed to antecedent wetness, amplifying the effect. Areas of near surface saturation reduced the capacity of the floodplain to reduce the flood peak reaching the catchment outlet by resulting in saturation excess and infiltration excess surface runoff on the floodplain during the large rainfall event and reducing infiltration losses of overbank flows crossing the floodplain surface.

Modeling uncertainties in this study reduced the ability for change detection, particularly in baseflow responses, and could be addressed with further local sampling to reduce model parameter uncertainty. Scenario comparisons highlighted the sensitivity of the modeled impacts of restoration to the estimated rate of mountain bedrock recharge of the alluvial aquifer. If this recharge source were much smaller than estimated, it is possible that the floodplain aquifer levels, channel connectivity, and baseflow would have been more sensitive to changes in alluvial aquifer recharge from overbank flooding. This would have meant that the impacts of channel restoration would have been more sensitive to changes in runoff due to hillslope vegetation. It also may have resulted in changes in baseflow response patterns between scenarios. The water table would have declined more in dry periods in the absence of overbank flows and channel infiltration recharge and rates of drainage due to channel depth may have been more important to determining the degree of aquifer-channel connectivity. These subsurface recharge rates are difficult to estimate from aquifer physical properties because of the irregular fracture network of the TMG quartzitic sandstones and cemented faults and layering of aquicludes creating springs and potentially unconnected aquifers (Xu et al., 2009). In model development for the Baviaanskloof, this was conceived of as a simple linear reservoir with outflow rates parameterized through calibration against floodplain groundwater level and streamflow data. Multicriteria calibration against multiple data sources was used to improve likely accuracy and ensemble modeling within the resulting accepted range of parameter values was used to carry forward model uncertainty into scenario modeling predictions, however further field data could be used in future to further test and improve model representation of this key process.

Further geomorphic study in the Baviaanskloof and similar catchments would be needed to better determine likely future states. Given the current levels of uncertainty and process simplifications in the model, the scenarios of restoration considered were extreme in their spatial extent to increase the likelihood of change detection. Actual restoration interventions implemented may be smaller and occur more slowly. There was also no consideration of the temporal dimension of the proposed changes. Different modeled scenarios of individual and combined changes could represent different stages in the future of the catchment due to both phased implementation of active restoration interventions and geomorphic landscape evolution occurring over time in response different activities. In addition, potential vegetation change on the floodplain, which may occur given the shallower water table in the restored channel scenario. It was assumed that while the type of vegetation present would likely change, this may not result in a very significant change in floodplain AET to that predicted here as the floodplain vegetation was already assumed to have a high ET demand and access to the water table. However this assumption could be tested in further studies.

Regardless of its accuracy in quantifying specific outcomes for the Baviaanskloof catchment, it can be reasonably assumed that the model used here represents a likely set of processes and combinations of connectivity thresholds for a semi-arid, mountainous catchment. The results of this study are therefore useful as a demonstration of the sensitivity of catchment hydrology in this type of area to the types of changes and combinations of changes considered. In this setting the dominant impact of large scale vegetation change on the overall yield of the catchment stood out above the other changes. The channel form

played a significant role in determining the long-term average floodplain groundwater depth, which was less sensitive to the vegetation change than might have been expected because of the less vulnerable, long-term floodplain aquifer recharge from the mountain block aquifer. Daily peak flow responses were vulnerable to interacting thresholds dictated by both the vegetation and channel network properties, determining surface runoff production from the hillslopes, initiation and extent of overbank flooding, wetness and infiltration capacity of the fans and floodplain during the event.

Part of the motivation for exploring the combination of hillslope, fan, and floodplain restoration interventions for the Baviaanskloof was because it represents full implementation of recently proposed activities for the area motivated by concerns about the loss of biodiversity and multiple ecosystem services in the region and concerns about regional water supply security in particular (Jansen, 2008; Mander et al., 2010). While the modeling results in this study suggest that full restoration would likely result in a decrease in the long-term annual average yield at the catchment outlet, predicting the quantitative impacts on realized downstream water supply availability will require further integration of these predictions into models of the water supply systems, as well as consideration of sediment transport to the downstream reservoir. The actual decrease in available supply with restoration would likely be smaller than the predicted decreases in average annual streamflow yield for several reasons. Firstly, predicted decreases in streamflow were greater for wet years and large flow events than for dry periods. Currently the downstream Kouga Dam reservoir routinely overflows in wet years and so decreased flows during these periods

may not result in an actual decrease in available supply. In addition, the large decrease in peak flows (56-60%) with restoration would likely result in a reduction in sediment transport to the reservoir, which would otherwise cause a loss in storage capacity over time. Nevertheless, model results representing the current understanding of catchment processes in the Baviaanskloof given available data, indicate a decrease and not an increase in yield available to downstream users given the catchment-wide full restoration scenario modeled here.

Results did indicate that restoration could improve water access for those living within the catchment who rely on pumping from floodplain aquifer and recreate floodplain wetland habitat, however local catchment residents would also likely be more subject to impacts of floodplain inundation. Again the modeling results of this study would need further comparison against local pumping requirements and costs and infrastructure, agriculture, and community flood vulnerabilities to be able assess tradeoffs of local wetland habitat benefits, local water supply benefits, local flood impacts, downstream water supply losses, and downstream flood impact reductions. In this case it is notable that thicket restoration alone was predicted to result in a deepening of the floodplain aquifer and reduction in inundation, while the combined restoration scenario results indicated a net rise in the water table and increase inundation. If further geomorphic studies indicate that active thicket restoration alone would not result in floodplain channel aggradation and that increasing groundwater access and wetland habitat were priorities, actively establishing a less incised river channel would be beneficial. Restoring the floodplain channel alone was predicted to

increase groundwater tables more than when hillslope thicket was also restored, however inundation impacts would be greater if thicket was not simultaneously restored. Tradeoffs are inevitable; however, this modeling exercise demonstrated that exploration of combined impacts of different restoration activities could yield an overall preferred scenario and more accurate prediction of impacts than considering different interventions in isolation. Further work could be done modeling different degrees and spatial configurations of hillslope, alluvial fan, and floodplain channel restoration deemed geomorphologically feasible to identify scenarios best meeting multiple catchment management objectives.

6.5 Conclusion

This modeling study of various restoration scenarios in the Baviaanskloof, a mountainous, semi-arid, meso-scale catchment, showed the importance of modeling changes to both vegetation and to channel properties together in this type of setting when these changes are likely to coincide due to geomorphological processes and/or diverse human activities. It was found that the modeled impacts of restoring hillslope thicket vegetation on water yields, flood peaks, and floodplain groundwater levels were significantly different depending on whether or not the channel network crossing the central valley alluvial fans and floodplain was predicted to change concurrently. Downslope geomorphologic effects of upslope changes, such as the impact land cover change on stream channels, are becoming increasingly well understood, however this is not yet being routinely incorporated into hydrologic modeling. While dynamically coupled eco-hydro-geomorphological models may

still be a long way off, conceptual models of local geomorphological responses can be incorporated through multiple static scenarios, as done here, to at least consider the potential impacts of combined changes or the level of prediction uncertainty introduced due to uncertain future geomorphic trajectories. This understanding may critically impact catchment management decisions. For example, in the Baviaanskloof, if widespread hillslope thicket restoration could result in aggradation in the floodplain channel over time due to reduced peak flow intensities, the average floodplain groundwater table would likely rise from its current state, increasing wetland habitat, local groundwater supply access, and local inundation impacts. If the channel is not predicted to change, and/or is predicted to incise further due to reduced sediment load, the groundwater table would be predicted drop with thicket restoration, having the opposite impact on conditions in the floodplain.

It is also not uncommon for different types of active anthropogenic interventions in different parts of a landscape to be planned independently by separate actors in a large catchment based on conceptual understandings of the independent effects of the activity. This study demonstrated the importance of modeling combined impacts of multiple planned interventions together. A cascade of surface and subsurface flow connectivity thresholds was observed and modeled for the Baviaanskloof, and the high variability rainfall pattern meant that these thresholds are only episodically met. As a result the combined impacts of different interventions at different locations were sometimes more complex than the sums of their parts. For example, in a scenario in which hillslope thicket, alluvial fans, and the floodplain channel were all restored in the Baviaanskloof, the predicted flood peak reduction

was less than the sum of predicted reductions from each intervention assumed to occur alone within the current catchment context. The combined effect of alluvial fan recharge and decreased aquifer drainage with the smaller floodplain channel resulted in near saturated conditions over more of the floodplain during very large flow events, reducing its capacity to buffer flood peaks even though it received less flow from surrounding restored hillslopes. This also highlighted the importance of developing locally appropriate conceptual models of these connections and thresholds when modeling change in a semi-arid meso-scale catchment setting.

This study demonstrated likely tradeoffs that would need to be considered when holistically planning restoration in the Baviaanskloof. It was predicted that restoring the hillslopes, fans, and floodplain together would result in a decrease in average annual water yield, peak flow, and baseflow with more AET predicted on both the hillslopes and floodplain. This could decrease water supply to downstream users although potentially increase quality and reduce downstream flood impacts. The groundwater table in the floodplain and floodplain inundation were also predicted to rise in this scenario, likely making groundwater supplies more accessible within the catchment and likely increasing floodplain wetland habitat, but also increasing local flooding impacts. This study demonstrated how different combinations of interventions could result in significantly different impacts. Further modeling of combinations and spatial extents of interventions could assist in balancing different catchment management objectives.

6.6 References

Ajami, H., Troch, P.A., Maddock, T., Meixner, T., and Eastoe, C. (2011). Quantifying mountain block recharge by means of catchment-scale storage-discharge relationships. Water Resour. Res. *47*, n/a – n/a.

Arnold, J.G., Allen, P.M., Volk, M., Williams, J., and Bosch, D.D. (2010). Assessment of different representations of spatial variability on SWAT model performance. Trans. ASAE *53*, 1433–1443.

Balling, R., and Wells, S. (1990). Historical Rainfall Patterns and Arroyo Activity Within the Zuni River Drainage-Basin, New-Mexico. Ann. Assoc. Am. Geogr. *80*, 603–617.

Beechie, T.J., Pollock, M.M., and Baker, S. (2008). Channel incision, evolution and potential recovery in the Walla Walla and Tucannon River basins, northwestern USA. Earth Surf. Process. Landf. *33*, 784–800.

Bobbins, K.L. (2011). Developing a form-process framework to describe the functioning of semi-arid alluvial fans in the Baviaanskloof Valley, South Africa.

Booth, D. (1990). Stream-Channel Incision Following Drainage-Basin Urbanization. Water Resour. Bull. *26*, 407–417.

Bosch, J.M., and Hewlett, J.D. (1982). A review of catchment experiments to determine the effect of vegetation changes on water yield and evapotranspiration. J. Hydrol. *55*, 3–23.

Bravard, J., Amoros, C., Pautou, G., Bornette, G., Bournaud, M., Creuzé des Châtelliers, M., Gibert, J., Peiry, J., Perrin, J., and Tachet, H. (1997). River incision in south-east France: morphological phenomena and ecological effects. Regul. Rivers Res. Manag. *13*, 75–90.

Brown, A.E., Zhang, L., McMahon, T.A., Western, A.W., and Vertessy, R.A. (2005). A review of paired catchment studies for determining changes in water yield resulting from alterations in vegetation. J. Hydrol. *310*, 28–61.

Cowling, R.M., and Mills, A.J. (2011). A preliminary assessment of rain throughfall beneath Portulacaria afra canopy in subtropical thicket and its implications for soil carbon stocks. South Afr. J. Bot. *77*, 236–240.

Essaid, H.I., and Hill, B.R. (2014). Watershed-scale modeling of streamflow change in incised montane meadows. Water Resour. Res. *50*, 2657–2678.

Euston-Brown, D.I.W. (2006). Baviaanskloof Mega-Reserve Project: Vegetation mapping contract report on methodology, vegetation classification and short descriptions of habitat units (South Africa: Eastern Cape Parks & Tourism Agency).

Gomez, B., Eden, D.N., Peacock, D.H., and Pinkney, E.J. (1998). Floodplain construction by recent, rapid vertical accretion: Waipaoa River, New Zealand. Earth Surf. Process. Landf. *23*, 405–413.

Gregory, K.J. (2006). The human role in changing river channels. Geomorphology *79*, 172–191.

Hammersmark, C., Rains, M., and Mount, J. (2008). Quantifying the hydrological effects of stream restoration in a montane meadow, northern California, USA. RIVER Res. Appl. *24*, 735–753.

Hammersmark, C.T., Dobrowski, S.Z., Rains, M.C., and Mount, J.F. (2010). Simulated Effects of Stream Restoration on the Distribution of Wet-Meadow Vegetation. Restor. Ecol. *18*, 882–893.

Hargreaves, G., and Samani, Z. (1982). Estimating potential evapotranspiration. J. Irrig. Drain. Div.-Asce *108*, 225–230.

He, M., and Hogue, T.S. (2012). Integrating hydrologic modeling and land use projections for evaluation of hydrologic response and regional water supply impacts in semi-arid environments. Environ. Earth Sci. *65*, 1671–1685.

Hipsey, M.R., Vogwill, R., Farmer, D., and Busch, B.D. (2011). A multi-scale ecohydrological model for assessing floodplain wetland response to altered flow regimes (Christchurch: Modelling & Simulation Soc Australia & New Zealand Inc).

James, L.A., and Marcus, W.A. (2006). The human role in changing fluvial systems: Retrospect, inventory and prospect. Geomorphology *79*, 152–171.

Jansen, H.C. (2008). Water for Food and Ecosystems in the Baviaanskloof Mega Reserve: Land and water resources assessment in the Baviaanskloof (Wageningen, The Netherlands: Alterra).

Karen, I. (2009). A top–down approach to characterise aquifer–river interaction processes. J. Hydrol. *365*, 145–155.

Keesstra, S.D., van Huissteden, J., Vandenberghe, J., Van Dam, O., de Gier, J., and Pleizier, I.D. (2005). Evolution of the morphology of the river Dragonja (SW Slovenia) due to land-use changes. Geomorphology *69*, 191–207.

Lechmere-Oertel, R.G., Kerley, G.I.H., and Cowling, R.M. (2005a). Patterns and implications of transformation in semi-arid succulent thicket, South Africa. J. Arid Environ. *62*, 459–474.

Lechmere-Oertel, R.G., Cowling, R.M., and Kerley, G.I.H. (2005b). Landscape dysfunction and reduced spatial heterogeneity in soil resources and fertility in semi-arid succulent thicket, South Africa. Austral Ecol. *30*, 615–624.

Loheide, S.P., and Booth, E.G. (2011). Effects of changing channel morphology on vegetation, groundwater, and soil moisture regimes in groundwater-dependent ecosystems. Geomorphology *126*, 364–376.

Loheide, S.P., and Gorelick, S.M. (2007). Riparian hydroecology: A coupled model of the observed interactions between groundwater flow and meadow vegetation patterning. Water Resour. Res. *43*, 16 PP.

van Luijk, G., Cowling, R.M., Riksen, M.J.P.M., and Glenday, J. (2013a). Hydrological implications of desertification: Degradation of South African semi-arid subtropical thicket. J. Arid Environ. *91*, 14–21.

van Luijk, G., Cowling, R.M., Riksen, M.J.P.M., and Glenday, J. (2013b). Hydrological implications of desertification: Degradation of South African semi-arid subtropical thicket. J. Arid Environ. *91*, 14–21.

Lynch, S.D. (2003). Development of a Raster Database of Annual, Monthly and Daily Rainfall for Southern Africa (Pretoria, South Africa: Water Research Commission (WRC)).

Mander, M., Blignaut, J., van Niekerk, M., Cowling, R.M., Horan, M., Knoesen, D., Mills, A.J., Powell, M., and Schulze, R.E. (2010). Baviaanskloof-Tsitsikamma Payment for Ecosystem Services: A Feasibility Assessment (South Africa: FutureWorks report for South African National Biodiversity Institute (SANBI)).

Maneta, M., Schnabel, S., and Jetten, V. (2008). Continuous spatially distributed simulation of surface and subsurface hydrological processes in a small semiarid catchment. Hydrol. Process. *22*, 2196–2214.

Meijninger, W.M.L., and Jarmain, C. (2014). Satellite-based annual evaporation estimates of invasive alien plant species and native vegetation in South Africa. Water SA *40*, 95–108.

Midgley, J.J., and Scott, D.F. (1994). Use of stable isotopes of water (d and o-18) in hydrological studies in the Jonkershoek valley.

Mills, A.J., and Cowling, R.M. (2010). Below-ground carbon stocks in intact and transformed subtropical thicket landscapes in semi-arid South Africa. J. Arid Environ. *74*, 93–100.

Mills, A. j., and Fey, M. v. (2004). Effects of vegetation cover on the tendency of soil to crust in South Africa. Soil Use Manag. *20*, 308–317.

Mirchi, A., Watkins, D., and Madani, K. (2010). Modeling for Watershed Planning, Management, and Decision Making (Hauppauge: Nova Science Publishers, Inc).

Ohara, N., Kavvas, M.L., Chen, Z.Q., Liang, L., Anderson, M., Wilcox, J., and Mink, L. (2014). Modelling atmospheric and hydrologic processes for assessment of meadow restoration impact on flow and sediment in a sparsely gauged California watershed. Hydrol. Process. *28*, 3053–3066.

Osterkamp, W.R., and Hupp, C.R. (2010). Fluvial processes and vegetation - Glimpses of the past, the present, and perhaps the future. Geomorphology *116*, 274–285.

Powell, R. (2015). Recent degradation along the upper-middle reaches of the Baviaanskloof River-floodplain: An examination of drivers of change and best rehabilitation practices. PhD dissertation. Rhodes University.

Price, K. (2011). Effects of watershed topography, soils, land use, and climate on baseflow hydrology in humid regions: A review. Prog. Phys. Geogr. *35*, 465–492.

Refsgaard, J.C., and Storm, B. (1995). MIKE SHE. In Computer Models of Watershed Hydrology, V.P. Singh, ed. (Water Resources Publications), pp. 809–846.

Roets, W., Xu, Y., Raitt, L., and Brendonck, L. (2008). Groundwater discharges to aquatic ecosystems associated with the Table Mountain Group (TMG) aquifer: A conceptual model. Water SA *34*, 77–88.

Schulze, R.E., and Maharaj, M. (2004). Development of Database of Gridded Daily Temperature for Southern Africa (Pretoria, South Africa: Water Research Commission (WRC)).

Sigwela, A.M., Kerley, G.I.H., Mills, A.J., and Cowling, R.M. (2009). The impact of browsing-induced degradation on the reproduction of subtropical thicket canopy shrubs and trees. South Afr. J. Bot. *75*, 262–267.

Smit, S. (2013). Observation of changes in vegetation cover density in the Baviaanskloof catchment using field sampling and remotely sensed NDVI (Normalized Difference Vegetation Index). BSc Thesis. University of Applied Science Van Hall Larenstein.

Soltau, L., Smith-Adao, L., and Bugan, R. (2011). Baviaanskloof resistivity survey to define water level and depth to bedrock (Stellenbosch, South Africa: Center for Scientific and Industrial Research (CSIR)).

Tague, C., Valentine, S., and Kotchen, M. (2008). Effect of geomorphic channel restoration on streamflow and groundwater in a snowmelt-dominated watershed. Water Resour. Res. *44*, 10 PP.

Uhlenbrook, S., Roser, S., and Tilch, N. (2004). Hydrological process representation at the meso-scale: the potential of a distributed, conceptual catchment model. J. Hydrol. *291*, 278–296.

Wheaton, J.M., Gibbins, C., Wainwright, J., Larsen, L., and McElroy, B. (2011). Preface: Multiscale Feedbacks in Ecogeomorphology. Geomorphology *126*, 265–268.

Xu, Y., Titus, R., Holness, S.D., Zhang, J., and Tonder, G.V. (2002). A hydrogeomorphological approach to quantification of groundwater discharge to streams in South Africa. Water SA *28*, 375–380.

Xu, Y., Wu, Y., and Beekman, E.H. (2003). The role of interflow in estimating recharge in mountainous catchments. In Groundwater Recharge Estimation in Southern Africa, Y. Xu, and E.H. Beekman, eds. (Paris, France: UNESCO),.

Xu, Y., Lin, L., Jia, H., South Africa., and Water Research Commission. (2009). Groundwater flow conceptualization and storage determination of the Table Mountain group (TMG) aquifers: report to the Water Research Commission (Gezina, Pretoria: Water Research Commission]).

Chapter 7 Conclusions and recommendations for further research

This dissertation comprised multiple studies through which a hydrologic model was developed for the Baviaanskloof, a semi-arid, mountainous, meso-scale catchment area (Chapters 1 and 2), and this model was further used to estimate the hydrologic impacts of degradation and restoration of three different components of the landscape: hillslope vegetation, alluvial fans, and the floodplain channel. Potential impacts on catchment outlet streamflow and floodplain groundwater levels were modeled for each change individually (Chapters 3-5) and for all three in combination (Chapter 6). The model development and the findings presented in this dissertation contribute to the field of hydrologic modeling, particularly for semi-arid areas and meso-scale catchments, and have import for catchment management and restoration planning in this type of environment. Particular contributions and ideas for further research based on this work are described below.

7.1 Hydrologic modeling of semi-arid meso-scale catchments

Through the process of developing of a model appropriate for assessing targeted restoration impacts in the Baviaanskloof catchment, this research contributes to ongoing development of modeling strategies suited to semi-arid mountainous meso-scale catchments.

Semi-arid catchments have generally proven more challenging to model accurately compared to more humid areas (Ackerman et al., 2005; Clark et al., 2008; He and Hogue, 2012; Maneta et al., 2008) and modeling meso-scale catchments (10-1,000 km^2) can also require greater model complexity than smaller catchments to achieve similar performance (Tetzlaff et al., 2008, 2010; Uhlenbrook et al., 2004). Many commonly used hydrologic model structures were developed and tested in smaller more humid catchments, while development of model structures better able to represent processes typical of semi-arid catchments has been more recent and more work and testing are needed. Modeling the Baviaanskloof required application of several novel approaches including use of a multi-scale model, to address the need for different levels of process representation in different parts of the catchment, and explicit consideration of alluvial fan processes in the model, a landform that is not specifically catered for in most medium complexity catchment models.

7.1.1 Multi-scale model development

The model development method applied in the Baviaanskloof case-study and the resulting multi-scale modeling approach have rarely been documented for this type of catchment and successful model calibration suggests that they could be beneficial in future research on semi-arid meso-scale catchments. In more arid areas, thresholds of surface flow connectivity throughout a catchment are only episodically met and large portions of flows reaching the catchment outlet may pass through complex surface-subsurface flow paths. In larger semi-arid catchments with sizeable lowland alluvial fill deposits, such as fans and

floodplains, these deposits are seldom saturated. They therefore act as buffers to surface flow such that surface-subsurface interactions between alluvial aquifers and channel networks play a large role in streamflow magnitude and timing (Ajami et al., 2011; Karen, 2009; Maneta et al., 2008). The challenges of capturing the complex flow paths and patterns of more arid catchments have often been addressed by modeling processes at higher spatial resolutions using gridded models (Clark et al., 2008; Maneta et al., 2008). Gridded models allow for more sophisticated, spatially explicit, consideration of infiltration along surface flow paths and local development of saturation in the landscape. They also allow for coupling of surface, groundwater, and hydraulic flow models that can capture temporally dynamic groundwater-channel interactions as well as overbank flooding. These elements can be critical to capturing semi-arid meso-scale catchment responses with desired accuracy levels. However, distributed gridded models can prove computationally intensive when modeling large catchment areas over long time periods. In addition, at larger catchment scales with more diverse landforms, geology, soils, and vegetation, sufficient data with which to calibrate a distributed model are often not available.

To develop a conceptual and numeric model of the 1,234 km^2 Baviaanskloof catchment, a partially data-driven 'downward' or 'top-down' approach (Chirico et al., 2003; Sivapalan et al., 2003; Young, 2003) was applied to determine levels of spatial and process discretization warranted by available data and characterize connectivity between discretized units, while also incorporating model structure requirements for detecting impacts of vegetation and channel changes (Chapter 1). Available climate, hillslope soil moisture and surface runoff,

floodplain groundwater, and streamflow data were assessed for patterns that would indicate when and how surface and subsurface flow paths between land units were active. It was found that, in the Baviaanskloof, interflow and bedrock aquifer outflow from mountainous areas surrounding the central valley floodplain were all important in recharging the floodplain aquifer, the level of which was important in determining catchment outlet streamflow. The importance of reasonably accurate characterization of this pattern of surface and subsurface flows reaching the floodplain was highlighted when the model was further used to look at change scenarios. For example, modeled antecedent floodplain groundwater depth proved to be an important factor in determining predicted catchment scale runoff in large flood events and the sensitivity of catchment flows not only to changes in the floodplain channel, but also to changes in hillslope vegetation and alluvial fans (Chapters 3-6).

A multi-scale model was proposed to address the need for higher resolution consideration of processes occurring in the floodplain, and the comparative data scarcity regarding processes occurring within the contributing mountain areas. Due to the size of the catchment and limited data on processes over much of the mountainous area, a relatively coarse scale hydrologic response unit (HRU) sub-model was applied to the mountain tributary subcatchments, using simple linear reservoirs to represent interflow and bedrock aquifer flow lumped by subcatchment. In this sub-model surface flow was routed across a catena of topographically defined HRUs. Surface and subsurface outflows from the subcatchments were then input into a higher resolution, gridded model of the central valley

alluvial fans and floodplain which allowed for temporally dynamic estimation of flow exchange between the alluvial aquifer and the floodplain channel based on relative water surface elevations and alluvial aquifer conductivity.

This multi-scale model reduced computational and calibration demands while still allowing for consideration of the finer scale floodplain processes expected to change in the alluvial fan and floodplain channel scenarios to be assessed. To the author's knowledge only (Hipsey et al., 2011) have published work on development of a similar multi-scale model of a semi-arid meso-scale catchment, however their study did not include a quantitative assessment of model output against observed data. After multi-criteria calibration of the parameter space against observed patterns in the streamflow and groundwater data (Chapter 2), the Baviaanskloof model was able to reproduce 2012-2013 observed daily streamflow with a Nash-Sutcliffe efficiency (NSE) of 0.87-0.92 and 1991-2013 monthly streamflow with an NSE of 0.79-0.85, predict mean flow within 0.5 m^3/s and maximum monthly flows within 1 m^3/s of the observed, and estimate floodplain groundwater fluctuations with an R^2 of 0.79-0.81 and an accuracy in the range of depth fluctuation within 0.5 m of the observations. Daily streamflow responses to minor rainfall events were over-estimated, but monthly flow errors did not show a systematic bias. During the multi-criteria calibration, additionally selecting for parameters sets that improved model representation of low flows and floodplain groundwater levels also served to improve average model performance against indicators of peak flows and overall flow patterns, rather than creating a significant performance tradeoff. The lack of major performance tradeoffs between different criteria

provided further support for the model's representation of different processes in the Baviaanskloof.

While there was room for improvement, these results indicated that this model structure was capable of recreating the catchment's streamflow and floodplain groundwater level responses to weather patterns to a degree considered useful for further application in estimating potential impacts of large scale changes. Remaining uncertainties in parameter values, which also represent potential structural inaccuracies, were brought into the scenario modeling assessment through application of ensembles of parameter sets for each scenario. Regardless of the model's local streamflow accuracy, it can be considered representative of a likely set of patterns of processes and flow path connectivities for a semi-arid, mountainous, meso-scale catchment with which to explore potential patterns of change in response to different types of degradation and restoration in this kind of environment.

Further research could be done to more fully assess the benefits and drawbacks of this model structure in the Baviaanskloof and other catchments. Different means of representing processes and landscape connectivity in the Baviaanskloof were considered in the model development process and selections made based on patterns in the available observation data as described in Chapter 1; however, alternative model structures were not quantitatively tested. Comparing the performance of a fully gridded model, in which surface and subsurface processes in the mountain subcatchments were also calculated at the grid cell level, and an entirely HRU-scale model, in which processes on alluvial fans and floodplains

and their channel interactions were also calculated at the level of the entire land unit, with the model structure used here would quantitatively test the capabilities of different structures in this kind of catchment setting. Computational requirements could also be compared. Each model type would need to be calibrated using the same procedure and surface and groundwater prediction performance requirements, allowing comparison of the resulting performance and parameter uncertainties given the level of data available with which to assess the model. Comparisons of changes in relative performance amongst model structures when using different types and amounts of data in the calibration would also be of use in demonstrating and providing guidance on model structure suitability given different levels of data availability. Ensemble model structure testing studies have been done for smaller and more data-rich catchments using simpler model structures (e.g. (Clark et al., 2008)); however are less apparent for meso-scale catchments or for assessments of model fit to data availability.

7.1.2 Alluvial fan modeling

Another contribution of this research towards modeling semi-arid mountainous catchments was the development of a model structure that included surface and subsurface processes of alluvial fans. Models of alluvial fans and their contributing catchment areas have been developed with different levels of complexity (Blainey and Pelletier, 2008; Herron and Wilson, 2001; Houston, 2002, 2002; Mukhopadhyay et al., 2003; Munevar and Marino, 1999; Niswonger et al., 2005), but to the author's knowledge there are no published

studies in which alluvial fans have been explicitly modeled as landscape elements within their larger catchment contexts. In the Baviaanskloof model, alluvial fans were a continuous part of the gridded surface and groundwater flow sub-model of the central valley alluvial fill. Using a gridded model with explicit topography for surface flow handling allowed for the convex shapes of the fans to result in dispersive flow and infiltration across the fan surfaces if and when flows exceeded defined channel capacities. Negligible channel capacities were applied to simulate unchannelized fans, such that there was no channelized connection of surface flow between the mountain tributary subcatchment outlet and the main trunk channel in the floodplain.

Scenarios with different alluvial fan channel properties were modeled to estimate impacts of human alteration and potential restoration of these forms on streamflow and groundwater in the Baviaanskloof (Chapter 4). The changes detected between scenarios also give an indication of the importance of the explicit consideration of alluvial fans in the model. The scenario in which all alluvial fans were given channelized connections to the main floodplain channel can be considered similar to a model in which alluvial fans were not included and landscape topography was assumed convergent because flows were rarely predicted to exceed the assumed channel capacity and disperse across the fan surface in this scenario. Comparing this scenario to one in which the majority of fans in the Baviaanskloof were assumed to have generally dispersive flow paths across their surfaces, showed that failure to consider the buffering impact of alluvial fans on surface flows could significantly alter model predictions of key hydrologic outcomes. Results indicated that, in a catchment

with similar characteristics, not including alluvial fan processes in a model could result in an overestimation of average annual catchment water yield in the range of 7-21%, overestimation of flood peaks on the order of 15-24%, underestimation of minimum monthly flows by close to 10%, and overestimating the depth the average floodplain water table depth by 3-6%. Such inaccuracies could arise when modeling ungauged catchments for which calibration is not possible. If a model that did not include alluvial fans were calibrated against sufficient observational data, such inaccuracies could be avoided in as much as the impacts of the fans could be implicitly considered through adjustment of parameters for processes of other landscape elements dictating infiltration and recharge of the floodplain aquifer. However, important prediction inaccuracies could still arise should this model be further applied outside of the conditions under which it was calibrated.

The accuracy of model handling of alluvial fan processes was not explicitly tested in this study and could the focus of future research. In the case of the Baviaanskloof catchment, ability to determine the realism in the representation of the fans was limited by limited data on fan surface flow and groundwater levels. Obtaining useful quantities of data on flows on alluvial fans in this setting provides a challenge because surface flows were infrequent and groundwater levels were relatively deep. However by modeling fans as part of a larger catchment model, data on floodplain groundwater and streamflow downstream of the fans can assist in constraining fan parameterization in a calibration exercise. Longer time-series and more spatially distributed data would better allow for this compared to what was

available for the Baviaanskloof, which was why alluvial fan and floodplain soils and vegetation were considered together in this study with only the topography differing.

7.1.3 Multi-criteria model calibration and sources of uncertainty

Multi-criteria calibration techniques have typically been applied to smaller and more data-rich catchments (Efstratiadis and Koutsoyiannis, 2010), despite the potential for these procedures to be particularly beneficial for complex models needed for semi-arid meso-scale catchments and in cases with limited available streamflow data. Application to the Baviaanskloof catchment demonstrated benefits of multi-criteria model calibration with multiple data types in reducing parameter uncertainty and increasing model performance, particularly in better capturing observed patterns of low flows and water table depths (Chapter 2). Only a relatively short two year dataset of gauged daily streamflow was available for the catchment; however, other available data at other spatial and temporal scales were used to both test and improve model performance. Parameter ranges were calibrated for the Baviaanskloof model using thresholds of accepted model performance for recreating observed patterns in catchment outlet streamflow data, channel flow connectivity through the floodplain, floodplain groundwater levels, and subcatchment surface flow occurrence.

A notable output of this process was the significant increase in model performance across the various measures that resulted when additional criteria based only on the short

gauged streamflow record were included in the calibration, as opposed to using a single measure of overall fit. When thresholds of Nash-Sutcliffe efficiency (NSE) for logged daily streamflow, absolute error in daily flow, and absolute error in maximum monthly flow were also included in the calibration procedure, in addition to the NSE of untransformed daily streamflow, the performance of the accepted model set improved not only in terms of these additional measures, but also in terms of recreating patterns of groundwater table fluctuations in the floodplain aquifer. This was in part due to the linkage between floodplain aquifer levels and baseflow observed in the catchment and included in the model structure. The accuracy of low flow values has more weight in determining the NSE of logged streamflow compared to using untransformed flow. Inclusion of this criterion selected for models better representing low flows, hence better representing groundwater patterns.

Additional inclusion of criteria directly based on groundwater level observations and other data types did result in further improvements in performance and narrowing of the accepted parameter space for the Baviaanskloof model, but the improvement was small after the additional streamflow based criteria had been applied. This suggests that, in cases when only catchment outlet streamflow exists with which to calibrate a model, inclusion of multiple criteria selecting for models that recreating a variety of patterns in the streamflow data has the potential to improve model representation of internal processes, within the limitations of the model structure. In the Baviaanskloof case this was observed even when the available gauged streamflow data was relatively short.

Remaining inaccuracies in the Baviaanskloof model could be addressed through further research and data collection. There was a ceiling of performance seen in the distribution of the performance measures of all the parameter sets tried in the calibration exercise. In addition, minor trade-offs in performance between criteria occurred, such as exclusion of some better performing models in terms of recreating groundwater level patterns, although mean accepted set performance remained unchanged or improved (Chapter 2). Performance limitations could represent inaccuracies in the model structure, the parameter values applied, and the observational data to which the models were compared. A likely major source of unquantified uncertainty was the assumed catchment scale precipitation, derived from extrapolation of station data to subcatchment areas using monthly regional multi-factor regression based precipitation surfaces (Lynch, 2003). Some models include precipitation adjustment factors as calibration parameters, which was not done in this study. As such potential inaccuracies in precipitation would be incorporated into adjustments in the other parameter values, such as infiltration and evaporation rates, in as much as adjustments to these processes would account for over or underprediction of rainfall. A potentially fruitful area of further research for this and other semi-arid meso-scale catchments, in which the spatial distribution of rainfall is particularly important, would be comparing precipitation estimates of satellite based products such as NASA's TRMM (Tropical Rainfall Measuring Mission) data-set to station data and model calibration and performance using different sets.

Some of the criteria and thresholds of acceptability used in the calibration procedure for the Baviaanskloof were selected to represent the need for accuracy in certain model outputs to be of use in a management context. In this case the assumed focus was on water supply management for those living within the Baviaanskloof catchment area, relying on floodplain groundwater, and those living downstream, relying on streamflow at the catchment outlet which contributes to a regional supply reservoir. Published multi-criteria model calibration studies have tended to select model performance measures based on available data types with goals of optimizing model realism in representation of certain catchment processes, but without a specific applied use of the model outputs being considered. As such model selection criteria have been somewhat arbitrary (Seibert and McDonnell, 2002). An exception is the Management-Objectives-Constrained Analysis of Uncertainty (MOCAU) approach proposed in (Zheng and Keller, 2007a, 2007b), in which models are assessed specifically based on their accuracy in prediction of selected outcomes that directly lead to management decisions. In their example models were assessed for accuracy in prediction of exceedance of legal water quality thresholds against an observed dataset, an outcome triggering activities to reduce point and non-point pollutant sources.

Methods for considering management objectives in model calibration and assessment of suitability warrant further development and application. This was touched upon in this study, but further work could be done in the Baviaanskloof case to define model performance criteria that would assess whether or a not the model was fit-for-purpose to inform decisions pertinent to a range of potential catchment management objectives, such as

ensuring water supply for human use locally and regionally as well as ensuring environmental flows, managing flood risks, and protecting and restoring floodplain wetland habitat. Further refining the Baviaanskloof model structure and parameterization to improve performance against an array of criteria would likely require further field data on different catchment processes. An assessment of model performance sensitivities to different parameters using management based criteria would highlight what kinds of field sampling would be most directly beneficial to management, which could help secure support for the work.

7.2 Catchment management and restoration planning

Modeling studies in this dissertation demonstrated the sensitivity of long-term average catchment scale water yield, flood peaks, low flows, and floodplain groundwater levels to changes in hillslope vegetation cover, alluvial fan surfaces, and the form of the central floodplain channel in the Baviaanskloof catchment. In general, restoration in all of these landscape elements to assumed pre-agricultural use states was predicted to result in greater retention of water within the landscape, greater vegetation water use, and reduced flood peaks and average yields at the catchment outlet. Restoration of hillslope vegetation cover was predicted to have the largest impact in reducing flood peaks (56-60%) and yields (22-27%), and when implemented alone, was also predicted to result in a decline in groundwater levels (6-10%, Chapter 3). Floodplain channel restoration had the largest impact on the floodplain groundwater level, resulting in a significant rise in the average water table (17-

21%), without resulting in a large decrease in overall yield (Chapter 5 and 6). When both hillslope vegetation and fan and floodplain channel network restoration were assumed to occur together a rise in the average floodplain groundwater table (8-11%) was predicted, despite the decrease in water yield from the surrounding hillslopes (Chapter 6). A notable increase in baseflow was not predicted in any restoration scenario (Chapters 3-6).

These results have implications for land use, restoration, and water supply management in the Baviaanskloof, and demonstrate likely patterns of response for similar semi-arid, mountainous, meso-scale catchments. These studies make a contribution to understanding of the catchment impacts of human induced changes in vegetation cover and channel networks, particularly needed in more vulnerable semi-arid settings. Novel contributions were catchment-scale assessment of the impacts of alluvial fan alterations and of the loss and restoration of Southern African subtropical thicket. This research demonstrated the importance of considering catchment connectivity of hydrologic and sediment flow paths, in terms of linked changes in vegetation and channel properties, when predicting impacts of future scenarios. The semi-distributed nature of the model structure allowed for an assessment of hydrologic impacts at different locations within the catchment, rather than only the catchment outlet, which highlighted tradeoffs to be considered between local and downstream benefits and drawbacks of proposed restoration changes.

The effects of both changes in vegetation cover change and floodplain channel form on streamflow, particularly on baseflow, have previously been observed to be context specific,

dependent on climate, geology, geomorphology, vegetation types, and the extent of the change. Increases in vegetation cover generally reduce flow peaks, but can either increase or decrease baseflow (Bosch and Hewlett, 1982; Brown et al., 2005; Price, 2011). Similarly, restoration of shallower floodplain channels from anthropogenically incised states has been predicted to increase or decrease baseflow in different settings (Essaid and Hill, 2014; Hammersmark et al., 2008; Ohara et al., 2014; Tague et al., 2008). Results for the Baviaanskloof demonstrate likely responses for semi-arid, mountainous, meso-scale catchments with sporadic rainfall, high conductivity soils, and significant subsurface recharge of the floodplain from surrounding mountains.

In the case of the Baviaanskloof, it had been initially hypothesized that hillslope thicket restoration could increase baseflow due to the significant increase in soil infiltration and conductivity seen under intact thicket compared with degraded areas (Lechmere-Oertel and Kerley, 2008; Lechmere-Oertel et al., 2005; van Luijk et al., 2013; Mills and Cowling, 2010; Mills and Fey, 2004a, 2004b; Mills et al., 2005) and the detected large contribution of hillslope interflow to floodplain aquifer recharge which in turn feeds baseflow (Chapters 1-3). However, although modeling did indicate an increase long-term average interflow with more intact thicket compared to a fully degraded case, and an increase in delayed flow at the catchment outlet following very large peak flow events, these increases were small, of short-duration, and infrequent due to the steep slopes, high conductivity soils, and rarity of heavy rainfall. The increase in canopy interception and ET demand dominated the response such that average baseflows were predicted to decrease with thicket restoration. The geomorphic

setting of the vegetation change was also seen to have an impact, as fans and floodplain were seen to dampen the impacts on flood peaks and yields (Chapters 3 and 6).

Given the large predicted change in water yield with thicket restoration, the assumed change in canopy interception, soil properties, and thicket vegetation water use deserve further exploration. Canopy interception reported for intact thicket in previous studies, and which was applied here, is high relative to observations in other semi-arid vegetation types, as noted by (Cowling and Mills, 2011), point soil sampling would not account for potential macro-porosity that may develop in restored thicket due to root networks, and no direct measurements of AET in spekboom thicket have been reported. Field studies and model calibration against longer datasets could be used to improve the accuracy of the model representation of thicket and changes in thicket cover.

For the Baviaanskloof, restoring more dispersive flow paths across the central valley alluvial fill, through restoration of fans and floodplain channels to less channelized and incised states, was predicted to decrease flood peaks while having minor impacts on overall yields. The low impact on yield was partially due to the high rate of drainage of recharge through the alluvium following large flood events meaning it was not long available for ET. Because the additional alluvial aquifer recharge during wet periods entered the channel relatively quickly, increases in baseflow were only predicted in weeks following a large event and were not maintained into prolonged drier periods. In the Baviaanskloof model, the relatively consistent recharge of the alluvial aquifer from the mountain bedrock compared to

the rate of channel drainage, and shallower water table at downstream narrow valley reaches, meant that the channel was predicted to intersect the water table at some locations throughout the modeled period. This included prolonged dry periods without overbank flooding recharge events. As a result, increasing floodplain channel incision was predicted increase baseflows, even though incision decreased alluvial aquifer recharge by reducing overbank flooding. Subsurface recharge from the mountains was sufficient to sustain increased aquifer-channel connectivity.

There have been relatively few studies of catchment-scale impacts of floodplain channel incision impacts and none of alluvial fans channelization. Further research on the impacts of these changes in a variety of catchment and climate settings would assist in highlighting different response patterns likely in different environments that could help inform restoration planning. The predicted response to restoring the incised floodplain channel in the Baviaanskloof differed from channel incision studies in snow-melt fed meadows (Hammersmark et al., 2008; Ohara et al., 2014; Tague et al., 2008). In the meadows, prolonged seasonal floodplain recharge periods, shorter seasonal dry periods, and slower draining aquifer material, resulted in a greater build-up of additional recharge in the restored case and a slower subsequent delayed outflow, which also did not need to last as long to result in increased baseflows over the relatively dry summer. Even in catchment settings with similar climates to the Baviaanskloof, the response to channel changes could be different given much lower rates of floodplain recharge from surrounding mountains and/or

a different floodplain shape such that recharge from overbank flooding was more critical to maintaining the aquifer-channel connection and baseflow.

This dissertation also demonstrated the importance of considering the combined impacts of coinciding restoration activities or changes in downslope catchment properties that may occur as a result of activities upslope due to geomorphic processes. For example large scale changes in vegetation cover have been observed to influence channel form (Booth, 1990; James and Marcus, 2006; Keesstra et al., 2005; Osterkamp and Hupp, 2010). In the Baviaanskloof case the predicted impact of vegetation restoration was different if it was assumed that this would not influence central valley channel network properties compared to if it was assumed channels would also return to their restored state. For example the floodplain groundwater table was predicted to decline by 6-10% with hillslope thicket restoration alone, but if channel restoration also occurred the water table was predicted to rise by 8-11%. Further geomorphic research would be needed to determine which scenario is more likely and over what time period.

These studies indicated the nature of some of the trade-offs that would need to be considered in restoration planning and catchment management in the Baviaanskloof. Further integration of the Baviaanskloof hydraulic-hydrologic model with sediment transport modeling, water quality modeling, reservoir water balance modeling for the downstream supply reservoir, groundwater withdrawal patterns in the floodplain, flooding impact assessments in the catchment and in downstream areas, and wetland and riparian habitat

models would be needed to fully understand the impacts of the modeled changes on realized water supply, flood impacts, and habitat. Nevertheless, the hydraulic-hydrologic model results alone indicate that full catchment restoration is likely to result in an increase in groundwater supply accessibility for local catchment residents, an increase in floodplain inundation impacts, an increase in wetland habitat, a decrease in water supply for downstream users, but an increase in quality, and a decrease in flood impacts downstream. It is likely that the water yield decrease would be less than the modeled change In catchment outlet water yield as reservoir evaporation and sedimentation have not been taken into account and the largest changes in yield were predicted during wet periods when the reservoir is often overflowing. Trade-offs between different local and regional benefits and drawbacks were evident in the predicted hydrologic outcomes. There would also be other ecosystem services and biodiversity outcomes that would need to be considered when planning restoration and land management, such as agricultural productivity, habitat provision, and carbon storage. Catchment management goals need to be set collectively to holistically assess potential future scenarios and determine what activities are desirable on balance. The model development and scenario assessments done here form one part of this larger analysis.

7.3 References

Ackerman, D., Schiff, K.C., and Weisberg, S.B. (2005). Evaluating HSPF in an arid, urbanized watershed. J. Am. Water Resour. Assoc. *41*, 477–486.

Ajami, H., Troch, P.A., Maddock, T., Meixner, T., and Eastoe, C. (2011). Quantifying mountain block recharge by means of catchment-scale storage-discharge relationships. Water Resour. Res. *47*, n/a – n/a.

Blainey, J.B., and Pelletier, J.D. (2008). Infiltration on alluvial fans in arid environments: Influence of fan morphology. J. Geophys. Res. Earth Surf. *113*, n/a – n/a.

Booth, D. (1990). Stream-Channel Incision Following Drainage-Basin Urbanization. Water Resour. Bull. *26*, 407–417.

Bosch, J.M., and Hewlett, J.D. (1982). A review of catchment experiments to determine the effect of vegetation changes on water yield and evapotranspiration. J. Hydrol. *55*, 3–23.

Brown, A.E., Zhang, L., McMahon, T.A., Western, A.W., and Vertessy, R.A. (2005). A review of paired catchment studies for determining changes in water yield resulting from alterations in vegetation. J. Hydrol. *310*, 28–61.

Chirico, G.B., Grayson, R.B., and Western, A.W. (2003). A downward approach to identifying the structure and parameters of a process-based model for a small experimental catchment. Hydrol. Process. *17*, 2239–2258.

Clark, M.P., Slater, A.G., Rupp, D.E., Woods, R.A., Vrugt, J.A., Gupta, H.V., Wagener, T., and Hay, L.E. (2008). Framework for Understanding Structural Errors (FUSE): A modular framework to diagnose differences between hydrological models. Water Resour. Res. *44*, W00B02.

Cowling, R.M., and Mills, A.J. (2011). A preliminary assessment of rain throughfall beneath Portulacaria afra canopy in subtropical thicket and its implications for soil carbon stocks. South Afr. J. Bot. *77*, 236–240.

Efstratiadis, A., and Koutsoyiannis, D. (2010). One decade of multi-objective calibration approaches in hydrological modelling: a review. Hydrol. Sci. J.-J. Sci. Hydrol. *55*, 58–78.

Essaid, H.I., and Hill, B.R. (2014). Watershed-scale modeling of streamflow change in incised montane meadows. Water Resour. Res. *50*, 2657–2678.

Hammersmark, C., Rains, M., and Mount, J. (2008). Quantifying the hydrological effects of stream restoration in a montane meadow, northern California, USA. RIVER Res. Appl. *24*, 735–753.

He, M., and Hogue, T.S. (2012). Integrating hydrologic modeling and land use projections for evaluation of hydrologic response and regional water supply impacts in semi-arid environments. Environ. Earth Sci. *65*, 1671–1685.

Herron, N., and Wilson, C. (2001). A water balance approach to assessing the hydrologic buffering potential of an alluvial fan. Water Resour. Res. *37*, PP. 341–351.

Hipsey, M.R., Vogwill, R., Farmer, D., and Busch, B.D. (2011). A multi-scale ecohydrological model for assessing floodplain wetland response to altered flow regimes (Christchurch: Modelling & Simulation Soc Australia & New Zealand Inc).

Houston, J. (2002). Groundwater recharge through an alluvial fan in the Atacama Desert, northern Chile: mechanisms, magnitudes and causes. Hydrol. Process. *16*, 3019–3035.

James, L.A., and Marcus, W.A. (2006). The human role in changing fluvial systems: Retrospect, inventory and prospect. Geomorphology *79*, 152–171.

Karen, I. (2009). A top–down approach to characterise aquifer–river interaction processes. J. Hydrol. *365*, 145–155.

Keesstra, S.D., van Huissteden, J., Vandenberghe, J., Van Dam, O., de Gier, J., and Pleizier, I.D. (2005). Evolution of the morphology of the river Dragonja (SW Slovenia) due to land-use changes. Geomorphology *69*, 191–207.

Lechmere-Oertel, R.G., and Kerley, G.I.H. (2008). Litter dynamics across browsing-induced fenceline contrasts in succulent thicket, South Africa. South Afr. J. Bot. *74*, 651–659.

Lechmere-Oertel, R.G., Cowling, R.M., and Kerley, G.I.H. (2005). Landscape dysfunction and reduced spatial heterogeneity in soil resources and fertility in semi-arid succulent thicket, South Africa. Austral Ecol. *30*, 615–624.

van Luijk, G., Cowling, R.M., Riksen, M.J.P.M., and Glenday, J. (2013). Hydrological implications of desertification: Degradation of South African semi-arid subtropical thicket. J. Arid Environ. *91*, 14–21.

Lynch, S.D. (2003). Development of a Raster Database of Annual, Monthly and Daily Rainfall for Southern Africa (Pretoria, South Africa: Water Research Commission (WRC)).

Maneta, M., Schnabel, S., and Jetten, V. (2008). Continuous spatially distributed simulation of surface and subsurface hydrological processes in a small semiarid catchment. Hydrol. Process. *22*, 2196–2214.

Mills, A., and Fey, M. (2004a). Transformation of thicket to savanna reduces soil quality in the Eastern Cape, South Africa. Plant Soil *265*, 153–163.

Mills, A.J., and Cowling, R.M. (2010). Below-ground carbon stocks in intact and transformed subtropical thicket landscapes in semi-arid South Africa. J. Arid Environ. *74*, 93–100.

Mills, A. j., and Fey, M. v. (2004b). Effects of vegetation cover on the tendency of soil to crust in South Africa. Soil Use Manag. *20*, 308–317.

Mills, A.J., Cowling, R.M., Fey, M.V., Kerley, G.I.H., Donaldson, J.S., Lechmere-Oertel, R.G., Sigwela, A.M., Skowno, A.L., and Rundel, P. (2005). Effects of goat pastoralism on ecosystem carbon storage in semiarid thicket, Eastern Cape, South Africa. Austral Ecol. *30*, 797–804.

Mukhopadhyay, B., Cornelius, J., and Zehner, W. (2003). Application of kinematic wave theory for predicting flash flood hazards on coupled alluvial fan–piedmont plain landforms. Hydrol. Process. *17*, 839–868.

Munevar, A., and Marino, M.A. (1999). Modeling analysis of ground water recharge potential on alluvial fans using limited data. Ground Water *37*, 649–659.

Niswonger, R.G., Prudic, D.E., Pohll, G., and Constantz, J. (2005). Incorporating seepage losses into the unsteady streamflow equations for simulating intermittent flow along mountain front streams. Water Resour. Res. *41*, W06006.

Ohara, N., Kavvas, M.L., Chen, Z.Q., Liang, L., Anderson, M., Wilcox, J., and Mink, L. (2014). Modelling atmospheric and hydrologic processes for assessment of meadow restoration impact on flow and sediment in a sparsely gauged California watershed. Hydrol. Process. *28*, 3053–3066.

Osterkamp, W.R., and Hupp, C.R. (2010). Fluvial processes and vegetation - Glimpses of the past, the present, and perhaps the future. Geomorphology *116*, 274–285.

Price, K. (2011). Effects of watershed topography, soils, land use, and climate on baseflow hydrology in humid regions: A review. Prog. Phys. Geogr. *35*, 465–492.

Seibert, J., and McDonnell, J.J. (2002). On the dialog between experimentalist and modeler in catchment hydrology: Use of soft data for multicriteria model calibration. Water Resour. Res. *38*, 1241.

Sivapalan, M., Blöschl, G., Zhang, L., and Vertessy, R. (2003). Downward approach to hydrological prediction. Hydrol. Process. *17*, 2101–2111.

Tague, C., Valentine, S., and Kotchen, M. (2008). Effect of geomorphic channel restoration on streamflow and groundwater in a snowmelt-dominated watershed. Water Resour. Res. *44*, 10 PP.

Tetzlaff, D., McDonnell, J.J., Uhlenbrook, S., McGuire, K.J., Bogaart, P.W., Naef, F., Baird, A.J., Dunn, S.M., and Soulsby, C. (2008). Conceptualizing catchment processes: simply too complex? Hydrol. Process. *22*, 1727–1730.

Tetzlaff, D., Carey, S.K., Laudon, H., and McGuire, K. (2010). Catchment processes and heterogeneity at multiple scales—benchmarking observations, conceptualization and prediction. Hydrol. Process. *24*, 2203–2208.

Uhlenbrook, S., Roser, S., and Tilch, N. (2004). Hydrological process representation at the meso-scale: the potential of a distributed, conceptual catchment model. J. Hydrol. *291*, 278–296.

Young, P. (2003). Top-down and data-based mechanistic modelling of rainfall–flow dynamics at the catchment scale. Hydrol. Process. *17*, 2195–2217.

Zheng, Y., and Keller, A.A. (2007a). Uncertainty assessment in watershed-scale water quality modeling and management: 1. Framework and application of generalized likelihood uncertainty estimation (GLUE) approach. Water Resour. Res. *43*, W08407.

Zheng, Y., and Keller, A.A. (2007b). Uncertainty assessment in watershed-scale water quality modeling and management: 2. Management objectives constrained analysis of uncertainty (MOCAU). Water Resour. Res. *43*, W08408.